![British Geological Survey logo]

A hydrochemical assessment of groundwater–surface water interaction in the Woodham Burn, a Magnesian Limestone catchment in County Durham

BRITISH GEOLOGICAL SURVEY

A hydrochemical assessment of groundwater–surface water interaction in the Woodham Burn, a Magnesian Limestone catchment in County Durham

B Palumbo-Roe, B Brauns, VJ Banks

Contributors

D Steele, S Gallagher

Keyworth, Nottingham   British Geological Survey   2020

BRITISH GEOLOGICAL SURVEY

The full range of our publications is available from BGS shops at Nottingham, Edinburgh, London and Cardiff (Welsh publications only) see contact details below or shop online at www.geologyshop.com

The London Information Office also maintains a reference collection of BGS publications, including maps, for consultation.

We publish an annual catalogue of our maps and other publications; this catalogue is available online or from any of the BGS shops.

The British Geological Survey carries out the geological survey of Great Britain and Northern Ireland (the latter as an agency service for the government of Northern Ireland), and of the surrounding continental shelf, as well as basic research projects. It also undertakes programmes of technical aid in geology in developing countries.

The British Geological Survey is a component body of UK Research and Innovation.

British Geological Survey offices

**Nicker Hill, Keyworth,
Nottingham NG12 5GG**

Tel 0115 936 3100

BGS Central Enquiries Desk

Tel 0115 936 3143
email enquiries@bgs.ac.uk

BGS Sales

Tel 0115 936 3241
email sales@bgs.ac.uk

**The Lyell Centre, Research Avenue South,
Edinburgh EH14 4AP**

Tel 0131 667 1000
email scotsales@bgs.ac.uk

**Natural History Museum, Cromwell Road,
London SW7 5BD**

Tel 020 7589 4090
Tel 020 7942 5344/45
email bgslondon@bgs.ac.uk

**Cardiff University, Main Building, Park Place,
Cardiff CF10 3AT**

Tel 029 2167 4280

**Maclean Building, Crowmarsh Gifford,
Wallingford OX10 8BB**

Tel 01491 838800

**Geological Survey of Northern Ireland, Department of Enterprise, Trade & Investment, Dundonald House, Upper Newtownards Road, Ballymiscaw,
Belfast, BT4 3SB**

Tel 01232 666595
www.bgs.ac.uk/gsni/

Natural Environment Research Council, Polaris House, North Star Avenue, Swindon SN2 1EU

Tel 01793 411500   Fax 01793 411501
www.nerc.ac.uk

**UK Research and Innovation, Polaris House,
Swindon SN2 1FL**

Tel   01793 444000
www.ukri.org

Website www.bgs.ac.uk
Shop online at   www.geologyshop.com

Acknowledgements

Contents

FIGURES

TABLES

Summary

The interaction between groundwater and surface water, in particular in the hyporheic zone, is recognised to influence chemical fluxes between river and groundwater and to transform reactive chemistries such as nutrients or legacy contaminants. Characterising this connectivity in the Skerne catchment in Co. Durham has been recognised to be important by the Environment Agency (EA) in order to protect the underlying Magnesian Limestone aquifer and dependent features. Of particular concern is the presence of an eastward moving, sulphate-rich, mine water plume related to the recovery of groundwater levels in the underlying Coal Measures strata and mine workings.

Building on a previous investigation across the entire Skerne catchment, this work, in collaboration with the EA, aimed to understand the existence of hydraulic connection between groundwater and surface water and the hyporheic zone characteristics in a 500 m stretch of the Woodham Burn, a tributary of the Skerne. We have employed multiple methods, both at the reach-scale and smaller sediment-scale, for identifying source areas of sulphate to the stream, characterising the subsurface flow and estimating the controls on sulphate fluxes and potential natural attenuation. The Woodham Burn was monitored during three sampling events in: April 2018, August 2018, and February 2019.

The stream water chemistry survey has confirmed sulphate concentrations in excess of the drinking water standard of 250 mg/l, with a median of 510 mg/l in the surface water, range 235-790 mg/l. Stream flow measurements complementary to the water chemistry analysis were not possible and therefore loads (flow multiplied by concentration) of sulphate could not be calculated. Given the lack of tributaries, the changes in surface water chemistry were, nevertheless, useful to attribute the observed changes to groundwater losses or gains, where groundwater and surface water concentrations are significantly different. The spatial survey of downstream changes in stream water chemistry has delineated a sulphate-rich recharge zone within the study reach, which is very localised, with sulphate concentrations up to 800 mg/l and electrical conductivity of 2000 µS/cm. The source appears to be groundwater discharging directly into the stream channel and in the form of a seep on the western bank. The contribution of this source to the stream was quantified as up to 50 percent increase in dissolved sulphate in surface water.

An additional area potentially recharging sulphate to the stream, more diffuse in nature, was identified through analysis of the water-soluble fraction of soil samples collected by augers and additional bank seepage measurements and it corresponds to the northern banks upstream of the first monitoring point.

Temperature vertical profiling of the riverbed along the 500 m study reach together with a corresponding survey of specific electrical conductivity (SEC) variation in the surface water were used to further detect areas of potential flow of surface water to groundwater or flow of groundwater to surface water, and to inform the site selection for the monitoring of subsurface flow at smaller scale with piezometers and minipiezometers.

At four locations, piezometers were installed with data loggers to provide continuous observations of hydraulic heads, temperature, and (at two points) SEC: two paired piezometers of shallow (0.4 m) and deeper (1.4 m) depth at three of the locations and only a single shallow piezometer for one site. Due to the loss of the surface water logger after a storm event, precise water level fluctuations in Woodham Burn were unknown, and recorded fluctuations in the subsurface were more difficult to correlate. At the same locations, plus an additional one, a network of multilevel minipiezometers (two to three per site) were driven into the hyporheic zone to a fixed depth of 0.9 m below the riverbed and used to draw pore water from 10, 20, 50 and 90 cm depth. The evidence from vertical gradients of conservative elements, chloride and lithium, measured in each multilevel minipiezometer, and evidence from the diurnal temperature variations and hydraulic head from logged data, converged to indicate an increase of hyporheic exchange flow (HEF) moving downstream in the burn, corresponding to the transition in the superficial deposits from alluvium to lacustrine deposits, while the most upstream sites showed the near absence of HEF and at least one clearly gaining reach in correspondence of the sulphate-rich instream discharge.

Evaluation of natural attenuation in the hyporheic zone was carried out via comparison of conservative and non-conservative solute gradients. In most of the sites where there was sufficient HEF, both nitrate and sulphate showed various extents of non-conservative behaviour compared to chloride in the subsurface flow. In particular, the most significant losses of nitrate were observed in piezometers at the most downstream section of the reach (-48% to -98%). Sulphate losses were generally lower than those for nitrate and varied greatly (9% to 100%), often larger at depth. Although nitrate and sulphate losses were observed during surface water downwelling in the studied hyporheic zone, a correspondent decrease in stream water concentrations was not evident. It is recommended to test the significance of hyporheic natural attenuation to improve the stream water quality at catchment scale, by carrying out surface water flow measurements combined with water quality analysis, which enable calculation of mass gains and losses to identify the net flux integrated over the entire stream.

The analysis of the deep hyporheic zone chemistry, the least affected by shallow hyporheic exchange of downwelling surface water, gave insights into hydrochemical differences along the reach and indicates potentially distinct groundwater sources. These differences appear to be related to geology: the most upstream monitoring locations sited on the alluvium have greater similarities to the Magnesian Limestone aquifer, as inferred by cluster analysis with additional EA groundwater monitoring boreholes. As previously identified points of limited HEF and groundwater dominated hyporheic water, these locations plausibly represent a groundwater recharge zone. On the other hand, the most downstream points located on the lacustrine deposits show a different hyporheic zone composition, distinctly closer to hyporheic waters previously sampled from Rushyford Beck, also on lacustrine deposits. Beside these hydrochemical differences, a greater one is represented by the discrete spring (Bubbly Spring) discharging through the stream bed and western stream banks. Its chemistry has strong similarities to other seeps in the burn and also to Stony Hall C borehole water, which is sourced from the Coal Measures. The spring composition (Mg-SO$_4$ water type) was very stable throughout the monitoring period and distinctively enriched in SO$_4$ (median 811 mg/l) together with Sr (median 984 µg/l) , Li (median 162 µg/l), Rb (median 7.19 µg/l) and U (median 4.04 µg/l) compared to all the other waters in Woodham Burn, while it was lower in Si, Ba, Mn and Fe. Two, both plausible, reaction paths can explain the spring composition: one is gypsum dissolution and dedolomitisation, the other one is acid neutralisation of coal mine water through the dissolution of dolomite. To explain the physical processes underpinning the emergence of this groundwater enriched in sulphate and the origin of this sulphate further investigation is needed. In particular residence time studies and isotope analysis of water and dissolved sulphate are recommended. To gain a broader perspective on groundwater discharge areas a spatial hydrochemical survey of springs and seeps in the catchment should also be undertaken.

1 Introduction

This report describes Phase 2 of a BGS-Environment Agency (EA) co-funded project aimed at the assessment of the potential contaminant pathways in the hyporheic zone of the Skerne catchment in Co. Durham, UK. The River Skerne is a southerly flowing tributary of the River Tees. This project contributes to the EA's main programme goal to understand connectivity between the River Skerne and the Magnesian Limestone aquifer, in order to design measures to improve protection of the groundwater resource in the context of the River Basin Management Planning.

Over the past years, the EA has been monitoring the quality of the surface waters to determine whether they have been impacted via baseflow from an eastwards moving mine water plume enriched in sulphate. The mine water plume is related to the recovery of groundwater levels in the Coal Measures within the Durham Coalfield to the south of the Butterknowle Fault and following closure of the Mainsforth and Fishburn Collieries in the early 1970s. These groundwater levels have exceeded those in the overlying Magnesian Limestone which covers the confined areas of the coal field. It has been confirmed that sulphate-rich groundwater is entering the Woodham Burn, a tributary of the River Skerne, with observed concentrations of sulphate greater than 300 mg/l near the town of Newton Aycliffe. The possible association of this sulphate-rich groundwater with the plume of mine water remains uncertain.

In the first phase of the BGS study a survey during the period June to September 2017 provided direct measurements of the shallow hyporheic zone composition at selected locations in the Skerne catchment (CR/19/004). Given the groundwater–surface water interaction and temporal variability expected to occur in response to seasonal controls on catchment hydrology it was recommended to extend the monitoring phase beyond the low flow conditions. Given the relatively high sulphate concentrations in both surface water and hyporheic zone and proximity to mine workings, Woodham Burn was the site recommended for the phase 2 investigation.

The focus of this report is the results of Phase 2 monitoring of the hyporheic zone and overlying surface water in the Woodham Burn. The monitoring program was designed to identify potential areas of subsurface recharge to the reach, the origin of the sulphate-rich groundwater inflows, and the potential attenuation of river- or groundwater-borne sulphate in the hyporheic zone. Monitoring activities took place from April 2018 to February 2019.

2 Aim and Objectives

Surface water – groundwater interactions occur at different scales with a continuum of "hyporheic flow paths" at channel scale, leaving and returning to the stream several times within a single reach, and groundwater flow paths at the reach and catchment scale, leaving or entering the stream according to their hydrogeologic or geomorphic drivers (Ibrahim et al. 2010).

Infiltration of stream water into near-stream sediments and return to the stream channel over relatively short distances, defined as "hyporheic exchange flow (HEF)" and associated with the reactivity of near-bed sediments, favour increased dilution, biodegradation, and adsorption or precipitation of mineral phases, which can reduce the concentration of contaminants in the subsurface (Buss et al. 2009).

Our aim is to gain a better understanding of surface water – groundwater interaction and to assess the spatial distribution and superimposition of two scales of subsurface flow paths (HEF and groundwater discharge) in the riverbed of a reach of the Woodham Burn, a tributary of the River Skerne, known for sulphate-rich surface waters. The stream is located in an area where the quality of the Magnesian Limestone aquifer is known to be impacted by mine water rebound in the Coal Measures within the Durham Coalfield to the south of the Butterknowle Fault.

By delivering this study, we will contribute to the evidence-based assessment of the risk posed by groundwater discharges to surface water quality within the project area and, at the same time, of the risk of surface waters intercepting and redistributing a component of the mine water plume in the catchment.

To achieve an improved conceptual model of surface water–groundwater interaction in the project area, we set these specific objectives through a monitoring programme and data analysis:

1. Assessing the quality of surface water and shallow groundwater by sampling in a range of hydrological conditions.
2. Determining the extent of hyporheic exchange flow.
3. Determining where and how groundwaters discharge.
4. Evaluating the natural bioremediation/attenuation potential to reduce high sulphate concentrations in the hyporheic zone and surface water.
5. Understanding potential contributions of deep groundwater, shallow groundwater to the surface system.

3 Site description

The Phase 1 investigation described both Rushyford Beck and Woodham Burn (Figure 1) as a single research area in setting the context of the conceptual ground model (Palumbo-Roe et al. 2019). For this phase of reporting, we have subdivided the sites to accommodate the findings of an extended literature review for descriptive purposes. The ultimate focus on researching the Woodham Burn site warrants a more detailed description of that area.
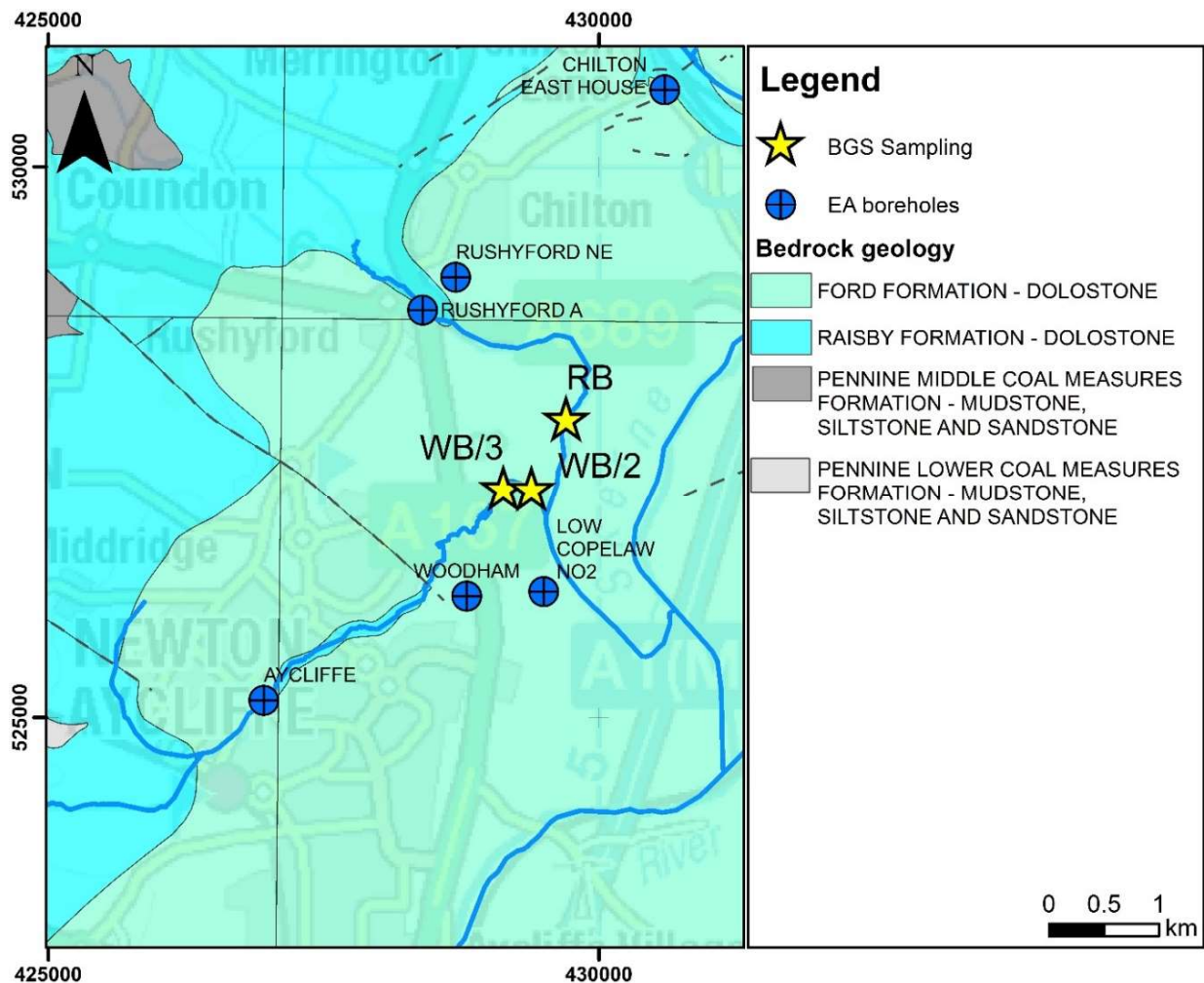
Figure 1 Bedrock geology and EA boreholes at monitoring point RB (Rushyford Beck)/WB (Woodham Burn). Dashed lines indicate inferred faults. Contains Ordnance Survey data © Crown Copyright and database right 2020. Ordnance Survey Licence no. 100021290.

3.1 RUSHYFORD BECK

3.1.1 Location

Rushyford Beck is sourced in the order of 3 km to the west of Chilton and 1 km to the north-east of the village of Coundon, further from the monitoring points than indicated by Figure 1. The first-order streams are commonly associated with small ponds and areas of woodland. From the headwaters, the beck flows in a southeasterly direction for approximately 5 km before flowing south to join the Woodham Burn.

3.1.2 Geology

The bedrock geology that underlies Rushyford Beck (Figure 1; Table 1), comprises the south-easterly dipping Raisby Formation, overlain to the southeast by the Ford Formation and underlain in the source area, extending for approximately 550 m, by the Pennine Middle Coal Measures Formation. The Ford Formation, capped by Glacial Till, dominates the sequence. Near the headwaters, the superficial deposits include pockets of Glacio-fluvial sand and gravel deposits. Ribbons of Alluvium line the course of the river and its tributaries (Figure 2). To the east of approximately easting 429435, the alluvial deposits give way to lacustrine clays and silts. The lacustrine clays (Nunstainton Grange Carrs) are considered the remnant of the glacial Lake Tees (Murton and Murton, 2012), which is further described in section 3.2.2. The River Skerne has previously been described as an overflow channel from the glacial Lake Wear that flowed south through the Ferrybridge Gap (Ogilvie, 1930).

Table 1 Geology underlying the Rushyford Beck and Woodham Burn.

Deposit type	Mapped Unit	Lithology
Superficial (0-15 m)	Alluvium	Organic clay
	Lacustrine deposits	Peaty, silty clays
	Glacio-fluvial sand and gravel	Sand and gravel
	Devensian Till	Gravelly silty sandy clay
Bedrock	Ford Formation of the Zechstein Group (Permian); formerly Middle Magnesian Limestone	Dolomitised platform limestones. Dolostone (very vuggy in field walls)
	Raisby Formation	Cream, brown and grey, fine-grained dolostone with grey, fine-grained limestone
	Pennine Middle Coal Measures Formation (Carboniferous)	Mudstone, sandstone and siltstone
	Pennine Lower Coal Measures Formation (Carboniferous)	Mudstone, siltstone and sandstone
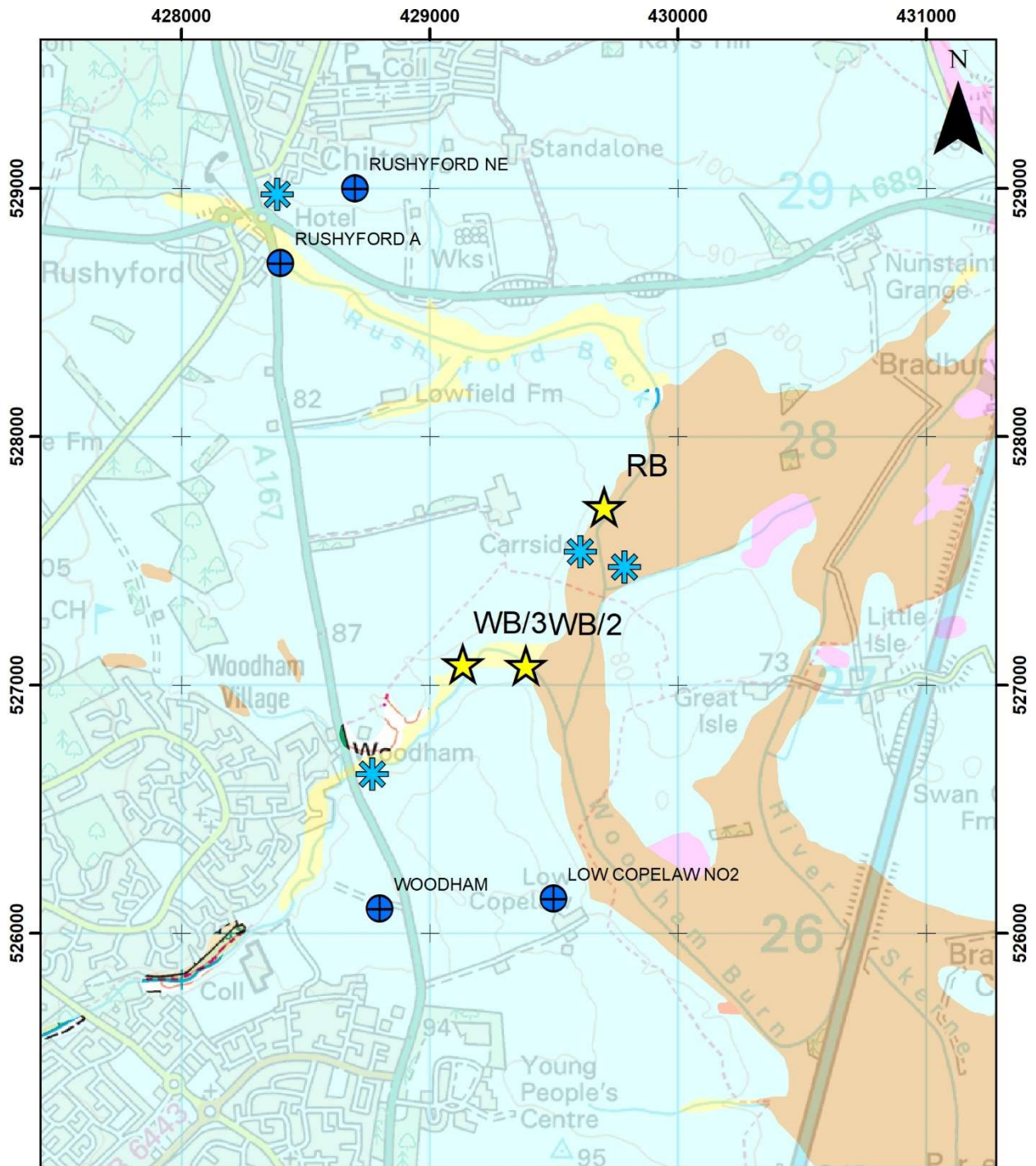
Figure 2 Superficial deposits at monitoring site RB (Rushyford Beck)/WB (Woodham Burn). Contains Ordnance Survey data © Crown Copyright and database rights 2020. Ordnance Survey Licence no. 100021290.

3.2   WOODHAM BURN

3.2.1   Location

Woodham Burn rises in the order of 2.5 km to the south-west of Shildon, near to the village of Newbiggin. From its headwaters, the burn flows east towards Newton Aycliffe, where it takes a broadly northeasterly course before turning to the southeast approximately 9 km from its source and 450 m from its confluence with the Rushyford Beck. From the confluence, Woodham Burn continues in a southeasterly direction towards the A1. The stream changes course again before reaching the A1, this time flowing north-northeast to join the River Skerne.

3.2.2   Geology

From its source, the bedrock geology that underlies Woodham Burn comprises the Pennine Lower Coal Measures Formation, Raisby Formation and the Ford Formation (Figure 1; Table 1). The unconformable nature of the contact between the Permian and Carboniferous strata is shown in Figure 3 and Figure 4 (an extract from BGS 1:63330 Geology Sheet 32, Barnard Castle (solid edition)).

The bedrock geology (Figure 1) forms a faulted ridge in the source area of the Rushyford Beck and Woodham Burn. Here the glacial deposits thin against the ridge and extensive windows through the superficial deposits are evident on BGS (1969).

Woodham Burn is incised through the Glacial Till and the Ford Formation into the underlying Raisby Formation between NGR 426941 525099 and a northwest to southeast striking fault at 428444 526189. Downstream of this, the Ford Formation dominates the bedrock geology and the superficial deposits comprise Glacial Till with ribbons of Alluvium along the course of the river and its tributaries (Figure 2). To the east of approximately easting 429435, the alluvial deposits give way to lacustrine clays and silts. Within the lacustrine clay deposits, isolated ponds with bulrushes were observed at NGR 429528 527127 and 429445 527127 75 and 76 m OD, respectively (in Figure 12).

It is plausible that the incision of Woodham Burn is fault guided, potentially forming the northeastern extension of a mapped fault along the same alignment to the southeast. The veneer of superficial deposits might lead to an under-representation of faults. A window through the superficial deposits has been mapped in the vicinity of NGR 428830 526776, immediately east of Woodham village (Figure 2). The BGS field slip (BGS 1989) indicates that this is associated with an inflow to the stream. The sampling point that has been referenced as *BP* (section 4.4) appears to be another window through the Glacial Till.

The lacustrine clays are considered to be a remnant of the proglacial Lake Tees (Murton and Murton, 2012). The glacial Lake Tees likely formed as the Eden-Stainmore ice stream reached the coast and its flow reduced, allowing a lobe of North Sea Ice to dam the lake (Davies et al. 2019). Hughes et al. (1998) note that in the Tees Estuary, two laminated clays occur: one close to OD and the other, accompanied by sands, is at around 20 m above OD and extending to around 30 m below OD, suggesting a complex interplay between recession and re-advance. The full history of the neotectonics of this area has still to be resolved.
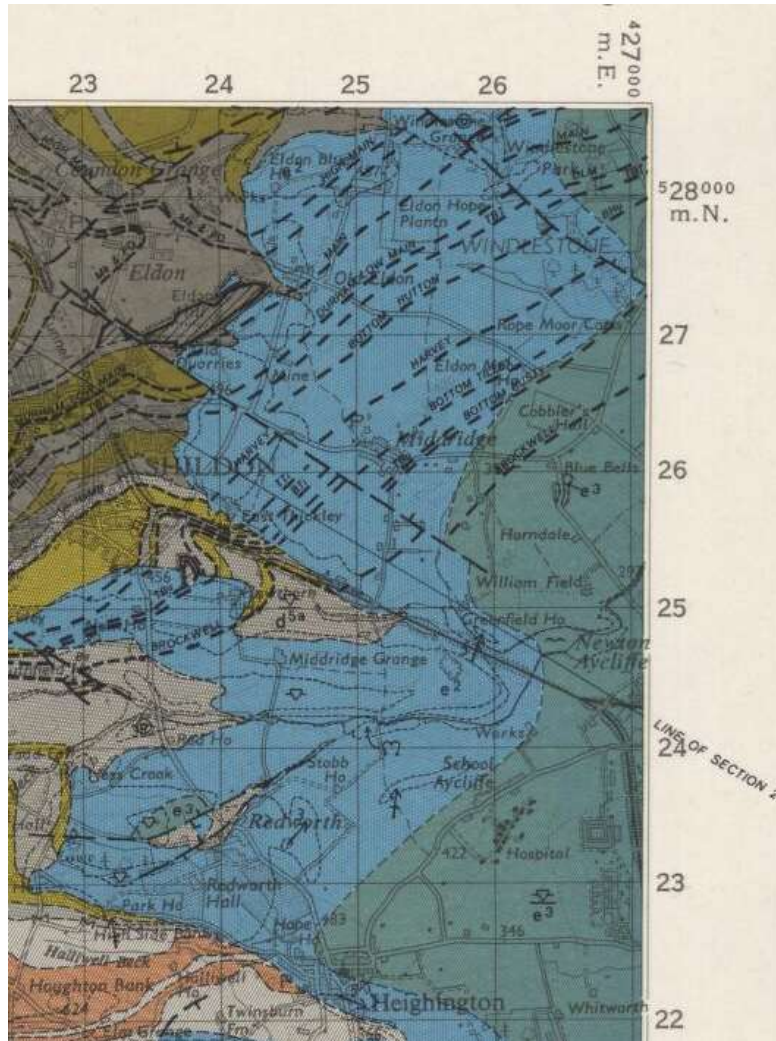
Figure 3 Extract of BGS 1:63330 Geology Sheet 32, Barnard Castle (solid edition, 1969) showing the line of the section presented as Figure 4.
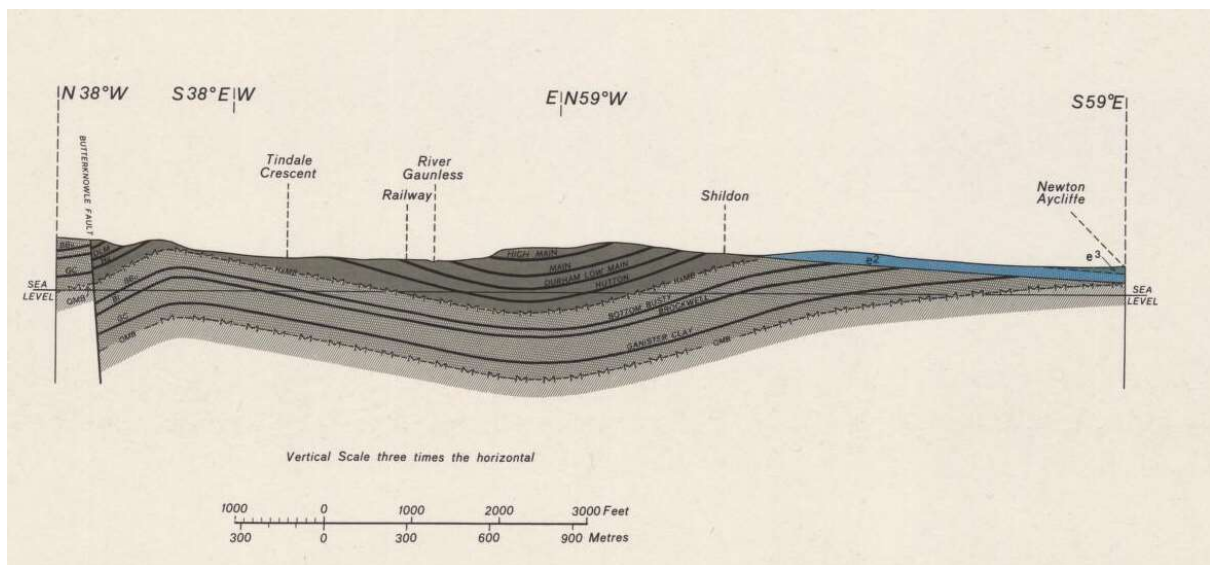
Figure 4 Cross Section 2 from BGS 1:63330 Geology Sheet 32, Barnard Castle (solid edition) presented to illustrate the unconformable nature of the Permian sediments (blue) over the Carboniferous strata (grey).

7

The lacustrine clays underlying the areas are called *Carrs*, a name that relates to the associated vegetation (water-tolerant trees, e.g. alder) and raised bog. Borehole evidence (Mordon Carrs) indicates that the peat deposits reach about 6 m in depth and that the underlying clays extend to about 16 m. As indicated above, the red, plastic clays give way to sand partings overlying the till deposits.

The River Skerne has previously been described as an overflow channel from the glacial Lake Wear, that flowed south through the Ferrybridge Gap (Ogilvie, 1930).

3.2.3 Hydrology and hydrogeology

Groundwater contours reported by White Young Green (2006) indicate that to the south of the Butterknowle Fault, there is an easterly hydraulic gradient in the Coal Measures and an easterly to southeasterly hydraulic gradient in the Permian strata. The overall flow in the Coal Measures is still understood to be easterly, but in the local vicinity of the Woodham Burn (Figure 10), the flow is to the northeast.

White Young Green (2006) reported on the monitoring of Stony Hall C Borehole (NGR 432570 529550) that was drilled into the Bottom Busty (Q2) workings in the south of Mainsforth Colliery workings (Figure 5). It was noted that the mine water level (78 m OD) was the lowest of the blocks (section 3.2.5.1). This informs the conceptual ground model (Figure 11).
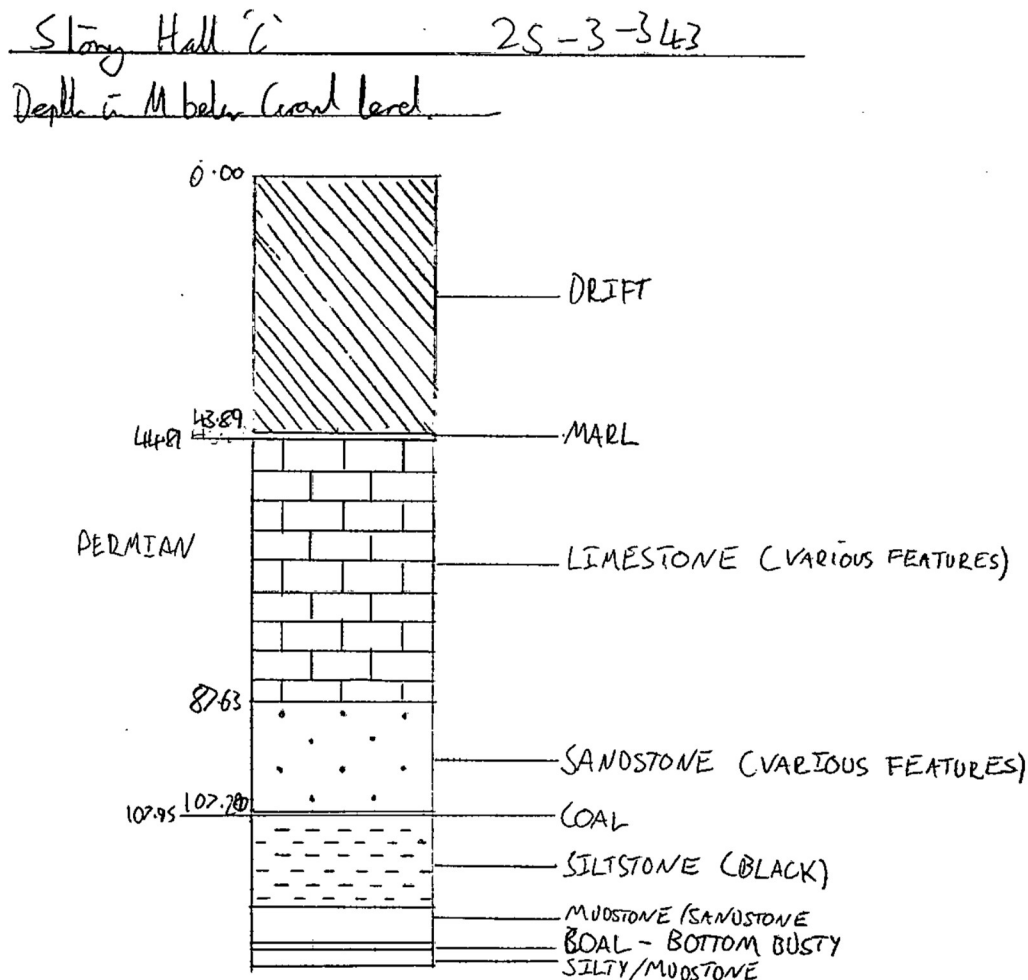
Figure 5 Borehole log for Stony Hall C (provided by the Environment Agency).

Up hydraulic gradient, boreholes to the north of Rushyford Beck (Rushyford to Bradbury) indicate an unsaturated zone of at least 5 to 7 m in thickness. The Low Copelaw borehole (700 m to the

southeast of the confluence of Rushyford Beck with Woodham Burn) indicates an unsaturated thickness of 17.31 m (Personal communication, Environment Agency 2020), with the groundwater water table reaching the basal 12 m of the superficial deposits that extend to 33.53 m below ground level. Beneath this, the Ford Formation extends to 49.38 m, this in turn underlain by the less permeable Raisby Formation. At the time of sampling the unsaturated thickness was likely in the order of 5 m (mean groundwater level 75.2 m OD during the period 18/04/2018 to 06/02/2019.

The association of Rushyford Beck and, to the east the River Skerne, with the lacustrine deposits, likely reflects their lower vertical permeability and propensity to support surface water above the groundwater table. However, if the lake formed in association with neotectonic movement on faults, it is plausible that confined groundwater might resurge along the contact between the till and the glacial lake deposits.

A small number of springs are associated with the till and the boundary between the till and the glaciofluvial sand and gravel deposits. The spring at Carrsides (NGR 429607 527534; Figure 2, Figure 6) is at the boundary between the till and lacustrine clay and silt deposits (to the east). For part of its course, the Rushyford Beck follows the boundary between the till and the lacustrine deposits, before turning south to flow across the lacustrine deposits.
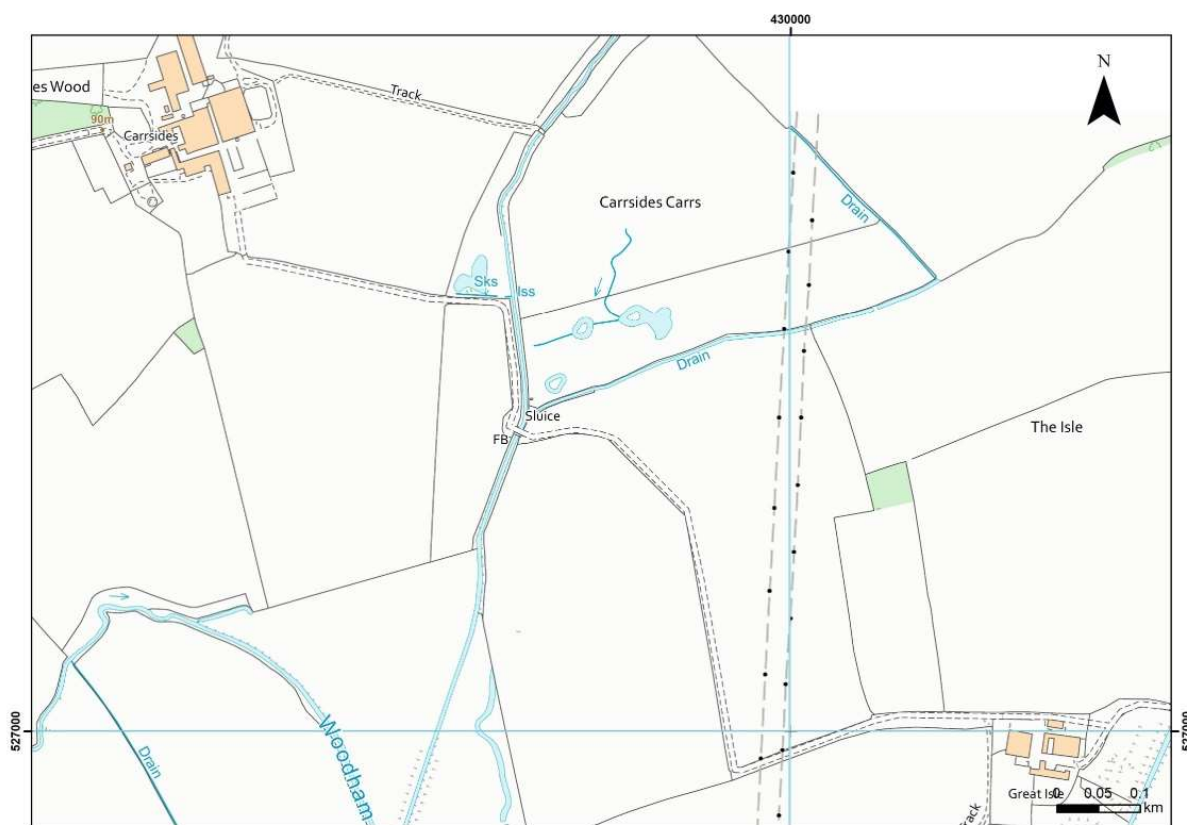
Figure 6 Carrsides spring and groundwater fed ponds. Contains Ordnance Survey data © Crown Copyright and database rights 2020. Ordnance Survey Licence no. 100021290.

3.2.4   Hydrogeochemistry

A survey carried out by the Environment Agency on the 18-02-2015 measured concentrations of 200 mg/l and 446 mg/l sulphate, respectively, in a spring discharging into the Woodham Burn and a pond, by the site of Woodham medieval village (Figure 7). From a concentration of 224 mg/l at the Woodham bridge, sulphate increases to 419 mg/l when the burn bends to a south-east direction, decreasing to 300 mg/l downstream the confluence with Rushyford Beck.

The results of the Phase 1 report established that at sampling points WB2 and WB3 (Figure 2), there was some dilution of sulphate concentrations in the sand and gravel of the riverbed hyporheic zone. The groundwater chemistry with high magnesium, calcium and bicarbonate suggested dolomitised limestone dissolution. It was also suggested that it is possible that there is a component of baseflow from the till, which may maintain a high flow to the stream, giving longer residence time for bedrock dissolution.

At site WB 3 (the upstream sample), the shallow sediment depth was not monitored, but the chloride (Cl) composition of the lower bed (-85; -115 cm depth) was similar to the surface water (Figure 8), which could be due to a high hyporheic exchange flow (HEF). Alternatively, the observed porewater Cl composition could be the result of a lateral or upwelling water inflow with Cl concentrations similar to the surface water. The high sulphate (SO_4) and corresponding relatively high dissolved oxygen (DO) values of the porewater suggest that the system did not have a strong reducing capacity. Furthermore, the hyporheic zone SO_4 concentration was similar to that at site WB 2 (downstream, Figure 3) at a depth of -20 to -40 cm.

Within the hyporheic zone at WB 2, SO_4 was found to behave conservatively with slightly attenuated concentrations in the hyporheic zone as a result of mixing of SO_4-rich surface water with moderately less enriched groundwater. However, at greater depth (-80 cm) SO_4 reduced significantly to 100 mg/l. It was not possible to interpret the SO_4 data at depth in terms of reduction mechanisms, as field parameters, such as oxidation-reduction potential (Eh) and DO, were not available. The inference of this monitoring was that there was hyporheic exchange in the first 30 cm of the riverbed at WB 2. The extent of surface water mixing with low-Cl porewater decreased with depth. The deeper groundwater has a lower Cl concentration and appears to dominate the hyporheic zone.
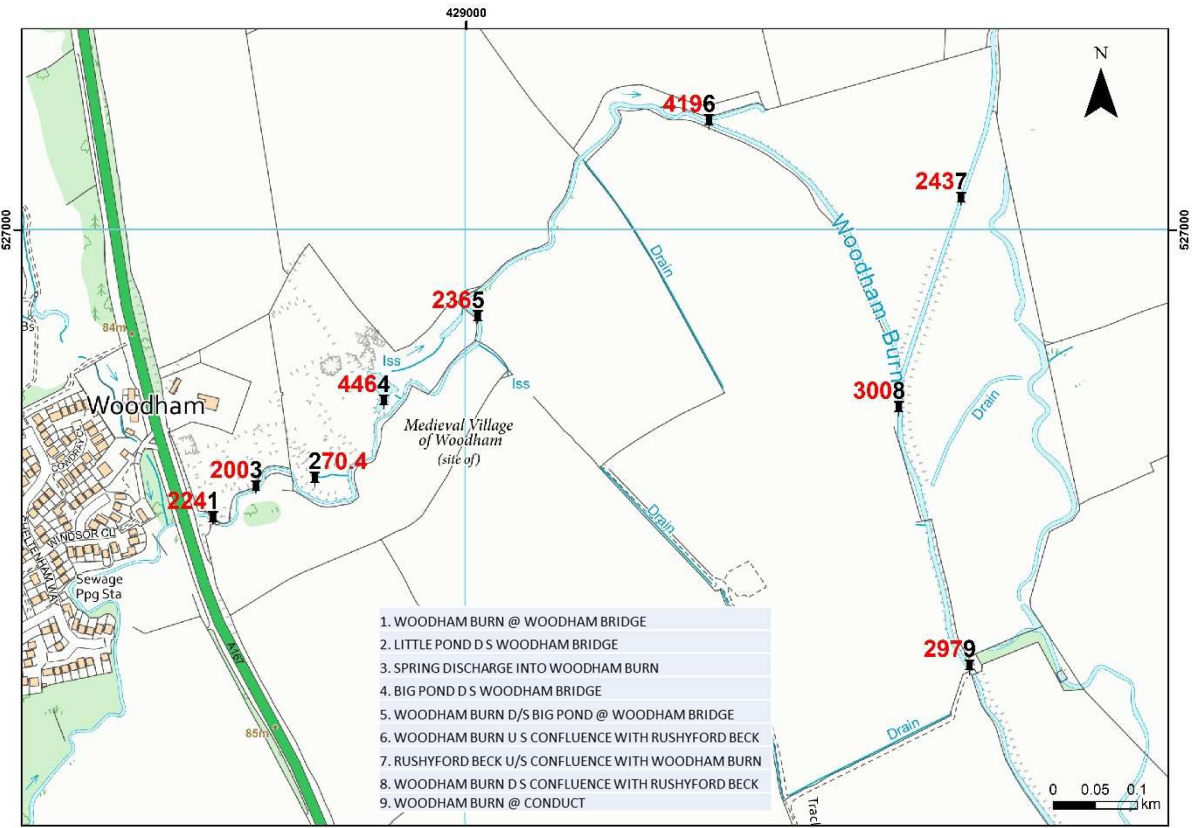
Figure 7 Sampling points and water sulphate concentrations (in red, mg/l) from a survey of the Woodham burn carried out by the Environment Agency on 18-2-2015. Contains Ordnance Survey data © Crown Copyright and database rights 2020. Ordnance Survey Licence no. 100021290.
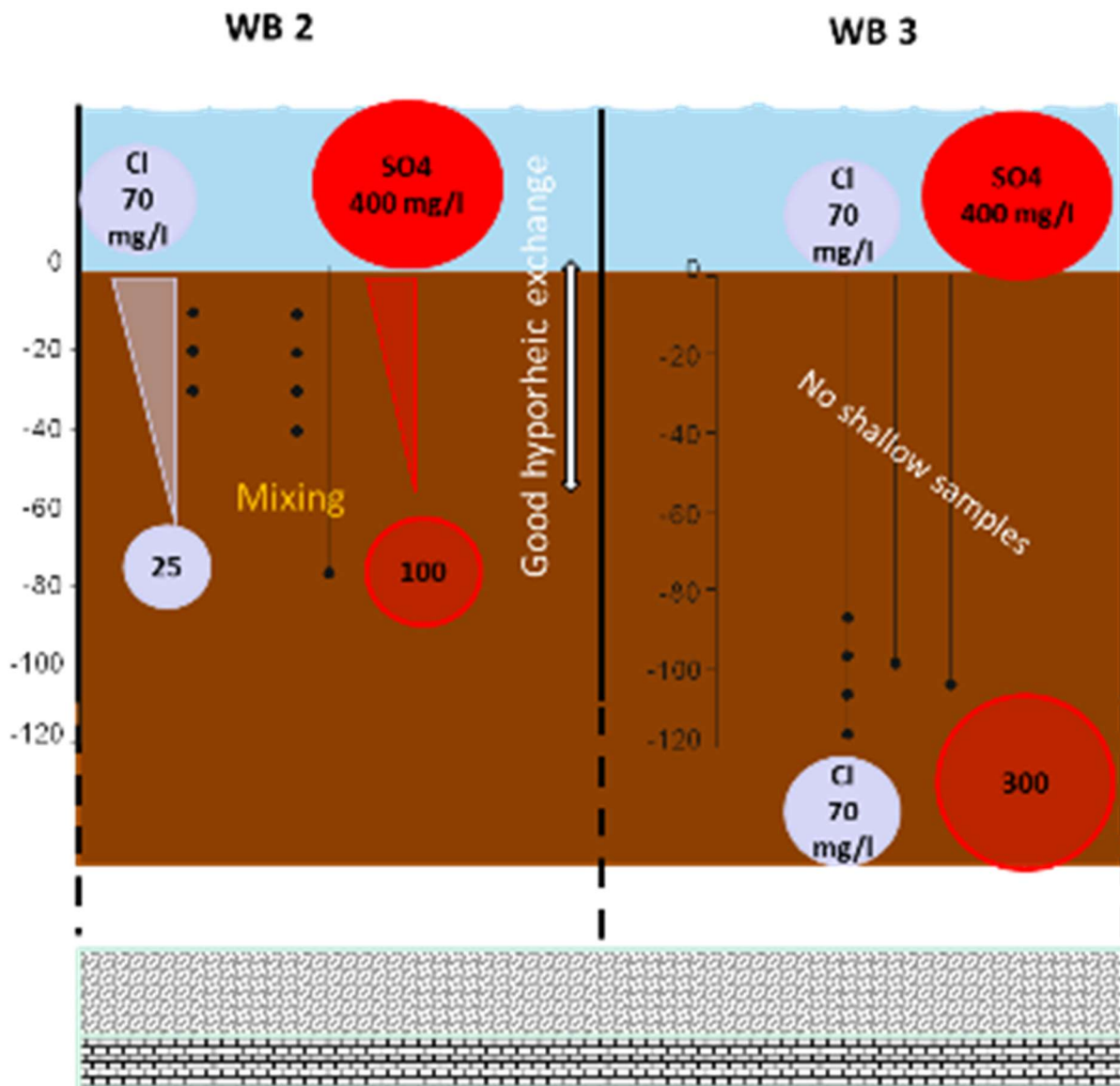
Figure 8 A schematic cross-section summarising solute concentrations observed at sites WB 2 and WB 3.

3.2.5 Conceptual ground model for Woodham Burn

3.2.5.1 PROXIMITY OF MINE WORKINGS

The area of the Durham Coalfield south of the Butterknowle Fault is shown in Figure 9 (White Young Green, 2006).

There are five mining blocks lying to the south of the Butterknowle Fault, three with Permian cover and two principally in the exposed coalfield (White Young Green, 2006). The blocks are:

1 The Ladysmith / Woodhouses / Etherley Lane Block (Coal Measures)

2 The North Eldon Block (Coal Measures)

3 The Eldon Block (Permian cover)

4 The Chilton Block (Permian cover)

5 The Fishburn / Mainsforth / Thrislington Block (Permian cover)
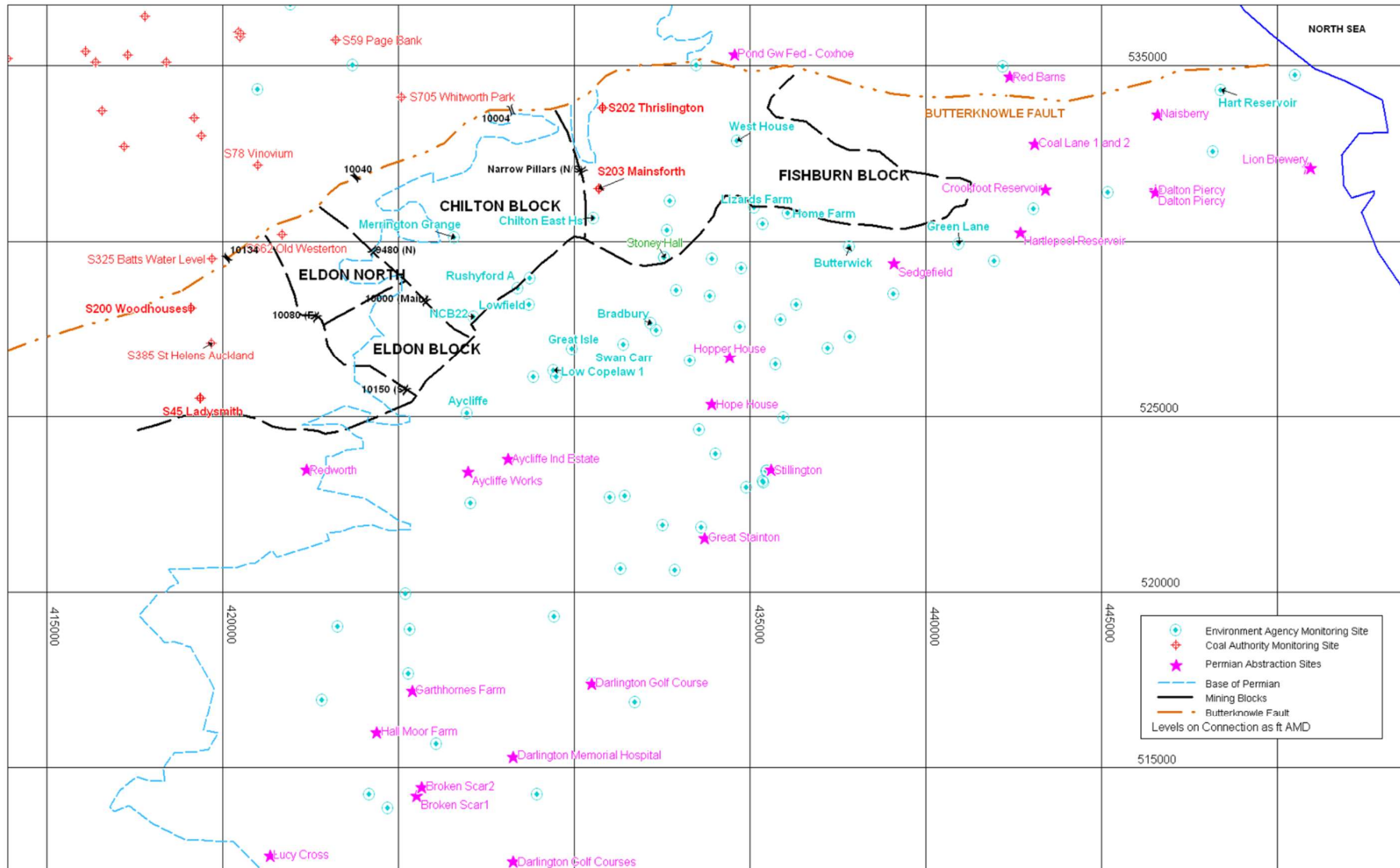
Figure 9 The area of the Durham Coalfield south of the Butterknowle Fault (from White Young Green, 2006, reproduced courtesy of the Coal Authority)

Figure 10 indicates that the edge of the coalfield (Chilton and Eldon blocks) lies immediately to the north of, and adjacent to the headwaters of Woodham Burn. It indicates a number of adits and shafts along this boundary with zones classified as B (on the coalfield) or C1 (on the coalfield areas with one, or both of: shallow mine workings, and nearby controlling outflow). Similarly, the Rushyford Beck rises over zone B (on the coalfield) and then flows across zone C2 (on the coalfield with shallow mine water that may be artesian) in the area of Rushyford to the edge of the coalfield.
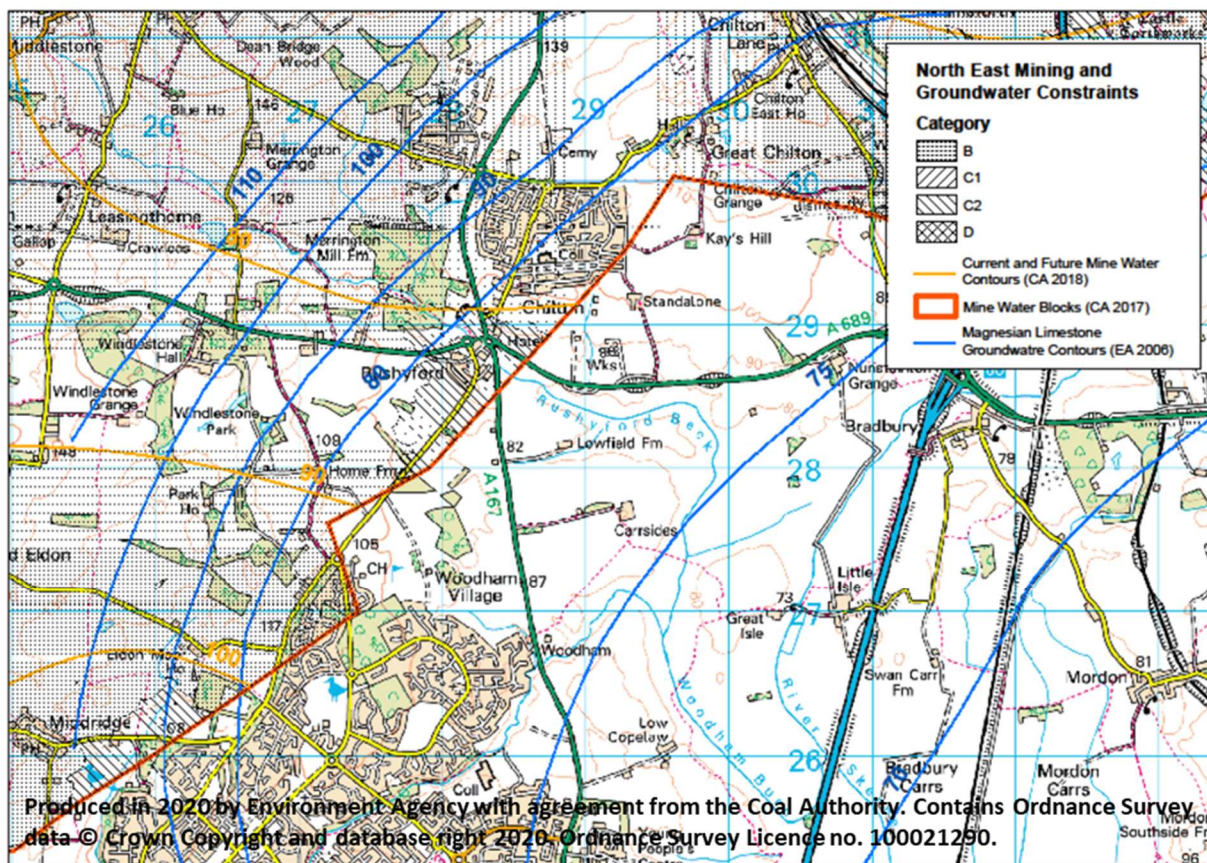
Figure 10 Map showing mining and groundwater constraints, specifically hatched areas of zone C2: on the coalfield with shallow mine water that may be artesian. Produced in 2020 by Environment Agency with agreement from the Coal Authority. Contains Ordnance Survey data © Crown Copyright and database rights 2020. Ordnance Survey Licence no. 100021290. Data also available on the Coal Authority online viewer (https://mapapps2.bgs.ac.uk/coalauthority/home.html).

A tributary to Woodham Burn, with its source to the northeast of Middridge (at 425908 524337) and flowing south immediately to the west of Woodham Village, likely receives groundwater from a zone of Coal Authority C2 designation (on the coalfield with shallow mine water that may be artesian in the Chilton Block; potentially the same source as for the Rushyford Beck). In this reach, the artesian levels in the Lower Pennine Coal Measures (98 m AOD, Figure 10) and the Permian strata (90 m AOD, Figure 10) are very similar and the stream follows the boundary between the Raisby and Ford formations. A thin layer of Glacial Till overlies the bedrock. Groundwater discharge is more likely where the confining effect of the till is reduced where it thins against the rising bedrock.

The pathways that hydraulically connect the mine workings and the aquifer are thought to be both direct contact (point sources) of mine entries (shafts and adits), boreholes and/or underground workings within the Permian aquifer and indirect connections (diffuse) between the mine workings and the aquifer, where flow is controlled by either natural or induced permeability (White Young

Green, 2006). These connections are controlled by the depth and type of mine workings, their proximity to the Permian Aquifer, the permeability, both natural and induced, of the strata separating the mine workings from the aquifer and the permeability of the aquifer in the area of the potential flow.

White Young Green (2006) estimated that the volume of mine water flowing out of the coal workings to the aquifer in the Chilton/ Eldon blocks is 57 L/s comprising 38 L/s from the Coal Measures and 19 L/s from the Permian strata. The volume of this water entering Rushyford Beck and Woodham Burn was not known at the time of writing.

3.2.5.2 AQUIFER –RIVER INTERACTION

The conceptual model developed for the Woodham Burn area from the EA Northumbria River Basin District Investigation (2012), and further considered in this study, distinguishes two sub-catchments: the upstream "Woodham Burn from Source to Rushyford Beck", where the stream from its source to the eastern part of the catchment flows over areas of thin drift (Glacial Till), generally less than 5 m thick, and the downstream "Woodham Burn from Rushyford Beck to Skerne" underlain by thick drift deposits. The thickness of the confining cover (Glacial Till) over the bedrock (Ford formation) is reflected on the groundwater–surface water interaction that could occur along these sections, with greater potential for groundwater–surface water connectivity along the upper reaches of the Woodham Burn before the confluence with the Rushyford Beck. Cairney (1972) and Carney and Hamill (1977) indeed indicated this area (the western part of the Skerne catchment) as the Magnesian Limestone aquifer's recharge zone.

Within the upstream "Woodham Burn from Source to Rushyford Beck" waterbody, data from the EA Northumbria River Basin District Investigation (2012) reported the groundwater levels recorded at Aycliffe borehole ~3 m below the stream bed, suggesting that groundwater was not currently supporting flows within the watercourse at that point. Due to the presence of the thin drift across the waterbody, flows may be lost to ground. Groundwater levels further to the south are known to be artesian which indicates that the Woodham Burn may gain base flow from groundwater at the downstream extent of the waterbody. Downstream of the confluence with Rushyford Beck, thick superficial deposits (10-30 m), are thought to underlie the "Woodham Burn from Rushyford Beck to Skerne" waterbody, limiting groundwater–surface water connectivity. In this area, groundwater level data recorded at Low Copelaw shows water levels to be depressed, currently lying at 74.6 m AOD which is over 17 m below ground level.

The conceptual ground model for the Woodham Burn area is shown in Figure 11. The extract from the Coal Authority Interactive Viewer (Figure 10) shows the potential for mine-related groundwater to enter the upper reaches of the Woodham Burn, as described above.

Discrete groundwater inflows were detected by the hyporheic zone monitoring during Phase 1.

In this study monitoring of the Woodham Burn was focused on the downstream stretch: "Woodham Burn from Source to Rushyford Beck". Whilst confined flow paths could develop within stratified Alluvium at any of the sampling positions, providing that it is of sufficient thickness, it is considered most likely that the inflows are sourced from the Permian bedrock in locations where the confining effect of the Glacial Till is reduced (see section 3.2.2). As the thickness of the Glacial Till increases, a greater proportion of the stream baseflow will be derived from the Glacial Till. At the confluence with the Rushyford Beck the stream course is influenced by the presence of the lacustrine deposits. The raised bog associated with these deposits potentially constitutes a source of low-pH base-flow from the lacustrine deposits, as the confining effect of the thicker Glacial Till deposits precludes groundwater discharge. It is plausible that the base-flow enters the stream by more permeable laminae within the lacustrine sequence with additional storage in the Alluvium. In the lacustrine deposits, some of the flow paths are likely to be confined by overlying, lower permeability laminae and the head would be controlled by the local topography. Depending on the detail of the topography, there is also a potential for subsurface connectivity via the superficial deposits with the River Skerne.
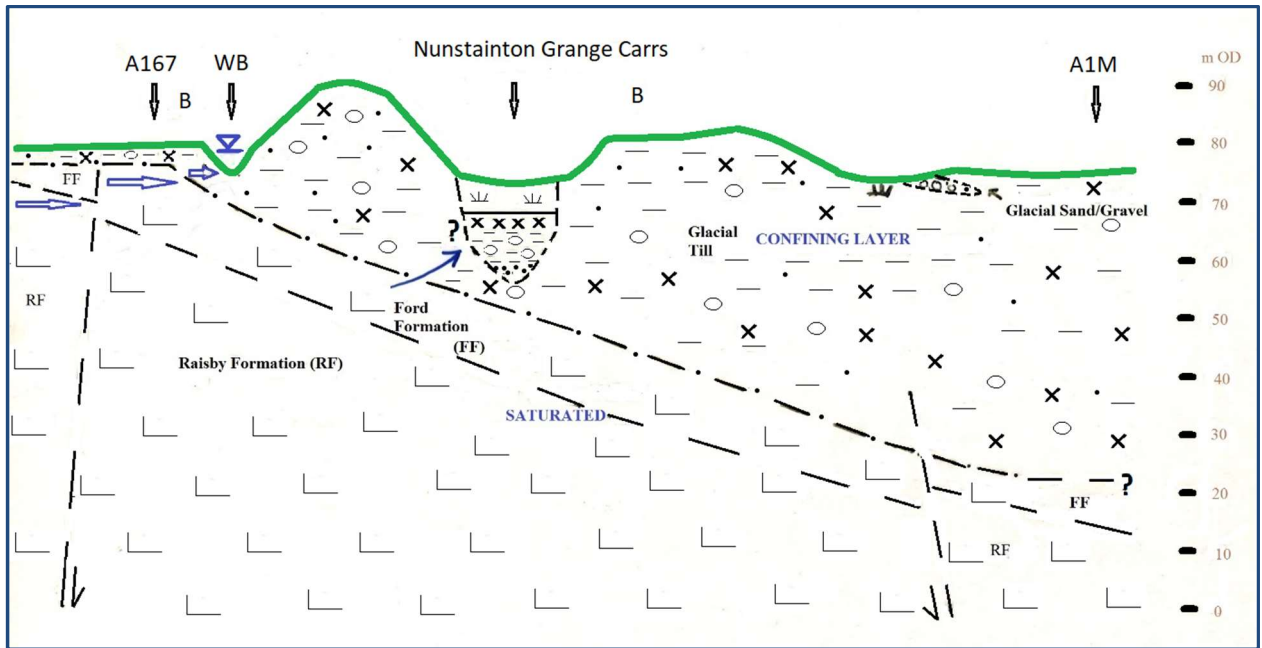
Figure 11 Conceptual ground model. Ground surface shown in green; faults based on bedrock exposure, borehole logs, stream morphologies; Fault dips interpreted based on Kurtas and Younger (2013). Potential flow paths indicated with Blue arrows; vertical exaggeration 16. ▽ Mine water level, indicating the recharge to Woodham Burn is plausible. For conceptualisation, the Mordon Carr stratigraphy (cf 3.1.2 Geology) is projected on to Figure 11 as indicative of the conditions associated with Nunstainton Grange Carrs, because there were no representative borehole logs available in this area. It is plausible that these areas have been deepened by sub-surface dissolution.

3.2.6 Uncertainty

One of the conclusions of the first phase of investigation (Palumbo-Roe et al. 2019) was that further sampling would be necessary to confirm these patterns and characterise the groundwater. This forms the focus of the current report.

There were a number of remnant uncertainties relating to the source of the very high SO_4 in surface water. A range of potential geological sources (gypsum, pyrite oxidation in the bedrock, till, pyrite in the lacustrine deposits) or additional sources, e.g. agricultural applications, agricultural lime, or colliery waste in superficial deposits (proximity of the colliery workings) were considered worthy of further consideration. The detail of the recharge flow paths and the groundwater monitoring borehole response zones are not known.

4 Methods

4.1 MONITORING PLAN

Developing an understanding of surface water–-groundwater interaction is complex and challenging, due to the interplay of multiple factors: geomorphic, hydrologic and hydrogeologic; multiple scales of interaction: basin, reach, channel unit, channel sub-unit, and particle scales, and the high spatial and temporal variability. The range of tools available to investigate surface water–groundwater connectivity, includes: hydrographic analysis, hydrogeological mapping, seepage measurements, and tracer studies, to cite a few (Brodie et al. 2007). The approach in this study was field-based monitoring with further data analysis to test the conceptual understanding and uncertainty identified in the previous phase of work in the catchment.

Specific objectives of the monitoring programme were:

- To measure hydraulic and chemical concentration gradients across the hyporheic zone of the Woodham Burn, using multilevel minipiezometers installed in the streambed, complemented by the analysis of within-reach changes of surface water chemistry.
- To analyse synoptic (between April 2018 and February 2019) variations in surface and pore water chemistry, while continuous piezometric measurements of hydraulic head and temperature were taken for a 47 day period in June / July 2018.
- To analyse spatial variations within a c. 500 m reach of the Woodham Burn instrumented at five locations.
- To carry out an additional hydrochemical survey of springs and field drainage pipes in the immediate surroundings of the study area to gain a broader perspective on groundwater discharge types.
- To sample and analyse groundwater, in the BGS laboratories, from a number of Environmental Agency monitoring boreholes on the Magnesian Limestone to complement historical Environment Agency data.

Figure 12 summarises the monitoring and sampling locations described in details in the following sections.
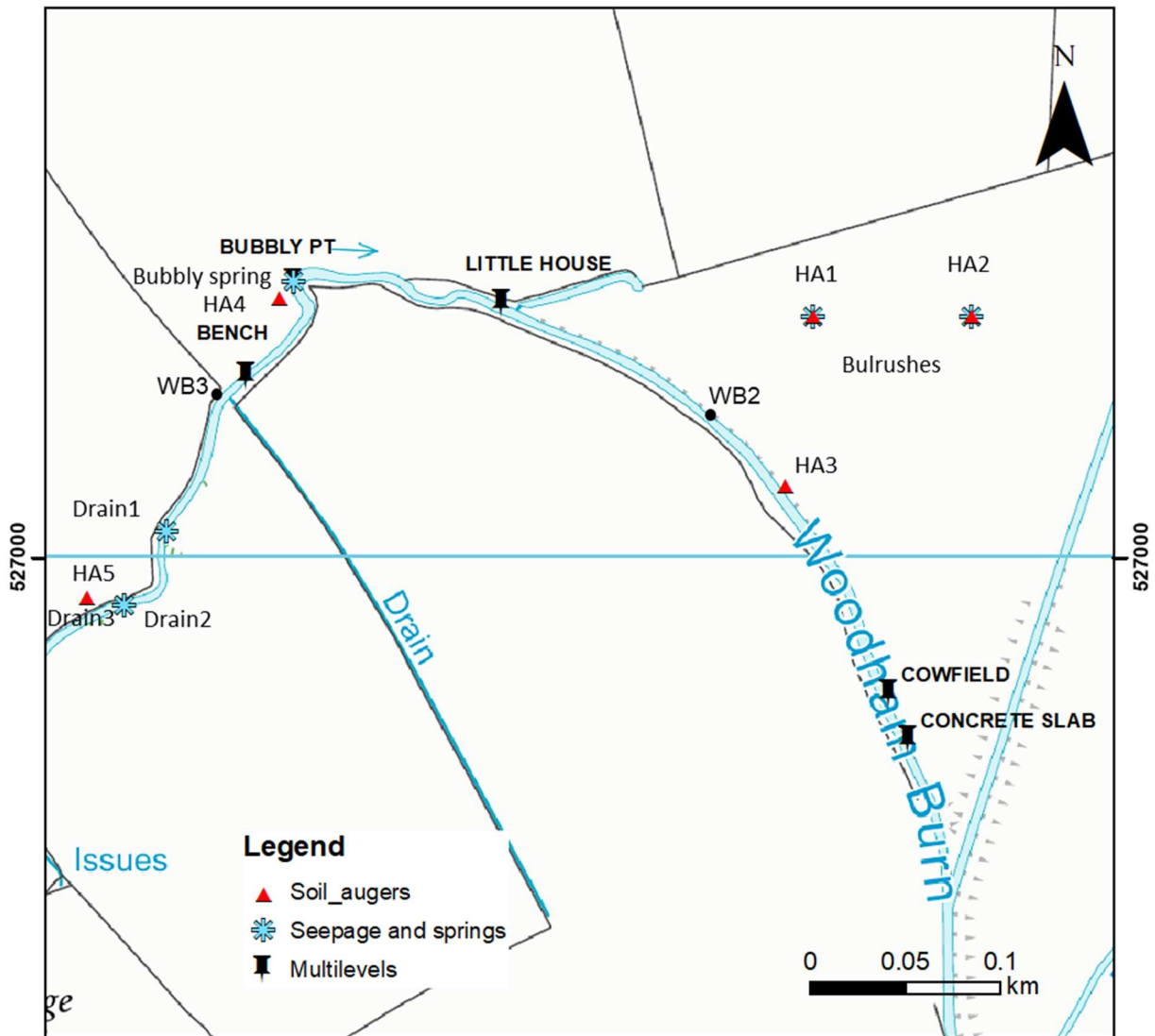
Figure 12 Monitoring and sampling locations in Woodham Burn. Contains Ordnance Survey data © Crown Copyright and database rights 2020. Licence no. 100021290.

4.2 RAINFALL, RIVER LEVEL, AND GROUNDWATER LEVEL DATA COLLECTION

The hyporheic zone sampling took place on three occasions: 25-26 April 2018, 01 August 2018, and 5-6 February 2019.

The data presented in Figure 13 comprise daily precipitation from the EA monitoring station Harpington Hill Farm at 433631 526654, and average daily river water levels from the EA monitoring station Preston-Le-Skerne at 429196 523796 throughout the period covering the sampling events. Groundwater levels at Low Copelaw Borehole for the same period with antecedent data from seven days before the first sampling are also included. Figure 14, Figure 15, and Figure 16 show the same data focussing on each sampling event and including the 7 days antecedent to the sampling.

17
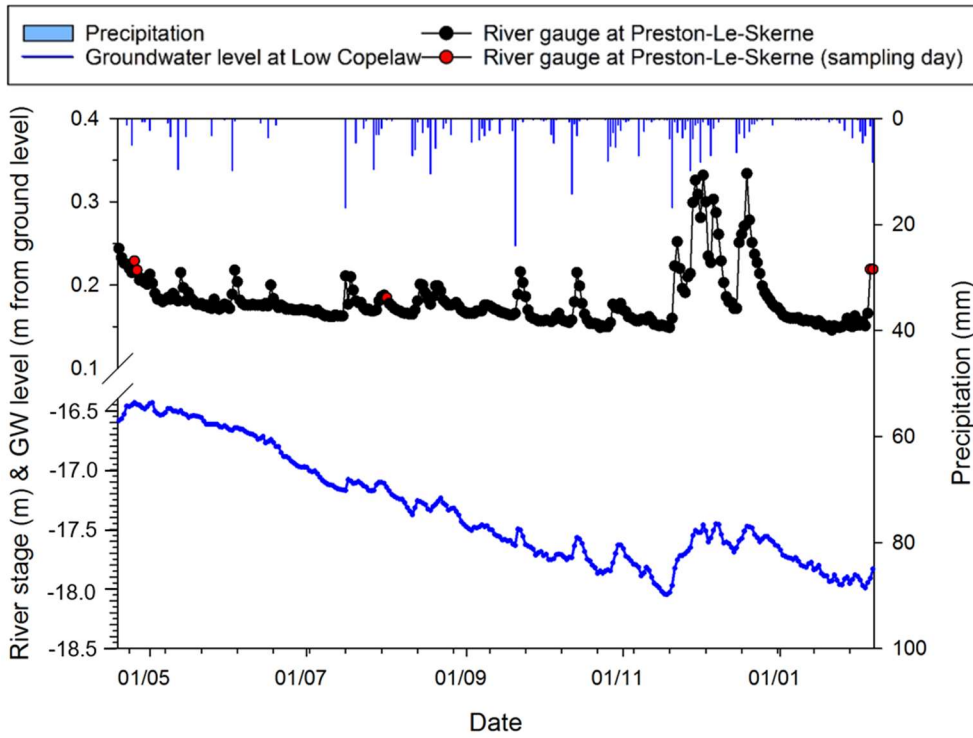
Figure 13 Water levels at Preston-Le-Skerne monitoring station from 18 April 2018 to 6 February 2019. Red dots indicate the days on which sampling took place. Secondary y-axis: daily precipitation data from the EA monitoring station Harpington Hill Farm at 433631 526654. Additional left y-axis: groundwater levels at Low Copelaw borehole.
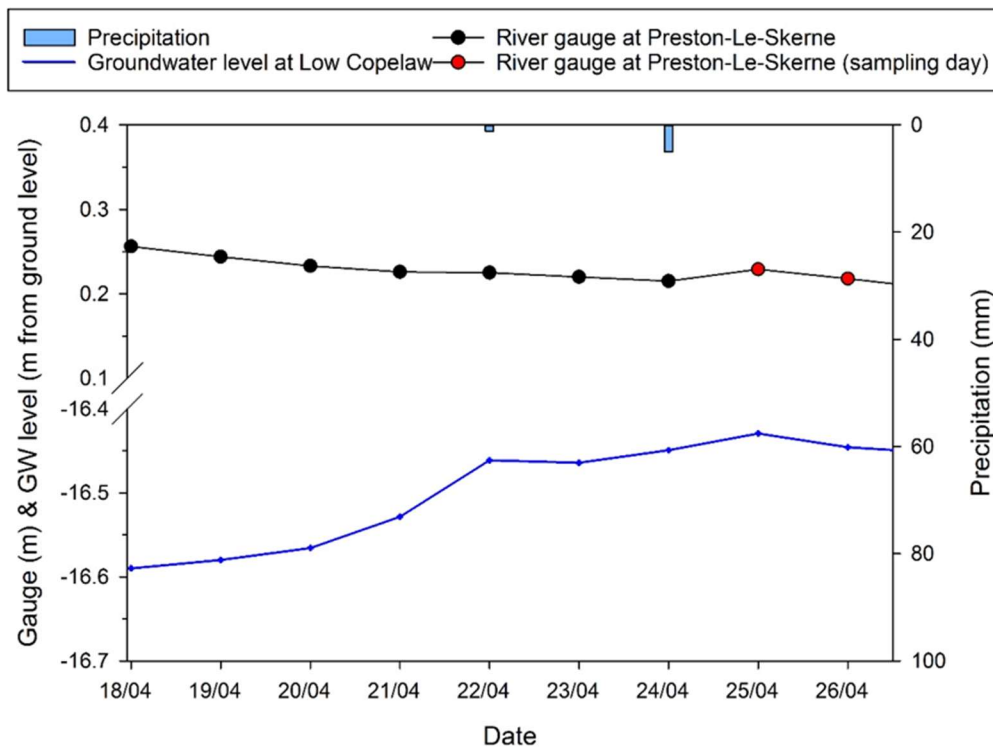
Figure 14 Water levels at Preston-Le-Skerne monitoring station, daily precipitation data from the EA monitoring station Harpington Hill Farm and groundwater levels at Low Copelaw Borehole during the sampling event in April 2018 and for the 7 days before.
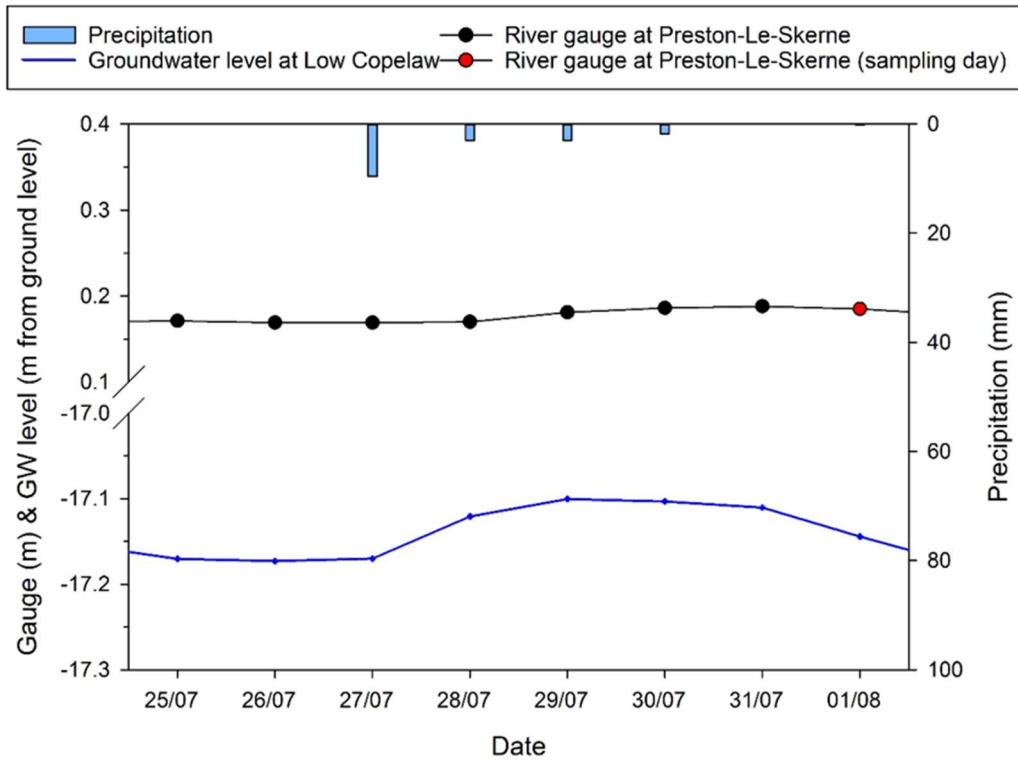
Figure 15 Water levels at Preston-Le-Skerne monitoring station, daily precipitation data from the EA monitoring station Harpington Hill Farm and groundwater levels at Low Copelaw borehole during the sampling event in August 2018 and for the 7 days before.
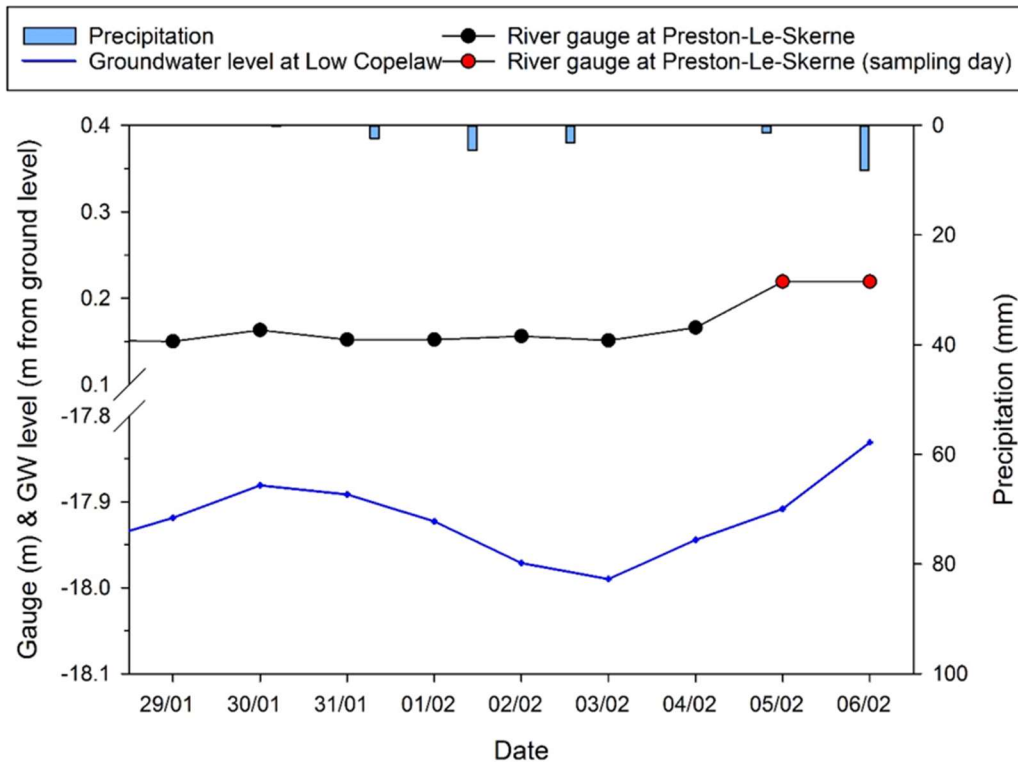
Figure 16 Water levels at Preston-Le-Skerne monitoring station, daily precipitation data from the EA monitoring station Harpington Hill Farm and groundwater levels at Low Copelaw Borehole during the sampling event in February 2019 and for the 7 days before.

4.3 CONDUCTIVITY AND TEMPERATURE SURVEY

Vertical temperature profiling of the riverbed and a longitudinal survey of specific electrical conductivity (SEC) variation in the surface water were used to detect stream locations with potential groundwater inflow, and to inform the site selection for the monitoring sites in this study. In addition to supporting the site selection, the high resolution longitudinal stream synoptic SEC measurements have been used to complement the surface water quality survey using spot sampling and chemical analysis.

Temperature profiles of riverbed sediment can be an informative tool to detect potential groundwater inflows into surface water during periods with distinct differences between surface water and groundwater temperatures (House et al. 2015). Using a hand-held temperature lance, this method can be applied as a quick and low-cost survey. Main restrictions of the applicability of this method are cobbly river sections, in which the lance cannot penetrate, and sections that are too deep or have too much flow to allow for safe access. Likewise, monitoring SEC is a simple, low-cost sensing technique allowing for high-resolution measurements. The method is most accurate when the tracer concentration in groundwater is clearly distinct from that in the river (Cook, 2013).

In this study, a combined temperature and SEC survey of the Woodham Burn was carried out on 23 April 2018 from 16:00 to 20:00 h (measurement points 1–70), and on 24 April 2018 from 12:00 to 13:00 to cover additional measurements (point 70–80). The temperature survey was conducted using a handheld thermocouple thermometer (Hanna Instruments) connected to an Oakton™ Type T thermocouple probe with a temperature accuracy of ± 0.8%. Measurements were taken at depths of 10–60 cm in 10 cm intervals where possible (restrictions occurred to high water level and/or rocky underground) at a total of 80 locations that were recorded using a handheld GPS. Distances between locations were planned to be 5 m, but needed occasional adjustment due to unsuitable ground conditions or inaccessibility of the specific locations. The resultant distances between points were approximately between 5–15 m. Measurements of specific electrical conductivity (SEC) and temperature of surface water at about 10 cm height above the river bottom were taken at each point of the sediment temperature measurement, using a multimeter probe. Specific care was taken to record the multimeter readings in the surface water before inserting the temperature lance into the sediment, which could have increased SEC readings caused by disturbed sediment. Likewise, to avoid disturbing sediment before measurement, the survey was conducted from downstream, to upstream.

4.4 MINIPIEZOMETER INSTALLATION

The spatial variation of the shallow hyporheic zone was addressed by sampling the stream reach with a network of multilevel minipiezometers in order to resolve vertical porewater chemistry differences across the stream section. The hyporheic zone multilevel minipiezometer designs adopted in this study are based on those described by Rivett et al. (2008). The hyporheic zone multilevel samplers comprise a 12 mm ID, 16 mm OD, 1200 to 1800 mm long, HDPE tube, fitted at one end with a machined, stainless steel drive-point that assists penetration of the device into sediments. Four discrete, depth sampling ports were installed around the central stock of the hyporheic zone multilevel sampler, comprising a Teflon tube (1.6 mm ID, 3.2 mm OD) measuring ~200 mm in length that was fitted at one end with nylon mesh screen (e.g. 45 μm mesh size) to prevent blockages due to sediment ingress. The sampling ports were installed at 10 cm intervals and marked at the top end of the Teflon tubes with different colour tape according to this scheme: yellow = 3 mm from datum (top of metal bolt of the stainless steel drive-point); green = 100 mm from datum; red = 200 mm from datum; black = 300 mm from datum.

To install the minipiezometer into the hyporheic zone, the device was inserted into a 1500 or 2000 mm long, metal drive tube (29 mm ID, 31.5 mm OD), leaving the 36 mm diameter drive-point protruding from the pipe end. During installation, the drive tube rests on the lip of the widest part of the drive-point cone. In order to drive the sampler into the hyporheic zone, a sledge hammer was used to apply force to a metal cap placed on the top of the drive tube. The metal cap was designed to limit metal fatigue and deformation. The samplers were driven into the hyporheic zone to a fixed depth of 90 cm below the riverbed. The drive tube was then removed.

Five locations were chosen for the installation of the multilevel minipiezometers. Site names and coordinates are reported in Table 2. Piezometer locations are prefixed by: Be for *Bench*, BP for *Bubbly Point*, LH for *Little House*, CF for *Cowfield*, and CS for *Concrete Slab*. The minipiezometers at each location were given the suffixes 1 (the piezometer closer to the northern stream bank) through 3 (further away from the northern bank). Depths intervals for each minipiezometer were further indicated as: _B (for black = 10 cm sediment depth), _R (for red = 20 cm sediment depth), _G (for green = 50 cm sediment depth), _Y (for yellow = 90 cm sediment depth). A total of 12 multilevel piezometers were installed: two at each site except for sites Be and LH (Table 2).

Table 2 Overview of installed multilevel piezometers.

Site	Multilevel Piezometers	Superficial deposits	Comments	Easting	Northing
Be	Be_HZ 01 Be_HZ 02 Be_HZ 03	Alluvium	Near WB3 – upstream drain Point 69 of T survey	429147	527096
BP	BP_HZ 01 BP_HZ 02	Alluvium	Point 63 of T survey	429172	527145
LH	LH_HZ 01 LH_HZ 02 LH_HZ 03	Alluvium	Point 53/54 of T survey	429281	527134
CF	CF_HZ 01 CF_HZ 02	Lacustrine Deposits	Point 16 of T survey	429485	526929
CS	CS_HZ 01 CS_HZ 02	Lacustrine Deposits	Point 10/11 of T survey	429495	526905

*At each site the multilevel number 1 indicate the piezometer closer to the stream bank.
* T survey = Temperature survey

4.5 PIEZOMETER DESIGN AND INSTALLATION

Observations of temperature and river level fluctuations versus temperature and hydraulic head in groundwater below the streambed can provide valuable information about the flow directions and potential interchange between the two zones. For example, a groundwater hydraulic head that exceeds river water levels indicates a gaining stream. Vice versa, a lower hydraulic head of groundwater than of the river water level indicates a losing stream. Thus piezometric measurements of the surface water and groundwater at different depths were taken at Woodhan Burn to determine whether or not groundwater is discharging to the Skerne via the Woodham Burn, and to inform analysis of the spatial and temporal variability of the subsurface recharge.

The installed observation points consisted of 25 mm ID, 33 mm OD diameter solid UPVC tubing with a 20 cm slotted (1 mm slots) screen on the bottom. A textile filter was fixed on the outside of the screen to protect against sediment ingress into the piezometers. A total of 8 piezometers (2 at Be, 1 at BP, 3 at LH, and 2 at CS) were installed on 24 May 2018. At all locations except BP, two paired piezometers of shallow (0.4 m) and deeper (1.4 m) depth were used. At BP, only a shallow piezometer was installed because a) the number of data loggers was limited to 8, and b) the more difficult access at this site would have made it too risky to handle heavy equipment in the stream, precluding installation of the deeper piezometer. An additional piezometer for the monitoring of surface water was installed at LH.

All shallow piezometers ("*location name*-S") were installed roughly in the centre of the riverbed and to a total depth of 0.4 m below the riverbed. The screened area of the piezometers was from 0.2 to 0.4 m. The deeper piezometers ("*location name*-D") intruded into the riverbed by 1.4 m and were screened at 1.2 to 1.4 m depth. Installation of the shallow piezometers comprised pushing the piezometer (which has a seal on the bottom) into the riverbed and, where needed, hammering it to the desired depth using a manual hammer. For the installation of the deep piezometers, a handheld percussion drill (Figure 17) was used to drive a metal outer pipe, with a metal drive point on the bottom, to the desired depth in the stream bed. The piezometer was then inserted into the outer tube, and the outer pipe was extracted using a manual lever system, which was powered by two people. A third person ensured that the piezometers stayed in place by pushing down on it from the top. The drive point was designed with a sacrificial cone that remained in the sediment.

Figure 17 Using the jackhammer for installation. A small podium was used in the river to ensure safe footing while handling (left). Lever-system (levers on not attached yet) to extract the outer metal pipe (right).

All piezometers were installed about 0.5 – 1.0 m downstream of multilevel samplers to avoid multilevel sample contamination by potential dissolution of metals from the sacrificial cone. The sediment was expected to collapse against the piezometer after extraction of the outer pipe, thereby avoiding a direct connection between the stream water and the bottom of the piezometer. Based on visual impressions, this seemed to be the case at all installation points.

At each site, automated pressure transducers were installed that were set to monitor pressure changes at 15-minute intervals. A list of the installed instruments is given in Table 3. An additional logger for measuring atmospheric pressure was added to one of the points.

Three different types of loggers were used:

1) Winsitu TROLLS (including BARO TROLL): These loggers are installed by attaching a Kevlar® string, and submersing them into the water. The TROLLS are not vented, i.e. they record total pressure and subtraction of atmospheric pressure (recorded by the BARO TROLL) is a required step in the data processing. The TROLL can easily be attached within the piezometer via Kevlar® string, which allows the piezometer to be capped with a normal cap. The BARO TROLL is installed in the same way, but kept well above the water column, as its function is to measure the changes in atmospheric pressure.

2) Solinst loggers: These loggers are installed in the same way as the TROLLS.

3) AQUATROLLS: All AQUATROLL loggers are vented by means of a thicker (about 4 mm) cable that is attached to the logger. It is crucial that no water/humidity enters the cable. Therefore, a desiccation unit is attached to the top end of the cable. When installing these loggers, the desiccation unit needs to a) be fixed well above the water level, and b) be protected from rainfall events by a larger cap that is installed on top of the desiccation unit Figure 18).
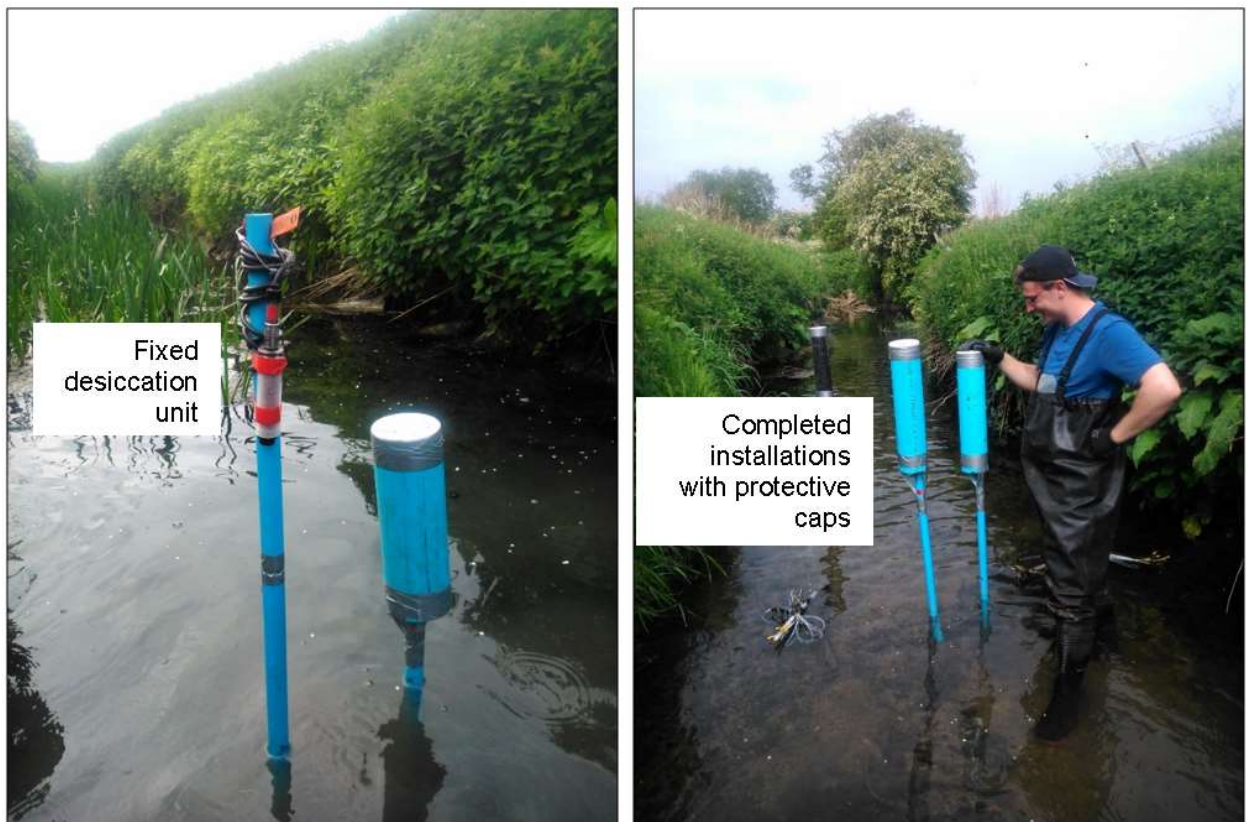
Figure 18 Installation of vented loggers (AQUATROLLS).

Table 3 List of installed loggers including location, type of logger, and recorded parameters.

Location	Type of logger	Logged parameters
Be – S	Winsitu TROLL	T, pressure, depth
Be – D	Solinst logger	T, pressure, depth
BP-S	Winsitu BARO TROLL	T, pressure, depth
	Solinst logger	T, pressure, depth
LH – SW	AQUATROLL 200	T, pressure, depth, SEC
LH – S	AQUTROLL 500	T, pressure, depth
LH – D	AQUATROLL 200	T, pressure, depth, SEC
CS – S	AQUTROLL 500	T, pressure, depth
CS – D	AQUTROLL 500	T, pressure, depth

Notes: All loggers are set to log at 15-minute intervals.
Loggers at Be and BP were started on 24 May at 16:00 hrs.
Loggers at LH and CS were started on 31 May at 16:00 hrs.

4.6 SOIL SAMPLING

Table 4 shows sampling locations and description of the soil samples collected around the burn (Figure 12) using a hand-held auger on the 18 July 2018.

Table 4 Soil survey at Woodham Burn.

SAMPLE	NRG		DESCRIPTION	COMMENTS
Bullrushes 1 HA1	NZ 27127	29528	HA1: 0.00-0.35 m Water and sludge with pond weed; 0.35 – 0.60 m Stiff dark grey to black, organic, very plastic CLAY.	Elevation 75 m OD
Bullrushes 2 HA2	NZ 27127	29445	HA2: 0.00-0.25 m Water and sludge with pond weed, more sedge associated than at the previous location; 0.25 – 0.60 m Soft to firm dark grey to black, organic, very plastic CLAY with some fine roots (1-2 mm diameter).	Elevation 76m OD
HA3 0.00 – 0.30 m	NZ 27038	29430	HA3: 0.00 – 0.40 m Light brown humic clayey silt TOPSOIL with some roots and rootlets (sampled 0.3-0.40 m);	Site adjacent to Woodham Burn; Elevation 77 m OD
HA3 0.30 – 0.73 m	NZ 27038	29430	0.40 – 0.73 m Light brown very silty humic CLAY	
HA3 0.73 – 0.80 m	NZ 27038	29430	0.73 – 0.80 m Stiff mottled greyish brown silty CLAY	
HA3 0.80 – 1.05 m	NZ 27038	29430	0.80 – 1.05 m Firm laminated grey and orange brown very silty CLAY, becoming slightly sandy with depth	
HA3 1.05 – 2.03 m	NZ 27038	29430	1.05 – 2.03 m As above but no lamination and a marginally increasing sand content.	
HA4 0.00 – 0.35 m	NZ 27136	29164	0.00 – 0.35 m greyish brown organic clayey silt/ silty clay TOPSOIL with occasional fragments of limestone, brick etc. becoming more clayey and stiffer with depth	HA4 near the outside of the meander where the spring was located on a previous visit and at the northern end of the ploughed zone (dredged arisings containing fragments of dolomitised limestone, brick and sheet asbestos). Spring still bubbling. Elevation 73 m OD
HA4 0.35 – 0.75 m	NZ 27136	29164	0.35 – 1.35 m Dark brown silty CLAY with occasional clasts of limestone, becoming slightly sandy with depth	
HA4 0.70 – 1.35 m	NZ 27136	29164		
HA4 1.35 – 1.65 m	NZ 27136	29164	Water strike at 1.45 m and hole complete at 1.65 m.	
HA5 0.00 – 0.70 m	NZ 26979	29063	HA5: 0.00 – 0.70 m Firm crumb structure greyish brown organic silty clay TOPSOIL becoming lighter brown firm clay with depth	Hand auger hole sited near to bank seepage previously observed and present at the time of sampling on the opposite bank. Elevation 69.5 m OD. Here in an open area of grass, thistles and dock leaves 5 m NW of a mayflower tree and approximately 10 m east of the overhead cables.
HA5 0.70 – 1.05 m	NZ 26980	29063	0.70 – 1.55 m Soft to firm grey and dark grey organic CLAY; As above, but becoming increasingly organic and peaty	
HA5 1.05 – 1.75 m	NZ 26981	29063	1.55 – 1.75 Soft to firm grey and dark grey peaty CLAY becoming reddish brown fibrous PEAT. Water strike at 1.05 and hole complete at 1.75m.	
Ploughed field at Be site			Firm dry brown pods collected at surface (0-0.10 m) formed during prolonged dry period - possibility of been washed out by intense rainfall the night before sampling	

4.6.1 Water-soluble fraction

In the laboratory, soil samples were air-dried and subject to 1/10 solid to liquid ratio leaching by deionised water to extract the water soluble fraction. 25 g of soil in 250 ml Millipore water were shaken in an orbital shaker for 10 minutes at 200 rpm and room temperature of 24 °C. The suspension was centrifuged at 8000 rpm for 15 minutes and the supernatant filtered through a 0.45 µm filter. The obtained solution was analysed for the anion concentrations using ion chromatography at the BGS lab facility.

4.7 POREWATER SAMPLE COLLECTION

Porewater samples were collected using the multilevel samplers. Porewaters were drawn from the Teflon tubes directly into either 250 ml DURAN® glass bottles where a vacuum was created using a hand vacuum pump or into 60 ml syringes. The maximum pressure applied via vacuum pump was -60 kPa. The sample tubes were purged before sampling by collecting and discarding 3 times the volume of water present in the sample tube.

The porewaters extracted from each minipiezometer and the surface waters were analysed in the field for DO, SEC, Eh (field measurement corrected to the standard hydrogen electrode, SHE), and temperature immediately after collection and avoiding contact with air for the DO measurements. Samples for major- and trace-element analysis, and alkalinity were filtered through 0.45 µm filters and collected in plastic 60 ml bottles. The aliquots for cation and trace elements were acidified to 1% v/v HNO_3 immediately. For Fe(II) analysis, 15 ml of the filtrate was added to 1.5 ml of a pre-made reagent containing the colour-forming agent 2,2' dipyridyl and analysed by colorimetric analysis at the BGS laboratory.

4.8 SURFACE-WATER SAMPLE COLLECTION

The primary focus of the surface-water sampling was to compare the hyporheic zone composition to the overlying surface water, and therefore the surface-water sampling was carried out simultaneously with the hyporheic-zone sampling. The sampling strategy resulted, at least on one occasion (February 2019), in the surface water sampling been carried out across two consecutive sampling days.

This is considered in the analysis of the spatial downstream compositional variation along the study stretch (section 5.4). Applications included solute mass balance methods to estimate instream gain, loss of solutes assumes steady state conditions in the river. In practice, this is rarely possible, but the assumption of steady-state conditions will be reasonable, provided that river chemistry and flow do not change significantly over the period of time required to collect the river chemistry samples or the period of time for water to flow from the most upstream to the most downstream site (whichever is greater) (Cook 2013). The potential influence of rainfall and resulting stream discharge variation from one day to the other, or one period to another, on surface water composition in this study is considered by referring to rainfall data and discharge for the sampling period when analysing the spatial variation in elemental compositions along the study reach. On this basis, for the third sampling round the last two points CF and CS cannot be integrated with the three upstream in the interpretation of the longitudinal solute changes.

Table 5 Water sampling dates.

Site	Point	Round 1 Sampling date	Round 2 Sampling date	Round 3 Sampling date
Be	1	26/04/2018	1/08/2018	6/02/2019
BP	2	25/04/2018	1/08/2018	6/02/2019
LH	3	26/04/2018	1/08/2018	6/02/2019
CF	4	26/04/2018	1/08/2018	5/02/2019
CS	5	26/04/2018	1/08/2018	5/02/2019

At each minipiezometer point, a sample of the surface water, taken from approx. 20–30 cm below surface level, at the time of the hyporheic zone porewater sampling, using a 600 ml TELESCOOP (In-Situ) sampling container attached to a telescopic sampling system, which allowed for sampling from the riverbank (and thus minimum disturbance of the bed sediment while sampling). Field measurements and sample preservation were carried out as per porewater samples (section 4.7).

4.9   SEEPAGE AND SPRINGS SAMPLE

During each of the porewater sampling rounds, the upwelling water at BP was sampled from the northern bank.

On 24 April 2018 two field drain pipes discharging water into the burn immediately upstream of the monitored reach of the burn, i.e. upstream of the Be location, were sampled. An area of stream bank seepage, also upstream of our study reach, was observed and sampled on the same occasion (Table 5). On 18 July 2018 a waterlogged area at the boundary between the alluvium and the lacustrine deposits, identifiable by the presence of bulrushes, was also sampled.

4.10   LABORATORY ANALYSIS

Alkalinity was determined by titrating 25 ml filtered water sample against 1.6 N H_2SO_4, using a bromocresol green indicator solution.

Determination of Cl, SO_4 and fluoride (F) was by ion chromatography and major and trace elements were determined by inductively-coupled plasma mass spectrometry (ICP-MS), with independent QC checks providing 96 +/- 3% accuracy (in-house QC solution) and 98 +/- 4% accuracy (NIST SRM 1643e). The Non Purgeable Organic Carbon (NPOC) content was determined using a Shimadzu TOC-V CPH analyser with an associated ASI-V auto-sampler. All analyses were carried out at the in-house BGS laboratory in Keyworth, UK.

The 2,2' dipyridyl-preserved water samples were analysed for Fe(II) using colorimetric analysis. It was noted that many of the Fe(II) data are exceeding the total Fe; for total Fe > 1 mg/l, Fe(II) was on average 10% higher. The Fe(II) results may have been subject to unquantified interference from other elements during the analysis, which was not further explored. Given the associated uncertainty, the Fe(II) data are not reported in the tables in the Appendix. Nevertheless the Fe(II) analysis indicates the predominance of dissolved Fe(II) over Fe(III).

Concentrations of major and trace elements determined in procedural blanks were negligible when compared with the reported data.

5 Data Processing

5.1 HYDROCHEMICAL CHARACTERISATION

A range of visualisation techniques and statistical methods were used to explain the overall hydrochemical patterns in terms of water origin, sources and sinks for different elements and chemical reactions and processes.

5.2 STATISTICS

Using a multivariate approach, the main patterns in the chemical composition of surface water and porewater were explored using cluster analysis. One primary application of cluster analysis is to explore similarities between observations, and to thereby possibly detect signatures of discharges into the surface system. Hierarchical clustering was carried out on the analyses of the porewater, surface water and selected boreholes, springs and seepage waters based on the geochemical data set consisting of the following elements: Ca -Mg- Na- K- HCO_3- Cl- SO_4- F- Si- Ba- Sr- Mn- Fe- Li- Rb- U. The samples were clustered into four groups, using Euclidean distance and the Ward's Linkage method. The data were standardised to convert all variables to a common scale by subtracting the means and dividing by the standard deviation before the distance matrix was calculated, to minimise the effect of scale differences.

Welch's One-Way ANOVA, which assumes unequal variances, with multiple comparisons using the Games-Howell method, was used to test differences between means for each parameter across the sites or sampling events. Nonparametric analysis, such as the Kruskal-Wallis test was used to determine whether the medians of two or more groups differ, since in some cases sample size is very small and the median is more meaningful for the study.

5.3 SATURATION INDICES

The saturation indexes of selected mineral phases in water samples were calculated using PHREEQC version 3 and the phreeqc.dat database.

5.4 ESTIMATING GROUNDWATER DISCHARGE TO THE STREAM FROM STREAM CHEMISTRY

Using a simple stream water solute mass-balance, we estimated the importance of subsurface sources of solute to the stream and/or in-stream attenuation processes. The method assumes steady-state conditions and so can only be applied when river flows are stable (Cook 2013). The method will be most accurate when the groundwater composition is very distinct from that in the river. The major drainage ditches in the Woodham Burn study catchment were dry at the time of all sampling events, so it is reasonable to assume any increase of stream solute concentrations within the reach is due to subsurface contribution by i) advective exchange via groundwater discharges or ii) diffuse exchange where groundwater discharges were insignificant.

Based on a significant change of solute concentrations between two locations in Woodham Burn (Be and LH) the fraction of groundwater inflow was estimated using:

(1) $M_3 = M_1 + M_{GW}$, where the load M_3 of a (conservative) element downstream of the GW inflow must equal the load upstream (M_1) plus the load M_{GW} added by the inflow.

(2) $C_3 Q_3 = C_1 Q_1 + C_{GW} Q_{GW}$, as $M = C Q$, where C is the concentration and Q the discharge.

(3) $Q_3 = Q_1 + Q_{GW}$, where by flow balance, the discharge Q_3 must equal the discharge Q_1 plus the discharge Q_{GW} of the inflow.

By combining the two equations (2) and (3), the ratio Q_{GW}/Q_3 was calculated:

$C_3 Q_3 = C_1 (Q_3 - Q_{GW}) + C_{GW} Q_{GW}$;

$Q_{GW}/Q_3 = [(C_3 - C_1)/(C_{GW} - C_1)] \times 100$.

Discharge measurements were not carried out at the time of the water sampling, but, based on the solute concentrations upstream and downstream and the concentration of the grounder inflow

(measured at Bubbly spring), we could calculate the fraction of groundwater inflow in surface water at point 3: Q_{GW}/Q_3.

5.5 ESTIMATING GROUNDWATER DISCHARGE TO THE STREAM FROM SPATIOTEMPORAL POREWATER VARIATION

Areas of groundwater discharge are expected to be represented by narrower temporal variations in the porewater composition of the impacted piezometers. To assess this, the relative standard deviation RSD%, i.e. the percent standard deviation from the mean of the composition in the three sampling events, (standard deviation*100/mean), of the conservative elements chloride and lithium, were examined by depth for each piezometer, in order to infer potential areas of subsurface flow and hyporheic exchange flow.

5.6 ASSESSMENT OF HYPORHEIC EXCHANGE FLOW (HEF)

The chemical gradients in the hyporheic zone and, although limited, hydraulic and temperature gradients measured in piezometers installed across the stream channel allowed assessment of HEF (cycling of water between surface water and sediments), using both close-to-the-bank- and middle-channel positioned piezometers.

Characterisation of water pathways in the streambed, and delineation of the HEF when surface water mixes with porewater in the streambed can be carried out using chloride concentrations as a tracer. Assuming the conservative behaviour of chloride, the stream component in the hyporheic porewater is estimated from a two end-member mixing equation. Lithium, another element with a near-conservative behaviour, is used to confirm the results based on chloride.

A two end-member (surface water and deep porewater) mixing equation to delineate HEF is applicable only if the end-members have different concentration of the tracer chloride. To assess the differences in mean chloride concentrations across surface water and piezometer depths, and therefore to test the condition that the potential end-members surface water and deep porewater are significantly different, the Kruskal-Wallis Test was used. It was indeed verified that for all piezometers, except the ones at BP site, the median chloride concentrations in surface water and in the deep porewater at 90 cm sediment depth were significantly different ($p < 0.05$). The median chloride values were higher in surface water.

The following calculation was used for the characterisation of the hyporheic zone and subsurface hydrogeology of each site using chloride concentrations in a mixing model. The BP site was not considered further, after showing there was not a significant difference in the concentration means of chloride in surface water and the deep porewater.

Mixing scores (Lansdown et al. 2015) were derived as:

$(Cl_{[PW]} - Cl_{[SW]})/(Cl_{[SW]} - Cl_{[90cm]})$, such that porewater at 90 cm has a score "-1" and surface water has "0", respectively. Sediment depths with score values close to -1 indicate porewater very similar to the deep one suggesting that groundwater is either isolated from the stream or extremely well connected with dominance of upwelling porewater. Score values between -1 and 0 indicate the presence of a surface water component in the porewater, i.e. HEF.

Key assumptions underlying the two end-member mixing approach are that: the water in the hyporheic zone is from two sources, namely stream water and groundwater, and each source has a spatially and temporally uniform conservative signature. For scores > 0 and/or <-1 horizontal flow (either lateral or inputs from the riparian zone or longitudinal flow along the river channel) could be inferred. With a chloride concentration of the horizontal flow lower than the deep porewater scores are <-1, or with a chloride concentration of the horizontal flow higher than surface water scores are >0. However, if chloride concentrations of the horizontal flows are the same as surface water and upwelling groundwater, the horizontal flows would not be detectable with this method.

5.7 EVALUATION OF NATURAL ATTENUATION

Using chloride as a conservative tracer of mixing between surface water and groundwater, zones of hyporheic flow exchange (HEF) have been identified along with other zones of very limited or no mixing or later flow.

For the sites with observed HEF, it is possible to calculate the expected concentrations of other elements, such as nitrate or sulphate, should they behave conservatively like chloride, i.e. due to only mixing of surface water and groundwater, using equation (1) and (2). Further analysis, using equation (3), of the difference between the measured concentration and the expected one given a conservative behaviour, gives an indication of the degree of non-conservative behaviour for that constituent.

The discharge ratio Q_{SW}/Q_{GW} of surface water /groundwater in the porewater at each piezometer depth is calculated as:

(1) $Q_{SW}/Q_{GW} = (C_{PW}-C_{90cm})/(C_{SW}-C_{90cm})$, using the element concentration (C) in surface water (SW), porewater (PW) and groundwater (90 cm) (given that the porewater composition at 90 cm depth is chosen to represent groundwater composition),

and $(Q_{SW}/Q_{GW})_{[Cl]} = (Cl_{PW}-Cl_{90cm})/(Cl_{SW}-Cl_{90cm})$, using chloride as conservative tracer.

The Q_{SW}/Q_{GW} ratio based on Cl can then be substitute in the generic eq (1) to calculate any other element concentration expected if conservative behaviour ($C_{PW\,exp}$):

$(Q_{SW}/Q_{GW})_{[Cl]} = (C_{PW\,exp} -C_{90cm})/(C_{SW}-C_{90cm})$;

and rearranging gives:

(2) $C_{PW\,exp} = (Q_{SW}/Q_{GW})_{[Cl]} \times (C_{SW}-C_{90cm}) + C_{90cm}$.

Thus the indication of the degree of non-conservative behaviour for that constituent is given by:

(3) Difference = $C_{PW\,meas} - C_{PW\,exp}$, where ($C_{PW\,meas}$) is the measured concentration.

6 Results

6.1 CONDUCTIVITY AND TEMPERATURE SURVEY

The combined temperature and SEC survey at Woodham Burn was carried out on 23 April 2018 from 16:00 to 20:00 h (measurement points 1–70), and on 24 April 2018 from 12:00 to 13:00 (point 70–80, east to west). Time lags between measurements are expected to have an effect on surface water temperature due to the diurnal signal of ambient air temperature. However, this potentially distorting effect will be less predominant in the subsurface, particularly in areas of groundwater upwelling because of the more stable groundwater temperatures, which (in the UK) are typically at around 8–10 °C throughout the year.

Figure 19 shows the combined results of both survey days for SEC concentrations in the surface water (A), and surface and subsurface temperatures from the most upstream point (80) to the most downstream (point 1). SEC measurements range from about 1200 to 2000 µS/cm, with a very marked increase from 1290 µS/cm at point 62, to 2000 µS/cm at point 63 (Figure 19 A). Concentrations downstream of point 63 quickly drop to a lower level at around 1400 µS/cm, but remain elevated compared to the area upstream of point 63. This indicates a strong inflow of high-conductivity water into the burn at point 63, which is likely locally confined.
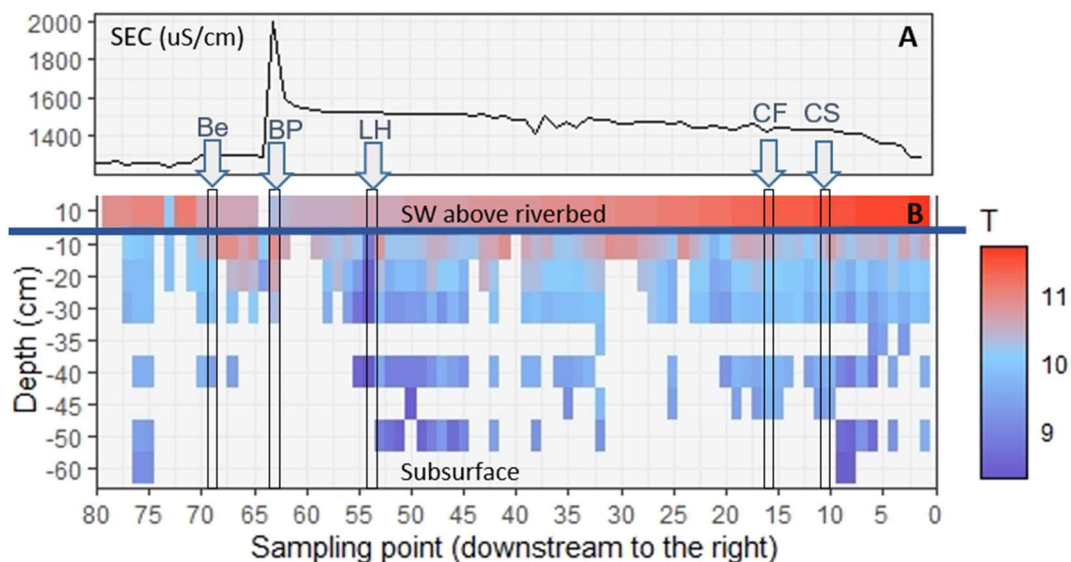
Figure 19 SEC concentrations in surface water (A), and temperature distribution at 10 cm above the riverbed, and at different depth intervals below the riverbed (B). The subsequently selected monitoring sites are indicated by arrows and below rectangles.

In terms of temperature (Figure 19 B), a trend of slightly increasing surface water temperatures from point 70 (measured at 20:00) to point 1 (measured four hours earlier) can be seen, which is likely caused by the gradual cooling of the surface water in the evening. For the same reason, temperatures at point 80–70 (taken the next day around 12:00) are generally slightly higher than those of the previous evening.

The overall temperature range was 8.3–11.7 °C, with the highest temperature occurring in surface water, and the lowest in the subsurface at point 54. The typically lower temperatures at depth indicate that groundwater temperature is around 8–9 °C (as expected), which is markedly cooler than the observed 10–11 °C in surface water. Thus, low temperatures close to the riverbed are likely indicative of upwelling groundwater, while temperatures >9 °C in the subsurface may indicate HEF and/or downwelling surface water. Figure 19 B shows that the most distinct area of low temperatures occurs around point 45—56 which has markedly lower temperatures at 30–40 cm depth (mostly between 8.3–9.4 °C) than other areas. The most distinct location is point 54

with a maximum of 8.8 °C at 10 cm depth, which is more similar to groundwater then to prevailing surface water temperatures, and thus indicative of an input of groundwater in this area. Though not precisely located at the same point, the more downstream transition in superficial deposits from alluvium to lacustrine deposits near point 35 (according to mapped change in geology, see Figure 2, and observed change in riverbed from sandy/silty to more gravelly/cobbly, see Appendix 1), could be in relation to the distinct flow behaviour in this section. Additional temperature measurements at depth between point 35–45 could have shed more light on this likely correlation, but were not possible to attain due to the firmness/too much gravel in the riverbed, through which the temperature lance could not penetrate.
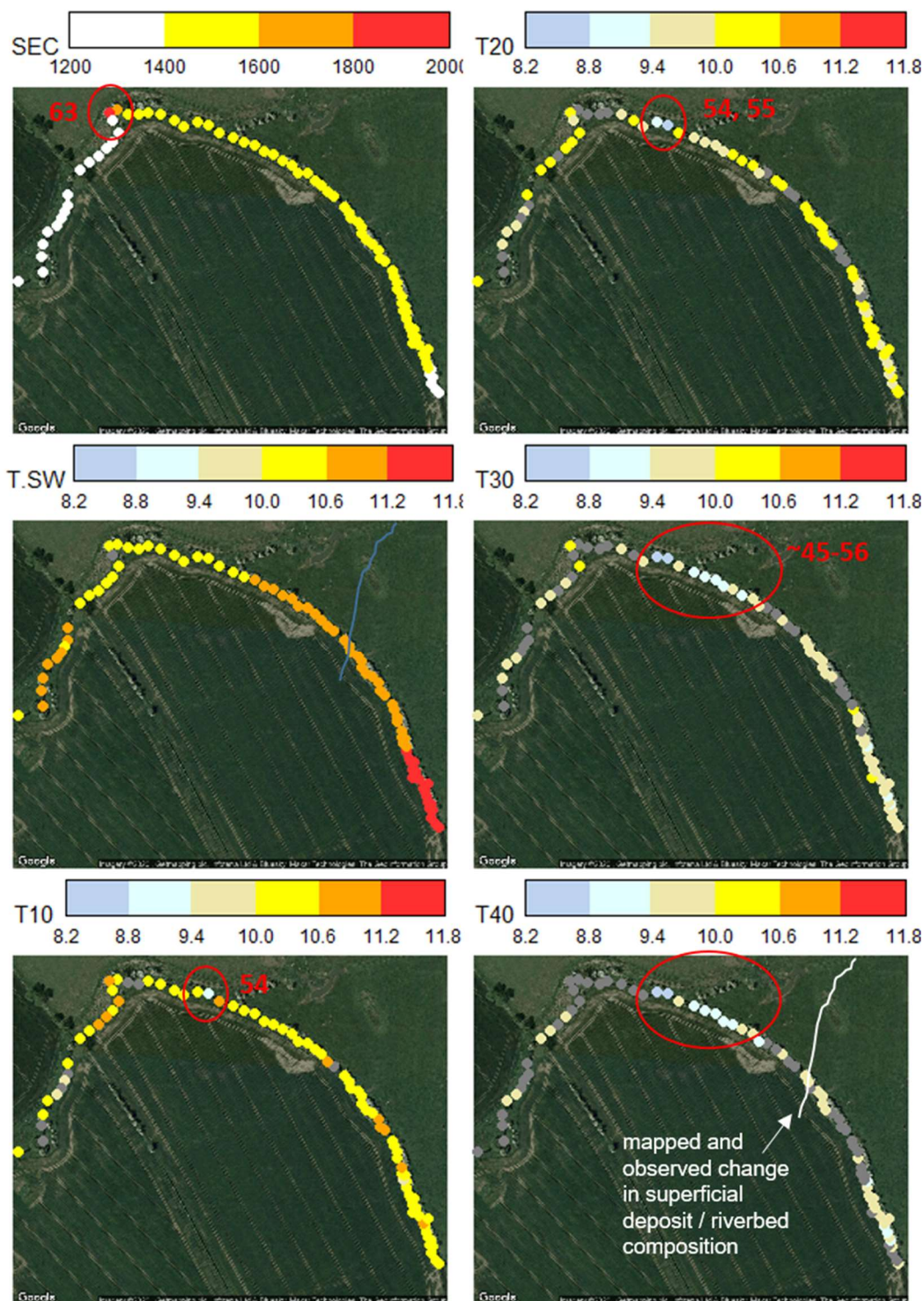
Figure 20 Plan view of SEC and temperature distribution (in surface water and at different depths (T10=10cm, T20=20cm, T30=30cm, T40=40cm) below the riverbed. Google maps imagery © 2020 Getmapping plc, Infoterra Ltd and Bluesky, Maxar technologies, The GeoInformation Group, Map data ©2020

Point 63 (marked up on the top-left plot in Figure 20), which is the point of high SEC measurement, did not show a strong drop in temperature with depth (10.6° C at 10 cm, and 10.3 °C at 20 cm depth, no penetration/measurement possible at higher depth), and adjacent sampling points showed similar values. Upwelling water into the riverbed could be visually observed nearby. It is likely that the upwelling water is coming through locally distinct pathways (thus not having much diffuse effect on nearby sediment) and/or that the upwelling water has a temperature close to that of the surface water.

In summary, the survey indicates 2 distinct areas of (potential) inflows into Woodham Burn:

1. A very localised inflow of high-conductivity water (2000 µS/cm, with an increase of 708 µS/cm from the nearest upstream measurement) at point 63. Temperature measurements at and near this location were limited due to gravel in the riverbed, but do not seem much lower than surface water temperatures (close to 10 °C).

2. A wider stretch of suspected groundwater inflow indicated by lower subsurface temperatures (8.3—9.4 °C) from about point 45-56, which coincides approximately with the area of change in superficial deposits. Contrary to point 63, there is no significant change in SEC. Thus, it can be concluded that the two recharge areas are unlikely to originate from the same source.

Based on the above, both locations were chosen as monitoring locations for hyporheic zone and water level/temperature monitoring as described in the following sections (sampling points BP at the point of high SEC and visually observed upwelling, and LH near point 54, correlating to the second area of interest. Note that installation directly at point 56 was not feasible due to accessibility restrictions for coming in with the more heavy installation equipment). Additional monitoring locations were chosen at point 69 (Be) to monitor upstream of point 63, and at two locations (between points 10/11 and at point 16; CF and CS, respectively) in the lacustrine deposit to compare the effects of lacustrine with alluvial deposits (see Figure 19 for location of the sampling points).

6.2   HYDROCHEMICAL PARAMETERS IN SURFACE WATER AND POREWATERS

Surface water was a $Ca-HCO_3$ type along all the monitoring points in the burn in April 2018, while it changed from $Ca-HCO_3$ type to $Ca-SO_4$ type downstream from Be in August 2018 and February 2019 (Figure 21).

All the surface waters were oversaturated in dolomite (SI 3.9 to 5.6), calcite (SI 2.0 to 3.0), and gypsum (SI range 1.1 to 1.6). Barium concentrations are controlled by barite solubility (SI 2.8 to 3.27). $Fe(OH)_3$ was oversaturated except for surface water at BP.

A range in temperature of 10.7 °C was measured between the three sampling events; the surface-water pH remained neutral throughout the monitored stream stretch and temporal sampling, ranging from 6.6 to 7.5. The waters were generally well oxygenated with a median DO of 9.7 mg/l, although a minimum value of 1 mg/l was measured. Conductivity was high, ranging from 1289 to 2191 µS/cm (Table 6). Descriptive statistics of surface water major and minor elements are shown in Table 7 and Table 8. Sulphate concentrations ranged from 235 mg/l to 790 mg/l, $N-NO_3$ from 0.20 to 3.7 mg/l and total phosphorus from 0.010 mg/l to 0.06 mg/l.

Most of the porewaters were of the $Ca-HCO_3$ type, except for the porewater at BP, which was a $Mg-SO_4$ water in the April and August 2018 sampling and a $Ca-SO_4$ type in February 2019 (Figure 21). LH also had two porewater samples (H01-Y AND H02-R) of $Ca-SO_4$ type. Within the $Ca-HCO_3$ hydrofacies type, some of the samples from CF and CS sites were relatively enriched in bicarbonate anions compared to the other sites.

All the porewaters were oversaturated in calcite (SI +1.9 to +3.9) and dolomite (SI +3.1 to +7.5). Gypsum was oversaturated, except for the deep porewater at locations CF and CS, which were slightly undersaturated (SI range -1.83 to +1.66). Ba concentration was controlled by barite (SI +1.04 to +3.97). $Fe(OH)_3$ was oversaturated except for in most of the porewaters at the BP.
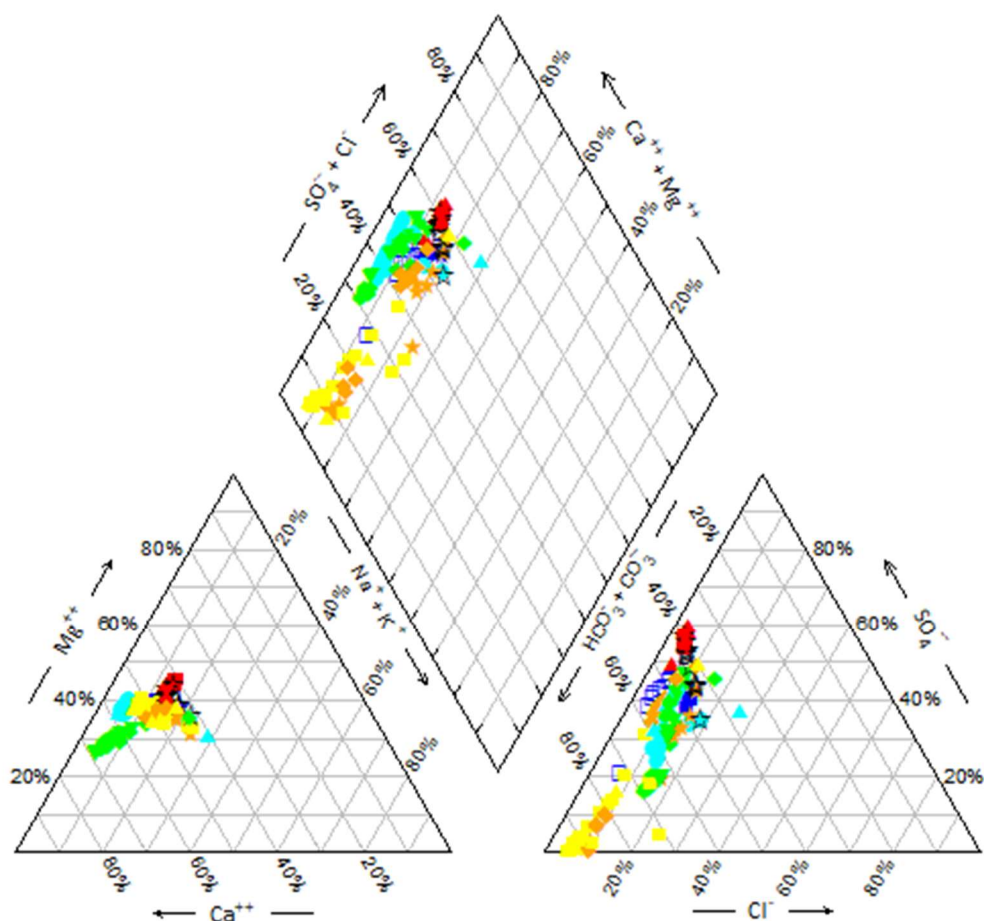
Figure 21 Piper plot. Surface water: star symbols. Porewater: BP: red; Be: light blue; LH: green; CF: orange; CS: yellow, Woodham Burn data from 1st phase investigation: blue.

DO levels in the porewater were significantly ($p < 0.05$) lower than in the surface water; although they remained oxic (median of 2.8 mg/l and a range of 0.2 mg/l to 9.6 mg/l). Redox measurements were significantly lower in the porewater (median 162; range -190 to 466 mV), while porewater and surface water alkalinity median (respectively 433-538 mg/l as HCO_3) and pH (6.98 and 7.07) were similar and typical of waters dominated by carbonate equilibrium reactions. NPOC was significantly higher in porewater. The sulphate concentrations in porewater (median ± standard deviation 185 ±259 mg/l) were significantly lower ($p < 0.05$) than in surface water (median ± standard deviation 509 ±166 mg/l) (Table 9). The nitrate concentrations in porewater (median ± standard deviation 0.03 ± 0.25 as N) were significantly lower ($p < 0.05$) than in the surface water (median ± standard deviation 1.06 ± 0.92). The phosphorus concentrations in porewater (median ± standard deviation 0.11±0.25) were significantly higher ($p < 0.05$) than in the surface water (median ± standard deviation 0.05±0.02 as P). The iron concentrations in porewater (median ± standard deviation 3657 ± 10835 µg/l) were significantly higher ($p < 0.05$) than in the surface water (median ± standard deviation 34 ± 34 µg/l) (Table 10).

Table 6 Descriptive statistics of field pH, dissolved oxygen, redox, temperature and conductivity for all surface waters (SW) and all porewaters (HZ).

Variable	Type	N	Mean	StDev	Minimum	Median	Maximum
pH	SW	14	7.07	0.22	6.55	7.07	7.50
	HZ	115	7.06	0.32	6.62	6.98	8.12
DO (mg/l)	SW	15	8.4	3.8	1.0	9.7	12.2
	HZ	108	3.1	1.4	0.2	2.8	9.6
Eh (mV)	SW	15	271	182	-170	313	459
	HZ	106	139	197	-190	162	466
Field Temp (ºC)	SW	14	11.0	3.6	5.0	10.8	15.7
	HZ	0	nd	nd	nd	nd	nd
Conductivity (µS/cm)	SW	14	1754	250	1289	1812	2191
	HZ	109	1266	505	352	1152	2284

Table 7 Descriptive statistics of major elements for all surface water (SW).

Variable (mg/l)	Type	N	Mean	StDev	Minimum	Median	Maximum
Ca	SW	15	184.00	37.83	120.00	187.24	241.70
Mg	SW	15	100.00	26.51	61.70	95.23	143.56
Na	SW	15	78.10	13.95	64.60	74.00	112.00
K	SW	15	8.58	1.13	7.09	8.69	10.40
HCO3	SW	15	546.0	95.4	403.5	537.8	705.3
Cl	SW	15	78.10	34.99	41.72	79.54	174.56
SO4	SW	15	516.0	166.2	235.4	509.3	789.9
N-NO3	SW	15	1.18	0.92	0.20	1.06	3.73
Br	SW	2	0.17	0.06	0.13	0.17	0.21
F	SW	15	0.30	0.08	0.19	0.27	0.45
NPOC	SW	15	2.07	1.07	0.63	1.81	4.37
Total P	SW	10	0.04	0.02	0.01	0.05	0.06
Total S	SW	15	172.4	55.0	80.0	171.4	259.2
Si	SW	15	4.52	0.74	3.55	4.29	5.96

Table 8 Descriptive statistics of minor and trace elements for all surface water (SW).

Variable (µg/l)	Type	N	Mean	StDev	Minimum	Median	Maximum
Al	SW	14	7.71	8.36	3.00	4.50	34.00
As	SW	14	0.18	0.06	0.05	0.18	0.31
B	SW	15	126.6	34.4	80.0	112.0	215.0
Ba	SW	15	63.9	15.6	32.4	67.9	85.6
Be	SW	0	*	*	*	*	*
Cd	SW	6	0.023	0.008	0.010	0.025	0.030
Ce	SW	5	0.02	0.02	0.01	0.02	0.05
Co	SW	12	0.16	0.05	0.05	0.17	0.21
Cr	SW	4	0.68	0.24	0.50	0.60	1.00
Cs	SW	5	0.010	0.003	0.006	0.009	0.015
Cu	SW	11	3.21	4.96	1.00	1.40	18.00
Dy	SW	4	0.008	0.002	0.006	0.008	0.009
Er	SW	3	0.003	0.001	0.003	0.003	0.004
Eu	SW	0	*	*	*	*	*
Fe	SW	15	41.35	34.08	10.00	34.00	140.40
Ga	SW	0	*	*	*	*	*
Gd	SW	7	0.005	0.001	0.004	0.005	0.008
Hf	SW	0	*	*	*	*	*
Ho	SW	0	*	*	*	*	*
La	SW	7	0.010	0.006	0.006	0.007	0.022
Li	SW	15	100.37	38.12	49.00	100.00	169.00
Lu	SW	0	*	*	*	*	*
Mn	SW	15	52.41	28.42	4.70	61.00	110.00
Mo	SW	10	0.46	0.26	0.17	0.47	0.84
Nb	SW	0	*	*	*	*	*
Nd	SW	4	0.024	0.014	0.011	0.02	0.044
Ni	SW	15	1.35	0.98	0.30	0.93	3.70
Pb	SW	15	0.13	0.08	0.05	0.12	0.32
Pr	SW	4	0.006	0.001	0.005	0.006	0.007
Rb	SW	15	4.859	0.949	3.6	4.89	6.98
Sb	SW	14	0.110	0.044	0.027	0.109	0.180
Se	SW	15	0.268	0.1084	0.060	0.300	0.400
Sm	SW	2	0.005	0.001	0.004	0.005	0.006
Sn	SW	4	0.019	0.006	0.010	0.020	0.025
Sr	SW	15	663.4	203.7	326.9	699.1	1022.5
Tb	SW	0	*	*	*	*	*
Th	SW	0	*	*	*	*	*
Ti	SW	15	0.060	0.016	0.030	0.060	0.091
Tl	SW	0	*	*	*	*	*
Tm	SW	15	3.14	0.61	2.21	3.13	3.84
U	SW	9	0.21	0.06	0.10	0.20	0.30
V	SW	0	*	*	*	*	*
W	SW	9	0.03	0.01	0.02	0.03	0.05
Y	SW	1	0.005	*	0.005	0.005	0.005
Yb	SW	15	8.49	2.76	5.20	8.70	16.00
Zn	SW	0	*	*	*	*	*
Zr	SW	15	0.06	0.02	0.03	0.06	0.09

Table 9 Descriptive statistics of major elements for all porewater (HZ).

Variable (mg/l)	Type	N	Mean	StDev	Minimum	Median	Maximum	Range
Ca	HZ	116	146.0	51.7	75.6	127.8	255.3	179.7
Mg	HZ	116	67.8	40.4	19.3	53.7	163.9	144.7
Na	HZ	116	37.9	27.2	7.0	27.6	89.7	82.7
K	HZ	116	4.6	3.7	0.3	3.2	11.3	11.0
HCO3	HZ	116	536.0	234.4	245.4	433.2	1382.0	1136.6
Cl	HZ	116	44.8	14.5	18.1	41.3	99.4	81.3
SO4	HZ	116	256.0	258.7	0.3	185.3	868.8	868.5
N-NO3	HZ	80	0.14	0.25	0.00	0.03	1.78	1.78
Br	HZ	31	0.18	0.07	0.05	0.20	0.29	0.24
F	HZ	116	0.30	0.11	0.12	0.30	0.63	0.51
NPOC	HZ	116	5.66	4.19	0.62	4.50	26.76	26.14
Total P	HZ	34	0.21	0.25	0.01	0.11	1.00	0.99
Total S	HZ	114	86.20	85.83	0.20	61.95	283.60	283.40
Si	HZ	116	9.44	2.83	3.81	9.16	17.91	14.10

Table 10 Descriptive statistics of minor and trace elements for all porewater (HZ).

Variable (µg/l)	Type	N	Mean	StDev	Minimum	Median	Maximum
Al	HZ	100	11.31	17.43	2.00	7.00	139.00
As	HZ	109	1.79	2.00	0.03	0.83	9.04
B	HZ	116	81.8	56.4	26.5	68.8	250.0
Ba	HZ	116	240.5	140.4	25.7	230.8	650.9
Be	HZ	20	0.016	0.007	0.010	0.010	0.030
Cd	HZ	18	0.027	0.012	0.010	0.025	0.040
Ce	HZ	57	0.078	0.076	0.006	0.057	0.40
Co	HZ	106	2.20	1.86	0.02	1.71	10.33
Cr	HZ	37	0.72	0.82	0.2	0.4	4.1
Cs	HZ	53	0.026	0.045	0.006	0.015	0.321
Cu	HZ	72	3.59	9.41	0.20	2.00	81.00
Dy	HZ	57	0.012	0.0092	0.005	0.009	0.052
Er	HZ	50	0.007	0.005	0.002	0.005	0.027
Eu	HZ	40	0.008	0.005	0.002	0.008	0.020
Fe	HZ	116	8024	10835	4	3657	50223
Ga	HZ	81	0.70	0.60	0.06	0.53	3.05
Gd	HZ	69	0.011	0.011	0.003	0.008	0.056
Hf	HZ	1	0.02	*	0.02	0.02	0.02
Ho	HZ	10	0.007	0.003	0.002	0.007	0.009
La	HZ	68	0.025	0.027	0.005	0.017	0.152
Li	HZ	116	47.0	58.3	3.0	23.5	204.0
Lu	HZ	8	0.005	0.003	0.002	0.004	0.010

Variable (µg/l)	Type	N	Mean	StDev	Minimum	Median	Maximum
Mn	HZ	115	1936	1796	1	1514	9580
Mo	HZ	84	0.86	0.70	0.08	0.72	3.90
Nb	HZ	1	0.02	*	0.02	0.02	0.02
Nd	HZ	22	0.052	0.072	0.007	0.027	0.270
Ni	HZ	116	1.83	1.70	0.20	1.45	11.70
Pb	HZ	98	0.24	0.48	0.02	0.14	4.46
Pr	HZ	14	0.0118	0.0125	0.003	0.007	0.040
Rb	HZ	116	2.83	2.12	0.48	2.21	8.29
Sb	HZ	90	0.12	0.09	0.01	0.10	0.52
Se	HZ	79	0.21	0.11	0.05	0.20	0.60
Sm	HZ	35	0.017	0.016	0.004	0.010	0.070
Sn	HZ	44	0.17	0.50	0.02	0.06	3.34
Sr	HZ	116	467.1	285.4	135.7	363.0	1120.0
Tb	HZ	9	0.007	0.003	0.002	0.008	0.010
Th	HZ	34	0.016	0.009	0.006	0.013	0.042
Ti	HZ	69	0.57	0.52	0.11	0.40	2.90
Tl	HZ	26	0.08	0.05	0.01	0.07	0.17
Tm	HZ	3	0.005	0.003	0.003	0.003	0.009
U	HZ	116	1.11	1.45	0.01	0.35	4.33
V	HZ	87	0.6	0.3	0.1	0.5	1.6
W	HZ	34	0.08	0.02	0.05	0.08	0.12
Y	HZ	87	0.05	0.04	0.01	0.04	0.26
Yb	HZ	51	0.010	0.006	0.004	0.009	0.030
Zn	HZ	110	8.3	5.6	1.3	7.1	39.6
Zr	HZ	50	0.167	0.10	0.05	0.15	0.52

6.3   ADDITIONAL WATERS

In this study, a small number of additional water types were collected from the river banks and from a waterlogged area at the boundary between the alluvial and the lacustrine deposits identifiable by the presence of bulrushes, as described in the Methods sections.

The chemical analysis is shown in Appendix 3.

6.4   SOIL WATER SOLUBLE SULPHATE

Table 11 reports the anion analysis of the water leachates (water-soluble fraction) obtained from soils from Woodham Burn. The "water soluble" represents the fraction likely forming the runoff composition. The sample locations are shown in Figure 12. It is evident that the bank area represented by HA3, south of the bulrushes, adjacent to Woodham Burn, was lower in soluble sulphate than locations HA4 (by BP) and HA5. An increasing trend in water-soluble sulphate with soil depth is measured at both locations.

Location HA5 sited near to bank seepage previously observed (Drain 2) and also present at the time of sampling on the opposite bank. The high sulphate concentration of the water-soluble fraction matches the high sulphate composition of Drain 2 seepage, to suggest a diffuse area of sulphate recharge to the burn, upstream of the first monitoring point, i.e. Be site, of our study.

Table 11 Concentrations of anions in water-soluble extracts (in mg/l) and sulphate water-soluble fraction (in mg/kg) from soils in Woodham Burn.

Sample	Water Leachate analysis (1:10 S:L ratio /25g sample in 250 ml water)								
	SEC	Cl-	SO42-	NO3-	Br-	NO2-	HPO42-	F-	Water soluble SO42-
	(µS/ cm)	(mg/l)	(mg/l)	(mg/l)	(mg/l)	(mg/l)	(mg/l)	(mg/l)	(mg/ kg)
HA3 0.00 – 0.30 m	nd	nd	low SO$_4$	nd	nd	nd	nd	nd	nd
HA3 0.30 – 0.73 m	nd	nd	low SO$_4$	nd	nd	nd	nd	nd	nd
HA3 0.80 – 1.05 m	44	1.24	3.4	6.3	<0.01	2.30	<0.01	0.67	34
HA3 1.05 – 2.03 m	nd	nd	low SO$_4$	nd	nd	nd	nd	nd	nd
HA4 0.00 – 0.35 m	nd	nd	low SO$_4$	nd	nd	nd	nd	nd	nd
HA4 0.35 – 0.75 m	nd	nd	low SO$_4$	nd	nd	nd	nd	nd	nd
HA4 0.70 – 1.35 m	64	0.81	8.4	10.9	<0.01	0.032	<0.01	0.47	84
HA4 1.35 – 1.65 m	67	1.48	12.1	6.5	<0.01	0.088	<0.01	0.40	121
HA5 0.00 – 0.70 m	84	3.15	13.4	11.6	<0.01	1.48	<0.01	0.72	134
HA5 0.70 – 1.05 m	94	1.60	29.2	0.4	<0.01	0.01	<0.01	0.72	292
HA5 1.05 – 1.75 m	234	5.66	96.2	0.8	<0.02	<0.01	<0.02	1.34	962
Ploughed field at Be site	nd	nd	low SO$_4$	nd	nd	nd	nd	nd	nd

6.5   SPATIAL AND TEMPORAL PATTERNS

6.5.1   Surface water spatio-temporal chemical variation

Surface water composition varied with both location and time. The range for most surface water parameters was narrower in August (lower relative standard deviation, RSD%) as shown in Table 12.

Figure 22 shows the spatial variation in Ca, Mg, Na and HCO$_3$, Cl, and SO$_4$ concentrations in surface water along the study reach and the temporal variation over the three sampling events. For each sampling event, Ca, Mg, HCO$_3$, SO$_4$ were elevated at the downstream end of the reach relatively to the upstream. This solute spatial variation shows a sharp increase in concentrations from point Be to BP, to then decrease from points BP to LH, remaining relatively constant and higher than the upstream point 1 throughout the remaining stretch of the study burn (points CF and CS). It is noticeable that the surface water composition of point BP is relatively constant throughout the three sampling events and enriched in Ca, Mg, HCO$_3$ and SO$_4$ (Na only for round 1 and 2), while depleted in Cl compared to the other points. This is a strong indication that point BP is a discharge point of a relative homogeneous subsurface flow into the burn. In contrast, the monitoring points upstream and downstream of the BP show higher variability over time.

Table 13 reports the percent difference of major solutes calculated between the most upstream and downstream points (points Be–CS), and between each relative upstream and downstream location. It shows that the greatest downstream increase in the reach is in SO$_4$. In the April 2018 sampling, the percent increase of SO$_4$ from the most upstream point Be to point CS, at the confluence with Rushyford Beck, was 56%, reaching 51% at point 3, highlighting a narrow area between point Be and LH where the change happens. Similar percent increase is measured in February 2019 (57% and 52%, respectively point Be–CS and point Be–LH), while a lower percent increase of 19% and 23% is measured in August 2018. Downstream of LH, the percent difference between points LH and CF and points CF and CS in Ca, Mg, Na, K, Cl and HCO$_3$ is mostly < 3% and variable between positive and negative. While the accuracy of the method has not been

tested in this study, the observed large differences are reliable and considered in further interpretation to indicate groundwater inflows. The low values cannot be considered in greater detail other than suggesting the lack of major load gains and losses downstream LH.

Table 12 Surface water composition variation across the whole study burn over time.

Variable	Sampling Date	N	Mean	StDev	RSD%	Minimum	Median	Maximum	Range
pH	Apr-18	5	6.9	0.2	2.7	6.6	7.0	7.1	0.5
	Aug-18	5	7.0	0.3	4.1	6.6	7.0	7.3	0.9
	Feb-19	5	7.2	0.2	3.2	6.9	7.2	7.5	0.6
DO	Apr-18	5	9.2	4.6	50.0	1.0	12.0	12.0	11.0
(mg/l)	Aug-18	5	7.5	3.7	49.0	1.0	9.2	9.7	8.7
	Feb-19	5	8.5	3.9	46.0	2.1	10.0	12.0	9.9
Eh	Apr-18	5	398	60	15	312	401	457	145
(mV)	Aug-18	5	60	145	241	-170	55	200	370
	Feb-19	5	354	84	24	239	362	459	220
T	Apr-18	5	11.0	1.0	8.4	10.2	11.6	12.6	2.4
(ºC)	Aug-18	5	14.0	2.0	14.0	11.0	15.2	15.7	4.7
	Feb-19	5	6.8	1.8	27.0	5.0	7.2	9.4	4.4
SEC	Apr-18	5	1612	370	23	1289	1520	2250	961
(µS/cm)	Aug-18	5	1844	173	9	1651	1814	2125	474
	Feb-19	5	1906	183	10	1678	1888	2191	513
NPOC	Apr-18	5	3.1	1.1	36.0	1.3	3.3	4.4	3.1
(mg/l)	Aug-18	5	1.4	0.5	34.0	1.0	1.2	2.2	1.3
	Feb-19	5	1.7	0.7	41.0	0.6	1.8	2.5	1.9
Ca	Apr-18	5	154	39	25	120	143	221	101
(mg/l)	Aug-18	5	209	21	10	183	205	242	59
	Feb-19	5	189	34	18	145	187	240	95
Mg	Apr-18	5	87	31	36	62	77	141	80
(mg/l)	Aug-18	5	117	17	15	95	115	144	48
	Feb-19	5	96	25	26	64	95	133	69
Na	Apr-18	5	70	7	11	65	67	82	18
(mg/l)	Aug-18	5	72	4	6	67	73	78	11
	Feb-19	5	92	15	16	80	85	112	32
HCO3	Apr-18	5	488	99	20	404	461	659	255
(mg/l)	Aug-18	5	602	56	9	538	590	693	155
	Feb-19	5	549	104	19	416	537	705	289
Cl	Apr-18	5	76	17	22	48	80	93	45
(mg/l)	Aug-18	5	55	9.3	17	42	55	68	26
	Feb-19	5	103	50	48	45	85	175	130
SO4	Apr-18	5	410	185	45	235	367	725	490
(mg/l)	Aug-18	5	614	109	18	491	599	790	299
	Feb-19	5	523	158	30	325	509	765	441
Fe	Apr-18	5	25	14	54	10	30	37	27
(µg/l)	Aug-18	5	33	20	59	19	26	67	48
	Feb-19	5	66	48	74	13	47	140	127
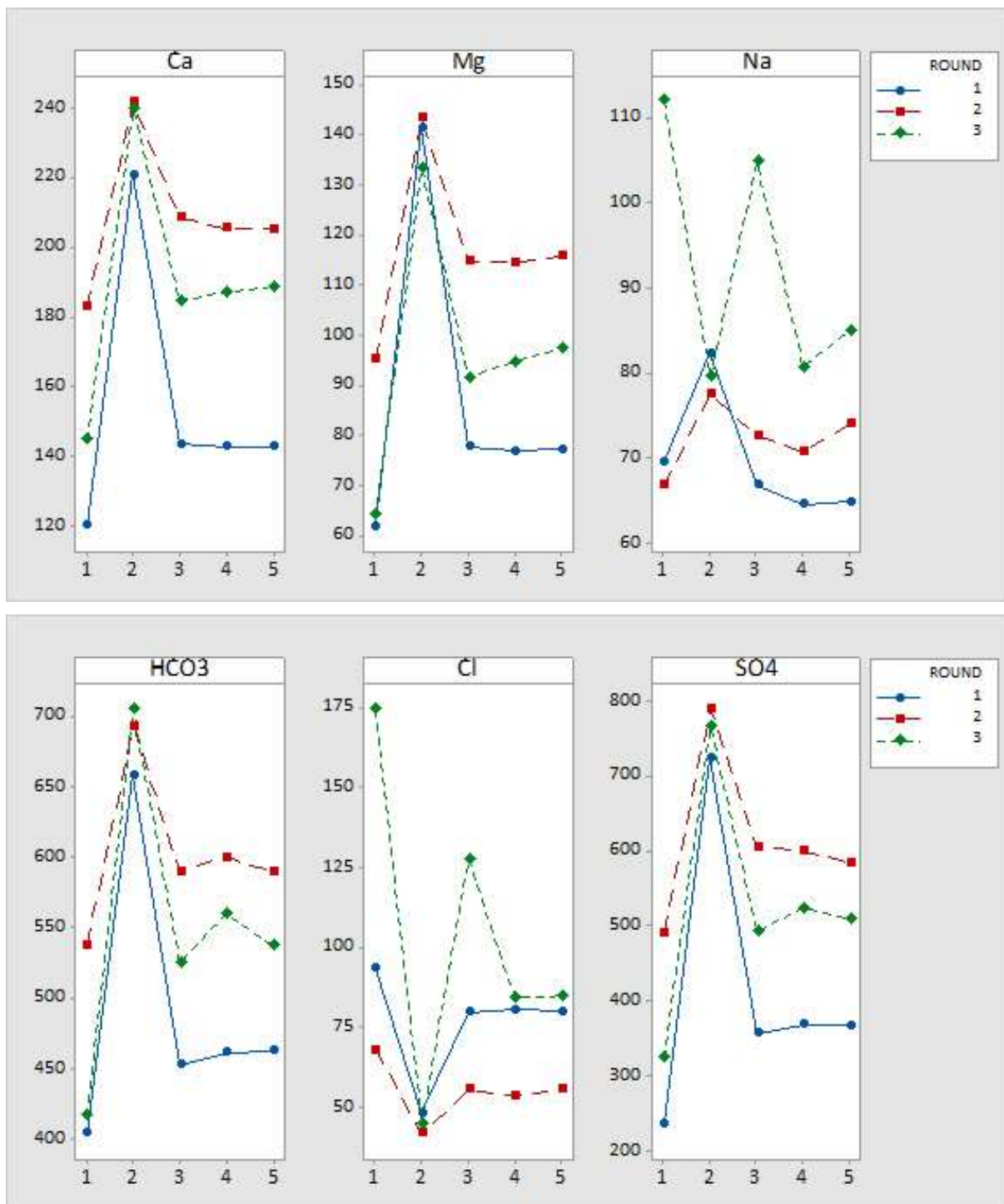
Figure 22 Compositional changes in surface water (concentrations in mg/l) along the burn at the three sampling events. Legend: 1: Be; 2: BP; 3: LH; 4: CF; 5: CS. Round 1: 25-26 April 2018, round 2: 1 August 2018; round 3: 5-6 February 2019.

Table 13 Percent difference calculated between the most upstream and downstream points (points Be–CS), and between each relative upstream and downstream location

	Concentration difference (%) (Cd/s-Cu/s)*100/Cu/s	Ca	Mg	Na	K	HCO3	Cl	SO4	N-NO3
Round 1: **Apr 2018**	**Point Be to CS**	**+19%**	**+25%**	**-7%**	**+3%**	**+15%**	**-14%**	**+56%**	**-15%**
	Point Be to LH	+20%	+26%	-4%	+3%	+12%	-15%	+51%	-15%
	Point LH to CF	-0.5%	-1.2%	-3.3%	1.5%	1.9%	1.3%	3.5%	1.9%
	Point CF to CS	-0.1%	+0.6%	+0.5%	-2.2%	0.4%	-0.9%	-0.5%	-1.4%
Round 2: **Aug 2018**	**Point Be to CS**	**+12%**	**+22%**	**+11%**	**+21%**	**+10%**	**-18%**	**+19%**	**-27%**
	Point Be to LH	+14%	+21%	+9%	+18%	+10%	-18%	+23%	-53%
	Point LH to CF	-1.5%	-0.3%	-2.6%	-2.4%	1.6%	-3.3%	-1.0%	-1.3%
	Point CF to CS	-0.1%	+1.0%	+4.7%	+4.8%	-1.7%	+3.7%	-2.4%	+59%
Round 3: **Feb 2019**	**Point Be to CS**	**NA**	**NA**	**NA**	**NA**	**NA**	**NA**	**NA**	**NA**
	Point Be to LH	+27%	+43%	-6%	+21%	+26%	-27%	+52%	-53%
	Point LH to CF	NA	NA	NA	NA	NA	NA	NA	NA
	Point CF to CS	+0.8%	+2.8%	+5.5%	+2.2%	-4.1%	+0.6%	-2.7%	-8.2%

+ indicate downstream increase

NA: not applicable as sampling dates for point CF and CS differ from points Be to LH.

6.5.2 Estimating groundwater discharge to Woodham Burn from stream chemistry

In the absence of direct rainfall input and surface water inflow between Be and point LH, we used a two component mixing equation to calculate the fraction of groundwater inflow at BP, responsible for the observed downstream solute concentration gains (Method Section 5.4). The results are in Table 14.

Table 14 Values of Q_2/Q_3, fraction of groundwater Q_{GW} in surface water Q_3 at point LH.

	Apr 18	Aug 18	Feb 19
Based on Ca concentrations	0.23	0.44	0.42
Based on Mg concentrations	0.20	0.41	0.40
Based on HCO3 concentrations	0.19	0.34	0.37
Based on SO4 concentrations	0.25	0.38	0.38

6.5.3 Porewater spatio-temporal chemical variation of conservative elements

Areas of groundwater discharge are expected to exhibit narrower temporal variations in the porewater composition in the impacted piezometers. The relative standard deviation RSD%, i.e. the percent standard deviation from the mean of the composition in the three sampling events, (standard deviation*100/mean), of the conservative chloride and lithium were examined by depth for each piezometer (Table 15 and Table 16).

The chloride concentration in porewater varied less than in surface water. Within the sediment zone, as shown in Figure 23, a generally greater RSD% was observed in the porewater composition at shallow depth, at least in one of the piezometers from each location. In particular, at CF, sediment porewaters at all depths show a large standard deviation in Cl composition similar in range to surface water. On the contrary, at BP, a narrow temporal variation is observed in the porewater composition and the overlying surface water.

Patterns for lithium are very similar to chloride (Figure 24), except for BP, where the porewater composition has a greater variation than the overlying surface water, although not significantly different from surface water. It is also noted that the lithium composition of the porewater from BP is distinctively different to the other sites.

Table 15 Surface water and pore water variation of Cl with time by each monitoring site. Depths intervals: _B (for black = 10 cm sediment depth), _R (for red = 20 cm sediment depth), _G (for green = 50 cm sediment depth), _Y (for yellow = 90 cm sediment depth)

Variable & Site	Location	N	Mean	StDev	%RSD	Minimum	Median	Maximum
CI - Be	Be_SW	3	111.90	55.70	49.78	67.90	93.20	174.60
	Be_HZ01_B	3	36.37	2.38	6.54	34.68	35.34	39.10
	Be_HZ01_R	3	34.74	0.96	2.76	33.96	34.45	35.81
	Be_HZ01_G	3	34.02	0.55	1.63	33.56	33.86	34.63
	Be_HZ01_Y	3	35.16	1.32	3.75	33.65	35.73	36.09
	Be_HZ02_B	2	38.93	0.64	1.63	38.48	38.93	39.38
	Be_HZ02_R	2	39.09	6.06	15.50	34.80	39.09	43.38
	Be_HZ02_G	2	35.88	0.12	0.32	35.79	35.88	35.96
	Be_HZ02_Y	2	39.16	3.15	8.04	36.93	39.16	41.39
	Be_HZ03_B	2	64.80	37.30	57.56	38.40	64.80	91.10
	Be_HZ03_R	2	51.40	24.20	47.08	34.20	51.40	68.50
	Be_HZ03_G	2	39.29	3.63	9.24	36.73	39.29	41.86
	Be_HZ03_Y	2	41.97	0.75	1.77	41.45	41.97	42.50
CI - BP	BP_SW	3	44.92	3.26	7.26	41.72	44.80	48.23
	BP_HZ01_B	3	41.05	0.63	1.53	40.34	41.31	41.51
	BP_HZ01_R	3	40.11	2.05	5.11	37.77	40.92	41.63
	BP_HZ01_G	3	40.30	1.89	4.69	38.12	41.29	41.48
	BP_HZ01_Y	3	41.08	1.75	4.26	39.07	41.89	42.28
	BP_HZ02_B	2	45.66	4.24	9.29	42.66	45.66	48.66
	BP_HZ02_R	2	44.72	4.90	10.96	41.26	44.72	48.18
	BP_HZ02_G	2	46.14	2.38	5.16	44.45	46.14	47.82
	BP_HZ02_Y	2	48.29	1.71	3.54	47.09	48.29	49.50
CI - CF	CF_SW	3	72.83	16.76	23.01	53.59	80.59	84.30
	CF_HZ01_B	3	63.59	9.32	14.66	56.69	59.88	74.19
	CF_HZ01_R	3	60.63	10.33	17.04	54.59	54.75	72.56
	CF_HZ01_G	3	55.47	13.15	23.71	47.42	48.33	70.65
	CF_HZ01_Y	3	52.15	11.36	21.78	40.58	52.57	63.29
	CF_HZ02_B	2	67.20	18.80	27.98	53.90	67.20	80.50
	CF_HZ02_R	2	71.50	16.80	23.50	59.70	71.50	83.40
	CF_HZ02_G	2	61.48	4.47	7.27	58.32	61.48	64.64
	CF_HZ02_Y	2	47.46	6.20	13.06	43.08	47.46	51.84
CI - CS	CS_SW	3	73.39	15.64	21.31	55.56	79.83	84.80
	CS_HZ01_B	2	36.07	0.46	1.27	35.74	36.07	36.39
	CS_HZ01_R	2	38.04	1.17	3.08	37.21	38.04	38.87
	CS_HZ01_G	2	31.92	3.71	11.62	29.30	31.92	34.54
	CS_HZ01_Y	2	25.15	9.96	39.60	18.10	25.15	32.19
	CS_HZ02_B	3	80.20	18.40	22.94	62.70	78.50	99.40
	CS_HZ02_R	3	75.86	13.42	17.69	62.86	75.05	89.67
	CS_HZ02_G	3	29.78	3.88	13.03	25.83	29.93	33.59
	CS_HZ02_Y	3	26.86	3.21	11.95	24.73	25.29	30.55
CI - LH	LH_SW	3	87.60	36.80	42.01	55.40	79.50	127.70
	LH_HZ01_B	3	49.73	4.55	9.15	45.58	49.01	54.60
	LH_HZ01_R	3	40.81	2.28	5.59	38.23	41.60	42.58
	LH_HZ01_G	3	40.83	5.44	13.32	34.65	42.91	44.92
	LH_HZ01_Y	3	41.78	6.05	14.48	35.86	41.51	47.96
	LH_HZ02_B	2	46.58	3.74	8.03	43.94	46.58	49.22
	LH_HZ02_R	2	38.19	4.35	11.39	35.11	38.19	41.26
	LH_HZ02_G	2	36.16	4.91	13.58	32.69	36.16	39.62
	LH_HZ02_Y	2	36.81	3.59	9.75	34.27	36.81	39.34
	LH_HZ03_B	2	36.15	2.15	5.95	34.64	36.15	37.67
	LH_HZ03_R	2	36.47	2.14	5.87	34.96	36.47	37.98
	LH_HZ03_G	2	36.16	1.56	4.31	35.05	36.16	37.26
	LH_HZ03_Y	2	35.80	1.67	4.66	34.62	35.80	36.98

Table 16 Surface water and pore water variation of Li with time by each monitoring site.

Variable & Site	Location	N	Mean	StDev	%RSD	Minimum	Median	Maximum
Li - Be	Be_SW	3	63	19	29	49	57	84
	Be_HZ01_B	3	13	3	20	10	13	15
	Be_HZ01_R	3	9	2	16	8	9	11
	Be_HZ01_G	3	9	1	11	8	9	10
	Be_HZ01_Y	3	10	2	16	8	10	11
	Be_HZ02_B	2	12	4	31	9	12	14
	Be_HZ02_R	2	20	13	64	11	20	29
	Be_HZ02_G	2	11	2	20	9	11	12
	Be_HZ02_Y	2	12	2	18	10	12	13
	Be_HZ03_B	2	25	23	90	9	25	41
	Be_HZ03_R	2	18	12	69	9	18	26
	Be_HZ03_G	2	9	0	0	9	9	9
	Be_HZ03_Y	2	10	1	7	9	10	10
Li - BP	BP_SW	3	160	8	5	156	156	169
	BP_HZ01_B	3	177	16	9	167	168	195
	BP_HZ01_R	3	177	18	10	162	171	197
	BP_HZ01_G	3	180	19	10	169	170	202
	BP_HZ01_Y	3	180	22	12	162	173	204
	BP_HZ02_B	2	156	1	1	155	156	157
	BP_HZ02_R	2	154	4	3	151	154	157
	BP_HZ02_G	2	153	5	3	149	153	156
	BP_HZ02_Y	2	132	38	29	105	132	158
Li - CF	CF_SW	3	93	25	27	65	100	113
	CF_HZ01_B	3	56	19	34	34	67	68
	CF_HZ01_R	3	47	13	28	33	49	59
	CF_HZ01_G	3	37	4	10	34	35	41
	CF_HZ01_Y	3	35	3	7	33	35	38
	CF_HZ02_B	2	73	30	42	51	73	94
	CF_HZ02_R	2	49	30	61	28	49	70
	CF_HZ02_G	2	41	3	7	39	41	43
	CF_HZ02_Y	2	38	0.	0	38	38	38
Li - CS	CS_SW	3	96	29	30	63	105	119
	CS_HZ01_B	2	22	1	6	21	22	23
	CS_HZ01_R	2	22	4	16	19	22	24
	CS_HZ01_G	2	19	1	4	18	19	19
	CS_HZ01_Y	2	24	9	35	18	24	30
	CS_HZ02_B	3	61	23	38	36	65	81
	CS_HZ02_R	3	42	5	12	37	42	47
	CS_HZ02_G	3	25	1	4	24	25	26
	CS_HZ02_Y	3	22	2	9	20	21	24
Li - LH	LH_SW	3	90.	23	26	65	95	111
	LH_HZ01_B	3	21	10	49	9	26	27
	LH_HZ01_R	3	7	3	43	3.5	8	9
	LH_HZ01_G	3	5	1	19	3.5	5	5
	LH_HZ01_Y	3	4	1	27	3	4	5
	LH_HZ02_B	2	34	30	87	13	34	55
	LH_HZ02_R	2	7	2	33	5	7	8
	LH_HZ02_G	2	4	1	20	3	4	4
	LH_HZ02_Y	2	4	1	20	3	4	4
	LH_HZ03_B	2	4	1	20	3	4	4
	LH_HZ03_R	1	3	-	-	3	3	3
	LH_HZ03_G	2	4	1	20	3	4	4
	LH_HZ03_Y	2	4	1	20	3	4	4
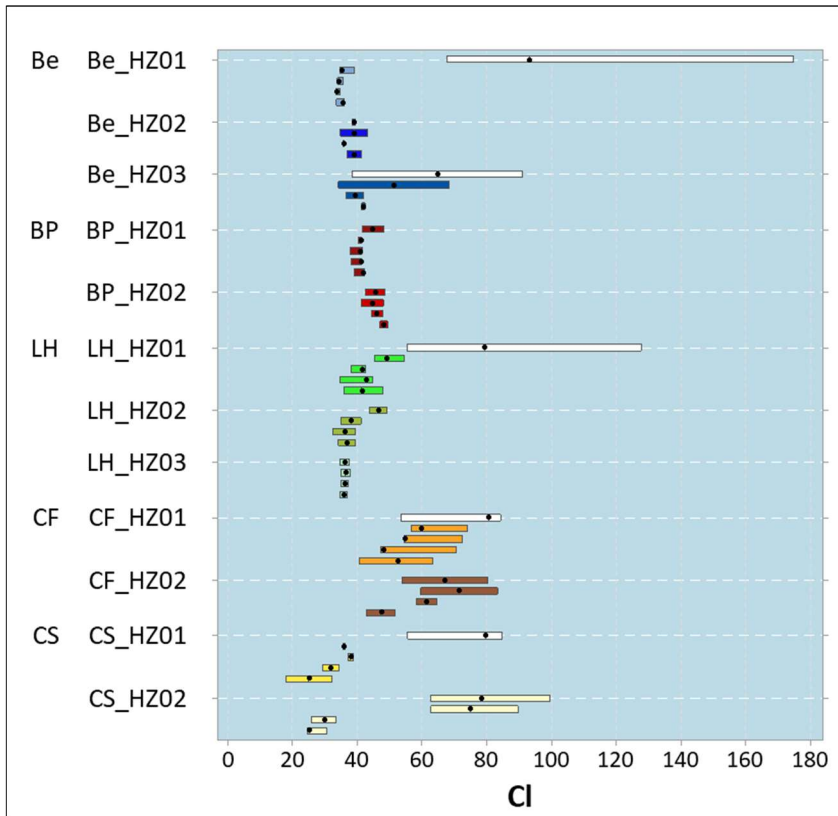
Figure 23 Median value (•) and interquartile range of Cl distribution with depth at each piezometer (all three sampling events). Surface water symbol in white. Units: mg/l.
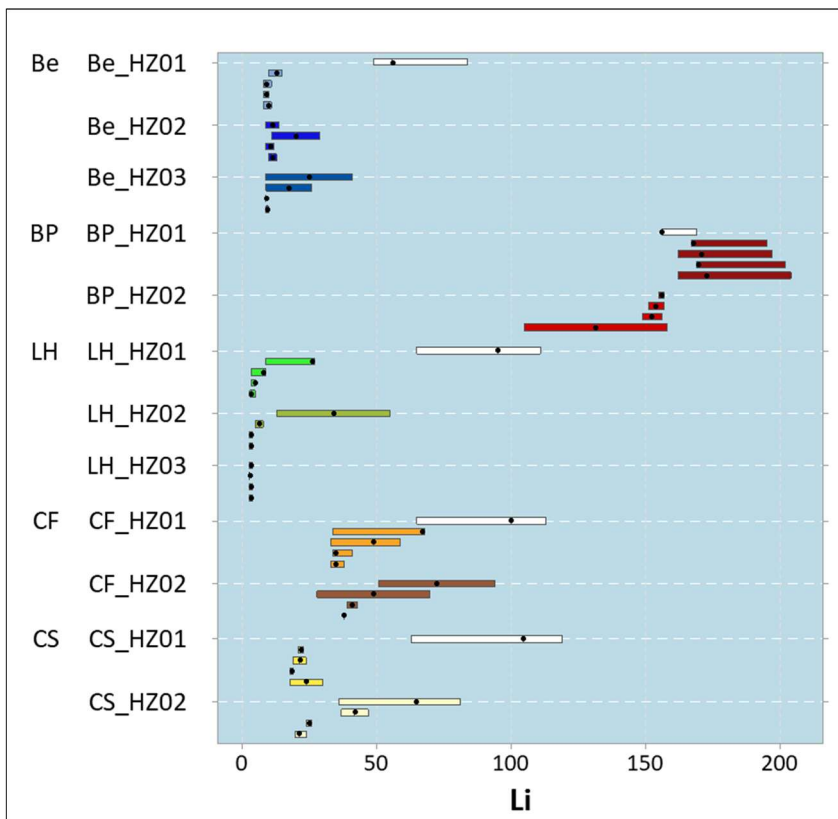
Figure 24 Median value (•) and interquartile range of Li distribution with depth at each piezometer (all three sampling events). Surface water symbol in white. Units: µg/l.

6.5.4 Delineation of hyporheic exchange flow using mixing scores

Figure 25 shows the distribution of the mixing score results (see also Method Section 5.6) for each site by sediment depth observed over all sampling events. It is noticeable that there are differences across the sites and within each site across the channel cross section.

At Be, the mixing score values cluster around -1 for piezometers Be-HZ01 and Be-HZ02, revealing little or no mixing of surface water and groundwater and a groundwater dominated riverbed; this suggests groundwater is either isolated from the stream or possibly upwelling. At piezometer Be-HZ03 the scores are between – 1 to 0, down to depth 20 cm, suggesting a component of downward HEF in the streambed up to that depth.

At LH, mixing scores lower than -1 suggest some horizontal flow between 10–50 cm depth for piezometer LH-HZ01, a shallow HEF up to 10 cm for piezometer LH-HZ02 and groundwater dominated riverbed/possible upwelling groundwater for piezometer LH-HZ03.

Sites CF and CS have fewer mixing scores close to -1 and are, instead, characterised by scores between -1 and 0 or greater than 0. At CF, for piezometer CF-HZ01 obvious downward HEF to a depth of 50 cm is inferred from the mixing scores. For CF-HZ02 HEF, is suggested at 10 cm depth by a score close to 0, while a lateral flow enriched in Cl compared to surface water at depth 20 to 50 cm is indicated by a mixing score greater than 0. Similarly, at the CS, the mixing scores suggest HEF down to 50 cm at piezometer CS-HZ01 and the presence of horizontal flow at shallow depth (10–20 cm) for piezometer CSHZ02, while the deeper horizon has a score close to -1.
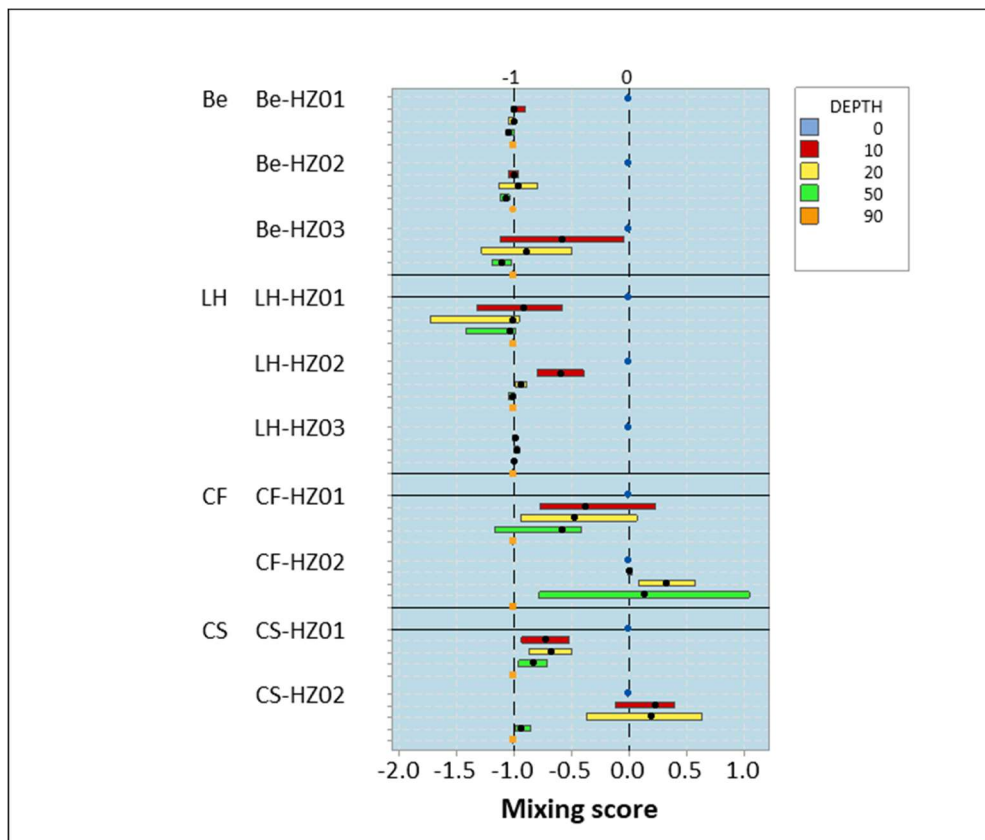
Figure 25 Box plot distribution of "Mixing Scores" by piezometer depth (over all 3 sampling events), derived from $(Cl_{[PW]} - Cl_{[SW]})/(Cl_{[SW]} - Cl_{[90cm]})$, such that porewater at 90 cm has a score "-1" and surface water has "0", respectively. Other scores > 0 and/or <-1 may suggest horizontal flow (either lateral inputs from the riparian zone or longitudinal flow along the river channel). Depth in cm. Median symbol " • ".

6.5.5 Piezometric measurement of hydraulic heads and temperature measurements

Measuring hydraulic heads along the reach can provide independent evidence to support the chloride vertical gradients results.

In this study, a long-term observation of hydraulic heads, temperature, and (at two points) SEC was planned. However, due to stronger than expected debris transport (e.g. tree logs) down the Woodham Burn after heavy rainstorms, the stability of the installed monitoring piezometers was challenged, and the installation failed after a 47 day period. At this point, data loggers had to be removed to ensure the safety of the equipment. Unfortunately, the piezometer and data logger installed to measure pressure, temperature and SEC in the surface water had already been lost. Due to the loss of the surface water logger, precise water level fluctuations in Woodham Burn are unknown, and recorded fluctuations in the subsurface are therefore more difficult to correlate.

The analysis of the head and temperature data is subdivided into the description of overall data characteristics and trends across the whole period (1 June, 16:00 to 16 July 2019, 22:00), and a detailed focus on rainstorm events. Raw data as well as standardised data are considered to explore similarities in trends across the different time series.

6.5.5.1 WATER LEVEL FLUCTUATIONS BELOW THE RIVERBED

Water level fluctuations over the interpreted time period are shown in Figure 26 and in more detail in Appendix 2, Figure 46. As a proxy for river stage at Woodham Burn, data from the Preston le Skerne river gauge has been used in these figures. The river stage at Preston le Skerne can be sub-divided in three periods, a) a strong level increase of about 15 cm in the first weeks of June, with relatively quick return to lower levels, b) a stable period between the second and last week of June, and c) and an overall increasing trend in river stage from beginning of July onwards.

The water levels logged in the piezometers at the monitoring points show a distinctly different pattern from the surface water data at Preston-Le-Skerne, with a broadly dampened response, as would be expected in the subsurface. An exception to this are two distinct peak periods in June. In summary, the logged period in the shallow and deep subsurface below the riverbed can be described as:

- A first recharge peak on 2 June 2019.
- Stable levels (similar to the initial levels) between 2 and 16 June 2019.
- A second recharge peak on 16 June 2019.
- Either stable or steadily increasing levels (depending on the measuring point) after the second recharge peak and until the end of the measuring period.

The extent of the temporary level increase during both peak periods differs by site and is most pronounced at LH 0.4 m and at CS (both depths). These three monitoring points are also the ones with the most pronounced gradual increase in levels over the last weeks of the monitoring period. This is potentially related to increased levels in Woodham Burn. LH 1.4 has a much less pronounced, but yet observable increasing trend toward the end of the monitoring period (best observed in Figure 27). The water level measurements therefore suggest that the sites around LH and CS have a different overall behaviour compared to the upstream area around Be and BP.

Logged water level time series (larger print in Appendix)	Data point	Max drop	Max rise	Mean	Standard deviation
	Preston Le Skerne	5.68	30.82	14.65	4.69
	Bench_0.4	-8.4	22.9	-3.4	3.5
	Bench_1.4	-16.2	23.0	-6.4	4.8
	BubblyPt_0.4	-14.4	5.4	-11.3	2.6
	LittleHouse_0.4	-14.7	33.1	-8.7	6.1
	Little House_1.4	-9.0	22.2	-4.8	3.8
	ConcreteSlab_0.4	-1.8	45.7	6.2	6.9
	ConcreteSlab_1.4	-1.9	46.3	6.0	6.9
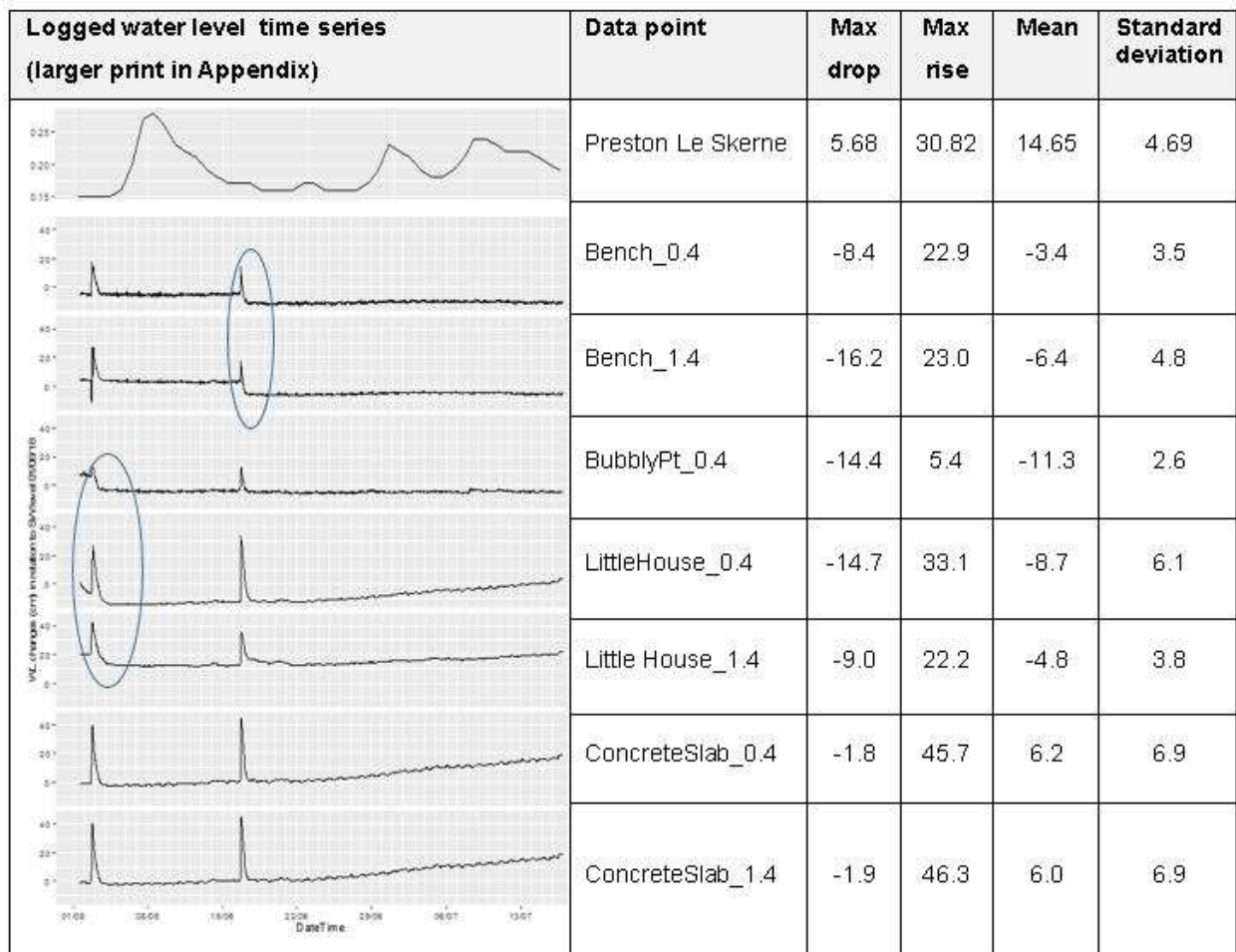
Figure 26 Water-level fluctuation below the river bed (as change in cm from initial level), and at Preston Le Skerne river gauge from 01 June to 16 July 2019 including basic summary statistics. The circled areas indicate sudden step changes that occurred at some of the installation after peaks in water levels. The most likely cause of this phenomenon is an issue with the installation, as further discussed in the text.

It is noteworthy that both recharge events affect all monitoring points, but to different extents. In all cases, except at CS, water levels after the first or second peak show a sudden 'step change' below the pre-peak level. This is a curious observation, and the most likely explanation is that the installations have been damaged after heavy rainfall due to resulting increases in surface water flow and debris transport. For example, cracking of the piping on the bottom combined with a bending of the upper part of the piezometer would have resulted in a higher position of the data logger (attached to the top part with a string, which would have then pulled upwards), and thus less water column above the data logger. Indeed, it is known that the piezometers Be and LH were bent when data were collected in July 2018 (contrary to the piezometers at BP and CS, which were found intact). It is therefore most likely that observed step changes in Be and LH are not real, and Figure 27 is based on an adjusted dataset in which these step changes were removed. For comparison with the same plot using raw data, see Appendix 2, Figure 48.

Another striking observation is that the water at LH 1.4 was about 20 cm higher than the stage of the Woodham Burn when installed. This could be an indication a confined/semi-confined groundwater layer at 1.4 m depth.
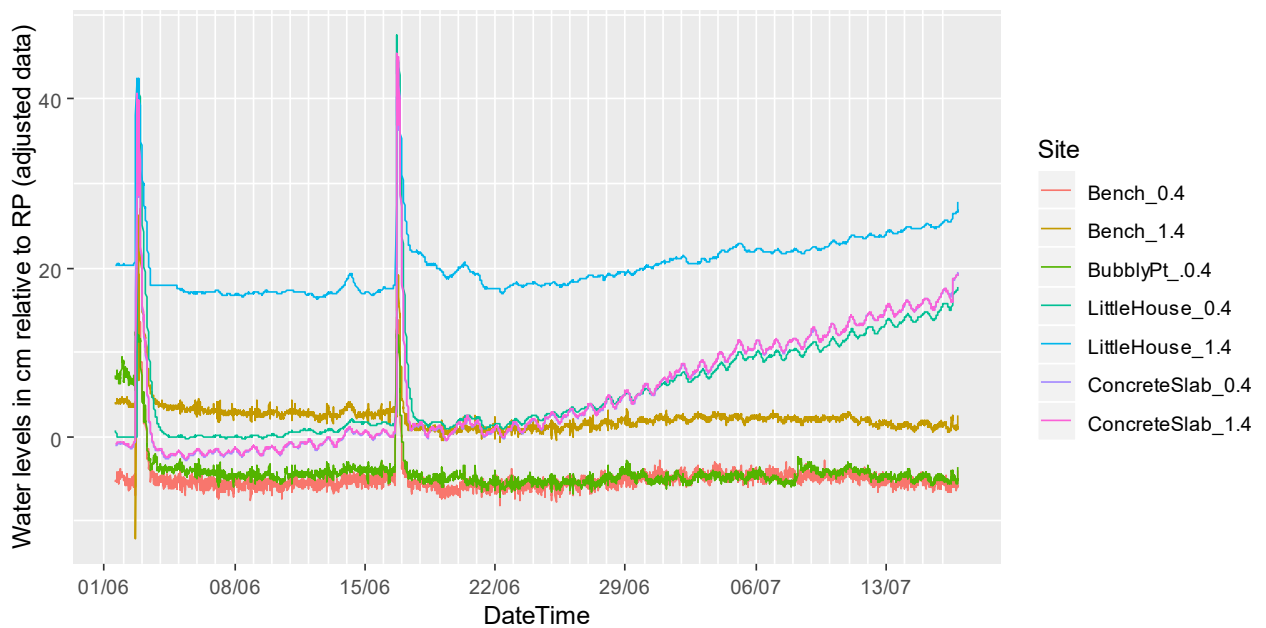
Figure 27 Piezometric water-level fluctuations for all monitoring sites in relation to the river stage on 01 June 2019 as reference point. The level fluctuation observed in CS 0.4 and CS_1.4 are nearly identical, hence the line for CS 0.4 is mostly overlain by the one of CS_1.4.

6.5.5.2 TEMPERATURE MEASUREMENTS

Temperature measurements below riverbed are a common method to estimate the degree of connectivity and exchange between the surface water and water in the hyporheic zone / in shallow groundwater. The underlying theory here is that surface water temperature will tend to equilibrate with the ambient air temperature in a typical diurnal cycle of warming and cooling, but water in the ground, if unaffected by surface water, will tend to equilibrate with the more stable surrounding soil / rock temperature. Measured diurnal temperature variations in the subsurface can therefore be a valuable indicator of active HEF and/or downwelling of surface water, as this will lead to a the propagation of the signal into depth. A limitation to this interpretation is that in very shallow sediments, a small diurnal signal may be observed due to the thermal conductivity of the sediment itself, even if no surface water infiltrates. The precise magnitude will be strongly dependent on the given sediment characteristics (Sebok and Müller, 2019), and the evaluation of this often goes beyond standard temperature surveys. Therefore, observations very near to the sediment-water boundary with only small diurnal signals should not be over-interpreted.

Conversely, a stable temperature of subsurface water at shallow depths of a river sediment, i.e. a complete masking of the expected diurnal temperature effect, can indicate that a) there is a hydraulic barrier disconnecting the surface and subsurface water, or b) subsurface water is discharging into the river (i.e. the river is a gaining stream at this segment). These two causes can be difficult to differentiate where stable temperatures are observed well below the river bed, but stable temperatures within the first decimetres below the riverbed can be attributed to groundwater upwelling with higher confidence. This is because a hydraulic barrier placed directly at the sediment/water interface would still show small diurnal temperature variations in the subsurface due to the thermal conductance of the sediment itself. In summary, it can be said that strong diurnal signals in subsurface water are a strong indication of surface water downwelling, and stable temperatures very close to the sediment/water interface are a strong indication of upwelling subsurface water.

The logged temperatures of the Woodham Burn investigation are shown in Figure 28 (refer to Appendix 2, Figure 47 for larger version of the plot without summary statistics). As would be expected, most sites at the shallow depth of 0.4 m show diurnal temperature signals, which may indicate that there is surface water downwelling into the hyporheic zone and mixing with groundwater. However, the lack of direct measurements of the surface water temperatures during

48

the observed period unfortunately limits the extent of data interpretation because it makes it difficult to ensure that the observed signal is not purely caused by thermal conductance of the sediment. It can be generally assumed though, that the more pronounced the diurnal temperature fluctuation, the more mixing and/or downwelling of surface water is likely taking place. Consequently, the visual inspection of the plotted signals in Figure 28 as well as the standard deviations (relating higher deviations to stronger signals) indicate a hierarchy from the most to least likely monitoring point to have downwelling surface water in the order:

CS 0.4 > LH 0.4 > Be 0.4 >>> BP (no diurnal signal).

An additional close-up example of the strong associations of diurnal signals between atmospheric temperature (used as a proxy for the variation pattern of surface water temperature) and CS 04 is included in Appendix 2, Figure 49).
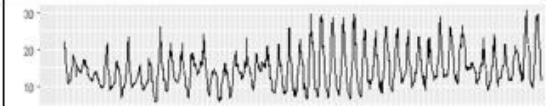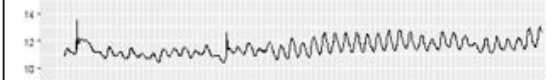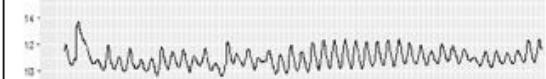
Logged temperature time series (larger print in Appendix)	Data point	Min	Max	Mean	Standard deviation
	Baro (air temperature)	5.68	30.82	14.65	4.69
	Bench_0.4	10.37	13.50	11.50	0.53
	Bench_1.4	8.88	9.91	9.44	0.30
	BubblyPt_0.4	9.25	9.74	9.28	0.02
	LittleHouse_0.4	9.69	13.70	10.98	0.64
	Little House_1.4	8.71	11.96	9.05	0.26
	ConcreteSlab_0.4	9.49	15.17	11.66	0.98
	ConcreteSlab_1.4	9.59	10.42	10.05	0.22

Figure 28 Temperature time series of surrounding air and water temperatures at the monitoring points at Woodham Burn, and summary statistics.

In addition to the susceptibility to the diurnal temperature signal (which has most effect on shallow monitoring points), overall trends in temperature at the sites can be indicative of the degree of connectivity of the deeper monitoring points with the surface water. The basic assumption for this is that a stable temperature (or very slight diurnal trends) is indicative of sites dominated by subsurface water, whereas sites with stronger temperature increase may be in more direct exchange with the increasingly warmer surface water in the summer months. Figure 29 below shows the similarity in rising trend of the two deeper monitoring sites Be 1.4 and CS 1.4, indicating

a likely connection of these sites with the surface water. A smaller trend is observed in LH 1.4, and no trend is observed at BP, which indicates low/no connectivity with or downwelling of surface water.

Figure 29 Plot of normalised temperatures at all sites, highlighting rising temperature trends at Be and CS 1.4, slight rising trend at LH 1.4, and no trend at BP.

6.5.5.3 CONDUCTIVITY MEASUREMENTS AT LITTLE HOUSE 1.4

Conductivity (SEC) was measured at the deeper monitoring point at LH throughout the monitored period with the same frequency as all other parameters. The measured time series, compared to changes in water levels and changes in temperature at LH 1.4 is shown in Figure 30. All parameters are standardised for comparison. SEC values ranged from 419 to 976 µS/cm (non-standardised data are included in Appendix 2, Figure 46 and Figure 47).

The most noteworthy feature of the time series is a pronounced decrease during the 2nd rain event on June 18 from around 670 to 410 µS/cm with a similarly pronounced recovery and increase to levels of around 850 within the same day. Assuming a relatively low conductivity of fresh precipitation, the decrease in conductivity is most likely related to downwelling of surface water, reflected also in increased water level and increased temperature at the measuring point. Shortly after, water levels are still higher than before the rain event, but temperature values drop back to approximately the same level as previously. Simultaneously, SEC values increase, potentially indicating that groundwater of higher conductivity is dominating the surface water–groundwater mix at the sampling point.
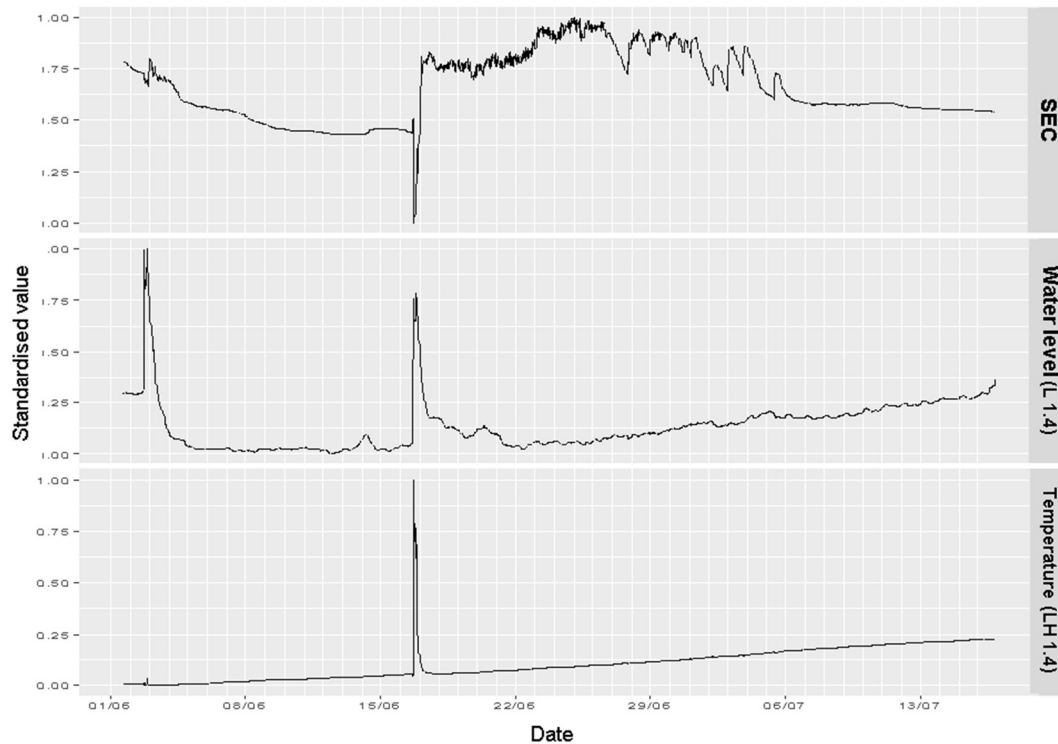
Figure 30 The measured conductivity time series, compared to changes in water levels and changes in temperature at LH 1.4.

6.5.5.4 SUMMARY AND INTERPRETATION

Temperature gradients and diurnal cycles indicate HEF at all sites except BP (where the upwelling water dominates the site). CF location was not covered with piezometer/loggers. The lack of a diurnal temperature signal at BP is a strong indication for upwelling groundwater of stable temperature. Water level measurements suggest that the sites around LH and CS have a different overall behaviour to the upstream area around Be and BP. Temperature peaks after rain storm events that partially coincide with a drop in SEC indicate at least intermittent surface water downwelling at all sites.

In summary, the following can be interpreted based on the hydraulic head and temperature measurements:

- Be: There seems to be some HEF, but likely no strong in- or outflow of the riverbed
- BP: Water from the subsurface is upwelling.
- LH: Surface water downwelling to some depth, but there are also indications for upwelling groundwater at the deeper monitoring point (1.4 m). This might be confined to some degree by sediment layers in the subsurface because the water level in the piezometer after installation was about 20 cm higher than the water level in the Woodham Burn.
- CS: Dominated by downwelling surface water.

51

6.5.6 Porewater spatio-temporal variations of non-conservative elements

Figure 31 and Figure 32 show the distribution of selected determinants over the sampling events across each piezometer depth.
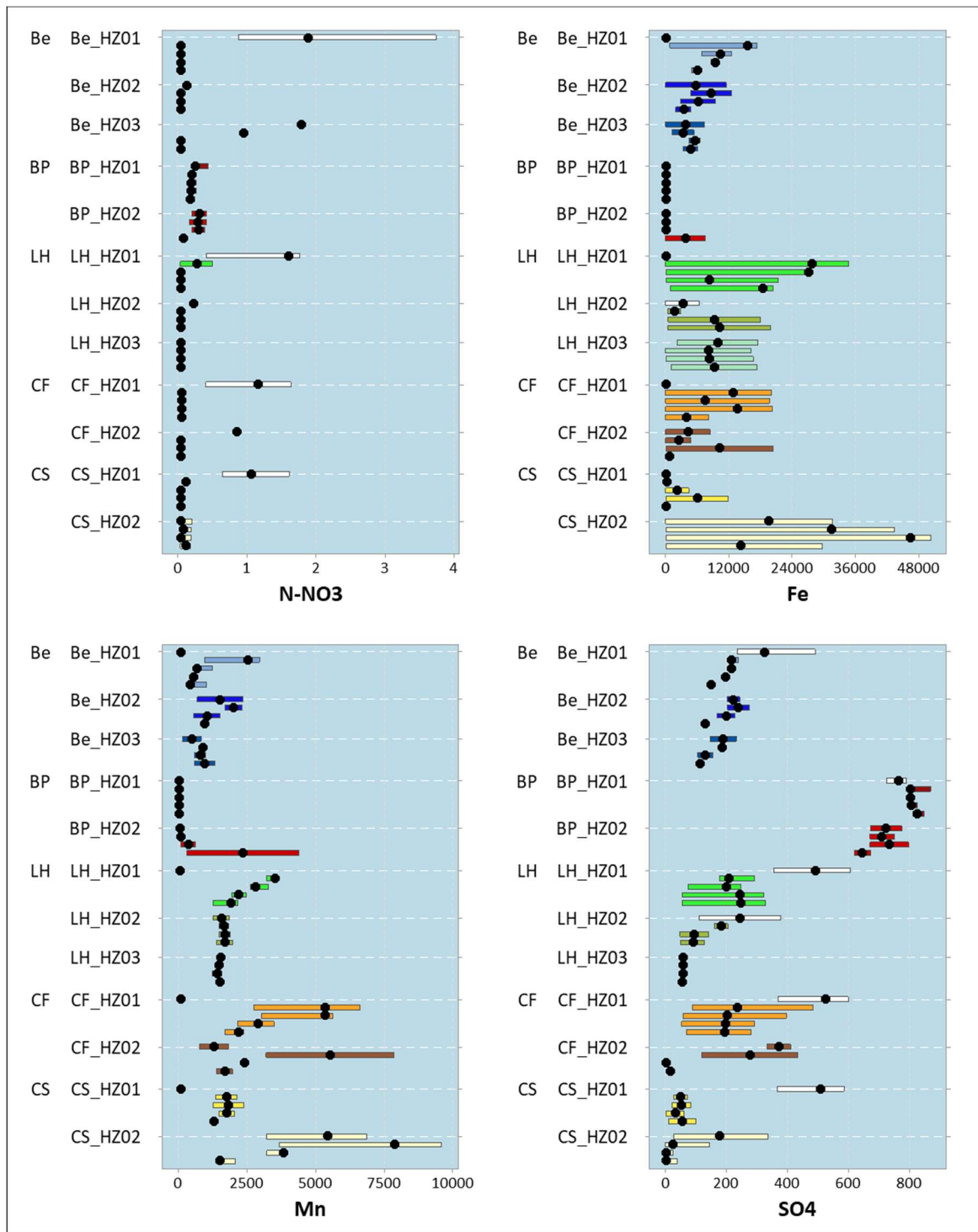
Figure 31 Median value (•) and interquartile range of selected solute distributions with depth at each piezometer (all three sampling events). Surface water symbol in white. Units: N-NO$_3$ and SO$_4$ in mg/l; Fe and Mn in µg/l.
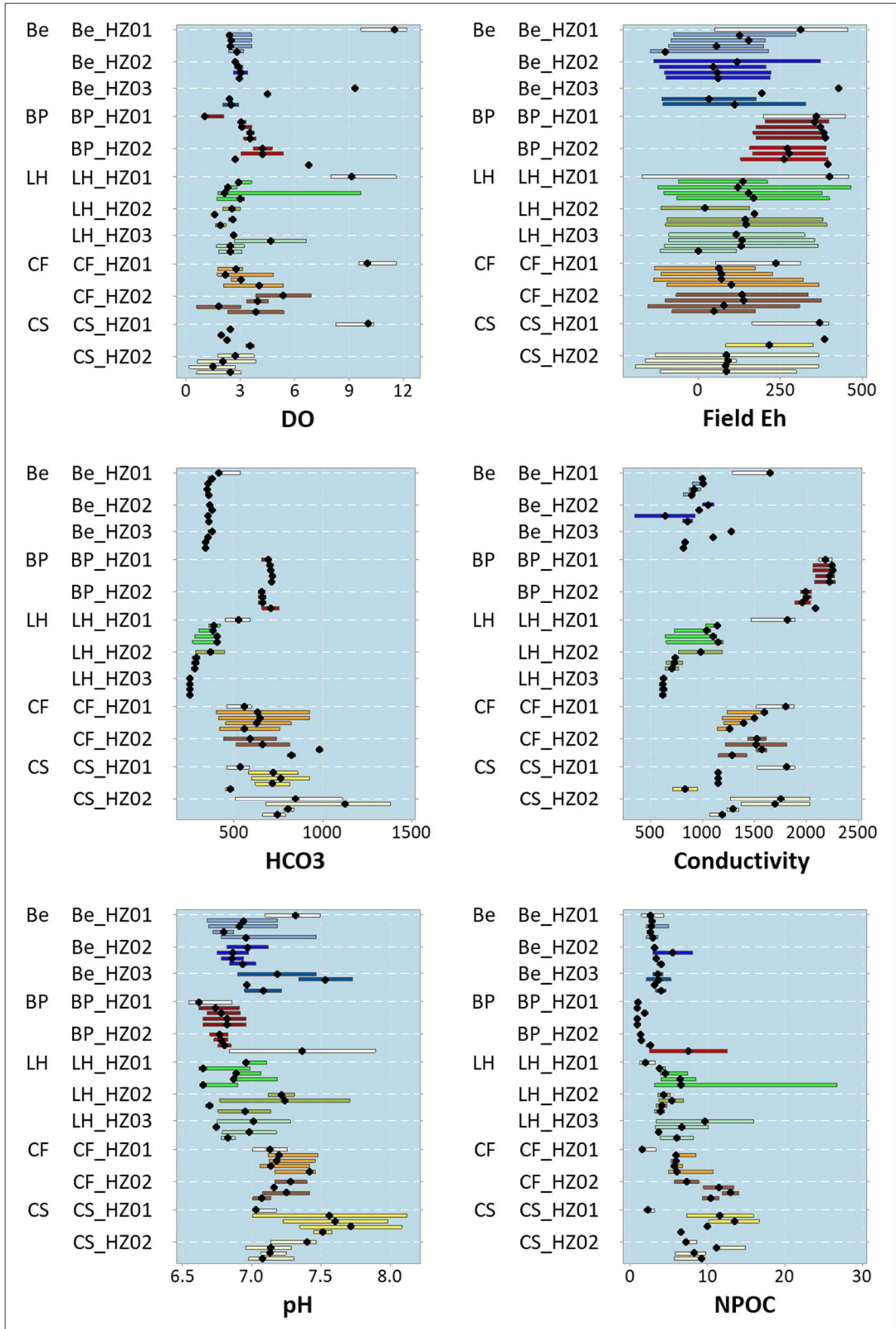
Figure 32 Median value (•) and interquartile range of DO (mg/l), Eh (mV), HCO₃ (mg/l), conductivity (µS/cm), pH and NPOC (mg/l) with depth at each piezometer (all three sampling events). Surface water symbol in white.

6.6 EVALUATION OF NATURAL ATTENUATION VIA COMPARISON OF CONSERVATIVE AND NON-CONSERVATIVE SOLUTE POREWATER GRADIENTS

Using Cl as a conservative tracer of mixing between surface water and groundwater, zones of hyporheic flow exchange between surface water and groundwater have been identified along with other zones of very limited or no mixing or lateral flow.

For the sites with observed HEF, it is possible to calculate the expected concentrations of other elements, such as e.g. nitrate or sulphate, should they behave conservatively like chloride, i.e. due to only mixing of surface water and groundwater (see Section 5.7).

Calculations of the apparent loss (negative difference) or gain (positive difference) for nitrate and sulphate, in the piezometers where a HEF was measured, are reported in Table 17, the higher the number indicating the degree of non-conservative behaviour.

Of all the sites where there was significant mixing between surface water and groundwater, most sites had significantly negative differences between observed and predicted concentrations, indicating non-conservative behaviour of both nitrate and sulphate and a loss from the water during surface water infiltration.

In particular large negative differences between observed nitrate and predicted nitrate (-48% to -98%) identifying significant loss of nitrate were observed in piezometers at CF and CS sites in all sampling events. Measured sulphate was also lower than predicted, indicating that both elements are depleted in the hyporheic zone. The difference was generally lower than for nitrate and varied greatly with the gradient depth (9% to 100%).

At Be, a percentage of surface water in the bed sediment greater than 10% ($Q_{sw}/Q_{GW}>0.10$) was measured only for piezometer Be-HZ03, in Apr-18. Here, the nitrate measured was between 2 - 4% less than what is expected with conservative behaviour, however with a depletion close to the analytical error of +/- 5%, it is therefore considered not significant. On the contrary, a 12% increase compared to the sulphate expected might suggest a source of sulphate other than surface water at depth of 20 cm of piezometer Be-HZ03.

At LH site, at the shallow depth of 10 cm for both LH-HZ01 and 02, nitrate was depleted (-29% and -40% in April), while the sulphate difference, although negative (-4%), was close to the analytical error and therefore not significant.

Table 17 Calculations of mixing ratios between surface water and groundwater in the hyporheic porewater based on chloride and sodium, and percent difference between concentrations of "measured" and "expected" nitrate and sulphate in the hyporheic porewater. The expected concentration is calculated based on the mixing ratio assuming nitrates and sulphates behave conservatively like chloride. A negative number represents a loss of nitrate or sulphate from the water. Only at locations where the mixing ratio was greater than 0.1, the differences were calculated.

Site	Q_{sw}/Q_{GW} [Cl]	Q_{sw}/Q_{GW} [Na]	NO_3 meas	NO_3 exp	SO_4 meas	SO_4 exp	$100*(NO_{3meas} - NO_{3exp})/NO_{3exp}$	$100*(SO_{4meas} - SO_{4exp})/SO_{4exp}$
April 2018								
Be								
Be_HZ03_B	0.96	0.86	7.88	8.02	232	230	*-2%*	*1%*
Be_HZ03_R	0.51	0.49	4.18	4.36	191	171	*-4%*	*12%*
LH								
LH_HZ01_B	0.43	0.40	2.21	3.13	177	183	*-29%*	*-4%*
LH_HZ02_B	0.21	0.17	0.98	1.63	111	116	*-40%*	*-4%*
CF								
CF_HZ01_B	0.63	0.56	0.15	4.60	234	304	*-97%*	*-23%*
CF_HZ01_R	0.54	0.45	0.15	3.94	203	288	*-96%*	*-42%*
CF_HZ01_G	0.43	0.35	0.15	3.16	196	269	*-95%*	*-37%*
CF_HZ02_B	1.00	0.93	3.73	7.20	333	367	*-48%*	*-9%*
CF_HZ02_R	1.10	1.11	0.15	7.90	119	402	*-98%*	*-70%*
CF_HZ02_G	0.23	0.32	0.15	1.74	4	100	*-91%*	*-96%*
CS								
CS_HZ01_B	<0.10	<0.10						
CS_HZ01_R	<0.10	<0.10						
CS_HZ01_G	<0.10	<0.10						
CS_HZ02_B	1.40	0.97	0.15	6.91	26	357	*-98%*	*-93%*
CS_HZ02_R	1.20	1.14	0.15	8.13	144	414	*-98%*	*-65%*
CS_HZ02_G								
August 2018								
Be								
Be_HZ03_B	<0.10	<0.10						
Be_HZ03_R	<0.10	<0.10						
LH								
LH_HZ01_B	<0.10	<0.10						
LH_HZ02_B	0.61	0.47	0.95	1.13	379	421	*-16%*	*-10%*
CF								
CF_HZ01_B	1.24	0.81	0.30	2.17	484	675	*-86%*	*-28%*
CF_HZ01_R	1.08	0.69	0.30	1.90	396	624	*-84%*	*-37%*
CF_HZ01_G	0.60	0.32	0.30	1.12	292	470	*-73%*	*-38%*
CF_HZ02_B	1.03	0.84	0.30	1.83	411	619	*-84%*	*-34%*
CF_HZ02_R	1.58	1.03	0.30	2.72	434	941	*-89%*	*-54%*
CF_HZ02_G	2.05	0.44	0.30	3.49	0.5	1222	*-91%*	*-100%*
CS								
CS_HZ01_B	0.49	0.33	0.30	1.46	28	291	*-79%*	*-91%*
CS_HZ01_R	0.51	0.32	0.30	1.52	21	303	*-80%*	*-93%*
CS_HZ01_G	0.30	0.18	0.15	0.95	1	182	*-84%*	*-99%*
CS_HZ02_B	1.24	1.00	0.30	3.46	337	722	*-91%*	*-53%*
CS_HZ02_R	1.64	0.94	0.30	4.55	23	960	*-93%*	*-98%*
CS_HZ02_G	0.15	0.07	0.15	0.56	0.3	90.7	*-73%*	*-100%*

Site	Q_{sw}/Q_{GW} [Cl]	Q_{sw}/Q_{GW} [Na]	NO_3 meas	NO_3 exp	SO_4 meas	SO_4 exp	100*(NO_{3meas} - NO_{3exp})/NO_{3exp}	100*(SO_{4meas} - SO_{4exp})/SO_{4exp}
February 2019								
Be								
Be_HZ03_B	nd	nd						
Be_HZ03_R	nd	nd						
LH								
LH_HZ01_B	<0.10	<0.10						
LH_HZ02_B	nd	nd						
CF								
CF_HZ01_B	0.23	0.45	0.30	2.46	89	273	**-88%**	**-67%**
CF_HZ01_R	0.07	0.35	0.30	1.98	57	228	**-85%**	-75%
CF_HZ01_G	-0.16	0.16	0.30	1.09	53	143	**-72%**	-63%
CF_HZ02_B	nd	nd						
CF_HZ02_R	nd	nd						
CF_HZ02_G	nd	nd						
CS								
CS_HZ01_B	nd	nd						
CS_HZ01_R	nd	nd						
CS_HZ01_G	nd	nd						
CS_HZ02_B	0.92	0.88	0.3	5.7	175	471	**-95%**	-63%
CS_HZ02_R	0.74	0.75	0.3	6.8	0.5	376	**-96%**	-100%
CS_HZ02_G	0.30	0.23	0.2	11.3	0.3	151	**-99%**	-100%

* only samples with Q>0.1 are shown.

6.7   CHARACTERISATION OF THE NATURE OF SUBSURFACE FLOW

6.7.1   Stoichiometry of carbonate dissolution and potential chemical reactions

The porewater analysis is here discussed with reference to the stoichiometry of carbonate/gypsum dissolution.

When the porewaters are plotted on $[Ca^{2+}+Mg^{2+}]/[HCO_3^-]$ scatterplot, most of the waters align between the 1:1 and the 2:1 equivalent ratio lines (Figure 33). Three patterns are evident in Figure 33:

   a. BP porewaters align along the 2:1 equivalent ratio $[Ca^{2+}+Mg^{2+}]/[HCO_3^-]$ line.
   b. CF and CS porewaters align along the 1:1 equivalent ratio $[Ca^{2+}+Mg^{2+}]/[HCO_3^-]$ line.
   c. Be and LH porewaters plot between the two lines.

Figure 33 also shows how porewater samples from Rushyford Beck and WB3 plot close to CF and CS sites, while WB2 close to LH and Be sites. This is consistent with the clustering results.
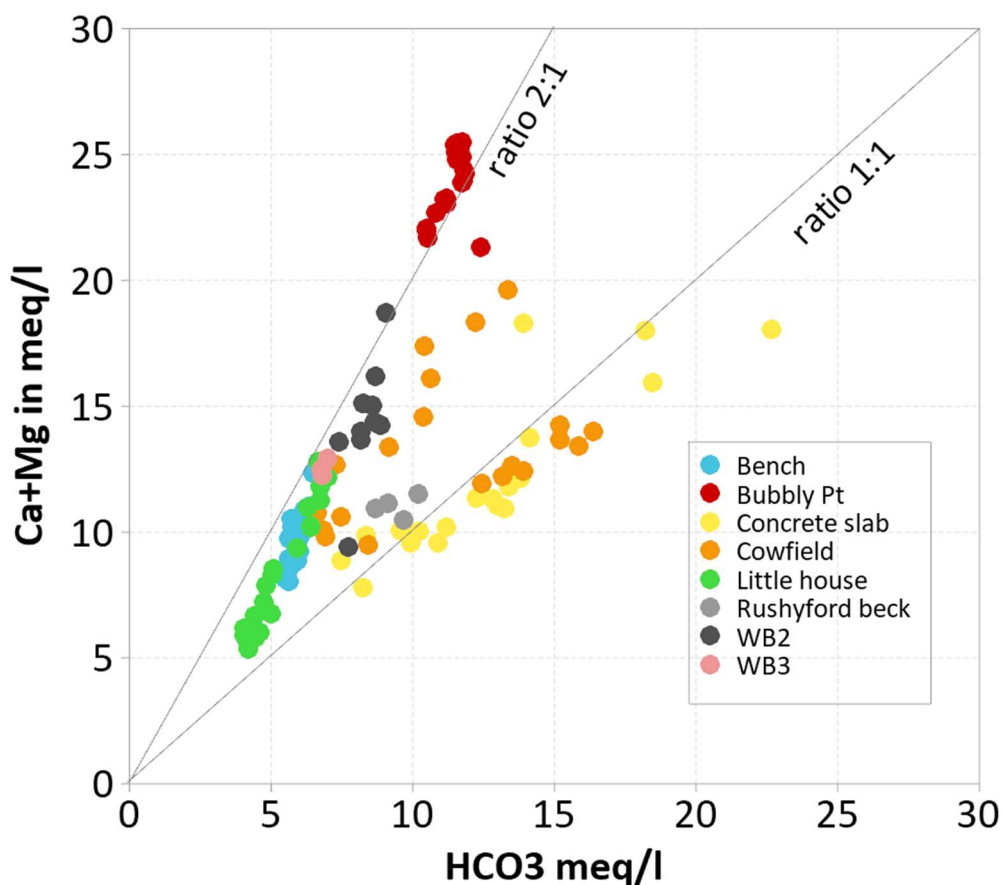
Figure 33 Ca+Mg in meq/l plotted against alkalinity as HCO_3 (in meq/l).

6.7.1.1 EQUIVALENT RATIO $[CA^{2+}+MG^{2+}]/[HCO_3^-]$ OF 2:1

BP porewaters, as well as Bubbly Spring, with a $[Ca^{2+}+Mg^{2+}]/[HCO_3^-]$ equivalent ratio of 2:1, have also high SO_4, high Mg contents and a Ca/Mg molar ratio close to 1 (Figure 34, Figure 35). These waters are also distinctively with a lower pH range (6.6-6.9) compared to the other sites. An equivalent ratio $[Ca^{2+}+Mg^{2+}]/[HCO_3^-]$ of 2:1 is the theoretical predicted equivalent ratio of the dissolution of dolomite in presence of acidic water, following the reaction:

(1) $CaMg(CO_3)_2 + 2H^+ \rightarrow Ca^{2+} + Mg^{2+} + 2HCO_3^-$
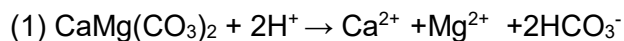
A source of acidity to drive reaction (1) can come from coal mine water due to the oxidation of pyrite according to various stages (Rose and Cravotta 1998) given as:

(2) $FeS_{2(s)} + 3.5\ O_2 + H_2O = Fe^{2+} + 2SO_4^{2-} + 2H^+$

(3) $Fe^{2+} + 0.25O_2 + H^+ = Fe^{3+} + 0.5\ H_2O$

(4) $FeS_{2(s)} + 14\ Fe^{3+} + 8H_2O = 15Fe^{2+} + 2SO_4^{2-} + 16H^+$

(5) $Fe^{3+} + 3H_2O = Fe(OH)_{3(s)} + 3H^+$
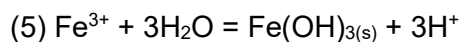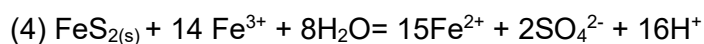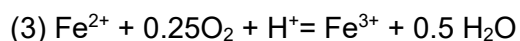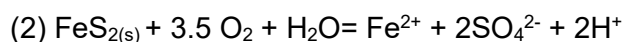
Hydrolysis and precipitation of iron hydroxides, denoted as $Fe(OH)_3$, would account for the low dissolved Fe content of the final water.

Another plausible water – rock interaction process to account for the above stoichiometry and major element chemistry of the Bubbly Spring and BP porewaters is dedolomitisation. The process of dedolomitisation may occur in aquifers containing dolostones associated with gypsiferous layers and consists of dolomite dissolution and concurrent precipitation of calcite, driven by dissolution of gypsum:

(6) $CaMg(CO_3)_2 + CaSO_4 .2H_2O + H_2CO_3 \rightarrow CaCO_3 + Ca^{2+} + Mg^{2+} + SO_4^{2-} + 2HCO_3^- + 2H_2O$

Plummer et al. (1980) illustrated the dominant groundwater reactions in the dedolomitisation of the Madison aquifer resulting in an increase in both calcium, magnesium as sulphate increases accompanied by a decrease in pH. The process was described as follows: "the dedolomitisation processes begins with the dissolution of calcium sulphates (anhydrite in the Madison aquifer) adding calcium to the recharge water near saturation with calcite and dolomite, and causing precipitation of calcite. Calcite precipitation causes the pH to decrease (due to H^+ released from HCO_3^- during incorporation of CO_3^{2-} in calcite). The decrease in pH increases the proportion of H_2CO_3 * (=H_2CO_3 + CO_2) in solution and thus increase the PCO_2. The decrease in CO_3^{2-} concentration with decreasing pH causes the water to be undersaturated with respect to dolomite, which leads to dolomite dissolution and an increase in dissolved magnesium. The mass of anhydrite and dolomite dissolved in this dedolomitisation process exceeds the mass of calcite precipitated, resulting in a net increase in dissolved calcium. Saturation or slight oversaturation with respect to both calcite and dolomite is expected".

In summary, the composition of BP spring and porewaters Ca-SO_4 type waters (Ca and Mg as the major cations in roughly equal equivalents, SO_4 and HCO_3 as the major anions at a roughly 2:1 ratio (equivalent ratios) and (Ca+Mg): HCO_3 at 2:1 (equivalent ratios)) suggests that the dissolution of dolomite is the predominant process in the evolution of the water. High sulphate content could be due either to gypsum dissolution and dedolomitisation and/or to the oxidation of pyrite/coal mine drainage and reaction with dolomitic rocks in the flow path. Gypsum is abundant in the Permian Magnesian Limestone aquifer while pyrite is present in the Coal Measures strata, and mass-balance modelling allows for both possibilities, as shown above. The very low iron concentration (< 10 µg/l) of BP waters (Figure 37) is problematic to be explained in the context of acid neutralisation of an iron-rich mine water plume through the dissolution of dolomite, as groundwater anoxic conditions (BP: DO of 0 mg/l) would have prevented the loss of iron from solution, unless a much more complicated flow path exists responsible for iron loss (adsorption?). However, iron-poor composition of Coal Measures aquifers is not unknown.

6.7.1.2 EQUIVALENT RATIO [Ca^{2+}+Mg^{2+}] / [HCO_3^-] OF 1:1

An equivalent ratio [Ca^{2+}+Mg^{2+}] / [HCO_3^-] of 1:1 suggests instead the dissolution of dolomite in presence of dissolved CO_2, typical of percolation through the soil and upper unsaturated zone, according to the reaction:

(7) $CaMg(CO_3)_2 + 2H_2O + 2CO_2 \rightarrow Ca^{2+} + Mg^{2+} + 4HCO_3^-$

CF and CS porewaters show a greater alkalinity than BP porewaters and their stoichiometry could be explained by reaction (7).

An alternative explanation for the observed water chemistry could be that incipient microbial sulphate reduction is occurring in the near sub-surface, since this process generates bicarbonate alkalinity. The low SO_4 concentrations does not contradict this possibility.

When the EA Magnesian Limestone monitoring borehole data are plotted on the $[Ca^{2+}+Mg^{2+}]/[HCO_3^-]$ scatterplot, most of the waters align broadly with the Woodham Burn porewaters and surface waters (Figure 38 and Figure 39), suggesting the baseline flow contribution of the Permian aquifer to the burn.

A high concentration of calcium, magnesium and sulphate in groundwater and surface water is ambiguous in terms of relation to specific rock alteration reactions and sources of sulphate. In some cases the study of sulphur isotopes could help to track the source of sulphate from coal mine drainage (Gammons et al. 2013) or distinguish sulphates either from Coal Measures strata or evaporites (Bottrell et al. 2006). If future sulphur isotope application is undertaken in our study area, consideration should be given to the recharge model of mine water. The White Young Green (2006) report describes several distinct hydro-geological zones in the area south of the Butterknowle Fault, based on the principal mining blocks and the relative piezometric heads in the mine workings and Permian aquifer. Depending on the hydraulic regime, either inflow from the mine workings into the overlying Permian aquifer or inflow from the Permian recharging the mine workings are both possible. If mine water is recharged from the overlying Permian limestone by way of discontinuities, mine water might receive sulphate from gypsum present in the Magnesian Limestone formations, imposing the gypsum related-sulphur isotope signature on the mine water.
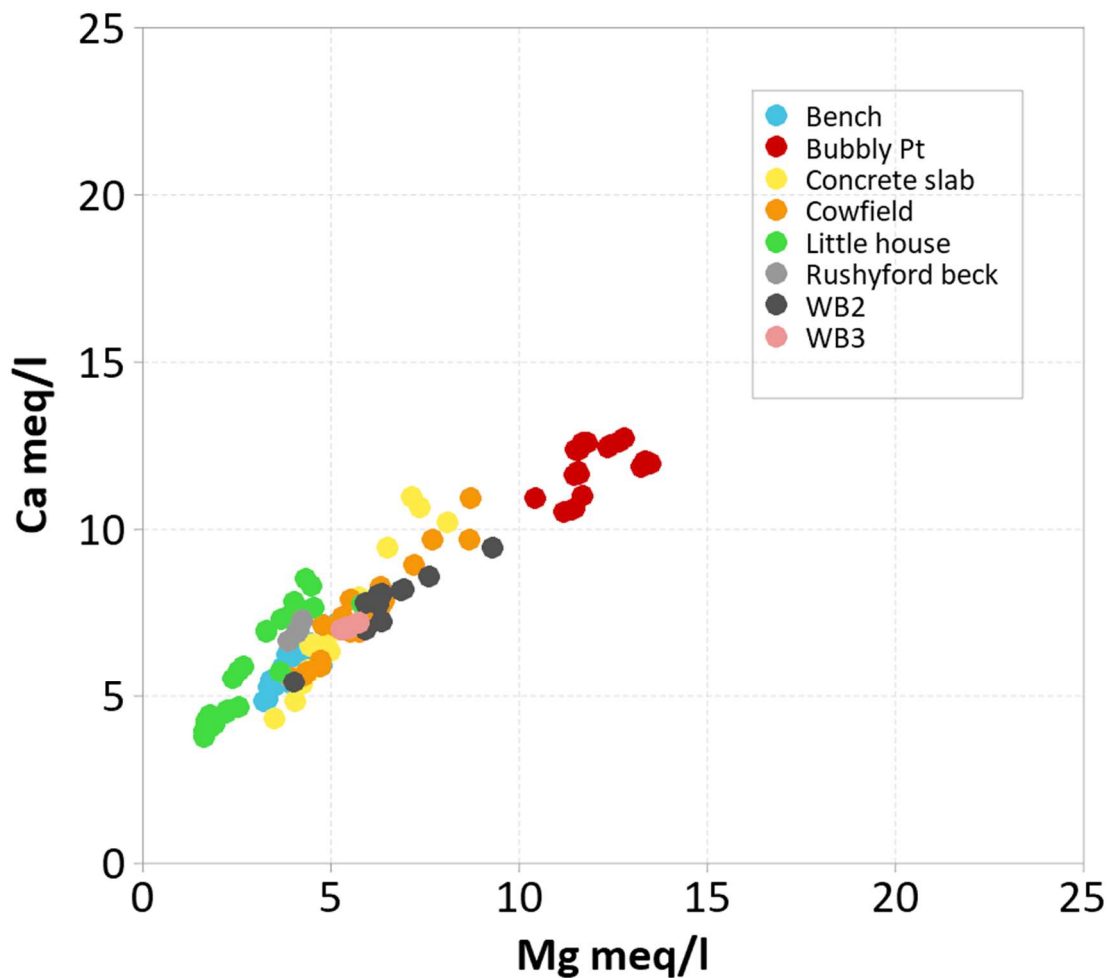
Figure 34 Ca (in meq/l) plotted against Mg (in meq/l).
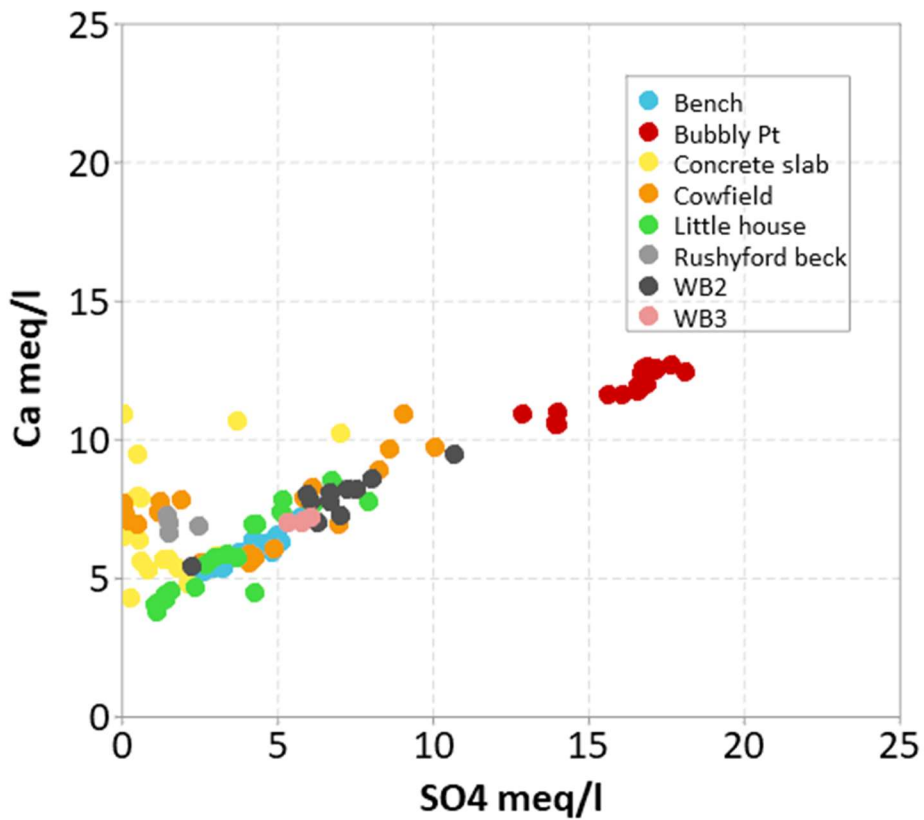
Figure 35 Ca (in meq/l) plotted against SO_4 (in meq/l).
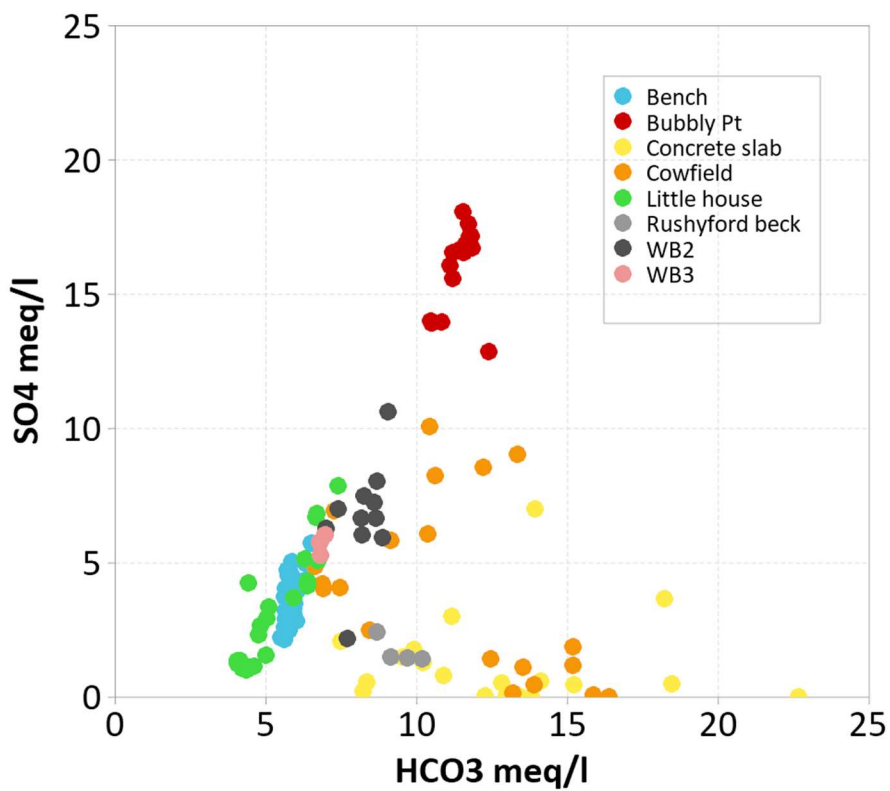
Figure 36 SO_4 (in meq/l) plotted against HCO_3 (in meq/l).
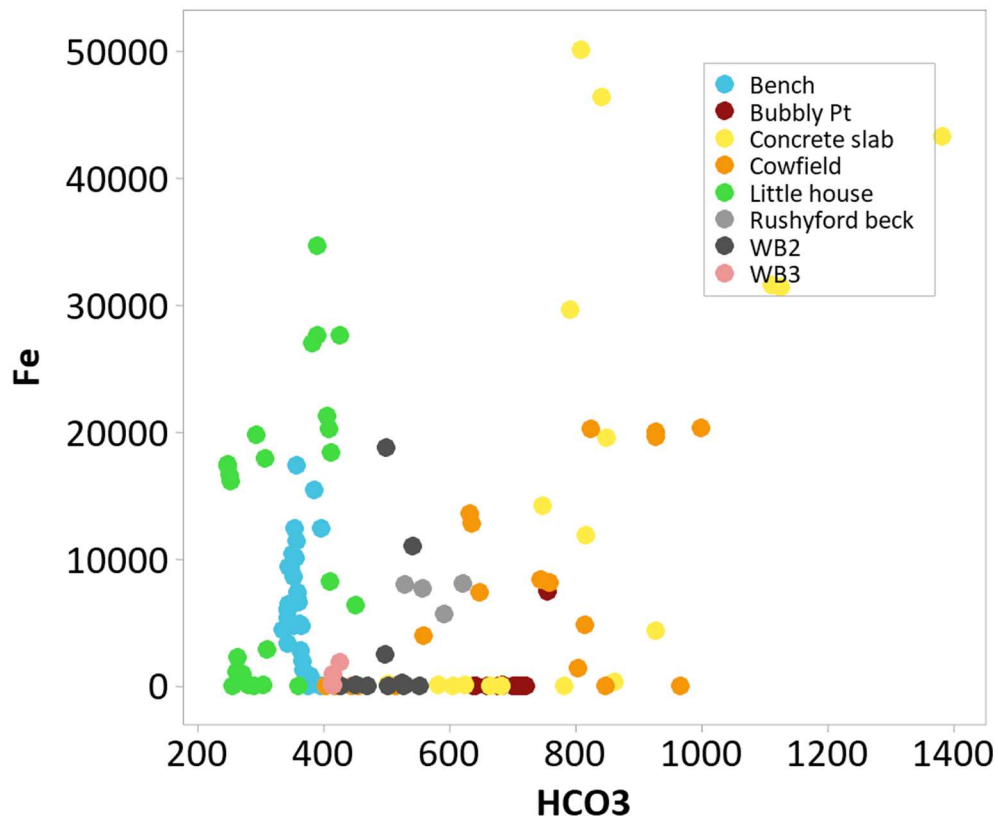
Figure 37 Fe (in μg/l) plotted against alkalinity as HCO$_3$ (in mg/l).
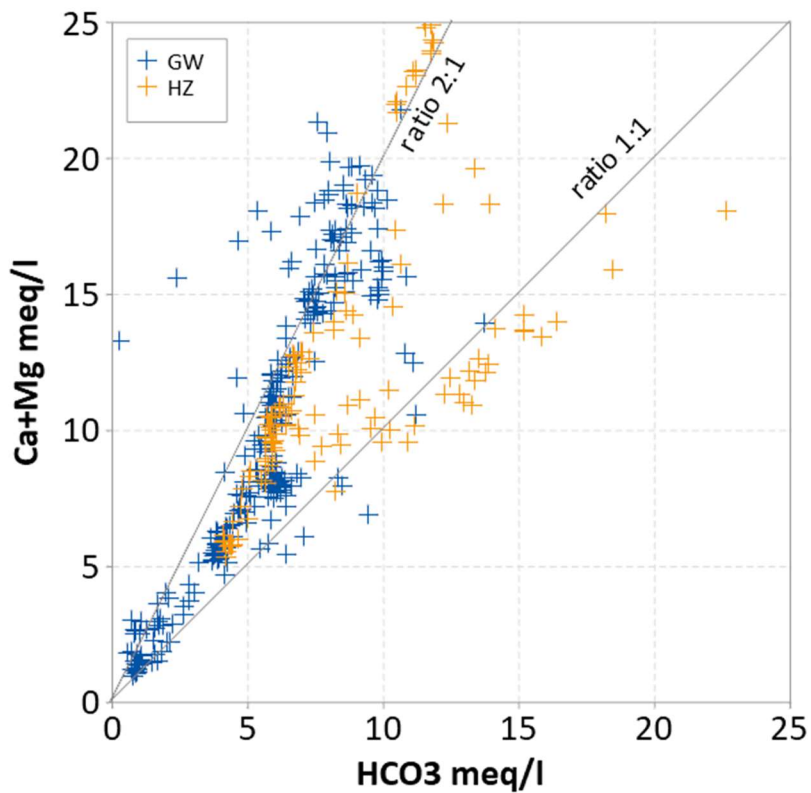
Figure 38 Ca+Mg (in meq/l) plotted against alkalinity as HCO$_3$ (in meq/l) in EA borehole monitoring sites (GW) and Woodham Burn porewater (HZ).
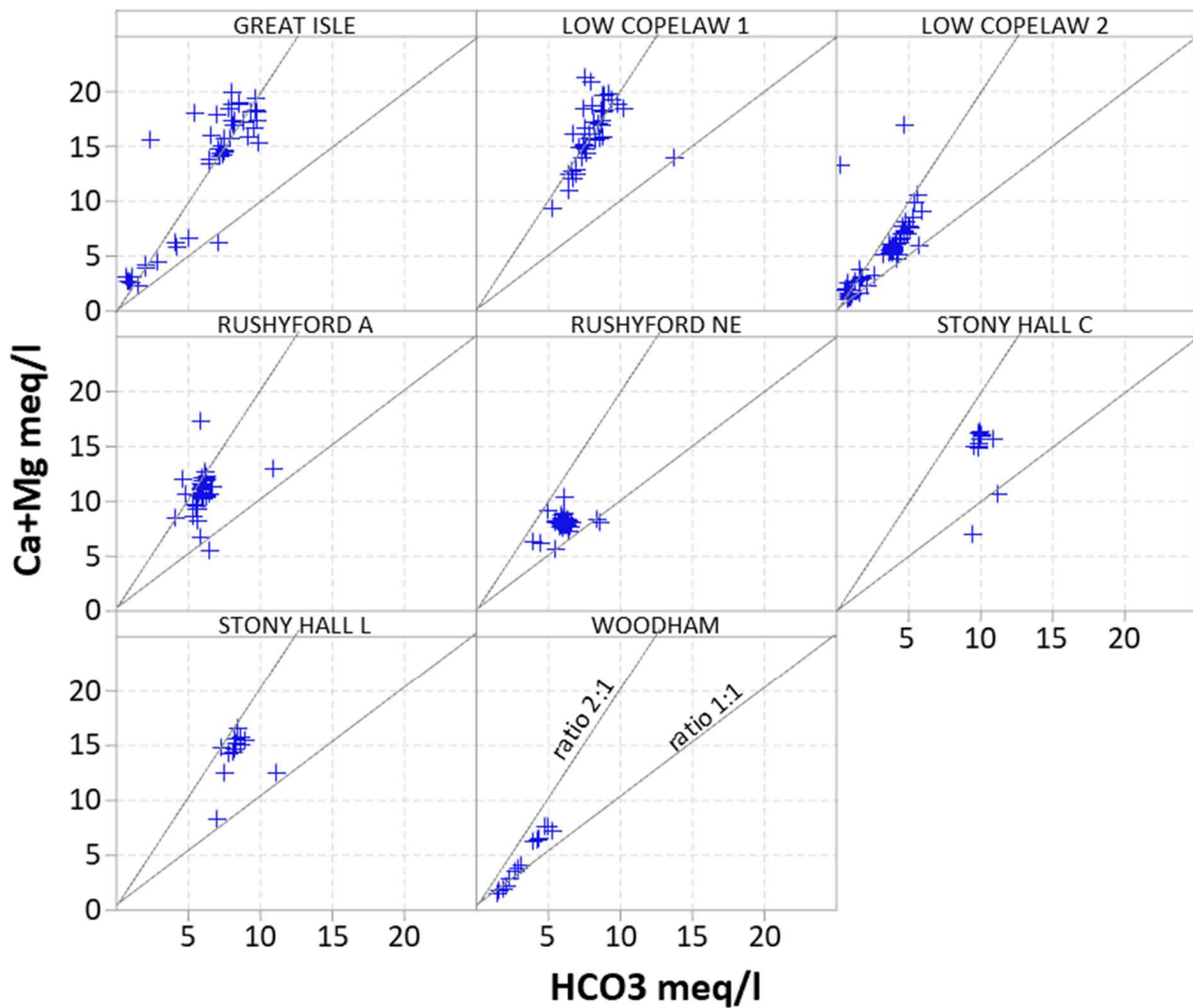
Figure 39 Ca+Mg (in meq/l) plotted against alkalinity as HCO$_3$ (in meq/l) in EA borehole monitoring sites, separated by site.

6.8 HYDROCHEMISTRY OF THE DEEP POREWATER

In order to identify the source of groundwater by hydrogeochemical approach, we investigated the major, minor and trace elements in the deep porewater (90 cm sediment depth), as it is less affected by hyporheic flow exchange and more representative of the shallow groundwater.

The investigation requires a detailed knowledge of end-members, i.e. mine water, Magnesian Limestone, surface runoff. However, comparison of the chemical analysis of our study with historical data was made difficult by insufficient analysis of the trace element data available. The work of Edmunds (1975) on brines provides trace element concentrations in the Coal Measures of northeast England. However it is thought that the mine water inflows into the Permian are more shallow mine waters. A limited dataset of boreholes analysed as part of Phase 1 is available (Palumbo-Roe, 2019).

Nevertheless there are sufficient trace element variations within the samples that have a potential diagnostic value as source or pathway indicator. These are highlighted in the following figures and tables.

Table 18 Statistics for deep porewater composition (depth 90 cm) at each site.

Variable	Site	N	Mean	StDev	Minimum	Median	Maximum
Field Eh (mV)	Be	7	45	200	-144	-98	328
	BP	4	338	108	177	390	396
	LH	7	115	221	-115	118	400
	CF	5	94	192	-96	101	369
	CS	5	141	187	-115	87	350
DO (mg/l)	Be	7	2.7	0.4	2.0	2.9	3.2
	BP	3	4.6	1.9	3.2	3.9	6.8
	LH	7	2.4	0.7	1.6	2.2	3.2
	CF	5	3.8	1.6	2.1	4.1	5.4
	CS	5	2.6	1.2	0.6	3.0	3.8
Conductivity (μS/cm)	Be	7	855	53	801	833	928
	BP	4	2172	99	2080	2163	2280
	LH	7	810	257	591	655	1202
	CF	5	1254	114	1148	1264	1428
	CS	5	1031	207	715	1070	1225
pH	Be	7	7.04	0.24	6.78	6.96	7.47
	BP	5	7.03	0.49	6.65	6.84	7.90
	LH	7	6.82	0.17	6.63	6.78	7.14
	CF	5	7.24	0.19	7.01	7.17	7.46
	CS	5	7.28	0.25	6.98	7.31	7.58
Ca (mg/l)	Be	7	107	5	97	108	113
	BP	5	238	17	219	241	255
	LH	7	109	38	81	85	167
	CF	5	139	17	112	143	158
	CS	5	110	20	86	107	131
Mg (mg/l)	Be	7	43	4	39	42	49
	BP	5	146	14	126	143	163
	LH	7	31	15	20	21	54
	CF	5	61	6	52	62	67
	CS	5	51	6	42	51	59
Na (mg/l)	Be	7	13.23	1.70	11.80	12.70	16.80
	BP	5	81.70	6.01	72.80	81.90	89.70
	LH	7	12.84	7.33	7.00	8.20	24.40
	CF	5	41.60	4.32	37.20	40.20	47.70
	CS	5	23.03	4.98	16.20	22.00	29.40
K (mg/l)	Be	7	1.26	0.30	0.93	1.20	1.87
	BP	5	10.33	1.34	7.99	10.77	11.28
	LH	7	1.31	1.09	0.32	0.87	3.08
	CF	5	4.12	1.49	2.52	4.03	6.23
	CS	5	3.18	0.87	1.70	3.43	4.03
HCO3	Be	7	351	10	341	350	365
	BP	5	711	34	659	714	754

Variable	Site	N	Mean	StDev	Minimum	Median	Maximum
(mg/)	LH	7	307	71	245	270	410
	CF	5	677	182	419	758	847
	CS	5	631	148	455	663	791
Cl (mg/l)	Be	7	38.25	3.47	33.65	36.93	42.5
	BP	5	43.97	4.23	39.07	42.28	49.5
	LH	7	38.65	4.85	34.27	36.98	47.96
	CF	5	50.27	8.99	40.58	51.84	63.29
	CS	5	26.17	5.55	18.1	25.29	32.19
SO4 (mg/l)	Be	7	133	19	104	137	159
	BP	5	755	103	619	811	848
	LH	7	131	113	50	59	328
	CF	5	114	118	6.80	68	280
	CS	5	30.2	42	1.00	10	100
$N-NO_3$ (mg/l)	Be	4	0.03	0.00	0.03	0.03	0.03
	BP	4	0.16	0.07	0.07	0.17	0.24
	LH	4	0.03	0.00	0.03	0.03	0.03
	CF	3	0.05	0.02	0.03	0.03	0.07
	CS	4	0.07	0.07	0.03	0.03	0.17
NPOC (mg/l)	Be	7	3.50	0.84	2.14	3.51	4.62
	BP	5	3.57	5.05	0.62	1.29	12.52
	LH	7	8.02	8.47	3.17	4.46	26.76
	CF	5	8.51	2.89	4.99	9.35	11.48
	CS	5	7.50	1.72	5.70	6.80	9.45
Total P (mg/l)	Be	4	0.07	0.03	0.04	0.06	0.11
	BP	1	0.01	*	0.01	0.01	0.01
	LH	1	0.06	*	0.06	0.06	0.06
	CF	1	0.03	*	0.03	0.03	0.03
	CS	1	0.10	*	0.10	0.10	0.10
Si (mg/l)	Be	7	9.1	0.7	8.1	8.9	10.3
	BP	5	6.5	1.5	5.1	5.9	9.0
	LH	7	8.9	0.7	8.2	8.5	10.1
	CF	5	10.0	1.6	8.1	10.0	11.7
	CS	5	13.4	2.4	10.5	14.6	16.0
F (mg/l)	Be	7	0.43	0.10	0.33	0.40	0.60
	BP	5	0.34	0.05	0.28	0.34	0.41
	LH	7	0.16	0.03	0.12	0.17	0.20
	CF	5	0.34	0.15	0.18	0.28	0.56
	CS	5	0.38	0.17	0.24	0.30	0.63
Ba (µg/l)	Be	7	218.4	38.1	163.6	224.3	281.4
	BP	5	41.77	14.84	28.5	36.7	65.6
	LH	7	433.4	135.9	267.4	430.7	650.9
	CF	5	231.3	31.7	176.8	240.8	259.7
	CS	5	322.8	200.6	138.0	252.2	570.3
Sr (µg/l)	Be	7	232	12	207	234	243
	BP	5	954	163	768	984	1120

Variable	Site	N	Mean	StDev	Minimum	Median	Maximum
	LH	7	194	62	146	157	290
	CF	5	572	116	375	630	658
	CS	5	494	147	321	483	644
Mn (µg/l)	Be	7	807	343	399	882	1315
	BP	4	1176	2148	7	153	4392
	LH	7	1670	348	1270	1601	2159
	CF	5	1923	391	1389	1966	2369
	CS	5	1511	331	1252	1370	2078
Fe (µg/l)	Be	7	4815	1673	1937	4932	6639
	BP	5	1509	3349	4	12	7500
	LH	7	11215	9751	492	17354	20335
	CF	5	2729	3465	11	1417	8211
	CS	5	8841	13177	7	190	29702
Li (µg/l)	Be	7	10	2	8	10	13
	BP	5	160	36	105	162	204
	LH	7	4	1	3	4	5
	CF	5	36	2	33	38	38
	CS	5	23	5	18	21	30
Rb (µg/l)	Be	7	0.92	0.17	0.67	0.90	1.19
	BP	5	7.01	1.11	5.26	7.19	8.29
	LH	7	0.73	0.20	0.49	0.70	0.99
	CF	5	2.70	0.54	2.28	2.35	3.34
	CS	5	2.74	0.57	2.08	3.01	3.34
U (µg/l)	Be	7	0.12	0.12	0.02	0.07	0.36
	BP	5	4.04	0.30	3.59	4.04	4.33
	LH	7	0.08	0.06	0.03	0.05	0.19
	CF	5	1.10	0.60	0.37	1.17	1.94
	CS	5	0.40	0.65	0.02	0.17	1.55
SO4/Sr MolarRatio	Be	7	522	64	455	513	621
	BP	5	726	37	672	735	764
	LH	7	536	291	314	345	1032
	CF	5	201	214	10	97	473
	CS	5	77	120	2	24	285
Na/Cl Molar ratio	Be	7	0.5	0.1	0.5	0.5	0.6
	BP	5	2.9	0.4	2.4	3.0	3.3
	LH	7	0.5	0.2	0.3	0.4	0.8
	CF	5	1.3	0.2	1.1	1.4	1.5
	CS	5	1.4	0.0	1.3	1.3	1.4
Ca/Mg Molar Ratio	Be	7	1.5	0.1	1.4	1.5	1.6
	BP	5	1.0	0.1	0.9	1.0	1.1
	LH	7	2.3	0.3	1.9	2.3	2.5
	CF	5	1.4	0.1	1.3	1.4	1.5
	CS	5	1.3	0.1	1.2	1.3	1.5
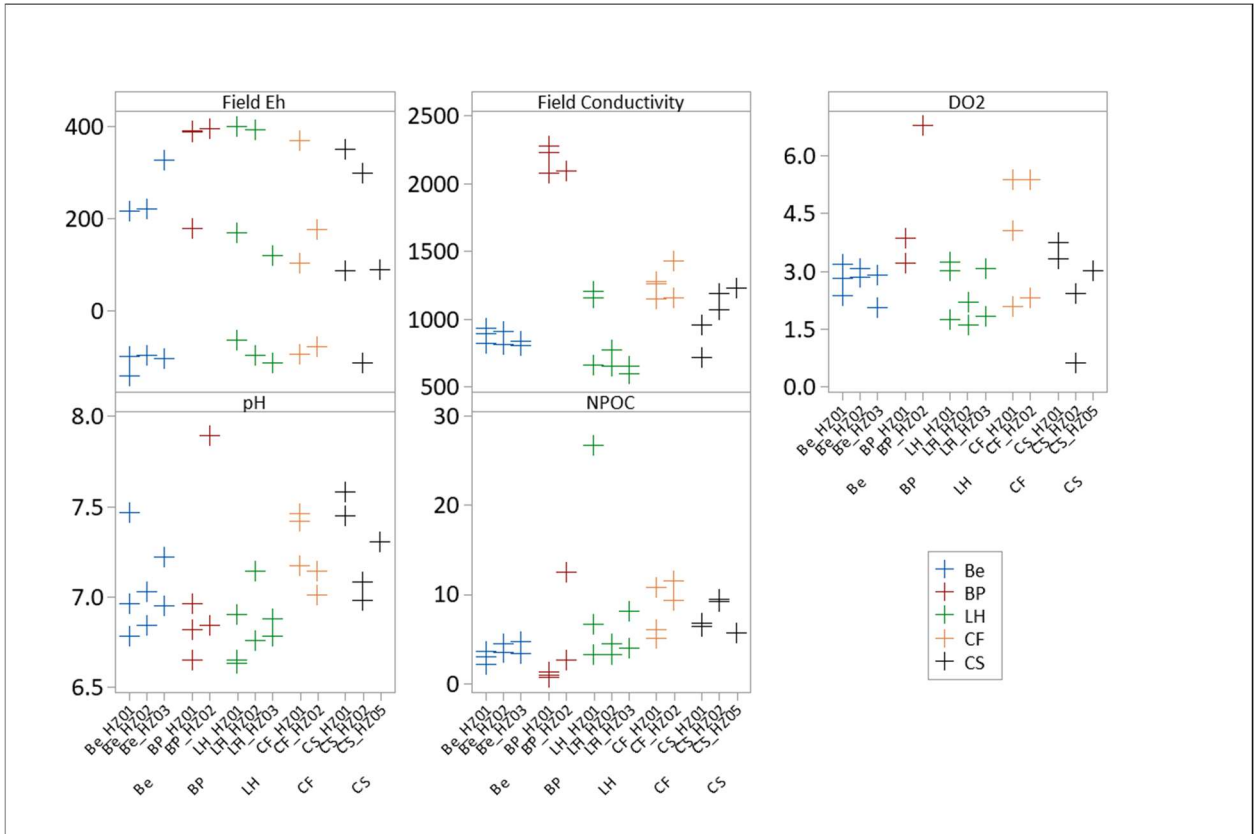
Figure 40 Individual value plot of field parameters at each minipiezometer depth of 90 cm. Units: Eh in mV, Conductivity in µS/cm, DO2 and NPOC in mg/l.
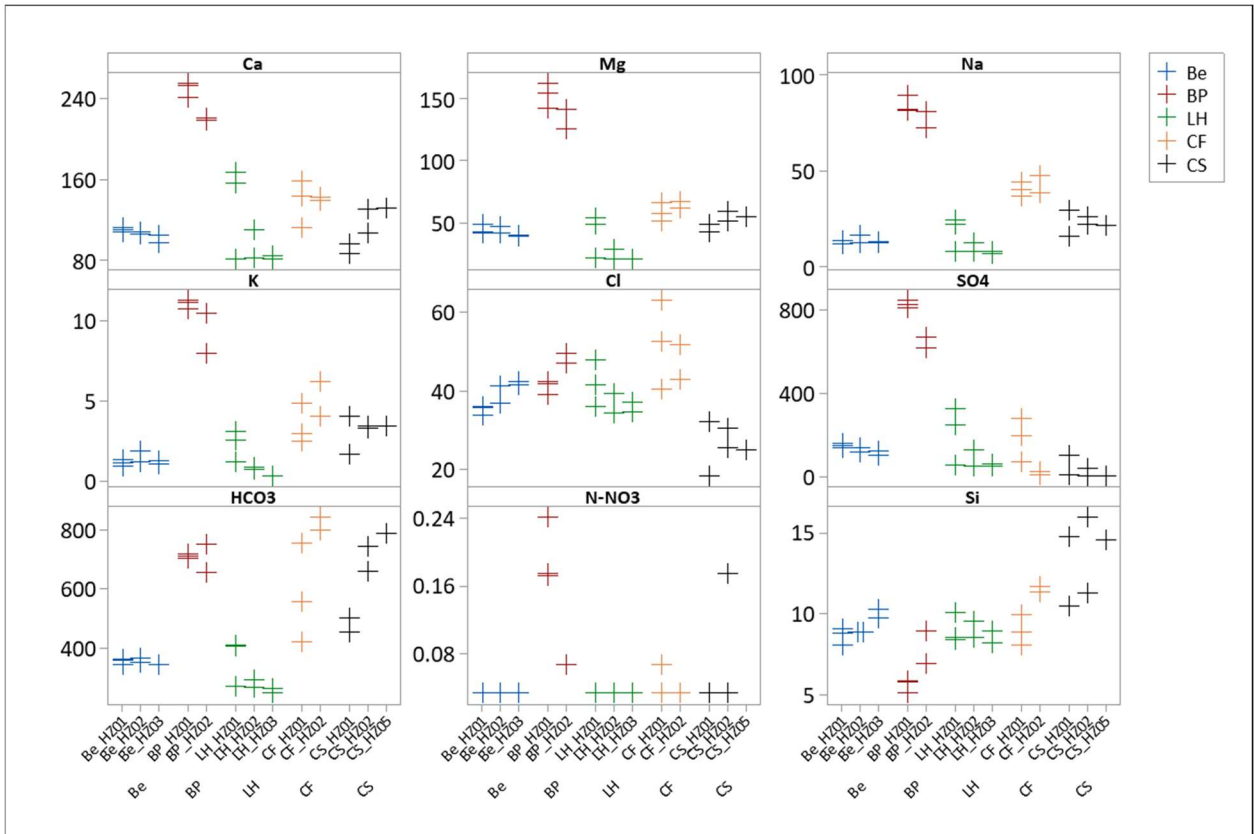
Figure 41 Individual value plot of major elements at each minipiezometer depth of 90 cm. Units: mg/l.
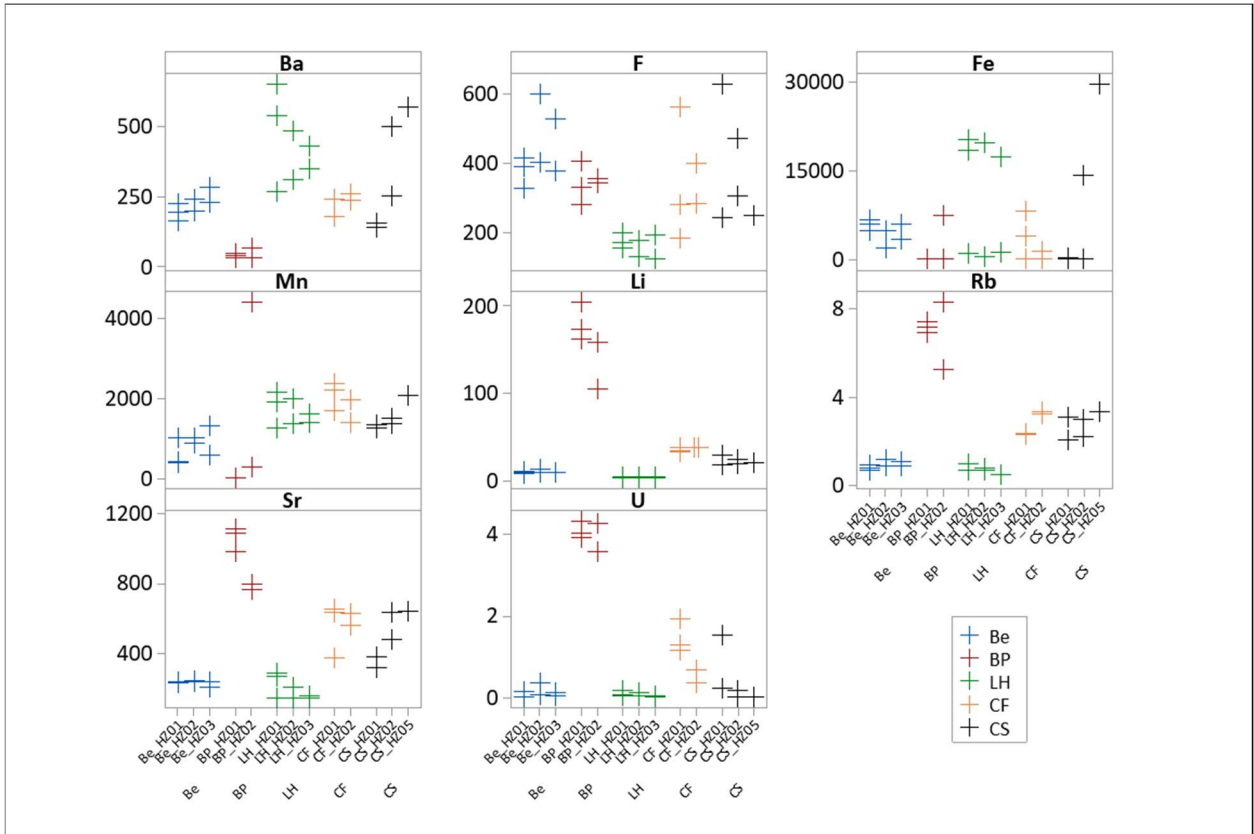
Figure 42 Individual value plot of selected minor and trace elements at each minipiezometer depth of 90 cm. Units: µg/l.
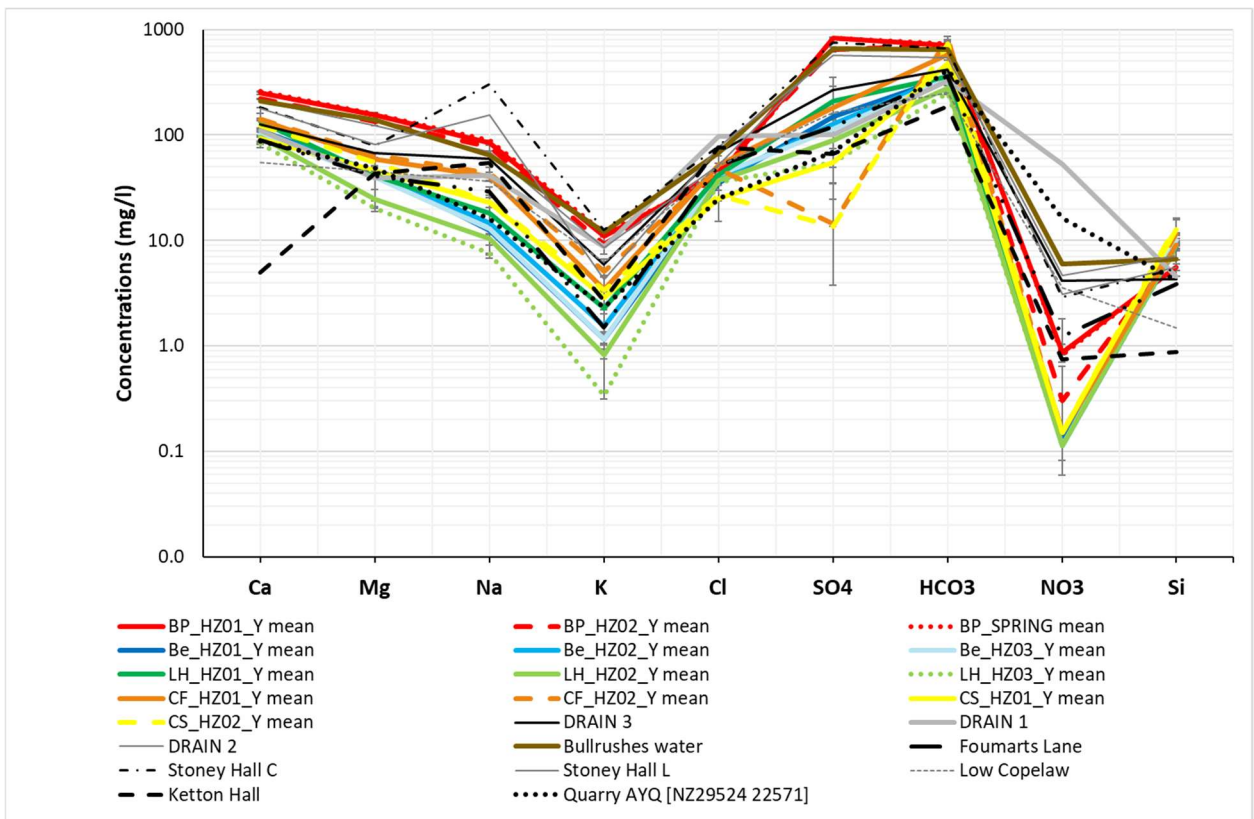
Figure 43 Schoeller diagram for major and minor elements in Woodham Burn deep porewaters and potential end-members.

67
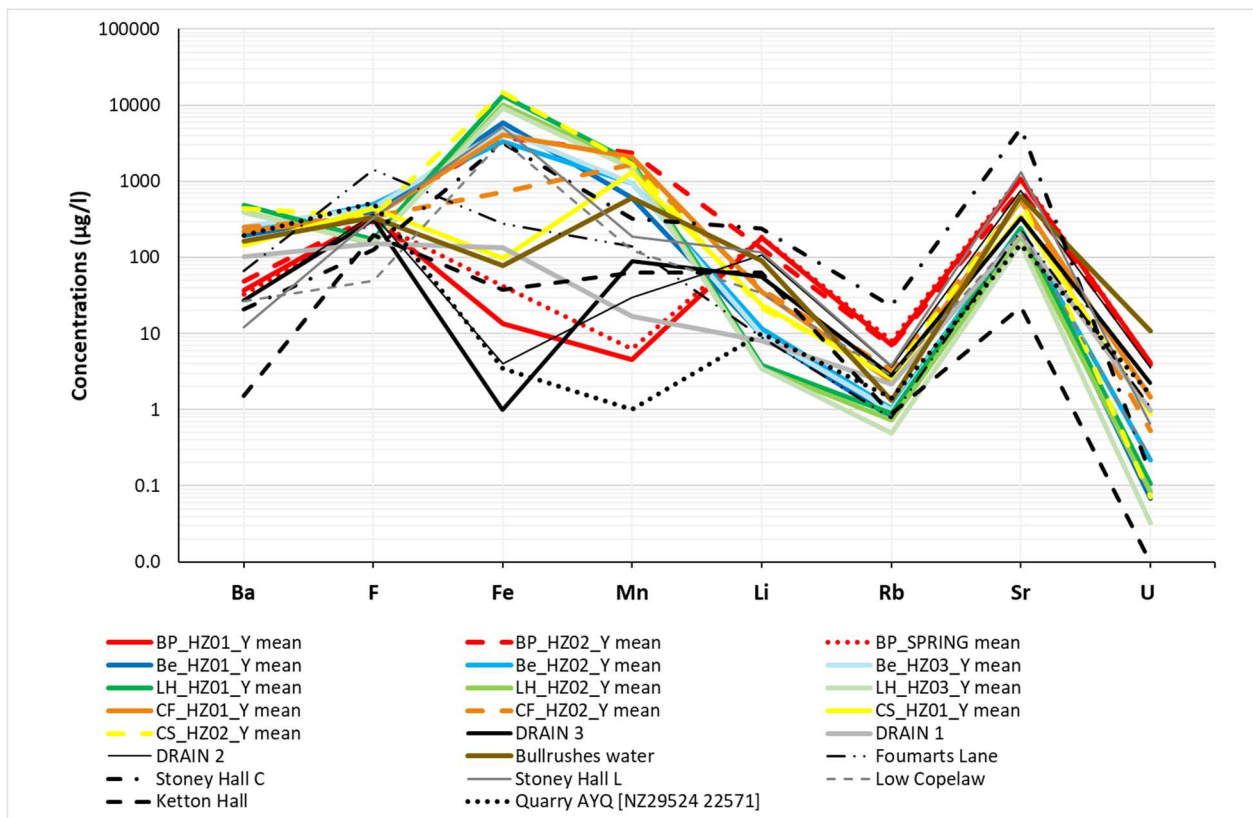
Figure 44 Schoeller diagram for minor and trace elements in Woodham Burn deep porewaters and potential end-members.

6.9 CLUSTERING/ SPATIAL VARIABILITY

The results of the clustering analysis summarise well the evidence collected so far; it was found that the porewater composition is not homogenous throughout the reach (Appendix 4).

The porewater spatial variability is shown as follows:

- The whole hyporheic zone at BP, the spring sampled at the same location, the spring water at the Bullrushes location and additional seepage (Drain 2) all cluster together in Cluster 1. All surface water at BP and most of the surface water downstream BP (except for April 2018) fall in the same group. The Stony Hall C borehole, monitoring the Coal Measures, also belongs to this cluster. The group has distinctively higher concentrations of Ca, Mg, Na, K, HCO_3, and SO_4 together with Sr, Li, Rb and U, compared to the other clusters, while it is lower in Si, Ba, Mn and Fe (cf. Table 18).
- Most of the porewater at location Be and all porewater at location LH grouped together in Cluster 2. The groundwater analyses from Foumarts Lane and Stillington OBH4 boreholes and from Aycliffe quarry also belonged to this cluster. The cluster has the highest Ba and the lowest Ca, Mg, Na, K, HCO_3, Cl, SO_4 as well as lower Sr, Li, Rb and U.
- Surface water during the April sampling event and some of the shallow porewaters at locations Be, CF and CS, also sampled during the same round, group together with the porewaters previously sampled at WB/3 and Rushyford Beck. Seepage (Drain 1 and Drain 3) also belong to this group, forming all together Cluster 3. The EA monitoring boreholes analysed by BGS (Ketton Hall, Low Copelaw, Stillington OBH2 and Stony Hall L) also all belong to this cluster. The Cluster is the highest in Cl, Na and K.
- The hyporheic zone at location CS and CF groups together with the porewaters previously sampled at WB/2 and Rushyford Beck, forming Cluster 4. This cluster has the highest HCO_3, Si, Mn and Fe, while relatively low SO_4.

The results show that most of the surface water at and downstream of BP is similar to the spring itself at BP, suggesting a strong groundwater contribution to the overall surface water system of Woodham Burn. It is worthwhile noticing though that the surface water from the April 2018 sampling grouped to land pipe drainage enriched in Na, Cl and K, which might have captured a greater runoff contribution to the Woodham Burn.
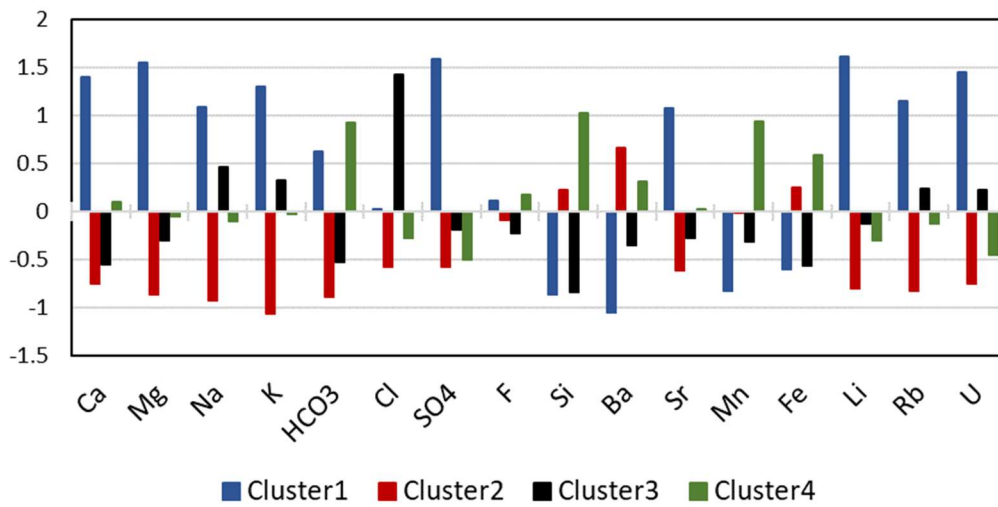
Figure 45 Z-scores for the cluster centroids. The centroids show the differences between clusters for key determinants.

7 Conclusions

The major findings of the study are summarised below.

The quality of surface water and shallow groundwater

The quality of surface water and shallow groundwater in the Woodham Burn was monitored during three sampling events: in April 2018, August 2018, and February 2019. The study reach covers the 500 m stretch upstream of the confluence with Rushyford Beck. A previous survey of water quality carried out by the Environment Agency in 2015 highlighted spring and pond features relatively enriched in sulphate (~ 400 mg/l) in the reach upstream of our monitoring sites.

The burn was found to have sulphate concentrations in excess of the drinking water standard of 250 mg/l, with a median of 510 mg/l in the surface water, range 235-790 mg/l; hyporheic porewater had a median sulphate concentration of 185 mg/l and a greater range from 0 to 870 mg/l.

Both spatial and temporal variability of water quality was significant as discussed in the following sections.

Hyporheic exchange flow (HEF)

At the sediment scale, stream water can move in and out of the sediment bed depending on permeability and location. From our network of piezometers we showed variation in the extent of HEF in the study reach. Evidence from vertical gradients of conservative elements, chloride and lithium, measured in each multilevel minipiezometer, and evidence from sediment temperature and water level logged data converge to indicate the near absence of HEF at the upstream sites Bench and Bubbly Point and clear HEF at the downstream sites Cowfield and Concrete Slab. Shallow intermittent HEF is present at Little House. The clear increase of HEF between the upstream points and two downstream monitoring points corresponds to the transition from alluvial to lacustrine deposits. As expected, there is no evidence of HEF at 1.4 m depth throughout the study reach.

Groundwater discharge locations

A longitudinal survey of vertical temperature profiling of the riverbed and conductivity of surface water, together with a solute mass balance approach from synoptic sampling of surface water, were used to infer potential stream groundwater inflow locations.

The sediment temperature survey indicated two areas of potential inflows into Woodham Burn:

-Bubbly Point: A very localised inflow of high-conductivity water (2000 µS/cm, with an increase of 708 µS/cm from the nearest upstream measurement). Temperature measurements at and near this location were limited due to gravel in the riverbed, but do not seem much lower than surface water temperatures (close to 10 °C). A discrete spring (Bubbly Spring) was found discharging through the stream bed and western stream banks. The homogenous vertical profiles porewater-surface water and water level, temperature logged data clearly indicate a gaining stream.

-Little House site: A wider stretch of suspected groundwater inflow indicated by lower subsurface temperatures (8.3–9.4 °C) than the surrounding sediments; the area coincides approximately with the area of change in superficial deposits.

The survey of surface water hydrochemistry confirmed that the stretch of the study corresponding to Bubbly Point was responsible for a 50% increase in the dissolved sulphate concentration compared to the nearest downstream point (Little House) in April 2018 and February 2019. A smaller percent change (20%) corresponded to the summer sampling (August 2018), with noticeably higher sulphate of the upstream surface water than in the other rounds. The fraction of this discharge in surface water was estimated between 0.2 to 0.4. Contrary to Bubbly Point, there was no significant change in SEC or other surface water measurements at Little House or other points along the study reach. However, the presence of other recharge areas cannot be

confirmed but not precluded on the basis of the stream chemistry survey approach only, given the stream chemistry-based method's assumptions and limitations.

It can also be said that the potential discharge area downstream of Bubbly Point is unlikely to originate from the same source as Bubbly Point.

An additional area potentially recharging sulphate to the stream, more diffuse in nature, was identified through analysis of the water-soluble fraction of soil samples collected by augers and bank seepage measurements and it corresponds to the northern banks upstream of the first monitoring point.

Nature of shallow groundwater

Most of the porewaters were of the $Ca-HCO_3$ type, and within the $Ca-HCO_3$ hydrofacies type. Some of the samples from Cowfield and Concrete Slab sites were relatively enriched in bicarbonate anions compared to the other sites. The exception to the calcium-bicarbonate facies is the porewater at Bubbly Point, which was a $Mg-SO_4$ water in the April and August 2018 sampling and a $Ca-SO_4$ type in February 2019. All the porewaters were oversaturated in calcite and dolomite and most of them also in gypsum, suggesting important water-rock interaction processes involving these minerals.

The composition of the spring and porewaters at Bubbly Point suggests that the dissolution of dolomite is a predominant process in the evolution of the water. High sulphate content could be due either to gypsum dissolution and dedolomitisation and/or to the oxidation of pyrite/coal mine drainage and reaction with dolomitic rocks in the flow path. Gypsum is abundant in the Permian Magnesian aquifer while pyrite is present in the Coal Measures strata, and mass-balance modelling allows for both possibilities as sources of sulphate. The very low iron concentration (<10 µg/l) of Bubbly Point waters is problematic in the context of acid neutralisation of iron-rich coal mine water through the dissolution of dolomite, as groundwater anoxic conditions (Bubbly Point DO of 0 mg/l) would have prevented the loss of iron from solution, unless a much more complicated flow path exists. However, iron-poor composition of Coal Measures aquifers is not unknown.

Cowfield and Concrete Slab porewaters show a greater alkalinity than Bubbly Point porewaters and their stoichiometry could be explained by the dissolution of dolomite in the presence of dissolved CO_2, typical of percolation through the soil and upper unsaturated zone. An alternative explanation for the observed water chemistry could be that incipient microbial sulphate reduction is occurring in the near sub-surface, since this process generates bicarbonate alkalinity. The low sulphate concentrations does not contradict this option.

When the EA Magnesian Limestone monitoring borehole data are plotted on the $[Ca^{2+}+Mg^{2+}]/[HCO_3^-]$ scatterplot, most of the waters align broadly along with the Woodham Burn porewaters and surface waters, suggesting the baseline flow contribution of the Permian aquifer to the Woodham Burn.

There are sufficient trace element variations within the water samples to have a potential diagnostic value as source or pathway indicators and additional insights come from the clustering of the observations based on the element chemistry. These are highlighted as follows:

- Bubbly Point spring and porewater, a $Mg-SO_4$ water type, are distinctively enriched in SO_4 (90 cm depth-porewater median 811 mg/l) together with Sr (median 984 µg/l) and the traces Li (median 162 µg/l), Rb (median 7.19 µg/l) and U (median 4.04 µg/l).

- The spring chemistry has strong similarities to water features in other locations in the burn, both upstream Bubbly Point (seepage Drain 2) and downstream (Bullrushes location). Also Stony Hall C borehole is similar to Bubbly Point waters.

- Most of the porewater at location Bench and all porewater at location Little House grouped together in a cluster. The groundwater analyses from Foumarts Lane and Stillington OBH4

boreholes and from Aycliffe quarry also belonged to this cluster. The cluster has the highest Ba and the lowest Ca, Mg, Na, K, HCO_3, Cl, SO_4 as well as low Sr, Li, Rb and U.

- The hyporheic zone at location Concrete Slab and Cowfield groups together with the porewaters previously sampled at WB/2 and Rushyford Beck. The group has the highest HCO_3, Si, Mn and Fe, while relatively low SO_4.

Natural attenuation

Evaluation of natural attenuation was carried out via comparison of conservative and non-conservative solute gradients. In most of the sites where there was sufficient HEF, both nitrate and sulphate showed various extents of non-conservative behaviour compared to chloride. In particular the most significant losses of nitrate were observed in piezometers at site Cowfield and Concrete Slab (-48% to -98%). Sulphate losses were generally lower than for nitrate and varied greatly with the gradient depth (9% to 100%) at those sites. Although nitrate and sulphate losses were observed during surface water downwelling in the studied hyporheic zone, a correspondent decrease in stream water concentrations was not evident.

Conceptual ground model

These findings appear to support the conceptual understanding and hypotheses of the conceptual model. The evidence suggests that the most likely sources of Sr, Li, Rb and U of Cluster 1 are the clays/ fireclays in the Carboniferous Coal Measures strata, as indicated by the Stony Hall C borehole, which falls within this cluster (see also Finkelman et al. 2019). This borehole comprises an observation well that extends to the Bottom Busty coal seam, potentially deriving water from the Coal Measures. The Glacial Till likely also contains derived Carboniferous material. However, it is unlikely that the Till is the primary source of these minor elements because they are not present in the other three clusters, supporting the hypothesis that the upstream end of Rushyford Beck receives a component of minewater discharge from mine water rebound. The low iron in the water at Bubbly Point together with the constancy of its groundwater chemistry suggest that this is a confined water contribution from the Coal Measures. It is most likely that this is rising on the unmapped extension of a fault as conjectured in the desk study.

It is plausible that the groundwater has become stratified (Nuttall and Younger, 2004) since the cessation of coal mine dewatering and that this might be reflected in the groundwater clusters that have been identified from this study. Stratification would potentially be disturbed by groundwater drawdown associated with groundwater abstractions, e.g. the groundwater abstractions shown on: https://magic.defra.gov.uk/MagicMap.aspx , some of which potentially impact on the research area.

Cluster 4, which primarily comprises the results of hyporheic zone samples, incorporates characteristics of carbonate-derived water, including the bicarbonate and mineral related Ba, Si and F (e.g. reticulate fluorspar described by Bridges and Pettigrew, 2013). This might be evidence of such stratification. The closer alignment of the stream with the strike of the bedrock, where it bends to flow in a south-south-east direction between the Little House and Concrete Slab sampling positions will facilitate groundwater seepage to the stream in areas where the superficial cover is thinner.

Clusters 2 and 3 are shown to have more similarity with Cluster 4 than with Cluster 1. To this end it should be noted that Cluster 3 comprises surface water and more of the higher groundwater level related sample results (April 2018), whilst Cluster 2 is more representative of hyporheic zone samples and lower groundwater conditions. Potentially this demonstrates either changing geochemical processes and or changing flow paths with changing groundwater conditions.

A modification to the conceptual understanding that results from this phase of research is the importance of the glacio-lacustrine deposits for HEF. This is likely facilitated by the laminated nature of the sediments with silty horizons forming flow paths and connectivity with the stream.

Uncertainties and Recommendations

The range of investigations has provided important baseline data to inform future river management strategies and has been instructive in improving the site conceptualisation in terms of potential contributions of deep groundwater, shallow groundwater or sub surface stormflow to the surface system and sulphate loads. However, it is clear that a number of uncertainties still remain and the following recommendations are suggested:

Sulphate-rich spring at Bubbly Point
Despite the similarity between the BP spring, and the Coal Measures borehole water, it has not been possible to positively identify the origin of the BP spring water. There remains significant uncertainty that the BP spring is related to the monitored plume of mine water within the Magnesian Limestone. To explain the physical processes underpinning the emergence of this groundwater enriched in sulphate and the origin of this sulphate, further investigation is needed. In particular residence time studies and isotope analysis of water and dissolved sulphate are recommended.

Sulphate-rich diffuse groundwater discharges

Besides localised upwelling of sulphate-rich groundwater discharging directly to the stream, we also have evidence of seeps and springs further away from the stream. To gain a broader perspective on groundwater discharge areas a spatial hydrochemical survey of springs and seeps in the catchment should be undertaken. Consideration should be given to trace elements and further comparison with hydrochemical data acquired in this study.

Natural attenuation

Although nitrate and sulphate losses were observed in the studied hyporheic zone in those losing sections of the reach (e.g. Cowfield and Concrete Slab sites), a correspondent decrease in stream water concentrations was not evident. To test the significance of hyporheic natural attenuation to improve the stream water quality at the catchment scale, surface water flow measurements combined with water quality analysis is recommended, which will enable the calculation of mass gains and losses, to identify the net flux integrated over the entire stream, over an extended section of the burn.

End-member characterisation

Cluster analysis has contributed to end-member characterisation. Consideration might be given to depth sampling in boreholes (i) to assess the extent of groundwater stratification and potentially (ii) to provide more data for end-member characterisation. Further to this, none of the boreholes sampled in this study was designed to monitor groundwater chemistry in the glacial till or the glacio-lacustrine deposits. Nested boreholes designed to better understand recharge and the baseline chemistry of groundwater in the superficial deposits would enable characterisation of this end-member. Parallel research to address the potential for sulphur isotope analysis could contribute to end-member characterisation. Further to this, the use of oxygen-18 and deuterium to distinguish SW/GW and look at evaporative effects offers potential for further cluster characterisation.

Connectivity with the superficial deposits

There is potential to test the hypothesised connectivity of the glacio-lacustrine deposits with the stream using tracer techniques during periods of falling groundwater levels.

Temporal mapping of springs

Spatial analysis of springs and discharge rates with mine water recovery to improve the conceptual understanding of the source term over time.

Upscaling the study

Uncertainty regarding catchment scale applicability can be addressed by using some of the key findings from this study. Specifically, the temperature and SEC surveys were efficient in detecting upwellings of groundwater, with potential for application utilising automated methods, potentially requiring a small boat with remote and logging methods.

Appendix 1 Temperature and conductivity survey of streambed and surface water

Table 19 Detailed results of the temperature and SEC survey.

Point	Easting (UTM)	Northing (UTM)	Riverbed composition	SW level (cm)	SEC (µS/cm)	T.SW (°C)	T10 (°C)	T20 (°C)	T30 (°C)	T35 (°C)	T40 (°C)	T45 (°C)	T50 (°C)	T60 (°C)
1	429508	526864	silty		1287	11.7	10.6	10.0	9.8		9.6		9.6	
2	429506	526867	silty	30	1284	11.7	10.3	10.1	9.9					
3	429505	526874	silty	30	1352	11.6	10.6	9.9	9.6	9.3				
4	429502	526880	silty	30	1363	11.6	10.2	10.2	9.9		9.5		9.2	
5	429499	526883	silty	50	1364	11.6	10.5	9.8	9.6	9.4				
6	429500	526887	silty	44	1389	11.6	10.4	9.7	9.3	9.2	8.8		8.6	
7	429498	526889	silty	30	1413	11.6	10.4	10.1	9.8		9.6		9.2	
8	429496	526895	silty	23	1407	11.5	10.2	9.6	9.2		8.8		8.5	8.4
9	429494	526900	sandy-gravel	18	1422	11.5	10.4	9.9	9.5		9.0		8.6	8.4
10	429493	526904	sandy	38	1429	11.5	10.7	10.3	9.9		9.7	9.5		
11	429498	526908	sandy	47	1427	11.5	10.3	10.0	9.8		9.6	9.4		
12	429488	526913	silty	41	1433	11.4	10.1	9.8	9.6		9.4			
13	429481	526915	silty	56	1435	11.4	10.3	10.0	10.0					
14	429484	526920		38	1440	11.4	10.2	10.0	9.9		9.6			
15	429482	526923	sandy	36	1443	11.4	10.3	10.1	9.9		9.7	9.6		
16	429482	526929	sandy	38	1418	11.4	10.5	10.1	9.9		9.8	9.7		
17	429480	526929	sandy	35	1459	11.3	10.5	10.3	9.8		9.5	9.3		
18	429478	526933	sandy	50	1448	11.3	10.6	10.1	9.8		9.6			
19	429476	526940	sandy	36	1434	11.3	10.5	10.1	9.9		9.7	9.4		
20	429475	526946		39	1442	11.2	10.1	9.6	9.3		9.2			
21	429472	526948	silty	43	1454	11.2	9.7	9.5	9.4					
22	429473	526952	gravel	54	1440	11.2	10.2	10.1	9.9					
23	429470	526955	gravel		1446	11.1	10.5	10.1	9.9					
24	429470	526961		85	1468	11.1	10.8							
25	429466	526970			1465	11.1	10.2	9.6	9.6		9.6	9.4		
26	429466	526976		25	1474	11.1	10.4	9.9	9.9					
27	429462	526983		15	1471	11.0	10.5	10.2	10.2					
28	429460	526988	sandy-gravel	19	1473	11.0	10.6	10.3						
29	429453	526998		29	1465	11.0	10.8							
30	429448	527001	gravel-cobble	31	1459	11.0	10.8							
31	429447	527009	gravel-cobble	29	1483	10.9	10.9							
32	429439	527016			1486	11.0	10.6	10.3	9.9	9.8			9.8	9.2
33	429433	527019	gravel-cobble	37	1492	10.9	10.5	10.2	9.9		9.7			
34	429429	527026	gravel-cobble	41	1439	10.9	10.3	10.0	9.8		9.5			
35	429429	527032	sandy	27	1471	10.9	10.2	10.1	9.8		9.4	9.1		
36	429425	527037	sandy	32	1439	10.9	10.2	10.1	9.8		9.4			
37	429417	527041	sandy	51	1501	10.9	10.5	10.1	9.7					

Point	Easting (UTM)	Northing (UTM)	Riverbed composition	SW level (cm)	SEC (µS/cm)	T.SW (°C)	T10 (°C)	T20 (°C)	T30 (°C)	T35 (°C)	T40 (°C)	T45 (°C)	T50 (°C)	T60 (°C)
38	429416	527047	sandy-gravel	31	1413	10.8	10.4	10.3	9.9		9.6		9.2	
39	429411	527053	sandy-gravel	46	1487	10.8	10.6	10.3	9.8		9.6			
40	429401	527063	gravel	28	1484	10.8								
41	429394	527068	gravel	28	1502	10.8	10.9							
42	429388	527074	gravel	25	1494	10.8	10.6	10.2	9.9		9.6		9.4	
43	429381	527080	sandy-gravel	35	1509	10.8	10.6	10.5						
44	429373	527086		31	1502	10.8	10.2							
45	429364	527087	sandy-gravel	20	1510	10.7	10.2	9.7	9.4		9.2		9.0	
46	429357	527095		16	1510	10.7	10.3	10.1	9.7		9.4		8.6	
47	429347	527100	sandy-gravel	45	1511	10.7	10.5	10.1	9.2		9.6		9.3	
48	429338	527105		35	1513	10.7	10.5	10.4	9.7		9.2		8.9	
49	429328	527108		39	1514	10.7	10.3	9.7	9.3		8.9		8.5	
50	429320	527115		23	1514	10.7	10.2	9.8	9.3		8.9	8.4		
51	429309	527118	sandy	28	1514	10.6	10.2	9.8	9.2		8.9		8.5	
52	429298	527123	gravel	34	1514	10.6	10.2	9.6	9.2		8.9		8.7	
53	429282	527128	gravel	25	1519	10.6	10.8	10.3	9.8		9.5		8.9	
54	429271	527136	gravel	35	1520	10.6	8.8	8.4	8.3		8.3			
55	429260	527138		46	1523	10.6	10.2	9.3	8.7		8.5			
56	429246	527134	gravel	14	1524	10.5	10.4	9.8	9.4					
57	429236	527139	gravel		1521	10.5	10.2	10.4						
58	429223	527146	gravel	53	1527	10.5	10.4	9.9	9.6					
59	429210	527148	boulders	19	1531	10.5	10.5							
60	429201	527145	boulders	20	1540	10.5								
61	429189	527146	boulders		1552	10.5								
62	429179	527150	boulders	29	1600	10.4	10.6							
63	429171	527147	boulders	29	2000	10.3	10.9	10.6	10.3					
64	429171	527147			1292		10.1	9.4						
65	429180	527128		52	1297	10.6	10.8	10.4	10.1					
66	429173	527118	gravel	57	1298	10.6	10.6	10.5						
67	429167	527111		36	1297	10.6	10.9	10.4	9.9		9.4			
68	429159	527103	gravel	47	1298	10.6	10.9							
69	429151	527097	sandy-gravel	36	1298	10.6	10.4	10.1	9.9		9.4			
70	429141	527089		38	1298	10.6	10.4	10.0	9.8		9.7			
71	429128	527064	sandy-gravel	25	1257	11.1	10.1	10.1						
72	429129	527053	sandy-gravel	25	1254	11.1								
73	429125	527046	sandy-gravel	25	1239	10.1	9.9	9.9						
74	429122	527039	sandy-gravel		1259	11.0								
75	429117	527032	silty-sandy	20	1260	11.0	9.9	9.8	9.8		9.6		9.3	9.1
76	429108	527026	silty-sandy	24	1260	11.0	10.0	9.8	9.8		9.6		9.4	9.1
77	429103	527012			1250	10.9	10.1	9.8	9.6					
78	429102	527000	boulders	13	1269	10.9								
79	429104	526985	boulders	26	1262	10.9								
80	429078	526974	silty-sandy	43	1260	10.6	10.2	10.1	9.9					

Figure 46 Hydraulic head measurements (including measurements of specific electrical conductivity).

Figure 47 Temperature measurements (including measurements of specific electrical conductivity).
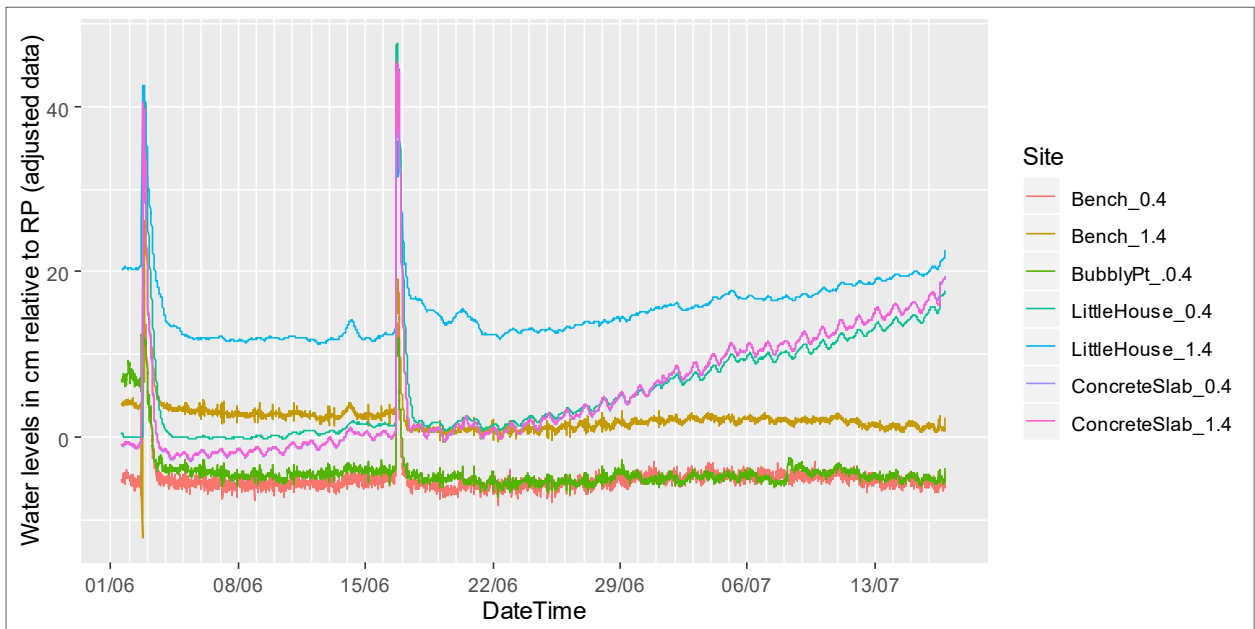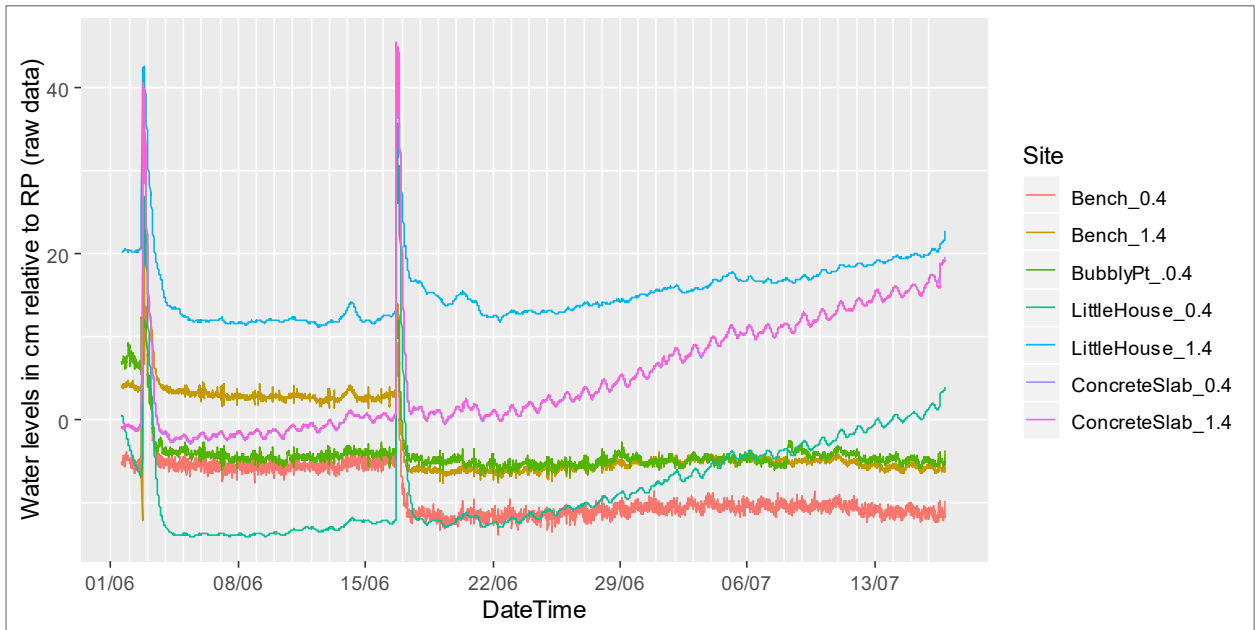
Figure 48 Comparison of water levels based on raw data (top) and treated data (bottom; step changes removed).
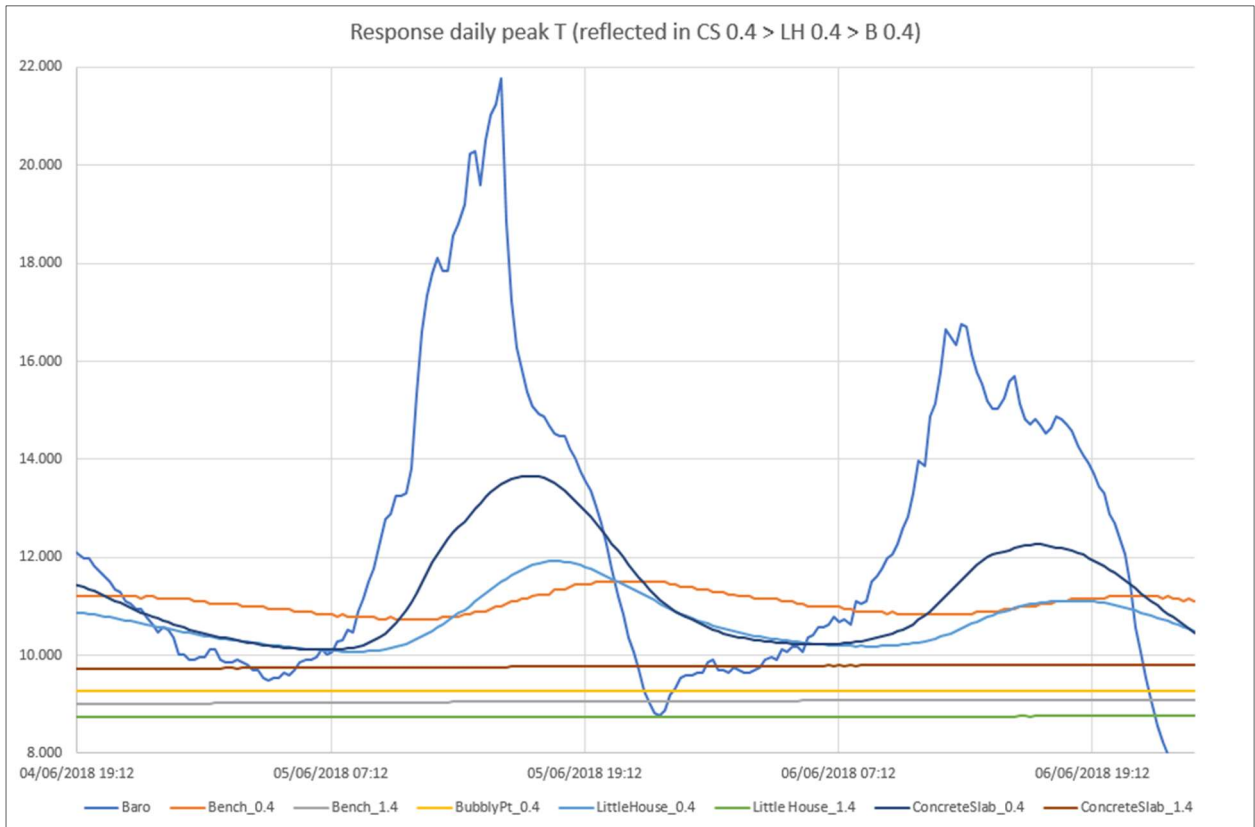
Figure 49 Detail of temperature variations 04-06 June, 2019, illustrating the propagation of the diurnal atmospheric temperature signal into the shallow sampling points (except BP).

Appendix 3 Chemical analysis

Table 20 Water chemical analysis at Bench (Be) site

Sample LIMS Code	Site ID	Sampling Date	T	Eh	pH	SEC	DO	TDS	Ca	Mg	Na	K	HCO₃⁻	Cl⁻	SO₄²⁻	NO₃⁻	Br⁻	NO₂⁻	HPO₄²⁻	F⁻	NPOC	Total P	Si
			°C	mV		µS cm⁻¹	mg l⁻¹	mg l⁻¹	mg l⁻¹	mg l⁻¹	mg l⁻¹	mg l⁻¹	mg l⁻¹	mg l⁻¹	mg l⁻¹	mg l⁻¹	mg l⁻¹	mg l⁻¹	mg l⁻¹	mg l⁻¹	mg l⁻¹	mg l⁻¹	mg l⁻¹
ICP-MS DL									*0.7*	*0.01*	*0.3*	*0.03*										*0.04*	*0.05*
14231-0012	Be_SW	26/04/2018	10.2	457	7.10	1289	11.5	999	120	61.7	69.6	7.09	404	93.2	235	8.36	0.215	<0.05	<0.1	0.412	4.37	0.06	3.55
14231-0013	Be_HZ01_B	26/04/2018	13.8	299	6.68	1015	2.4	816	125	55.4	14.4	1.54	378	35.3	207	0.2	<0.1	<0.05	<0.1	0.201	3.10	<0.04	9.56
14231-0014	Be_HZ01_R	26/04/2018	13.7	205	6.69	1009	2.4	791	122	54.0	14.5	1.05	358	34.0	208	0.2	<0.1	<0.05	<0.1	0.325	2.67	<0.04	9.62
14231-0015	Be_HZ01_G	26/04/2018	12.1	201	6.72	983	2.4	767	118	52.9	14.0	0.98	351	33.9	196	0.2	<0.1	<0.05	<0.1	0.350	2.55	<0.04	9.86
14231-0016	Be_HZ01_Y	26/04/2018	12.4	215	6.78	928	2.4	731	113	48.6	13.7	1.37	360	36.1	159	0.2	<0.1	<0.05	<0.1	0.389	3.59	<0.04	9.11
14231-0017	Be_HZ02_B	26/04/2018	10.2	374	6.82	1005	2.8	818	128	54.8	17.4	1.59	374	39.4	202	0.560	<0.1	<0.05	<0.1	0.357	2.91	<0.04	9.15
14231-0018	Be_HZ02_R	26/04/2018	10.8	209	6.75	992	2.7	795	124	53.8	14.1	1.18	364	34.8	203	0.2	<0.1	<0.05	<0.1	0.364	2.94	<0.04	9.95
14231-0019	Be_HZ02_G	26/04/2018	10.4	223	6.78	934	2.6	746	115	50.0	13.4	1.46	362	35.8	168	0.2	<0.1	<0.05	<0.1	0.316	3.56	<0.04	9.70
14231-0020	Be_HZ02_Y	26/04/2018	11.4	220	6.84	907	2.9	716	108	47.1	16.8	1.87	365	41.4	137	0.2	<0.1	<0.05	<0.1	0.402	4.38	<0.04	8.88
14231-0021	Be_HZ03_B	26/04/2018	nd	430	6.90	1280	9.3	970	119	57.6	61.9	6.61	394	91.1	232	7.88	0.202	<0.05	<0.1	0.312	4.24	<0.04	3.81
14231-0022	Be_HZ03_R	26/04/2018	10.9	195	7.34	1106	4.5	840	114	50.9	40.9	3.68	367	68.5	191	4.18	0.157	<0.05	<0.1	0.382	5.26	<0.04	6.62
14231-0023	Be_HZ03_G	26/04/2018	11.3	178	6.98	832	2.4	633	98.1	40.0	12.6	1.09	334	41.9	106	0.2	<0.1	<0.05	<0.1	0.325	2.97	<0.04	10.3
14231-0024	Be_HZ03_Y	26/04/2018	11.1	328	7.22	833	2.0	637	97.2	38.8	13.1	1.26	341	42.5	103	0.2	<0.1	<0.05	<0.1	0.376	3.29	<0.04	10.3
Sample LIMS Code	Site ID	Sampling Date	T	Eh	pH	SEC	DO	TDS	Ca	Mg	Na	K	HCO₃⁻	Cl⁻	SO₄²⁻	NO₃⁻	Br⁻	NO₂⁻	HPO₄²⁻	F⁻	NPOC	Total P	Si
			°C	mV		µS cm⁻¹	mg l⁻¹	mg l⁻¹	mg l⁻¹	mg l⁻¹	mg l⁻¹	mg l⁻¹	mg l⁻¹	mg l⁻¹	mg l⁻¹	mg l⁻¹	mg l⁻¹	mg l⁻¹	mg l⁻¹	mg l⁻¹	mg l⁻¹	mg l⁻¹	mg l⁻¹
ICP-MS DL									*0.6*	*0.07*	*0.5*	*0.03*										*0.04*	*0.05*
14283-0052	Be_SW	01/08/2018	15.5	259	7.32	1651	9.65	999	183	95.2	66.8	7.45	538	67.9	491	3.86	0.133	<0.005	<0.01	0.191	1.48	<0.04	4.75
14283-0029	Be_HZ01_B	01/08/2018	18.8	131	6.94	968	2.27	816	132	53.8	16.7	1.50	383	39.1	239	0.2	<0.1	<0.05	<0.1	0.447	2.75	0.39	11.0
14283-0030	Be_HZ01_R	01/08/2018	18.9	123	6.91	904	2.48	791	122	50.0	13.4	1.05	349	35.8	218	0.2	<0.1	<0.05	<0.1	0.407	4.96	0.11	10.6
14283-0031	Be_HZ01_G	01/08/2018	20.1	115	6.87	871	2.38	767	119	47.0	12.3	1.00	343	33.6	194	0.2	<0.1	<0.05	<0.1	0.264	2.63	0.19	10.0
14283-0032	Be_HZ01_Y	01/08/2018	20.7	103	6.96	816	2.8	731	108	42.4	12.0	1.14	342	35.7	140	0.08	<0.05	<0.025	<0.05	0.326	2.93	0.08	8.78
14283-0036	Be_HZ02_B	01/08/2018	19.1	70	7.12	1111	2.6	818	126	50.7	13.4	1.16	356	38.5	243	0.2	<0.1	<0.05	<0.1	0.334	3.43	0.34	9.89
14283-0035	Be_HZ02_R	01/08/2018	19.1	87	6.98	949	3.14	795	145	62.6	27.7	3.07	394	43.4	275	0.2	<0.1	<0.05	<0.1	0.319	8.11	0.07	10.2
14283-0034	Be_HZ02_G	01/08/2018	19.3	101	6.94	352	3.42	746	126	51.2	13.1	1.12	347	36.0	227	0.03	0.064	<0.01	<0.02	0.579	3.14	0.14	9.49
14283-0033	Be_HZ02_Y	01/08/2018	19.9	106	7.03	808	3.07	716	106	42.0	12.5	1.20	350	36.9	120	0.08	<0.05	<0.025	<0.05	0.602	3.51	0.04	8.88
14283-0037	Be_HZ03_B	01/08/2018	nd	nd	7.47	nd	nd	970	117	44.8	15.2	1.21	357	38.4	146	0.2	<0.1	<0.05	<0.1	0.142	2.95	<0.04	10.5
14283-0038	Be_HZ03_R	01/08/2018	nd	nd	7.73	nd	nd	840	119	45.9	13.2	1.06	342	34.2	179	0.2	<0.1	<0.05	<0.1	0.278	2.13	<0.04	9.79
14283-0039	Be_HZ03_G	01/08/2018	21.1	92	6.95	836	2.37	633	108	43.1	12.1	1.05	342	36.7	154	0.08	0.052	<0.025	<0.05	0.464	3.27	<0.04	9.57
14283-0040	Be_HZ03_Y	01/08/2018	20.6	97	6.95	801	2.91	637	105	40.2	12.7	1.06	342	41.4	124	0.08	0.051	<0.025	<0.05	0.530	4.62	0.04	9.78
Sample LIMS Code	Site ID	Sampling Date	T	Eh	pH	SEC	DO	TDS	Ca	Mg	Na	K	HCO₃⁻	Cl⁻	SO₄²⁻	NO₃⁻	Br⁻	NO₂⁻	HPO₄²⁻	F⁻	NPOC	Total P	Si
			°C	mV		µS cm⁻¹	mg l⁻¹	mg l-1	mg l-1	mg l-1	mg l-1	mg l-1	mg l-1	mg l-1	mg l-1	mg l-1	mg l-1	mg l-1	mg l-1	mg l-1	mg l-1	mg l-1	mg l-1
ICP-MS DL									*0.04*	*0.004*	*0.4*	*0.03*	*5.0*								*0.5*	*0.02*	*0.042*
14412-0028	Be_SW	06/02/2019	7.2	313	7.50	1678	12.2	999	145	64.1	112	7.99	416	175	324	16.5	<0.2	<0.1	<0.2	0.211	2.54	0.05	3.66
14412-0027	Be_HZ01_B	06/02/2019	7.3	128	7.19	1002	3.6	816	125	46.2	13.1	0.9	356	34.7	217	<0.3	<0.1	<0.05	<0.1	0.262	2.42	0.71	9.34
14412-0029	Be_HZ01_R	06/02/2019	7	155	7.19	1017	3.6	791	124	47.7	13.6	0.9	353	34.4	217	<0.3	<0.1	<0.05	<0.1	0.273	2.13	0.26	9.16
14412-0031	Be_HZ01_G	06/02/2019	nd	nd	nd	921	3.6	767	118	44.9	12.7	0.92	354	34.6	201	<0.3	<0.1	<0.05	<0.1	0.268	2.18	0.11	8.44
14412-0032	Be_HZ01_Y	06/02/2019	5.8	-144	7.47	894	3.2	731	110	41.2	11.8	0.93	359	33.6	150	<0.3	<0.1	<0.05	<0.1	0.415	2.14	0.11	8.09

Table 20 Water chemical analysis at Bench (Be) site (continued)

Sample LIMS Code	Site ID	Ba	Sr	Mn	Fe	Li	Be	B	Al	Ti	V	Cr	Co	Ni	Cu	Zn	Ga	As	Se	Rb	Y	Zr	Nb	Mo	Ag	Cd	Sn	Sb	Cs
		µg l⁻¹	µg l⁻¹	µg l⁻¹	µg l⁻¹	µg l⁻¹	µg l⁻¹	µg l⁻¹	µg l⁻¹	µg l⁻¹	µg l⁻¹	µg l⁻¹	µg l⁻¹	µg l⁻¹	µg l⁻¹	µg l⁻¹	µg l⁻¹	µg l⁻¹	µg l⁻¹	µg l⁻¹	µg l⁻¹	µg l⁻¹	µg l⁻¹	µg l⁻¹	µg l⁻¹	µg l⁻¹	µg l⁻¹	µg l⁻¹	µg l⁻¹
ICP-MS DL		0.1	0.2	0.3	2	3	0.01	18	2	0.2	0.1	0.2	0.02	0.1	0.6	0.8	0.05	0.06	0.1	0.01	0.01	0.09	0.02	0.08	0.05	0.02	0.03	0.02	0.005
14231-0012	Be_SW	67.9	327	41.6	30	49	<0.01	99	3	<0.2	0.3	1.0	0.19	3.7	2.8	5.3	<0.05	0.31	0.4	3.87	0.02	<0.09	<0.02	0.84	<0.05	<0.02	<0.03	0.18	0.006
14231-0013	Be_HZ01_B	193	263	2956	817	13	<0.01	59	5	<0.2	0.6	<0.2	6.44	3.2	1.5	24.4	0.50	1.07	<0.1	2.06	0.06	<0.09	<0.02	0.76	<0.05	0.04	<0.03	0.14	<0.005
14231-0014	Be_HZ01_R	186	234	1249	6923	11	<0.01	54	3	0.3	0.4	0.2	3.64	2.5	1.6	21.2	0.20	1.25	<0.1	1.26	0.04	<0.09	<0.02	0.29	<0.05	<0.02	<0.03	0.06	<0.005
14231-0015	Be_HZ01_G	208	227	577	8631	10	0.01	54	<2	<0.2	0.4	<0.2	0.50	0.7	0.7	3.4	0.06	0.44	<0.1	0.93	0.05	<0.09	<0.02	0.17	<0.05	<0.02	<0.03	<0.02	<0.005
14231-0016	Be_HZ01_Y	224	233	1016	4932	11	0.01	63	9	<0.2	0.3	<0.2	1.12	0.9	0.8	39.6	0.21	1.00	<0.1	0.94	0.06	<0.09	<0.02	0.59	<0.05	<0.02	<0.03	0.10	0.006
14231-0017	Be_HZ02_B	171	273	2350	32	14	0.01	67	15	0.5	0.5	<0.2	2.80	1.9	0.8	20.7	0.51	0.84	0.2	2.78	0.06	<0.09	<0.02	0.96	<0.05	0.04	0.17	0.26	0.006
14231-0018	Be_HZ02_R	195	242	1686	4792	11	0.01	58	7	<0.2	0.4	<0.2	5.64	3.0	<0.6	22.1	0.36	1.03	<0.1	1.55	0.06	<0.09	<0.02	0.43	<0.05	<0.02	0.09	0.25	<0.005
14231-0019	Be_HZ02_G	199	248	1518	2827	12	0.03	56	96	1.8	1.2	0.3	3.60	1.7	1.0	21.8	0.34	0.64	<0.1	2.05	0.26	<0.09	<0.02	0.36	<0.05	0.04	0.08	0.10	0.015
14231-0020	Be_HZ02_Y	241	243	1017	1937	13	0.01	57	20	0.7	0.4	<0.2	1.47	1.1	1.3	11.6	0.22	0.77	<0.1	1.19	0.08	<0.09	<0.02	0.82	<0.05	<0.02	0.07	0.13	0.006
14231-0021	Be_HZ03_B	85.0	321	144	20	41	<0.01	87	6	<0.2	0.4	0.7	0.42	3.4	2.7	4.4	<0.05	0.32	0.4	3.82	0.04	<0.09	<0.02	0.85	<0.05	<0.02	0.06	0.19	0.017
14231-0022	Be_HZ03_R	214	263	976	1227	26	0.03	71	139	2.9	0.5	0.5	2.00	2.9	1.8	10.5	0.26	0.81	0.3	2.75	0.24	<0.09	<0.02	0.76	<0.05	0.03	0.05	0.16	0.031
14231-0023	Be_HZ03_G	218	198	990	4477	9	0.01	49	3	<0.2	0.6	<0.2	1.51	0.8	2.3	6.1	0.22	0.62	<0.1	0.92	0.06	<0.09	<0.02	0.29	<0.05	<0.02	0.04	0.05	0.006
14231-0024	Be_HZ03_Y	228	207	1315	3335	10	0.02	47	15	0.6	0.7	<0.2	2.11	0.9	0.8	8.6	0.31	0.59	<0.1	1.05	0.08	<0.09	<0.02	0.40	<0.05	<0.02	<0.03	0.07	0.008
ICP-MS DL		0.9	2	2	7	3	0.5	11	2	0.2	0.1	0.3	0.05	0.1	1	2	0.08	0.07	0.1	0.05	0.02	0.05	0.02	0.3	0.05	0.04	0.04	0.05	0.02
14283-0052	Be_SW	81.4	567	66.0	26	84	<0.5	108	4	<0.2	0.3	<0.3	0.16	0.8	<1	6	<0.08	0.16	0.4	4.00	0.03	<0.05	<0.02	<0.3	<0.05	<0.04	<0.04	0.10	<0.02
14283-0029	Be_HZ01_B	242	290	2530	15454	15	<0.5	46	19	0.6	0.7	<0.3	6.56	3.4	<1	4	0.92	3.16	0.2	1.74	0.07	<0.05	<0.02	0.6	<0.05	<0.04	0.27	0.06	<0.02
14283-0030	Be_HZ01_R	212	249	666	10432	9	<0.5	43	8	<0.2	1.0	<0.3	0.73	1.1	<1	5	0.25	1.66	0.2	1.03	0.03	<0.05	<0.02	<0.3	<0.05	<0.04	<0.04	0.08	<0.02
14283-0031	Be_HZ01_G	251	241	528	9431	8	<0.5	37	33	0.9	0.7	<0.3	0.28	0.4	<1	3	0.27	0.30	<0.1	0.76	0.09	<0.05	<0.02	<0.3	<0.05	<0.04	<0.05	<0.05	<0.02
14283-0032	Be_HZ01_Y	192	232	427	6026	10	<0.5	40	5	<0.2	0.5	<0.3	0.11	0.2	<1	<2	0.15	0.27	<0.1	0.78	0.03	<0.05	<0.02	<0.3	<0.05	<0.04	<0.05	<0.05	<0.02
14283-0036	Be_HZ02_B	241	258	688	11474	9	<0.5	41	5	<0.2	0.6	<0.3	1.28	1.1	5	13	0.24	2.57	<0.1	0.98	<0.02	<0.05	<0.02	<0.3	<0.05	<0.04	<0.05	<0.05	<0.02
14283-0035	Be_HZ02_R	211	347	2320	12458	29	<0.5	58	17	0.3	0.6	<0.3	4.32	2.1	<1	2	0.90	3.32	0.2	2.52	0.04	<0.05	<0.02	0.7	<0.05	<0.04	<0.04	0.09	<0.02
14283-0034	Be_HZ02_G	230	250	559	9367	9	<0.5	41	2	<0.2	0.5	<0.3	0.59	0.8	1	5	0.21	0.48	<0.1	0.90	<0.02	<0.05	<0.02	<0.3	<0.05	<0.04	<0.04	<0.05	<0.02
14283-0033	Be_HZ02_Y	198	239	882	4790	10	<0.5	41	10	0.6	0.5	<0.3	0.69	0.4	<1	<2	0.35	0.69	<0.1	0.90	0.03	<0.05	<0.02	0.3	<0.05	<0.04	<0.05	<0.05	<0.02
14283-0037	Be_HZ03_B	231	239	826	7378	9	<0.5	44	<2	0.3	0.3	<0.3	0.49	0.5	<1	<2	0.32	0.56	<0.1	1.04	0.02	<0.05	<0.02	<0.3	<0.05	<0.04	<0.05	<0.05	<0.02
14283-0038	Be_HZ03_R	246	239	780	5383	9	<0.5	41	3	0.2	0.1	<0.3	0.28	0.4	1	3	0.29	0.34	<0.1	0.87	<0.02	<0.05	<0.02	<0.3	<0.05	<0.04	<0.05	<0.05	<0.02
14283-0039	Be_HZ03_G	276	231	587	6485	9	<0.5	40	13	0.5	0.5	<0.3	0.58	0.5	<1	2	0.23	0.57	<0.1	0.87	0.06	<0.05	<0.02	<0.3	<0.05	<0.04	<0.04	<0.05	<0.02
14283-0040	Be_HZ03_Y	281	237	594	6045	9	<0.5	42	8	0.4	0.5	<0.3	0.48	0.4	1	4	0.24	0.56	<0.1	0.90	0.04	<0.05	<0.02	<0.3	<0.05	<0.04	<0.04	<0.05	<0.02
ICP-MS DL		0.05	0.06	0.2	0.4	7	0.08	53	2	0.02	0.4	0.2	0.2	0.05	0.2	0.3	0.3	0.03	0.05	0.05	0.2	0.04	0.08	0.04	0.05	0.01	0.01	0.008	0.03
14412-0028	Be_SW	85.55	447.91	71.8	82.4	56	<0.08	80	4	0.12	<0.4	<0.2	0.2	1.39	1.6	7.8	<0.3	0.23	0.33	3.6	<0.2	<0.04	<0.08	0.32	<0.05	0.01	0.02	0.168	<0.03
14412-0027	Be_HZ01_B	232.89	257.55	943.7	17389.9	10	<0.08	<53	7	0.25	<0.4	<0.2	2.7	1.78	3.8	8	<0.3	2.4	0.06	0.92	<0.2	0.05	<0.08	0.19	<0.05	<0.01	0.03	0.02	<0.03
14412-0029	Be_HZ01_R	203.1	259.12	635.5	12423.6	8	<0.08	<53	4	0.23	<0.4	<0.2	0.4	0.46	0.4	12	<0.3	0.83	0.06	0.74	<0.2	0.04	<0.08	0.12	<0.05	<0.01	<0.01	0.035	<0.03
14412-0031	Be_HZ01_G	224.39	254.17	554.4	10157	9	<0.08	<53	4	0.11	<0.4	<0.2	<0.2	0.32	0.3	4.7	<0.3	0.19	0.05	0.74	<0.2	0.04	<0.08	0.1	<0.05	<0.01	<0.01	0.019	<0.03
14412-0032	Be_HZ01_Y	163.64	236.68	399	6638.5	8	<0.08	<53	10	0.3	<0.4	<0.2	<0.2	0.23	<0.2	1.3	<0.3	0.15	<0.05	0.67	<0.2	0.04	<0.08	0.14	<0.05	<0.01	<0.01	0.014	<0.03

Table 20 Water chemical analysis at Bench (Be) site (continued)

Sample LIMS Code	Site ID	La	Ce	Pr	Nd	Sm	Eu	Gd	Tb	Dy	Ho	Er	Tm	Yb	Lu	Hf	Ta	W	Tl	Pb	Th	U
		µg l⁻¹	µg l⁻¹	µg l⁻¹	µg l⁻¹	µg l⁻¹	µg l⁻¹	µg l⁻¹	µg l⁻¹	µg l⁻¹	µg l⁻¹	µg l⁻¹	µg l⁻¹	µg l⁻¹	µg l⁻¹	µg l⁻¹	µg l⁻¹	µg l⁻¹	µg l⁻¹	µg l⁻¹	µg l⁻¹	µg l⁻¹
ICP-MS DL		*0.005*	*0.03*	*0.04*	*0.07*	*0.006*	*0.002*	*0.003*	*0.002*	*0.005*	*0.002*	*0.002*	*0.002*	*0.004*	*0.002*	*0.01*	*0.02*	*0.05*	*0.02*	*0.04*	*0.005*	*0.01*
14231-0012	Be_SW	<0.005	<0.03	<0.04	<0.07	<0.006	<0.002	0.004	<0.002	0.006	<0.002	0.003	<0.002	<0.004	<0.002	<0.01	<0.02	<0.05	0.03	0.07	<0.005	2.21
14231-0013	Be_HZ01_B	0.015	<0.03	<0.04	<0.07	<0.006	<0.002	0.008	<0.002	0.007	<0.002	0.004	<0.002	0.005	<0.002	<0.01	<0.02	<0.05	0.03	0.05	<0.005	0.630
14231-0014	Be_HZ01_R	0.010	<0.03	<0.04	<0.07	<0.006	0.003	0.007	<0.002	<0.005	<0.002	0.003	<0.002	<0.004	<0.002	<0.01	<0.02	<0.05	<0.02	<0.04	<0.005	0.180
14231-0015	Be_HZ01_G	0.006	<0.03	<0.04	<0.07	<0.006	<0.002	0.004	<0.002	0.006	<0.002	0.003	<0.002	<0.004	<0.002	<0.01	<0.02	<0.05	0.02	<0.04	<0.005	0.040
14231-0016	Be_HZ01_Y	0.018	0.03	<0.04	<0.07	0.008	<0.002	0.007	<0.002	0.007	<0.002	0.005	<0.002	0.005	<0.002	<0.01	<0.02	<0.05	0.02	0.09	0.01	0.160
14231-0017	Be_HZ02_B	0.025	0.04	<0.04	<0.07	0.010	<0.002	0.009	<0.002	0.006	<0.002	0.006	<0.002	0.006	<0.002	<0.01	<0.02	<0.05	0.03	0.14	0.01	0.620
14231-0018	Be_HZ02_R	0.021	0.04	<0.04	<0.07	<0.006	<0.002	0.007	<0.002	0.008	<0.002	0.004	<0.002	0.007	<0.002	<0.01	<0.02	<0.05	0.02	0.10	0.01	0.180
14231-0019	Be_HZ02_G	0.152	0.40	0.04	0.25	0.056	0.015	0.053	0.009	0.050	0.008	0.024	0.003	0.014	0.003	<0.01	<0.02	<0.05	0.02	1.06	0.04	0.200
14231-0020	Be_HZ02_Y	0.027	0.06	<0.04	<0.07	0.010	0.005	0.012	<0.002	0.012	<0.002	0.005	<0.002	0.005	<0.002	<0.01	<0.02	<0.05	0.02	0.22	0.01	0.360
14231-0021	Be_HZ03_B	0.007	<0.03	<0.04	<0.07	<0.006	0.002	0.005	<0.002	<0.005	<0.002	0.005	<0.002	0.007	<0.002	<0.01	<0.02	<0.05	0.03	0.10	0.01	1.98
14231-0022	Be_HZ03_R	0.132	0.38	0.04	0.27	0.056	0.015	0.056	0.010	0.052	0.009	0.027	0.003	0.016	0.004	<0.01	<0.02	<0.05	0.02	0.86	0.04	1.23
14231-0023	Be_HZ03_G	0.012	<0.03	<0.04	<0.07	0.010	0.004	0.006	<0.002	0.006	<0.002	0.004	<0.002	0.005	<0.002	<0.01	<0.02	<0.05	0.02	0.11	0.01	0.090
14231-0024	Be_HZ03_Y	0.030	0.06	<0.04	<0.07	0.010	<0.002	0.011	<0.002	0.013	<0.002	0.009	<0.002	0.010	<0.002	<0.01	<0.02	<0.05	0.02	0.18	0.01	0.140

Sample LIMS Code	Site ID	La	Ce	Pr	Nd	Sm	Eu	Gd	Tb	Dy	Ho	Er	Tm	Yb	Lu	Hf	Ta	W	Tl	Pb	Th	U
		µg l⁻¹	µg l⁻¹	µg l⁻¹	µg l⁻¹	µg l⁻¹	µg l⁻¹	µg l⁻¹	µg l⁻¹	µg l⁻¹	µg l⁻¹	µg l⁻¹	µg l⁻¹	µg l⁻¹	µg l⁻¹	µg l⁻¹	µg l⁻¹	µg l⁻¹	µg l⁻¹	µg l⁻¹	µg l⁻¹	µg l⁻¹
ICP-MS DL		*0.03*	*0.04*	*0.05*	*0.2*	*0.03*	*0.008*	*0.007*	*0.007*	*0.007*	*0.007*	*0.008*	*0.007*	*0.008*	*0.007*	*0.01*	*0.02*	*0.05*	*0.01*	*0.02*	*0.009*	*0.009*
14283-0052	Be_SW	<0.03	<0.04	<0.05	<0.2	<0.03	<0.008	<0.007	<0.007	<0.007	<0.007	<0.008	<0.007	<0.008	<0.007	<0.01	<0.02	<0.05	0.06	0.05	<0.009	3.43
14283-0029	Be_HZ01_B	0.03	0.09	<0.05	<0.2	<0.03	0.014	0.010	<0.007	0.010	<0.007	<0.008	<0.007	0.018	<0.007	<0.01	<0.02	0.05	<0.01	0.23	0.015	0.444
14283-0030	Be_HZ01_R	<0.03	<0.04	<0.05	<0.2	<0.03	0.008	0.008	<0.007	<0.007	<0.007	<0.008	<0.007	<0.008	<0.007	<0.01	<0.02	<0.05	<0.01	0.08	<0.009	0.077
14283-0031	Be_HZ01_G	0.04	0.13	<0.05	<0.2	<0.03	0.008	0.013	<0.007	0.009	<0.007	<0.008	<0.007	<0.008	<0.007	<0.01	<0.02	<0.05	<0.01	0.33	0.010	0.014
14283-0032	Be_HZ01_Y	<0.03	<0.04	<0.05	<0.2	<0.03	0.008	<0.007	<0.007	<0.007	<0.007	<0.008	<0.007	<0.008	<0.007	<0.01	<0.02	<0.05	<0.01	0.03	<0.009	0.024
14283-0036	Be_HZ02_B	<0.03	<0.04	<0.05	<0.2	<0.03	<0.008	<0.007	<0.007	<0.007	<0.007	<0.008	<0.007	<0.008	<0.007	<0.01	<0.02	<0.05	<0.01	<0.02	<0.009	0.072
14283-0035	Be_HZ02_R	<0.03	0.08	<0.05	<0.2	<0.03	<0.008	<0.007	<0.007	<0.007	<0.007	<0.008	<0.007	<0.008	<0.007	<0.01	<0.02	0.06	<0.01	0.19	<0.009	1.02
14283-0034	Be_HZ02_G	<0.03	<0.04	<0.05	<0.2	<0.03	<0.008	<0.007	<0.007	<0.007	<0.007	<0.008	<0.007	<0.008	<0.007	<0.01	<0.02	<0.05	<0.01	<0.02	<0.009	0.023
14283-0033	Be_HZ02_Y	<0.03	<0.04	<0.05	<0.2	<0.03	<0.008	<0.007	<0.007	<0.007	<0.007	<0.008	<0.007	<0.008	<0.007	<0.01	<0.02	<0.05	<0.01	0.16	<0.009	0.072
14283-0037	Be_HZ03_B	<0.03	<0.04	<0.05	<0.2	<0.03	<0.008	<0.007	<0.007	<0.007	<0.007	<0.008	<0.007	<0.008	<0.007	<0.01	<0.02	<0.05	<0.01	<0.02	<0.009	0.068
14283-0038	Be_HZ03_R	<0.03	<0.04	<0.05	<0.2	<0.03	<0.008	<0.007	<0.007	<0.007	<0.007	<0.008	<0.007	<0.008	<0.007	<0.01	<0.02	<0.05	<0.01	<0.02	<0.009	0.035
14283-0039	Be_HZ03_G	<0.03	0.06	<0.05	<0.2	<0.03	<0.008	0.016	<0.007	0.011	<0.007	0.011	<0.007	0.009	<0.007	<0.01	<0.02	<0.05	<0.01	0.12	0.012	0.055
14283-0040	Be_HZ03_Y	<0.03	<0.04	<0.05	<0.2	<0.03	0.014	<0.007	<0.007	<0.007	<0.007	<0.008	<0.007	<0.008	<0.007	<0.01	<0.02	<0.05	<0.01	0.07	0.011	0.037

Sample LIMS Code	Site ID	La	Ce	Pr	Nd	Sm	Eu	Gd	Tb	Dy	Ho	Er	Tm	Yb	Lu	Hf	Ta	W	Tl	Pb	Th	U
		µg l-1	µg l-1	µg l-1	µg l-1	µg l-1	µg l-1	µg l-1	µg l-1	µg l-1	µg l-1	µg l-1	µg l-1	µg l-1	µg l-1	µg l-1	µg l-1	µg l-1	µg l-1	µg l-1	µg l-1	µg l-1
ICP-MS DL		*0.005*	*0.004*	*0.003*	*0.005*	*0.003*	*0.003*	*0.004*	*0.003*	*0.006*	*0.006*	*0.006*	*0.06*	*0.02*	*0.02*	*0.08*	*0.03*	*0.009*	*0.03*	*0.009*	*0.04*	*0.009*
14412-0028	Be_SW	0.012	0.012	0.006	0.018	0.004	<0.003	0.006	<0.003	<0.006	<0.006	<0.06	<0.02	<0.02	<0.08	<0.03	<0.009	<0.03	0.05	0.32	<0.009	2.415
14412-0027	Be_HZ01_B	0.023	0.057	0.007	0.041	0.008	<0.003	0.008	<0.003	<0.006	<0.006	<0.06	<0.02	<0.02	<0.08	<0.03	<0.009	<0.03	<0.009	0.19	<0.009	0.073
14412-0029	Be_HZ01_R	0.009	0.016	0.004	0.019	0.01	<0.003	0.004	<0.003	<0.006	<0.006	<0.06	<0.02	<0.02	<0.08	<0.03	<0.009	<0.03	<0.009	0.05	<0.009	0.04
14412-0031	Be_HZ01_G	0.005	0.02	<0.003	0.008	<0.003	<0.003	<0.004	<0.003	<0.006	<0.006	<0.06	<0.02	<0.02	<0.08	<0.03	<0.009	<0.03	<0.009	<0.04	<0.009	0.031
14412-0032	Be_HZ01_Y	0.016	0.068	0.007	0.019	0.018	<0.003	0.006	<0.003	0.007	<0.006	<0.06	<0.02	<0.02	<0.08	<0.03	<0.009	<0.03	<0.009	0.14	<0.009	0.022

Table 21 Water chemical analysis at Bubbly Point (BP) site

Sample LIMS Code	Site ID	Sampling Date	T	Eh	pH	SEC	DO	TDS	Ca	Mg	Na	K	HCO₃⁻	Cl⁻	SO₄²⁻	NO₃⁻	Br⁻	NO₂⁻	HPO₄²⁻	F⁻	NPOC	Total P	Si
			°C	mV		µS cm⁻¹	mg l⁻¹	mg l⁻¹	mg l⁻¹	mg l⁻¹	mg l⁻¹	mg l⁻¹	mg l⁻¹	mg l⁻¹	mg l⁻¹	mg l⁻¹	mg l⁻¹	mg l⁻¹	mg l⁻¹	mg l⁻¹	mg l⁻¹	mg l⁻¹	mg l⁻¹
ICP-MS DL									*0.7*	*0.01*	*0.3*	*0.03*										*0.04*	*0.05*
14231-0011	**BP_SW**	25/04/2018	nd	nd	nd	nd	nd	1888	221	141	82.3	9.73	659	48.2	725	1.94	<0.2	<0.1	<0.2	0.384	1.29	<0.04	5.60
14231-0001	**BP_HZ01_B**	25/04/2018	12.6	399	6.62	2250	3.0	2047	242	162	88.0	10.6	699	41.5	803	1.13	<0.2	<0.1	<0.2	0.419	1.12	<0.04	5.86
14231-0003	**BP_HZ01_R**	25/04/2018	12.9	374	6.68	2284	3.6	2041	238	161	87.9	10.6	701	41.6	800	1.15	<0.2	<0.1	<0.2	0.394	1.80	<0.04	5.92
14231-0004	**BP_HZ01_G**	25/04/2018	12.4	389	6.65	2273	3.3	2047	240	164	89.3	10.7	705	41.5	796	1.16	<0.2	<0.1	<0.2	0.378	0.824	<0.04	5.87
14231-0005	**BP_HZ01_Y**	25/04/2018	11.9	389	6.65	2280		2066	241	163	89.7	10.8	707	41.9	811	1.07	<0.2	<0.1	<0.2	0.407	1.29	<0.04	5.86
14231-0006	**BP_HZ02_B**	25/04/2018	11.5	391	6.70	2054	4.8	1801	212	139	80.2	9.17	637	48.7	673	1.82	<0.2	<0.1	<0.2	0.373	1.41	<0.04	5.79
14231-0002	**BP_HZ02_R**	25/04/2018	11.4	390	6.73	2048	5.4	1800	213	139	80.1	9.16	638	48.2	670	1.82	<0.2	<0.1	<0.2	0.388	1.56	<0.04	5.71
14231-0007	**BP_HZ02_GG**	25/04/2018	10.5	395	6.76	2043	2.7	1795	211	136	79.4	9.10	640	47.8	671	1.70	<0.2	<0.1	<0.2	0.394	2.14	<0.04	5.79
14231-0008	**BP_HZ02_Y**	25/04/2018	11.7	396	6.84	2095	6.8	1834	221	142	81.4	10.5	659	49.5	672	0.30	<0.2	<0.1	<0.2	0.355	12.5	<0.04	6.92
14231-0010	**BP_SPRING**	25/04/2018	nd	nd	nd	nd	0.0	2134	253	168	93.2	11.6	724	43.0	840	0.96	<0.2	<0.1	12	0.427	2.09	<0.04	5.80
Sample LIMS Code	Site ID	Sampling Date	T	Eh	pH	SEC	DO	TDS	Ca	Mg	Na	K	HCO₃⁻	Cl⁻	SO₄²⁻	NO₃⁻	Br⁻	NO₂⁻	HPO₄²⁻	F⁻	NPOC	Total P	Si
			°C	mV		µS cm⁻¹	mg l⁻¹	mg l⁻¹	mg l⁻¹	mg l⁻¹	mg l⁻¹	mg l⁻¹	mg l⁻¹	mg l⁻¹	mg l⁻¹	mg l⁻¹	mg l⁻¹	mg l⁻¹	mg l⁻¹	mg l⁻¹	mg l⁻¹	mg l⁻¹	mg l⁻¹
ICP-MS DL									*0.6*	*0.07*	*0.5*	*0.03*										*0.04*	*0.05*
14283-0053	**BP_SW**	01/08/2018	11	413	6.55	2125	1.02	1888	242	144	77.6	10.4	693	41.7	790	1.08	<0.2	<0.1	<0.2	0.269	0.96	<0.04	5.96
14283-0041	**BP_HZ01_B**	01/08/2018	15.7	412	6.74	2064	3.33	2047	250	150	80.6	11.0	703	40.3	869	0.88	<0.2	<0.1	<0.2	0.331	0.88	<0.04	5.79
14283-0042	**BP_HZ01_R**	01/08/2018	17.8	383	6.78	2066	3	2041	254	154	81.6	11.2	710	37.8	812	0.83	<0.2	<0.1	<0.2	0.312	2.28	<0.04	5.96
14283-0043	**BP_HZ01_G**	01/08/2018	14.6	377	6.82	2089	3.55	2047	251	151	80.9	11.0	715	38.1	824	0.82	<0.2	<0.1	<0.2	0.319	1.05	<0.04	5.89
14283-0044	**BP_HZ01_Y**	01/08/2018	14.9	386	6.82	2080	3.86	2066	255	155	81.9	11.3	714	39.1	848	0.77	<0.2	<0.1	<0.2	0.331	0.90	<0.04	5.78
14283-0045	**BP_HZ02_B**	01/08/2018	15.4	366	6.83	1945	3.73	1801	234	141	76.3	10.0	677	42.7	774	0.88	<0.2	<0.1	<0.2	0.347	1.10	<0.04	5.81
14283-0046	**BP_HZ02_R**	01/08/2018	15.1	375	6.83	1968	3.03	1800	233	139	76.6	9.94	682	41.3	750	0.72	<0.2	<0.1	<0.2	0.324	1.22	<0.04	5.87
14283-0047	**BP_HZ02_GG**	01/08/2018	15.3	339	6.85	1892	2.72	1795	236	140	77.3	9.85	682	44.5	796	0.87	<0.2	<0.1	<0.2	0.272	2.98	<0.04	5.79
14283-0048	**BP_HZ02_Y**	01/08/2018	nd	nd	7.90	nd	nd	1834	219	126	72.8	7.99	754	47.1	619	0.30	<0.2	<0.1	<0.2	0.343	2.55	<0.04	8.95
14283-0062	**BP_SPRING**	01/08/2018	nd	nd	7.14	nd	nd	2134	263	158	85.2	11.9	736	36.8	840	0.75	<0.5	<0.25	<0.5	<0.25	2.05	<0.04	5.82
Sample LIMS Code	Site ID	Sampling Date	T	Eh	pH	SEC	DO	TDS	Ca	Mg	Na	K	HCO₃⁻	Cl⁻	SO₄²⁻	NO₃⁻	Br⁻	NO₂⁻	HPO₄²⁻	F⁻	NPOC	Total P	Si
			°C	mV		µS cm⁻¹	mg l⁻¹	mg l⁻¹	mg l⁻¹	mg l⁻¹	mg l⁻¹	mg l⁻¹	mg l⁻¹	mg l⁻¹	mg l⁻¹	mg l⁻¹	mg l⁻¹	mg l⁻¹	mg l⁻¹	mg l⁻¹	mg l⁻¹	mg l⁻¹	mg l⁻¹
ICP-MS DL									*0.04*	*0.004*	*0.4*	*0.03*	*5.0*								*0.5*	*0.02*	*0.042*
14412-0022	**BP_SW**	06/02/2019	9.4	362	6.86	2191	2.1	1888	240	133	79.6	10.4	705	44.8	765	0.88	<0.2	<0.1	<0.2	0.370	0.63	<0.02	4.9
14412-0021	**BP_HZ01_B**	06/02/2019	8.6	356	6.91	2259	3.0	2047	253	142	81.5	11.0	721	41.3	805	0.78	<0.2	<0.1	<0.2	0.260	0.67	<0.02	4.97
14412-0023	**BP_HZ01_R**	06/02/2019	8.3	378	6.92	2259	3.1	2041	249	140	81	10.9	714	40.9	803	0.70	<0.2	<0.1	<0.2	0.350	1.54	<0.02	5.2
14412-0024	**BP_HZ02_G**	06/02/2019	9.4	384	6.96	2231	3.8	2047	249	141	81.7	10.9	716	41.3	808	0.74	<0.2	<0.1	<0.2	0.357	0.87	<0.02	5.08
14412-0025	**BP_HZ01_Y**	06/02/2019	9.2	391	6.96	2231	3.2	2066	253	143	82.7	11.1	719	42.3	825	0.76	<0.2	<0.1	<0.2	0.278	0.62	<0.02	5.09
14412-0030	**BP_SPRING**	06/02/2019	7.6	290	6.94	2345	3.6	2134	263	150	86.8	11.9	740	38.4	796	<1.5	<0.5	<0.25	<0.5	0.293	0.74	<0.02	5.16

Table 21 Water chemical analysis at Bubbly Point (BP) (continued)

Sample LIMS Code	Site ID	Ba	Sr	Mn	Fe	Li	Be	B	Al	Ti	V	Cr	Co	Ni	Cu	Zn	Ga	As	Se	Rb	Y	Zr	Nb	Mo	Ag	Cd	Sn	Sb	Cs
		$\mu g\,l^{-1}$	$\mu g\,l^{-1}$	$\mu g\,l^{-1}$	$\mu g\,l^{-1}$	$\mu g\,l^{-1}$	$\mu g\,l^{-1}$	$\mu g\,l^{-1}$	$\mu g\,l^{-1}$	$\mu g\,l^{-1}$	$\mu g\,l^{-1}$	$\mu g\,l^{-1}$	$\mu g\,l^{-1}$	$\mu g\,l^{-1}$	$\mu g\,l^{-1}$	$\mu g\,l^{-1}$	$\mu g\,l^{-1}$	$\mu g\,l^{-1}$	$\mu g\,l^{-1}$	$\mu g\,l^{-1}$	$\mu g\,l^{-1}$	$\mu g\,l^{-1}$	$\mu g\,l^{-1}$	$\mu g\,l^{-1}$	$\mu g\,l^{-1}$	$\mu g\,l^{-1}$	$\mu g\,l^{-1}$	$\mu g\,l^{-1}$	$\mu g\,l^{-1}$
ICP-MS DL		*0.1*	*0.2*	*0.3*	*2*	*3*	*0.01*	*18*	*2*	*0.2*	*0.1*	*0.2*	*0.02*	*0.1*	*0.6*	*0.8*	*0.05*	*0.06*	*0.1*	*0.01*	*0.01*	*0.09*	*0.02*	*0.08*	*0.05*	*0.02*	*0.03*	*0.02*	*0.005*
14231-0011	**BP_SW**	32.4	848	4.7	10	169	<0.01	215	4	<0.2	<0.1	<0.2	0.05	0.5	<0.6	7.3	<0.05	0.09	0.1	6.11	0.02	<0.09	<0.02	0.20	<0.05	<0.02	<0.03	0.05	0.015
14231-0001	**BP_HZ01_B**	34.9	968	2.1	4	195	<0.01	242	3	<0.2	<0.1	<0.2	0.04	0.6	4.0	21.5	<0.05	<0.06	<0.1	6.64	0.02	<0.09	<0.02	<0.08	<0.05	0.02	<0.03	<0.02	0.018
14231-0003	**BP_HZ01_R**	28.5	947	1.0	4	197	<0.01	242	2	0.2	<0.1	<0.2	0.03	0.3	1.6	9.5	<0.05	0.07	<0.1	6.65	0.01	<0.09	<0.02	<0.08	<0.05	0.02	<0.03	<0.02	0.321
14231-0004	**BP_HZ01_G**	29.3	952	0.6	4	202	<0.01	249	3	<0.2	<0.1	<0.2	0.02	0.4	2.3	9.1	<0.05	0.08	<0.1	6.86	0.01	<0.09	<0.02	<0.08	<0.05	<0.02	<0.03	<0.02	0.020
14231-0005	**BP_HZ01_Y**	28.5	984	0.2	4	204	<0.01	250	3	<0.2	<0.1	<0.2	<0.02	0.3	1.0	7.8	<0.05	<0.06	0.1	6.90	0.01	<0.09	<0.02	<0.08	<0.05	<0.02	<0.03	<0.02	0.022
14231-0006	**BP_HZ02_B**	25.7	774	30.2	22	157	<0.01	208	14	0.4	<0.1	<0.2	0.18	0.6	1.6	6.3	<0.05	0.09	0.1	5.26	0.05	<0.09	<0.02	<0.08	<0.05	0.03	<0.03	0.02	0.025
14231-0002	**BP_HZ02_R**	29.0	770	34.8	4	157	<0.01	211	3	<0.2	<0.1	<0.2	0.18	0.6	4.7	10.4	<0.05	0.07	0.1	5.10	0.04	<0.09	<0.02	<0.08	<0.05	0.04	<0.03	0.02	0.023
14231-0007	**BP_HZ02_GG**	26.1	763	85.7	28	156	<0.01	205	18	0.6	<0.1	<0.2	0.42	0.9	1.6	14.7	<0.05	0.09	0.1	5.23	0.07	<0.09	<0.02	0.08	<0.05	0.04	<0.03	0.03	0.026
14231-0008	**BP_HZ02_Y**	32.1	802	298	6	158	<0.01	196	5	<0.2	0.1	<0.2	0.91	1.4	4.9	14.0	<0.05	0.58	0.2	8.29	0.07	<0.09	<0.02	0.20	<0.05	0.04	<0.03	0.12	0.025
14231-0010	**BP_SPRING**	26.2	1071	4.3	7	206	<0.01	253	4	<0.2	<0.1	<0.2	0.03	0.4	0.7	15.0	<0.05	<0.06	<0.1	7.91	0.03	<0.09	<0.02	<0.08	<0.05	0.02	<0.03	<0.02	0.015

Sample LIMS Code	Site ID	Ba	Sr	Mn	Fe	Li	Be	B	Al	Ti	V	Cr	Co	Ni	Cu	Zn	Ga	As	Se	Rb	Y	Zr	Nb	Mo	Ag	Cd	Sn	Sb	Cs
		$\mu g\,l^{-1}$	$\mu g\,l^{-1}$	$\mu g\,l^{-1}$	$\mu g\,l^{-1}$	$\mu g\,l^{-1}$	$\mu g\,l^{-1}$	$\mu g\,l^{-1}$	$\mu g\,l^{-1}$	$\mu g\,l^{-1}$	$\mu g\,l^{-1}$	$\mu g\,l^{-1}$	$\mu g\,l^{-1}$	$\mu g\,l^{-1}$	$\mu g\,l^{-1}$	$\mu g\,l^{-1}$	$\mu g\,l^{-1}$	$\mu g\,l^{-1}$	$\mu g\,l^{-1}$	$\mu g\,l^{-1}$	$\mu g\,l^{-1}$	$\mu g\,l^{-1}$	$\mu g\,l^{-1}$	$\mu g\,l^{-1}$	$\mu g\,l^{-1}$	$\mu g\,l^{-1}$	$\mu g\,l^{-1}$	$\mu g\,l^{-1}$	$\mu g\,l^{-1}$
ICP-MS DL		*0.9*	*2*	*2*	*7*	*3*	*0.5*	*11*	*2*	*0.2*	*0.1*	*0.3*	*0.05*	*0.1*	*1*	*2*	*0.08*	*0.07*	*0.1*	*0.05*	*0.02*	*0.05*	*0.02*	*0.3*	*0.05*	*0.04*	*0.04*	*0.05*	*0.02*
14283-0053	**BP_SW**	46.2	994	22.0	21	156	<0.5	165	5	0.2	0.1	<0.3	0.08	0.3	<1	7	<0.08	<0.07	0.1	6.14	<0.02	<0.05	<0.02	<0.3	<0.05	<0.04	<0.04	<0.05	<0.02
14283-0041	**BP_HZ01_B**	41.6	1054	14.0	13	167	<0.5	174	3	<0.2	<0.1	<0.3	<0.05	0.3	<1	7	<0.08	<0.07	0.1	6.92	<0.02	<0.05	<0.02	<0.3	<0.05	<0.04	<0.04	<0.05	<0.02
14283-0042	**BP_HZ01_R**	36.9	1078	5.0	9	171	<0.5	183	<2	<0.2	0.1	<0.3	<0.05	0.4	<1	6	<0.08	<0.07	0.1	6.99	<0.02	<0.05	<0.02	<0.3	<0.05	<0.04	<0.04	<0.05	0.09
14283-0043	**BP_HZ01_G**	35.9	1067	5.0	8	170	<0.5	176	<2	<0.2	<0.1	<0.3	0.05	0.3	<1	9	<0.08	<0.07	0.1	6.92	<0.02	<0.05	<0.02	<0.3	<0.05	<0.04	<0.04	<0.05	<0.02
14283-0044	**BP_HZ01_Y**	36.7	1094	7.0	12	173	<0.5	183	<2	<0.2	0.2	<0.3	<0.05	0.4	<1	13	<0.08	<0.07	<0.1	7.19	<0.02	<0.05	<0.02	<0.3	<0.05	<0.04	<0.04	<0.05	<0.02
14283-0045	**BP_HZ02_B**	39.6	934	53.0	45	155	<0.5	163	4	0.4	0.2	<0.3	0.33	0.7	<1	7	<0.08	0.08	<0.1	5.86	0.05	<0.05	<0.02	<0.3	<0.05	<0.04	<0.04	<0.05	<0.02
14283-0046	**BP_HZ02_R**	33.0	930	109	20	151	<0.5	163	6	0.3	0.2	<0.3	0.35	0.7	<1	5	<0.08	<0.07	0.1	5.65	0.04	<0.05	<0.02	<0.3	<0.05	<0.04	<0.04	<0.05	<0.02
14283-0047	**BP_HZ02_GG**	40.4	936	621	88	149	<0.5	164	9	0.2	0.2	<0.3	2.51	1.2	<1	4	0.17	0.19	<0.1	4.28	0.07	<0.05	<0.02	<0.3	<0.05	<0.04	0.06	<0.05	<0.02
14283-0048	**BP_HZ02_Y**	65.6	768	4392	7500	105	<0.5	123	2	<0.2	0.2	<0.3	10.3	3.1	<1	3	1.76	2.07	<0.1	5.26	0.05	0.08	<0.02	0.4	<0.05	<0.04	<0.04	<0.05	<0.02
14283-0062	**BP_SPRING**	27.7	1192	<2	<7	178	<0.5	182	2	<0.2	<0.1	<0.3	<0.05	0.3	<1	7	<0.08	<0.07	<0.1	7.93	<0.02	<0.05	<0.02	<0.3	<0.05	<0.04	<0.04	<0.05	<0.02

Sample LIMS Code	Site ID	Ba	Sr	Mn	Fe	Li	Be	B	Al	Ti	V	Cr	Co	Ni	Cu	Zn	Ga	As	Se	Rb	Y	Zr	Nb	Mo	Ag	Cd	Sn	Sb	Cs
		$\mu g\,l^{-1}$	$\mu g\,l^{-1}$	$\mu g\,l^{-1}$	$\mu g\,l^{-1}$	$\mu g\,l^{-1}$	$\mu g\,l^{-1}$	$\mu g\,l^{-1}$	$\mu g\,l^{-1}$	$\mu g\,l^{-1}$	$\mu g\,l^{-1}$	$\mu g\,l^{-1}$	$\mu g\,l^{-1}$	$\mu g\,l^{-1}$	$\mu g\,l^{-1}$	$\mu g\,l^{-1}$	$\mu g\,l^{-1}$	$\mu g\,l^{-1}$	$\mu g\,l^{-1}$	$\mu g\,l^{-1}$	$\mu g\,l^{-1}$	$\mu g\,l^{-1}$	$\mu g\,l^{-1}$	$\mu g\,l^{-1}$	$\mu g\,l^{-1}$	$\mu g\,l^{-1}$	$\mu g\,l^{-1}$	$\mu g\,l^{-1}$	$\mu g\,l^{-1}$
ICP-MS DL		*0.05*	*0.06*	*0.2*	*0.4*	*7*	*0.08*	*53*	*2*	*0.02*	*0.4*	*0.2*	*0.2*	*0.05*	*0.2*	*0.3*	*0.3*	*0.03*	*0.05*	*0.05*	*0.2*	*0.04*	*0.08*	*0.04*	*0.05*	*0.01*	*0.01*	*0.008*	*0.03*
14412-0022	**BP_SW**	35.42	1022.49	11.7	13.3	156	<0.08	169	3	0.06	<0.4	<0.2	<0.2	0.49	1.2	8.9	<0.3	0.05	0.06	6.98	<0.2	<0.04	<0.08	<0.04	<0.05	<0.01	<0.01	0.027	<0.03
14412-0021	**BP_HZ01_B**	60.63	1104.37	43.9	15.7	168	<0.08	174	<2	<0.02	<0.4	<0.2	<0.2	0.48	2	12	<0.3	0.05	0.09	6.84	<0.2	<0.04	<0.08	<0.04	<0.05	<0.01	<0.01	0.027	<0.03
14412-0023	**BP_HZ01_R**	35.58	1083.85	6.1	11.4	162	<0.08	186	<2	0.11	<0.4	<0.2	<0.2	0.41	1.6	10.6	<0.3	0.03	0.07	6.8	<0.2	<0.04	<0.08	<0.04	<0.05	<0.01	<0.01	0.02	0.06
14412-0024	**BP_HZ02_G**	42.29	1086.77	9.9	21.6	169	<0.08	185	<2	<0.02	<0.4	<0.2	<0.2	0.4	1.3	9.4	<0.3	0.05	0.09	6.95	<0.2	<0.04	<0.08	<0.04	<0.05	<0.01	<0.01	0.01	<0.03
14412-0025	**BP_HZ01_Y**	45.93	1119.98	6.5	24.3	162	<0.08	180	<2	0.15	<0.4	<0.2	<0.2	0.38	1.5	15.8	<0.3	0.04	0.06	7.43	<0.2	<0.04	<0.08	<0.04	<0.05	0.01	<0.01	0.016	<0.03
14412-0030	**BP_SPRING**	43.89	1213.01	13.5	115.6	177	<0.08	191	12	0.25	<0.4	<0.2	<0.2	0.43	0.8	12	<0.3	0.06	<0.05	8.33	<0.2	<0.04	<0.08	<0.04	<0.05	<0.01	<0.01	0.017	<0.03

Table 21 Water chemical analysis at Bubbly Point (BP) (continued)

Sample LIMS Code	Site ID	La	Ce	Pr	Nd	Sm	Eu	Gd	Tb	Dy	Ho	Er	Tm	Yb	Lu	Hf	Ta	W	Tl	Pb	Th	U
		µg l⁻¹	µg l⁻¹	µg l⁻¹	µg l⁻¹	µg l⁻¹	µg l⁻¹	µg l⁻¹	µg l⁻¹	µg l⁻¹	µg l⁻¹	µg l⁻¹	µg l⁻¹	µg l⁻¹	µg l⁻¹	µg l⁻¹	µg l⁻¹	µg l⁻¹	µg l⁻¹	µg l⁻¹	µg l⁻¹	µg l⁻¹
ICP-MS DL		*0.005*	*0.03*	*0.04*	*0.07*	*0.006*	*0.002*	*0.003*	*0.002*	*0.005*	*0.002*	*0.002*	*0.002*	*0.004*	*0.002*	*0.01*	*0.02*	*0.05*	*0.02*	*0.04*	*0.005*	*0.01*
14231-0011	BP_SW	0.006	<0.03	<0.04	<0.07	<0.006	<0.002	<0.003	<0.002	<0.005	<0.002	<0.002	<0.002	<0.004	<0.002	<0.01	<0.02	<0.05	0.08	0.06	<0.005	3.84
14231-0001	BP_HZ01_B	<0.005	<0.03	<0.04	<0.07	<0.006	<0.002	<0.003	<0.002	<0.005	<0.002	<0.002	<0.002	<0.004	<0.002	<0.01	<0.02	<0.05	0.07	0.05	<0.005	4.23
14231-0003	BP_HZ01_R	<0.005	<0.03	<0.04	<0.07	<0.006	<0.002	<0.003	<0.002	<0.005	<0.002	<0.002	<0.002	<0.004	<0.002	<0.01	<0.02	<0.05	0.08	<0.04	<0.005	4.22
14231-0004	BP_HZ01_G	<0.005	<0.03	<0.04	<0.07	<0.006	<0.002	<0.003	<0.002	<0.005	<0.002	<0.002	<0.002	<0.004	<0.002	<0.01	<0.02	<0.05	0.08	0.05	<0.005	4.30
14231-0005	BP_HZ01_Y	<0.005	<0.03	<0.04	<0.07	<0.006	0.002	<0.003	<0.002	<0.005	<0.002	0.002	<0.002	<0.004	<0.002	<0.01	<0.02	<0.05	0.08	<0.04	<0.005	4.33
14231-0006	BP_HZ02_B	0.027	0.06	<0.04	<0.07	0.011	0.006	0.010	<0.002	0.009	<0.002	0.006	<0.002	<0.004	<0.002	<0.01	<0.02	<0.05	0.14	0.14	<0.005	3.88
14231-0002	BP_HZ02_R	0.015	<0.03	<0.04	<0.07	<0.006	<0.002	0.008	<0.002	0.005	<0.002	0.003	<0.002	<0.004	<0.002	<0.01	<0.02	<0.05	0.16	0.06	<0.005	3.95
14231-0007	BP_HZ02_GG	0.034	0.07	<0.04	0.08	0.010	0.004	0.013	<0.002	0.012	0.002	0.006	<0.002	<0.004	<0.002	<0.01	<0.02	<0.05	0.15	0.13	<0.005	3.95
14231-0008	BP_HZ02_Y	0.023	0.04	<0.04	<0.07	0.007	<0.002	0.009	<0.002	0.008	<0.002	0.004	<0.002	0.007	<0.002	<0.01	<0.02	<0.05	0.17	0.08	<0.005	4.29
14231-0010	BP_SPRING	0.018	<0.03	<0.04	<0.07	<0.006	0.003	0.006	<0.002	<0.005	<0.002	0.003	<0.002	<0.004	<0.002	<0.01	<0.02	<0.05	0.09	0.11	<0.005	4.33

Sample LIMS Code	Site ID	La	Ce	Pr	Nd	Sm	Eu	Gd	Tb	Dy	Ho	Er	Tm	Yb	Lu	Hf	Ta	W	Tl	Pb	Th	U
		µg l⁻¹	µg l⁻¹	µg l⁻¹	µg l⁻¹	µg l⁻¹	µg l⁻¹	µg l⁻¹	µg l⁻¹	µg l⁻¹	µg l⁻¹	µg l⁻¹	µg l⁻¹	µg l⁻¹	µg l⁻¹	µg l⁻¹	µg l⁻¹	µg l⁻¹	µg l⁻¹	µg l⁻¹	µg l⁻¹	µg l⁻¹
ICP-MS DL		*0.03*	*0.04*	*0.05*	*0.2*	*0.03*	*0.008*	*0.007*	*0.007*	*0.007*	*0.007*	*0.008*	*0.007*	*0.008*	*0.007*	*0.01*	*0.02*	*0.05*	*0.01*	*0.02*	*0.009*	*0.009*
14283-0053	BP_SW	<0.03	<0.04	<0.05	<0.2	<0.03	<0.008	<0.007	<0.007	<0.007	<0.007	<0.008	<0.007	<0.008	<0.007	<0.01	<0.02	<0.05	0.08	0.05	<0.009	3.84
14283-0041	BP_HZ01_B	<0.03	<0.04	<0.05	<0.2	<0.03	<0.008	<0.007	<0.007	<0.007	<0.007	<0.008	<0.007	<0.008	<0.007	<0.01	<0.02	<0.05	0.07	0.04	<0.009	3.92
14283-0042	BP_HZ01_R	<0.03	<0.04	<0.05	<0.2	<0.03	<0.008	<0.007	<0.007	<0.007	<0.007	<0.008	<0.007	<0.008	<0.007	<0.01	<0.02	<0.05	0.07	<0.02	<0.009	3.91
14283-0043	BP_HZ01_G	<0.03	<0.04	<0.05	<0.2	<0.03	0.008	<0.007	<0.007	<0.007	<0.007	<0.008	<0.007	<0.008	<0.007	<0.01	<0.02	<0.05	0.07	<0.02	<0.009	3.93
14283-0044	BP_HZ01_Y	<0.03	<0.04	<0.05	<0.2	<0.03	<0.008	<0.007	<0.007	<0.007	<0.007	<0.008	<0.007	<0.008	<0.007	<0.01	<0.02	<0.05	0.07	<0.02	<0.009	3.94
14283-0045	BP_HZ02_B	<0.03	<0.04	<0.05	<0.2	<0.03	0.009	<0.007	<0.007	<0.007	<0.007	<0.008	<0.007	0.009	<0.007	<0.01	<0.02	<0.05	0.12	0.10	<0.009	3.84
14283-0046	BP_HZ02_R	<0.03	<0.04	<0.05	<0.2	<0.03	<0.008	<0.007	<0.007	<0.007	<0.007	<0.008	<0.007	<0.008	<0.007	<0.01	<0.02	<0.05	0.15	0.06	<0.009	3.86
14283-0047	BP_HZ02_GG	0.04	0.10	<0.05	<0.2	<0.03	<0.008	0.009	<0.007	0.009	<0.007	<0.008	<0.007	<0.008	<0.007	<0.01	<0.02	<0.05	0.11	0.09	0.010	3.85
14283-0048	BP_HZ02_Y	<0.03	<0.04	<0.05	<0.2	<0.03	<0.008	<0.007	<0.007	<0.007	<0.007	<0.008	<0.007	<0.008	<0.007	<0.01	<0.02	<0.05	0.02	0.02	<0.009	3.59
14283-0062	BP_SPRING	<0.03	<0.04	<0.05	<0.2	<0.03	<0.008	<0.007	<0.007	<0.007	<0.007	<0.008	<0.007	<0.008	<0.007	<0.01	<0.02	<0.05	0.06	<0.02	<0.009	3.97

Sample LIMS Code	Site ID	La	Ce	Pr	Nd	Sm	Eu	Gd	Tb	Dy	Ho	Er	Tm	Yb	Lu	Hf	Ta	W	Tl	Pb	Th	U
		µg l⁻¹	µg l⁻¹	µg l⁻¹	µg l⁻¹	µg l⁻¹	µg l⁻¹	µg l⁻¹	µg l⁻¹	µg l⁻¹	µg l⁻¹	µg l⁻¹	µg l⁻¹	µg l⁻¹	µg l⁻¹	µg l⁻¹	µg l⁻¹	µg l⁻¹	µg l⁻¹	µg l⁻¹	µg l⁻¹	µg l⁻¹
ICP-MS DL		*0.005*	*0.004*	*0.003*	*0.005*	*0.003*	*0.003*	*0.004*	*0.003*	*0.006*	*0.006*	*0.06*	*0.02*	*0.02*	*0.08*	*0.03*	*0.009*	*0.03*	*0.009*	*0.04*	*0.009*	*0.009*
14412-0022	BP_SW	<0.005	0.011	<0.003	<0.005	<0.003	<0.003	<0.004	<0.003	<0.006	<0.006	<0.06	<0.02	<0.02	<0.08	<0.03	<0.009	<0.03	0.091	0.05	<0.009	3.84
14412-0021	BP_HZ01_B	<0.005	0.006	<0.003	<0.005	<0.003	<0.003	<0.004	<0.003	<0.006	<0.006	<0.06	<0.02	<0.02	<0.08	<0.03	<0.009	<0.03	0.065	0.06	<0.009	4.03
14412-0023	BP_HZ01_R	0.008	0.013	0.003	0.007	0.008	<0.003	<0.004	<0.003	<0.006	<0.006	<0.06	<0.02	<0.02	<0.08	<0.03	<0.009	<0.03	0.069	<0.04	<0.009	3.95
14412-0024	BP_HZ02_G	<0.005	0.008	<0.003	<0.005	<0.003	<0.003	<0.004	<0.003	<0.006	<0.006	<0.06	<0.02	<0.02	<0.08	<0.03	<0.009	<0.03	0.069	<0.04	<0.009	3.94
14412-0025	BP_HZ01_Y	<0.005	0.007	<0.003	0.011	<0.003	<0.003	<0.004	<0.003	<0.006	<0.006	<0.06	<0.02	<0.02	<0.08	<0.03	<0.009	<0.03	0.068	0.17	<0.009	4.04
14412-0030	BP_SPRING	0.028	0.071	0.005	0.022	<0.003	<0.003	0.012	<0.003	0.01	<0.006	<0.06	<0.02	<0.02	<0.08	<0.03	<0.009	<0.03	0.064	0.05	<0.009	4.09

Table 22 Water chemical analysis at Little House (LH) site

Sample LIMS Code	Site ID	Sampling Date	T	Eh	pH	SEC	DO	TDS	Ca	Mg	Na	K	HCO₃⁻	Cl⁻	SO₄²⁻	NO₃⁻	Br⁻	NO₂⁻	HPO₄²⁻	F⁻	NPOC	Total P	Si
			°C	mV		µS cm⁻¹	mg l⁻¹	mg l⁻¹	mg l⁻¹	mg l⁻¹	mg l⁻¹	mg l⁻¹	mg l⁻¹	mg l⁻¹	mg l⁻¹	mg l⁻¹	mg l⁻¹	mg l⁻¹	mg l⁻¹	mg l⁻¹	mg l⁻¹	mg l⁻¹	mg l⁻¹
ICP-MS DL									*0.7*	*0.01*	*0.3*	*0.03*										*0.04*	*0.05*
14231-0037	**LH_SW**	26/04/2018	11.6	401	6.96	1471	11.6	1190	143	77.7	66.8	7.32	452	79.5	356	7.09	<0.1	<0.05	<0.1	0.206	3.26	0.05	3.94
14231-0025	**LH_HZ01_B**	26/04/2018	12.3	212	6.62	1031	3.6	787	115	44.0	31.2	3.51	359	54.6	177	2.21	<0.1	<0.05	<0.1	0.195	3.75	<0.04	7.36
14231-0026	**LH_HZ01_R**	26/04/2018	12.3	466	6.89	729	2.1	545	91.0	27.0	10.5	1.59	303	38.2	74.0	0.2	<0.1	<0.05	<0.1	0.171	3.90	<0.04	8.94
14231-0027	**LH_HZ01_G**	26/04/2018	14.1	379	6.87	645	2.1	482	82.9	22.7	7.8	1.28	279	34.6	53.9	0.2	<0.1	<0.05	<0.1	0.197	3.99	<0.04	8.44
14231-0028	**LH_HZ01_Y**	26/04/2018	11.7	400	6.65	655	3.2	470	81.0	21.3	7.8	1.20	270	35.9	53.8	0.2	<0.1	<0.05	<0.1	0.168	3.18	<0.04	8.53
14231-0029	**LH_HZ02_B**	26/04/2018	16.2	157	7.31	770	2.0	588	93.6	30.8	18.4	1.85	288	43.9	111	0.985	<0.1	<0.05	<0.1	0.201	3.54	<0.04	7.35
14231-0030	**LH_HZ02_R**	26/04/2018	16.5	172	6.77	738	1.6	639	89.8	26.4	14.9	1.22	268	35.1	204	0.2	<0.1	<0.05	<0.1	0.358	3.72	<0.04	7.74
14231-0031	**LH_HZ02_G**	26/04/2018	12.5	382	6.67	651	2.4	455	80.8	20.9	7.9	0.76	264	32.7	47.8	0.2	<0.1	<0.05	<0.1	0.126	3.35	<0.04	8.56
14231-0032	**LH_HZ02_Y**	26/04/2018	11.9	393	7.14	648	1.6	460	81.9	20.5	8.2	0.77	264	34.3	50.3	0.2	<0.1	<0.05	<0.1	0.128	3.17	<0.04	8.54
14231-0033	**LH_HZ03_B**	26/04/2018	13.5	325	7.28	651	2.6	460	82.9	20.3	8.3	0.36	262	34.6	51.5	0.2	<0.1	<0.05	<0.1	0.129	3.38	<0.04	8.16
14231-0034	**LH_HZ03_R**	26/04/2018	13.7	355	6.76	648	2.7	447	79.1	19.6	7.5	0.32	254	35.0	51.4	0.2	<0.1	<0.05	<0.1	0.118	3.29	<0.04	7.76
14231-0035	**LH_HZ03_G**	26/04/2018	13.9	365	7.18	658	3.2	445	75.6	19.3	9.4	0.39	254	35.1	51.8	0.2	<0.1	<0.05	<0.1	0.119	3.79	<0.04	7.26
14231-0036	**LH_HZ03_Y**	26/04/2018	13.9	118	6.88	652	3.1	456	81.7	20.2	8.0	0.35	260	34.6	51.3	0.2	<0.1	<0.05	<0.1	0.120	3.88	<0.04	8.20

Sample LIMS Code	Site ID	Sampling Date	T	Eh	pH	SEC	DO	TDS	Ca	Mg	Na	K	HCO₃⁻	Cl⁻	SO₄²⁻	NO₃⁻	Br⁻	NO₂⁻	HPO₄²⁻	F⁻	NPOC	Total P	Si
			°C	mV		µS cm⁻¹	mg l⁻¹	mg l⁻¹	mg l⁻¹	mg l⁻¹	mg l⁻¹	mg l⁻¹	mg l⁻¹	mg l⁻¹	mg l⁻¹	mg l⁻¹	mg l⁻¹	mg l⁻¹	mg l⁻¹	mg l⁻¹	mg l⁻¹	mg l⁻¹	mg l⁻¹
ICP-MS DL									*0.6*	*0.07*	*0.5*	*0.03*									*0.5*	*0.04*	*0.05*
14283-0051	**LH_SW**	01/08/2018	15.2	379	6.96	1819	9.16	1190	209	115	72.6	8.81	590	55.4	605	1.80	<0.2	<0.1	<0.2	0.244	1.21	<0.04	5.18
14283-0017	**LH_HZ01_B**	01/08/2018	19.3	146	6.65	1153	2.78	787	154	54.8	30.1	2.83	424	45.6	292	0.2	<0.1	<0.05	<0.1	0.288	4.56	0.05	10.01
14283-0018	**LH_HZ01_R**	01/08/2018	21.6	79	6.87	1039	2.29	545	147	44.5	21.2	1.86	381	42.6	248	0.2	<0.1	<0.05	<0.1	0.197	7.43	<0.04	10.50
14283-0019	**LH_HZ01_G**	01/08/2018	21.4	99	6.85	1140	1.78	482	171	52.4	23.6	2.23	404	44.9	321	0.2	<0.1	<0.05	<0.1	0.155	8.50	<0.04	10.10
14283-0020	**LH_HZ01_Y**	01/08/2018	19.8	140	6.63	1155	1.73	470	167	54.1	24.4	2.56	407	48.0	328	0.2	0.106	<0.05	<0.1	0.198	26.8	<0.04	10.08
14283-0021	**LH_HZ02_B**	01/08/2018	20.6	90	7.12	1196	3.01	588	156	70.7	40.6	4.75	450	49.2	379	0.948	<0.1	<0.05	<0.1	0.308	5.15	<0.04	7.34
14283-0022	**LH_HZ02_R**	01/08/2018			7.71			639	118	32.2	14.7	1.07	309	41.3	161	0.2	<0.1	<0.05	<0.1	0.197	6.91	<0.04	8.33
14283-0023	**LH_HZ02_G**	01/08/2018	21.6	108	6.72	814	2.75	455	116	30.8	13.6	1.03	306	39.6	141	0.08	0.052	<0.025	<0.05	0.200	4.73	<0.04	9.37
14283-0024	**LH_HZ02_Y**	01/08/2018	20.1	105	6.76	770	2.2	460	111	28.7	12.5	0.87	291	39.3	128	0.08	<0.05	<0.025	<0.05	0.176	4.46	<0.04	9.54
14283-0025	**LH_HZ03_B**	01/08/2018	18.8	116	6.75	600	2.67	460	88.7	21.1	7.4	0.38	246	37.7	64	0.158	<0.05	<0.025	<0.05	0.159	15.9	<0.04	8.86
14283-0026	**LH_HZ03_R**	01/08/2018	21.2	114	6.73	590	6.64	447	85.4	20.3	7.0	0.35	250	38.0	64	0.08	<0.05	<0.025	<0.05	0.194	10.1	<0.04	9.10
14283-0027	**LH_HZ03_G**	01/08/2018	21.9	100	6.79	589	1.69	445	85.5	20.4	7.1	0.36	249	37.3	62	0.08	<0.05	<0.025	<0.05	0.210	3.52	<0.04	9.04
14283-0028	**LH_HZ03_Y**	01/08/2018	22.7	87	6.78	591	1.83	456	84.6	20.3	7.0	0.32	245	37.0	59	0.08	<0.05	<0.025	<0.05	0.192	8.14	<0.04	8.95

Sample LIMS Code	Site ID	Sampling Date	T	Eh	pH	SEC	DO	TDS	Ca	Mg	Na	K	HCO₃⁻	Cl⁻	SO₄²⁻	NO₃⁻	Br⁻	NO₂⁻	HPO₄²⁻	F⁻	NPOC	Total P	Si
			°C	mV		µS cm⁻¹	mg l⁻¹	mg l-1	mg l-1	mg l-1	mg l-1	mg l-1	mg l-1	mg l-1	mg l-1	mg l-1	mg l-1	mg l-1	mg l-1	mg l-1	mg l-1	mg l-1	mg l-1
ICP-MS DL									*0.04*	*0.004*	*0.4*	*0.03*	*5.0*								*0.5*	*0.02*	*0.042*
14412-0017	**LH_SW**	06/02/2019	7.3	459	7.11	1890	8.0	1190	185	91.5	105	9.65	524	128	492	7.80	<0.2	<0.1	<0.2	0.246	1.96	0.05	4.03
14412-0018	**LH_HZ01_B**	06/02/2019	7.7	138	6.99	1146	2.9	787	140	39.6	22.6	2.04	388	49.0	207	<0.3	<0.1	<0.05	<0.1	0.142	3.77	0.42	9.38
14412-0020	**LH_HZ01_R**	06/02/2019	7.1	123	7.07	1081	2.8	545	139	39.6	17.8	1.88	388	41.6	200	<0.3	<0.1	<0.05	<0.1	0.138	4.53	0.17	8.86
14412-0026	**LH_HZ01_G**	06/02/2019	8.1	154	7.19	1105	9.6	482	149	46.9	21.6	2.61	409	42.9	244	<0.3	<0.1	<0.05	<0.1	0.157	6.39	<0.02	8.22
14412-0019	**LH_HZ01_Y**	06/02/2019	7.8	169	6.90	1202	3.0	470	157	48.5	22.0	3.08	410	41.5	247	<0.3	<0.1	<0.05	<0.1	0.154	6.58	0.06	8.38

Table 22 Water chemical analysis at Little House (LH) site (continued)

Sample LIMS Code	Site ID	Ba	Sr	Mn	Fe	Li	Be	B	Al	Ti	V	Cr	Co	Ni	Cu	Zn	Ga	As	Se	Rb	Y	Zr	Nb	Mo	Ag	Cd	Sn	Sb	Cs
		µg l⁻¹	µg l⁻¹	µg l⁻¹	µg l⁻¹	µg l⁻¹	µg l⁻¹	µg l⁻¹	µg l⁻¹	µg l⁻¹	µg l⁻¹	µg l⁻¹	µg l⁻¹	µg l⁻¹	µg l⁻¹	µg l⁻¹	µg l⁻¹	µg l⁻¹	µg l⁻¹	µg l⁻¹	µg l⁻¹	µg l⁻¹	µg l⁻¹	µg l⁻¹	µg l⁻¹	µg l⁻¹	µg l⁻¹	µg l⁻¹	µg l⁻¹
ICP-MS DL		0.1	0.2	0.3	2	3	0.01	18	2	0.2	0.1	0.2	0.02	0.1	0.6	0.8	0.05	0.06	0.1	0.01	0.01	0.09	0.02	0.08	0.05	0.02	0.03	0.02	0.005
14231-0037	LH_SW	64.8	467	39.9	11	65	<0.01	106	3	0.2	0.2	0.7	0.18	2.7	3.3	9.2	<0.05	0.21	0.3	4.12	0.02	<0.09	<0.02	0.67	<0.05	0.03	<0.03	0.14	0.010
14231-0025	LH_HZ01_B	241	302	3524	23	27	<0.01	71	<2	<0.2	<0.1	0.2	4.50	2.7	6.5	13.2	0.80	0.73	0.2	2.85	0.03	<0.09	<0.02	0.80	<0.05	0.02	<0.03	0.19	0.007
14231-0026	LH_HZ01_R	205	200	3280	89	8	<0.01	45	<2	<0.2	<0.1	0.2	3.70	2.0	3.2	8.8	0.76	0.50	<0.1	1.30	0.02	<0.09	<0.02	0.44	<0.05	<0.02	<0.03	0.09	<0.005
14231-0027	LH_HZ01_G	218	159	1950	91	5	0.02	37	11	0.3	0.2	0.6	2.69	3.3	3.0	6.8	0.49	0.57	<0.1	1.01	0.05	<0.09	<0.02	0.54	<0.05	<0.02	<0.03	0.15	0.011
14231-0028	LH_HZ01_Y	267	146	1270	925	3	<0.01	37	<2	<0.2	<0.1	0.4	6.13	11.7	3.5	9.5	0.30	0.55	<0.1	0.70	0.02	<0.09	<0.02	1.20	<0.05	<0.02	<0.03	0.22	0.011
14231-0029	LH_HZ02_B	289	207	1272	12	13	<0.01	51	6	<0.2	0.3	<0.2	1.09	1.7	<0.6	7.2	0.31	0.68	0.2	1.44	0.04	<0.09	<0.02	0.83	<0.05	<0.02	<0.03	0.17	0.010
14231-0030	LH_HZ02_R	349	176	1477	430	8	0.01	51	10	<0.2	0.1	0.2	2.34	3.5	6.2	15.4	0.36	0.64	<0.1	1.17	0.04	<0.09	<0.02	0.81	<0.05	<0.02	<0.03	0.12	0.011
14231-0031	LH_HZ02_G	297	147	1481	498	3	0.02	35	<2	<0.2	<0.1	1.1	4.32	6.8	3.1	11.3	0.38	0.51	<0.1	0.71	0.02	<0.09	<0.02	0.64	<0.05	<0.02	<0.03	0.11	0.008
14231-0032	LH_HZ02_Y	312	146	1382	492	3	0.02	36	2	<0.2	<0.1	1.7	5.16	9.3	2.0	10.8	0.35	0.56	<0.1	0.76	0.02	<0.09	<0.02	0.82	<0.05	<0.02	<0.03	0.19	0.012
14231-0033	LH_HZ03_B	355	149	1438	2248	3	0.02	37	9	0.3	<0.1	1.7	1.80	2.8	0.7	6.0	0.37	0.25	<0.1	0.54	0.03	<0.09	<0.02	0.69	<0.05	<0.02	<0.03	0.05	0.012
14231-0034	LH_HZ03_R	329	143	1315	10	2	<0.01	34	3	<0.2	<0.1	0.3	1.49	2.8	1.8	6.3	0.32	0.41	<0.1	0.51	0.01	<0.09	<0.02	0.74	<0.05	<0.02	<0.03	0.05	0.010
14231-0035	LH_HZ03_G	315	136	1239	55	3	<0.01	34	10	0.4	<0.1	4.1	1.18	2.7	1.9	6.2	0.32	0.33	<0.1	0.53	0.03	<0.09	<0.02	0.85	<0.05	<0.02	<0.03	0.06	0.013
14231-0036	LH_HZ03_Y	349	147	1384	1112	3	0.01	34	3	0.2	<0.1	1.2	1.61	3.5	4.7	9.5	0.34	0.31	<0.1	0.49	0.02	<0.09	<0.02	0.51	<0.05	<0.02	<0.03	0.08	0.038

Sample LIMS Code	Site ID	Ba	Sr	Mn	Fe	Li	Be	B	Al	Ti	V	Cr	Co	Ni	Cu	Zn	Ga	As	Se	Rb	Y	Zr	Nb	Mo	Ag	Cd	Sn	Sb	Cs
		µg l⁻¹	µg l⁻¹	µg l⁻¹	µg l⁻¹	µg l⁻¹	µg l⁻¹	µg l⁻¹	µg l⁻¹	µg l⁻¹	µg l⁻¹	µg l⁻¹	µg l⁻¹	µg l⁻¹	µg l⁻¹	µg l⁻¹	µg l⁻¹	µg l⁻¹	µg l⁻¹	µg l⁻¹	µg l⁻¹	µg l⁻¹	µg l⁻¹	µg l⁻¹	µg l⁻¹	µg l⁻¹	µg l⁻¹	µg l⁻¹	µg l⁻¹
ICP-MS DL		0.9	2	2	7	3	0.5	11	2	0.2	0.1	0.3	0.05	0.1	1	2	0.08	0.07	0.1	0.05	0.02	0.05	0.02	0.3	0.05	0.04	0.04	0.05	0.02
14283-0051	LH_SW	75.9	743	61.0	67	111	<0.5	133	11	0.4	0.2	<0.3	0.14	0.7	<1	9	<0.08	0.15	0.3	4.94	0.05	<0.05	<0.02	<0.3	<0.05	<0.04	<0.04	0.07	<0.02
14283-0017	LH_HZ01_B	430	337	3595	27709	26	<0.5	61	6	0.2	0.6	<0.3	3.15	1.6	<1	2	1.32	2.57	0.2	1.90	0.04	0.06	<0.02	0.8	<0.05	<0.04	0.13	0.07	<0.02
14283-0018	LH_HZ01_R	526	277	2801	27067	9	<0.5	44	10	0.9	0.4	<0.3	1.71	1.6	<1	4	1.06	1.68	0.2	1.36	0.06	0.07	<0.02	0.5	<0.05	<0.04	0.06	0.06	<0.02
14283-0019	LH_HZ01_G	601	303	2485	21330	5	<0.5	40	7	0.2	0.4	<0.3	1.16	3.9	81	8	0.91	0.56	0.2	1.09	0.05	0.06	<0.02	0.3	<0.05	<0.04	3.34	0.09	<0.02
14283-0020	LH_HZ01_Y	651	290	2159	20335	5	<0.5	40	9	0.8	1.0	0.4	2.49	5.6	<1	8	0.80	0.84	0.2	0.99	0.10	0.10	<0.02	0.5	<0.05	<0.04	0.10	0.12	0.02
14283-0021	LH_HZ02_B	209	453	1854	6428	55	<0.5	82	13	0.7	0.2	<0.3	3.83	2.6	<1	7	0.72	0.79	0.2	3.18	0.05	<0.05	<0.02	0.4	<0.05	<0.04	0.07	0.13	<0.02
14283-0022	LH_HZ02_R	416	221	1834	2908	5	<0.5	36	6	<0.2	0.1	<0.3	1.05	3.8	<1	4	0.72	0.31	0.1	0.81	0.04	<0.05	<0.02	<0.3	<0.05	<0.04	0.35	0.07	<0.02
14283-0023	LH_HZ02_G	488	211	1897	17988	4	<0.5	35	37	1.5	0.9	<0.3	0.82	1.9	<1	8	0.77	0.77	0.1	0.70	0.15	0.07	<0.02	<0.3	<0.05	<0.04	0.04	0.08	0.02
14283-0024	LH_HZ02_Y	484	204	1979	19845	4	<0.5	33	20	1.1	0.8	<0.3	0.87	2.0	<1	6	0.74	0.78	0.1	0.69	0.12	0.07	<0.02	0.3	<0.05	<0.04	0.08	0.07	<0.02
14283-0025	LH_HZ03_B	464	164	1625	17538	4	<0.5	32	17	1.2	0.8	<0.3	0.18	0.6	<1	6	0.61	0.35	0.1	0.55	0.09	<0.05	<0.02	<0.3	<0.05	<0.04	<0.04	<0.05	<0.02
14283-0026	LH_HZ03_R	443	161	1603	16201	3	<0.5	30	25	1.5	0.5	<0.3	0.23	0.6	<1	5	0.58	0.42	0.1	0.51	0.10	<0.05	<0.02	<0.3	<0.05	<0.04	0.16	<0.05	<0.02
14283-0027	LH_HZ03_G	431	157	1577	16626	4	<0.5	30	16	1.0	0.6	<0.3	0.15	0.5	<1	3	0.57	0.30	<0.1	0.48	0.10	0.06	<0.02	<0.3	<0.05	<0.04	0.04	<0.05	0.02
14283-0028	LH_HZ03_Y	431	157	1601	17354	4	<0.5	30	16	1.4	0.7	<0.3	0.41	1.1	<1	4	0.60	0.35	0.1	0.50	0.07	<0.05	<0.02	<0.3	<0.05	<0.04	0.32	<0.05	0.08

Sample LIMS Code	Site ID	Ba	Sr	Mn	Fe	Li	Be	B	Al	Ti	V	Cr	Co	Ni	Cu	Zn	Ga	As	Se	Rb	Y	Zr	Nb	Mo	Ag	Cd	Sn	Sb	Cs
		µg l-1	µg l-1	µg l-1	µg l-1	µg l-1	µg l-1	µg l-1	µg l-1	µg l-1	µg l-1	µg l-1	µg l-1	µg l-1	µg l-1	µg l-1	µg l-1	µg l-1	µg l-1	µg l-1	µg l-1	µg l-1	µg l-1	µg l-1	µg l-1	µg l-1	µg l-1	µg l-1	µg l-1
ICP-MS DL		0.05	0.06	0.2	0.4	7	0.08	53	2	0.02	0.4	0.2	0.2	0.05	0.2	0.3	0.3	0.03	0.05	0.05	0.2	0.04	0.08	0.04	0.05	0.01	0.01	0.008	0.03
14412-0017	LH_SW	69.46	680.34	62.4	46.9	95	<0.08	108	9	0.2	<0.4	<0.2	<0.2	1.08	1.4	9.5	<0.3	0.18	0.25	4.85	<0.2	<0.04	<0.08	0.24	<0.05	0.03	0.01	0.121	<0.03
14412-0018	LH_HZ01_B	416	281	3221	34720	9	<0.08	<53	12	0.51	0.4	0.2	1.9	1.44	<0.2	4.1	<0.3	2.12	0.15	1.2	<0.2	0.09	<0.08	0.14	<0.05	<0.01	0.02	0.048	<0.03
14412-0020	LH_HZ01_R	524	253	2614	27677	3.5	<0.08	<53	14	0.35	<0.4	0.3	1	1.32	<0.2	2.6	<0.3	1.32	0.16	0.93	<0.2	0.11	<0.08	0.09	<0.05	0.01	0.02	0.052	<0.03
14412-0026	LH_HZ01_G	413	272	2197	8222	3.5	<0.08	<53	4	0.43	<0.4	<0.2	0.9	1.66	1.1	9.1	<0.3	0.37	0.16	1.12	<0.2	0.05	<0.08	0.11	<0.05	<0.01	0.02	0.05	<0.03
14412-0019	LH_HZ01_Y	540	270	1916	18442	3.5	<0.08	<53	27	2.04	1.1	0.3	0.8	2.31	0.3	5	<0.3	0.58	0.17	0.97	<0.2	0.19	<0.08	0.2	<0.05	0.02	<0.01	0.083	<0.03

Table 22 Water chemical analysis at Little House (LH) site (continued)

Sample LIMS Code	Site ID	La	Ce	Pr	Nd	Sm	Eu	Gd	Tb	Dy	Ho	Er	Tm	Yb	Lu	Hf	Ta	W	Tl	Pb	Th	U
		µg l⁻¹	µg l⁻¹	µg l⁻¹	µg l⁻¹	µg l⁻¹	µg l⁻¹	µg l⁻¹	µg l⁻¹	µg l⁻¹	µg l⁻¹	µg l⁻¹	µg l⁻¹	µg l⁻¹	µg l⁻¹	µg l⁻¹	µg l⁻¹	µg l⁻¹	µg l⁻¹	µg l⁻¹	µg l⁻¹	µg l⁻¹
ICP-MS DL		*0.005*	*0.03*	*0.04*	*0.07*	*0.006*	*0.002*	*0.003*	*0.002*	*0.005*	*0.002*	*0.002*	*0.002*	*0.004*	*0.002*	*0.01*	*0.02*	*0.05*	*0.02*	*0.04*	*0.005*	*0.01*
14231-0037	LH_SW	<0.005	<0.03	<0.04	<0.07	<0.006	<0.002	<0.003	<0.002	<0.005	<0.002	<0.002	<0.002	0.005	<0.002	<0.01	<0.02	<0.05	0.04	0.09	<0.005	2.48
14231-0025	LH_HZ01_B	<0.005	<0.03	<0.04	<0.07	<0.006	<0.002	0.003	<0.002	<0.005	<0.002	0.003	<0.002	0.005	<0.002	<0.01	<0.02	<0.05	<0.02	0.18	<0.005	1.10
14231-0026	LH_HZ01_R	<0.005	<0.03	<0.04	<0.07	<0.006	<0.002	<0.003	<0.002	<0.005	<0.002	<0.002	<0.002	<0.004	<0.002	<0.01	<0.02	<0.05	<0.02	0.07	<0.005	0.260
14231-0027	LH_HZ01_G	0.015	0.04	<0.04	<0.07	0.009	0.002	0.009	<0.002	0.008	<0.002	0.005	<0.002	0.004	<0.002	<0.01	<0.02	<0.05	<0.02	0.27	0.01	0.260
14231-0028	LH_HZ01_Y	<0.005	<0.03	<0.04	<0.07	<0.006	<0.002	<0.003	<0.002	<0.005	<0.002	0.002	<0.002	<0.004	<0.002	<0.01	<0.02	<0.05	<0.02	0.07	<0.005	0.190
14231-0029	LH_HZ02_B	0.010	<0.03	<0.04	<0.07	<0.006	0.003	0.005	<0.002	<0.005	<0.002	0.005	<0.002	<0.004	<0.002	<0.01	<0.02	<0.05	<0.02	0.09	<0.005	0.890
14231-0030	LH_HZ02_R	0.017	<0.03	<0.04	<0.07	<0.006	<0.002	0.008	<0.002	<0.005	<0.002	0.004	<0.002	0.005	<0.002	<0.01	<0.02	<0.05	<0.02	0.16	<0.005	0.620
14231-0031	LH_HZ02_G	0.006	<0.03	<0.04	<0.07	<0.006	<0.002	<0.003	<0.002	<0.005	<0.002	0.003	<0.002	<0.004	<0.002	<0.01	<0.02	<0.05	<0.02	0.16	<0.005	0.120
14231-0032	LH_HZ02_Y	0.005	<0.03	<0.04	<0.07	<0.006	<0.002	<0.003	<0.002	<0.005	<0.002	<0.002	<0.002	<0.004	<0.002	<0.01	<0.02	<0.05	<0.02	0.15	<0.005	0.120
14231-0033	LH_HZ03_B	0.020	0.04	<0.04	<0.07	<0.006	<0.002	0.007	<0.002	0.008	<0.002	0.006	<0.002	0.006	0.002	<0.01	<0.02	<0.05	<0.02	0.22	0.01	0.080
14231-0034	LH_HZ03_R	0.008	<0.03	<0.04	<0.07	<0.006	<0.002	<0.003	<0.002	<0.005	<0.002	<0.002	<0.002	0.005	<0.002	<0.01	<0.02	<0.05	<0.02	0.07	<0.005	0.110
14231-0035	LH_HZ03_G	0.018	0.04	<0.04	<0.07	0.013	<0.002	0.004	<0.002	0.005	<0.002	0.003	<0.002	<0.004	<0.002	<0.01	<0.02	<0.05	<0.02	0.20	<0.005	0.080
14231-0036	LH_HZ03_Y	0.008	<0.03	<0.04	<0.07	<0.006	<0.002	0.004	<0.002	<0.005	<0.002	<0.002	<0.002	0.006	<0.002	<0.01	<0.02	<0.05	<0.02	0.20	<0.005	0.040

Sample LIMS Code	Site ID	La	Ce	Pr	Nd	Sm	Eu	Gd	Tb	Dy	Ho	Er	Tm	Yb	Lu	Hf	Ta	W	Tl	Pb	Th	U
		µg l⁻¹	µg l⁻¹	µg l⁻¹	µg l⁻¹	µg l⁻¹	µg l⁻¹	µg l⁻¹	µg l⁻¹	µg l⁻¹	µg l⁻¹	µg l⁻¹	µg l⁻¹	µg l⁻¹	µg l⁻¹	µg l⁻¹	µg l⁻¹	µg l⁻¹	µg l⁻¹	µg l⁻¹	µg l⁻¹	µg l⁻¹
ICP-MS DL		*0.03*	*0.04*	*0.05*	*0.2*	*0.03*	*0.008*	*0.007*	*0.007*	*0.007*	*0.007*	*0.008*	*0.007*	*0.008*	*0.007*	*0.01*	*0.02*	*0.05*	*0.01*	*0.02*	*0.009*	*0.009*
14283-0051	LH_SW	<0.03	<0.04	<0.05	<0.2	<0.03	<0.008	<0.007	<0.007	0.007	<0.007	<0.008	<0.007	<0.008	<0.007	<0.01	<0.02	<0.05	0.07	0.17	<0.009	3.64
14283-0017	LH_HZ01_B	<0.03	<0.04	<0.05	<0.2	<0.03	0.009	0.011	<0.007	0.011	<0.007	<0.008	<0.007	0.013	<0.007	<0.01	<0.02	0.05	<0.01	0.08	0.014	0.581
14283-0018	LH_HZ01_R	<0.03	0.05	<0.05	<0.2	<0.03	<0.008	0.010	<0.007	0.018	<0.007	<0.008	<0.007	0.021	<0.007	<0.01	<0.02	<0.05	<0.01	0.23	0.014	0.131
14283-0019	LH_HZ01_G	<0.03	0.15	<0.05	<0.2	<0.03	<0.008	<0.007	<0.007	0.007	<0.007	<0.008	<0.007	0.020	<0.007	<0.01	<0.02	<0.05	<0.01	4.46	0.010	0.066
14283-0020	LH_HZ01_Y	0.03	0.11	<0.05	<0.2	<0.03	0.012	0.022	<0.007	0.011	<0.007	0.009	<0.007	0.030	<0.007	<0.01	<0.02	<0.05	<0.01	0.42	0.018	0.078
14283-0021	LH_HZ02_B	<0.03	0.11	<0.05	<0.2	<0.03	0.013	0.011	<0.007	0.015	<0.007	<0.008	<0.007	0.011	<0.007	<0.01	<0.02	<0.05	<0.01	0.28	0.011	1.80
14283-0022	LH_HZ02_R	<0.03	0.04	<0.05	<0.2	<0.03	<0.008	<0.007	<0.007	<0.007	<0.007	<0.008	<0.007	0.016	<0.007	<0.01	<0.02	<0.05	<0.01	0.10	<0.009	0.200
14283-0023	LH_HZ02_G	0.08	0.20	<0.05	<0.2	0.04	0.016	0.055	0.008	0.034	0.007	0.016	<0.007	0.019	<0.007	<0.01	<0.02	<0.05	<0.01	0.89	0.032	0.057
14283-0024	LH_HZ02_Y	0.06	0.17	<0.05	<0.2	0.04	0.016	0.032	<0.007	0.025	<0.007	0.011	<0.007	0.025	<0.007	<0.01	<0.02	<0.05	<0.01	0.96	0.031	0.046
14283-0025	LH_HZ03_B	0.04	0.10	<0.05	<0.2	<0.03	<0.008	0.022	0.008	0.012	0.007	0.011	<0.007	0.019	0.007	<0.01	<0.02	<0.05	<0.01	0.28	0.020	0.043
14283-0026	LH_HZ03_R	0.06	0.12	<0.05	<0.2	<0.03	0.018	0.023	0.008	0.016	0.007	0.011	<0.007	0.009	<0.007	<0.01	<0.02	<0.05	<0.01	0.21	0.024	0.035
14283-0027	LH_HZ03_G	0.05	0.13	<0.05	<0.2	<0.03	0.020	0.021	0.007	0.016	0.009	0.014	<0.007	0.015	0.008	<0.01	<0.02	<0.05	<0.01	0.15	0.026	0.033
14283-0028	LH_HZ03_Y	0.04	0.09	<0.05	<0.2	0.03	<0.008	0.016	<0.007	0.012	<0.007	<0.008	<0.007	0.015	<0.007	<0.01	<0.02	<0.05	<0.01	0.24	0.014	0.025

Sample LIMS Code	Site ID	La	Ce	Pr	Nd	Sm	Eu	Gd	Tb	Dy	Ho	Er	Tm	Yb	Lu	Hf	Ta	W	Tl	Pb	Th	U
		µg l-1	µg l-1	µg l-1	µg l-1	µg l-1	µg l-1	µg l-1	µg l-1	µg l-1	µg l-1	µg l-1	µg l-1	µg l-1	µg l-1	µg l-1	µg l-1	µg l-1	µg l-1	µg l-1	µg l-1	µg l-1
ICP-MS DL		*0.005*	*0.004*	*0.003*	*0.005*	*0.003*	*0.003*	*0.004*	*0.003*	*0.006*	*0.006*	*0.06*	*0.02*	*0.02*	*0.08*	*0.03*	*0.009*	*0.03*	*0.009*	*0.04*	*0.009*	*0.009*
14412-0017	LH_SW	0.007	0.027	0.005	0.044	0.006	<0.003	0.005	<0.003	<0.006	<0.006	<0.06	<0.02	<0.02	<0.08	<0.03	<0.009	<0.03	0.064	0.22	<0.009	2.972
14412-0018	LH_HZ01_B	0.024	0.119	0.004	0.026	0.01	<0.003	0.008	<0.003	0.007	<0.006	<0.06	<0.02	<0.02	<0.08	<0.03	<0.009	<0.03	<0.009	0.22	<0.009	0.124
14412-0020	LH_HZ01_R	0.028	0.089	0.008	0.042	0.022	<0.003	0.006	<0.003	0.011	<0.006	<0.06	<0.02	<0.02	<0.08	<0.03	<0.009	<0.03	<0.009	0.35	<0.009	0.046
14412-0026	LH_HZ01_G	<0.005	0.027	<0.003	0.015	<0.003	<0.003	<0.004	<0.003	<0.006	<0.006	<0.06	<0.02	<0.02	<0.08	<0.03	<0.009	<0.03	<0.009	0.05	<0.009	0.086
14412-0019	LH_HZ01_Y	0.066	0.147	0.017	0.09	0.027	0.004	0.028	<0.003	0.019	0.006	<0.06	<0.02	<0.02	<0.08	<0.03	<0.009	<0.03	<0.009	0.85	0.022	0.049

Table 23 Water chemical analysis at Cowfield (CF) site

Sample LIMS Code	Site ID	Sampling Date	T	Eh	pH	SEC	DO	TDS	Ca	Mg	Na	K	HCO₃⁻	Cl⁻	SO₄²⁻	NO₃⁻	Br⁻	NO₂⁻	HPO₄²⁻	F⁻	NPOC	Total P	Si
			°C	mV		µS cm⁻¹	mg l⁻¹	mg l⁻¹	mg l⁻¹	mg l⁻¹	mg l⁻¹	mg l⁻¹	mg l⁻¹	mg l⁻¹	mg l⁻¹	mg l⁻¹	mg l⁻¹	mg l⁻¹	mg l⁻¹	mg l⁻¹	mg l⁻¹	mg l⁻¹	mg l⁻¹
ICP-MS DL									*0.7*	*0.01*	*0.3*	*0.03*								*0.04*			*0.05*
14231-0046	**CF_SW**	26/04/2018	11.7	312	7.01	1520	11.6	1209	143	76.7	64.6	7.43	461	80.6	369	7.22	<0.1	<0.05	<0.1	0.375	3.34	0.05	3.80
14231-0038	**CF_HZ01_B**	26/04/2018	14.6	175	7.12	1238	2.8	951	122	57.0	55.7	6.57	402	74.2	234	0.2	<0.1	<0.05	<0.1	0.176	5.74	<0.04	8.32
14231-0039	**CF_HZ01_R**	26/04/2018	13.4	227	7.13	1192	2.2	919	115	52.5	53.5	6.03	417	72.6	203	0.2	<0.1	<0.05	<0.1	0.224	5.93	<0.04	8.78
14231-0040	**CF_HZ01_G**	26/04/2018	13.6	321	7.06	1205	3.0	953	118	57.2	51.5	5.78	454	70.6	196	0.2	<0.1	<0.05	<0.1	0.203	6.78	<0.04	8.83
14231-0041	**CF_HZ01_Y**	26/04/2018	12.9	369	7.46	1148	2.1	890	112	51.5	44.3	4.84	419	63.3	195	0.2	<0.1	<0.05	<0.1	0.180	5.97	<0.04	8.08
14231-0042	**CF_HZ02_B**	26/04/2018	12.2	336	7.40	1440	6.9	1139	139	69.8	63.4	7.40	443	80.5	333	3.73	<0.1	<0.05	<0.1	0.237	5.75	<0.04	4.79
14231-0043	**CF_HZ02_R**	26/04/2018	12.0	376	7.17	1225	3.4	949	112	47.5	66.4	8.19	513	83.4	119	0.2	0.117	<0.05	<0.1	0.215	9.50	<0.04	8.42
14231-0044	**CF_HZ02_G**	26/04/2018	11.7	310	7.42	1623	0.6	1310	147	74.2	53.1	7.82	966	58.3	3.76	0.2	0.225	<0.05	<0.1	0.325	11.9	<0.04	12.6
14231-0045	**CF_HZ02_Y**	26/04/2018		175	7.01	1428	2.3	1180	139	66.8	47.7	6.23	847	51.8	21.6	0.2	0.207	<0.05	<0.1	0.281	11.5	<0.04	11.3
Sample LIMS Code	**Site ID**	**Sampling Date**	**T**	**Eh**	**pH**	**SEC**	**DO**	**TDS**	**Ca**	**Mg**	**Na**	**K**	**HCO₃⁻**	**Cl⁻**	**SO₄²⁻**	**NO₃⁻**	**Br⁻**	**NO₂⁻**	**HPO₄²⁻**	**F⁻**	**NPOC**	**Total P**	**Si**
			°C	mV		µS cm⁻¹	mg l⁻¹	mg l⁻¹	mg l⁻¹	mg l⁻¹	mg l⁻¹	mg l⁻¹	mg l⁻¹	mg l⁻¹	mg l⁻¹	mg l⁻¹	mg l⁻¹	mg l⁻¹	mg l⁻¹	mg l⁻¹	mg l⁻¹	mg l⁻¹	mg l⁻¹
ICP-MS DL									*0.6*	*0.07*	*0.5*	*0.03*								*0.5*		*0.04*	*0.05*
14283-0050	**CF_SW**	01/08/2018	15.7	263	7.13	1809	9.54	1209	205	115	70.7	8.60	600	53.6	599	1.78	<0.2	<0.1	<0.2	0.303	1.20	<0.04	5.05
14283-0009	**CF_HZ01_B**	01/08/2018	16.4	75	7.2	1631	3.13	951	195	93.3	64.8	8.16	634	56.7	484	0.3	<0.2	<0.1	<0.2	0.443	8.48	<0.04	10.70
14283-0010	**CF_HZ01_R**	01/08/2018	16.8	96	7.18	1512	4.83	919	179	87.2	61.2	7.00	647	54.6	396	0.3	<0.2	<0.1	<0.2	0.457	5.25	<0.04	10.99
14283-0011	**CF_HZ01_G**	01/08/2018	16.9	72	7.14	1424	3.05	953	166	76.4	50.1	4.46	631	48.3	292	0.3	<0.2	<0.1	<0.2	0.482	5.70	<0.04	11.10
14283-0012	**CF_HZ01_Y**	01/08/2018	16.8	112	7.17	1264	5.38	890	158	66.7	40.2	2.97	557	40.6	280	0.2	0.105	<0.05	<0.1	0.564	10.8	<0.04	9.98
14283-0013	**CF_HZ02_B**	01/08/2018	16.9	141	7.17	1614	3.85	1139	194	105	65.6	9.10	743	53.9	411	0.3	<0.2	<0.1	<0.2	0.423	8.87	0.06	10.18
14283-0014	**CF_HZ02_R**	01/08/2018	16.9	108	7.16	1812	4.54	949	219	106	71.7	10.0	813	59.7	434	0.3	<0.2	<0.1	<0.2	0.475	13.4	<0.04	12.12
14283-0015	**CF_HZ02_G**	01/08/2018	18.2	54	7.08	1521	3.03	1310	155	76.4	52.7	8.20	999	64.6	0.50	0.3	0.275	<0.1	<0.2	0.406	14.1	0.06	14.32
14283-0016	**CF_HZ02_Y**	01/08/2018	17.7	128	7.14	1155	5.39	1180	143	62.0	38.6	4.03	803	43.1	6.8	0.2	0.217	<0.05	<0.1	0.400	9.35	<0.04	11.73
Sample LIMS Code	**Site ID**	**Sampling Date**	**T**	**Eh**	**pH**	**SEC**	**DO**	**TDS**	**Ca**	**Mg**	**Na**	**K**	**HCO₃⁻**	**Cl⁻**	**SO₄²⁻**	**NO₃⁻**	**Br⁻**	**NO₂⁻**	**HPO₄²⁻**	**F⁻**	**NPOC**	**Total P**	**Si**
			°C	mV		µS cm⁻¹	mg l⁻¹	mg l⁻¹	mg l⁻¹	mg l⁻¹	mg l⁻¹	mg l⁻¹	mg l⁻¹	mg l⁻¹	mg l⁻¹	mg l⁻¹	mg l⁻¹	mg l⁻¹	mg l⁻¹	mg l⁻¹	mg l⁻¹	mg l⁻¹	mg l⁻¹
ICP-MS DL									*0.04*	*0.004*	*0.4*	*0.03*	*5.0*							*0.5*		*0.02*	*0.042*
14412-0013	**CF_SW**	05/02/2019	5	239	7.26	1884	10.0	1209	187	94.7	80.6	8.69	560	84.3	524	5.1	<0.2	<0.1	<0.2	0.269	1.551	0.03	4.29
14412-0012	**CF_HZ01_B**	05/02/2019	5.1	64	7.48	1596	1.8	951	158	77.6	56.7	7.53	926	59.9	88.8	<0.6	<0.2	<0.1	<0.2	0.258	5.934	0.75	10.18
14412-0014	**CF_HZ01_R**	05/02/2019	4.6	71	7.46	1505	1.7	919	156	71.8	52.4	6.27	926	54.7	57.0	<0.6	<0.2	<0.1	<0.2	0.280	6.08	0.56	10.1
14412-0015	**CF_HZ01_G**	05/02/2019	4.7	71	7.42	1396	2.5	953	148	64.2	44.3	3.98	823	47.4	53.4	<0.6	<0.2	<0.1	<0.2	0.297	5.252	0.13	9.93
14412-0016	**CF_HZ01_Y**	05/02/2019	4.7	101	7.42	1276	4.1	890	144	57.9	37.2	2.52	758	52.6	68.3	<0.3	0.20	<0.05	<0.1	0.278	4.992	0.03	8.9

Table 23 Water chemical analysis at Cowfield (CF) (continued)

Sample LIMS Code	Site ID	Ba	Sr	Mn	Fe	Li	Be	B	Al	Ti	V	Cr	Co	Ni	Cu	Zn	Ga	As	Se	Rb	Y	Zr	Nb	Mo	Ag	Cd	Sn	Sb	Cs
		µg l⁻¹	µg l⁻¹	µg l⁻¹	µg l⁻¹	µg l⁻¹	µg l⁻¹	µg l⁻¹	µg l⁻¹	µg l⁻¹	µg l⁻¹	µg l⁻¹	µg l⁻¹	µg l⁻¹	µg l⁻¹	µg l⁻¹	µg l⁻¹	µg l⁻¹	µg l⁻¹	µg l⁻¹	µg l⁻¹	µg l⁻¹	µg l⁻¹	µg l⁻¹	µg l⁻¹	µg l⁻¹	µg l⁻¹	µg l⁻¹	µg l⁻¹
ICP-MS DL		0.1	0.2	0.3	2	3	0.01	18	2	0.2	0.1	0.2	0.02	0.1	0.6	0.8	0.05	0.06	0.1	0.01	0.01	0.09	0.02	0.08	0.05	0.02	0.03	0.02	0.005
14231-0046	CF_SW	58.3	467	35.2	37	65	<0.01	106	3	0.2	0.2	0.5	0.16	2.4	1.4	8.7	<0.05	0.17	0.4	4.21	0.03	<0.09	<0.02	0.61	<0.05	<0.02	<0.03	0.15	0.008
14231-0038	CF_HZ01_B	158	375	2742	14	34	<0.01	78	3	<0.2	0.5	0.3	3.54	2.8	4.8	8.8	0.66	2.28	0.2	3.95	0.04	0.10	<0.02	1.84	<0.05	0.02	<0.03	0.20	0.008
14231-0039	CF_HZ01_R	149	369	3015	13	33	0.01	86	4	<0.2	0.4	0.6	3.85	2.5	6.9	9.9	0.78	2.25	0.2	3.81	0.04	0.10	<0.02	1.44	<0.05	<0.02	<0.03	0.18	0.014
14231-0040	CF_HZ01_G	178	379	2149	13	35	0.01	89	5	<0.2	1.3	0.3	3.59	2.8	5.1	10.6	0.53	2.61	0.3	4.32	0.07	0.17	<0.02	1.65	<0.05	<0.02	<0.03	0.27	0.014
14231-0041	CF_HZ01_Y	177	375	2196	11	33	<0.01	86	3	<0.2	0.4	1.2	3.04	3.0	5.6	8.5	0.57	1.44	0.2	2.28	0.04	0.11	<0.02	1.60	<0.05	<0.02	<0.03	0.23	0.012
14231-0042	CF_HZ02_B	174	434	762	29	51	<0.01	98	16	0.2	0.7	0.3	1.37	3.0	5.9	13.4	0.18	0.67	0.3	5.26	0.07	0.09	<0.02	1.38	<0.05	0.04	0.04	0.27	0.012
14231-0043	CF_HZ02_R	177	343	3200	31	28	0.02	66	11	0.4	1.3	1.0	3.35	4.2	3.2	7.1	0.80	1.88	0.3	4.48	0.10	0.23	<0.02	2.94	<0.05	<0.02	0.04	0.30	0.011
14231-0044	CF_HZ02_G	260	620	2417	57	39	<0.01	89	2	0.2	0.2	<0.2	2.31	1.3	4.1	7.3	0.66	1.70	0.3	3.41	0.03	0.20	<0.02	0.83	<0.05	<0.02	<0.03	0.11	0.021
14231-0045	CF_HZ02_Y	260	560	1966	27	38	0.02	93	5	0.3	0.5	<0.2	2.39	2.6	4.4	6.1	0.53	1.99	0.2	3.24	0.07	0.30	<0.02	1.42	<0.05	<0.02	<0.03	0.23	0.028
ICP-MS DL		0.9	2	2	7	3	0.5	11	2	0.2	0.1	0.3	0.05	0.1	1	2	0.08	0.07	0.1	0.05	0.02	0.05	0.02	0.3	0.05	0.04	0.04	0.05	0.02
14283-0050	CF_SW	75.9	752	110	34	113	<0.5	132	5	<0.2	0.2	<0.3	0.17	0.7	1	6	<0.08	0.17	0.3	4.89	0.04	<0.05	<0.02	<0.3	<0.05	<0.04	<0.04	0.08	<0.02
14283-0009	CF_HZ01_B	225	634	6623	12864	68	<0.5	87	3	<0.2	0.6	<0.3	5.79	2.2	<1	4	2.60	4.70	0.3	4.32	0.03	0.11	<0.02	2.4	<0.05	<0.04	<0.04	0.10	<0.02
14283-0010	CF_HZ01_R	198	627	5631	7399	59	<0.5	93	2	<0.2	0.3	<0.3	4.16	1.8	<1	3	2.31	3.74	0.2	2.82	<0.02	0.09	<0.02	1.6	<0.05	<0.04	<0.04	0.08	<0.02
14283-0011	CF_HZ01_G	331	661	3482	13580	41	<0.5	92	<2	0.3	0.5	<0.3	4.35	2.1	<1	4	1.33	5.79	0.2	2.43	0.02	0.11	<0.02	1.6	<0.05	<0.04	0.05	0.08	<0.02
14283-0012	CF_HZ01_Y	241	658	2369	3979	38	<0.5	93	<2	<0.2	0.4	<0.3	3.44	1.9	<1	6	1.01	3.37	0.1	2.35	<0.02	0.06	<0.02	2.2	<0.05	<0.04	<0.04	0.11	<0.02
14283-0013	CF_HZ02_B	169	670	1832	8433	94	<0.5	103	3	0.4	1.0	0.3	4.65	3.8	<1	5	0.73	4.34	0.3	5.72	0.03	0.18	<0.02	2.4	<0.05	<0.04	0.07	0.13	<0.02
14283-0014	CF_HZ02_R	243	686	7852	4829	70	<0.5	72	3	0.2	0.6	<0.3	7.17	4.5	<1	<2	3.05	3.26	0.3	4.76	0.03	0.24	<0.02	3.9	<0.05	<0.04	0.06	0.13	<0.02
14283-0015	CF_HZ02_G	401	710	2397	20412	43	<0.5	81	51	1.8	0.6	0.4	1.95	1.1	<1	5	1.01	5.56	0.4	3.46	0.11	0.31	<0.02	0.7	<0.05	<0.04	0.10	0.12	0.02
14283-0016	CF_HZ02_Y	237	630	1389	1417	38	<0.5	98	11	0.7	0.3	<0.3	1.07	0.7	<1	<2	0.65	4.08	0.2	3.34	0.04	0.14	<0.02	0.8	<0.05	<0.04	<0.04	0.10	0.04
		µg l-1	µg l-1	µg l-1	µg l-1	µg l-1	µg l-1	µg l-1	µg l-1	µg l-1	µg l-1	µg l-1	µg l-1	µg l-1	µg l-1	µg l-1	µg l-1	µg l-1	µg l-1	µg l-1	µg l-1	µg l-1	µg l-1	µg l-1	µg l-1	µg l-1	µg l-1	µg l-1	µg l-1
ICP-MS DL		0.05	0.06	0.2	0.4	7	0.08	53	2	0.02	0.4	0.2	0.2	0.05	0.2	0.3	0.3	0.03	0.05	0.05	0.2	0.04	0.08	0.04	0.05	0.01	0.01	0.008	0.03
14412-0013	CF_SW	68.53	699.1	81.4	140.4	100	<0.08	112	15	0.51	<0.4	<0.2	<0.2	0.91	1	5.2	<0.3	0.18	0.21	4.89	<0.2	<0.04	<0.08	0.17	<0.05	0.02	0.02	0.098	<0.03
14412-0012	CF_HZ01_B	174	532	5361	20074	67	<0.08	73	5	0.11	0.8	<0.2	4	1.45	4.3	7.2	<0.3	5.76	0.25	3.11	<0.2	0.25	<0.08	1.19	<0.05	<0.01	0.05	0.102	<0.03
14412-0014	CF_HZ01_R	166	549	5353	19664	49	<0.08	73	5	0.23	0.8	<0.2	3.1	1.21	2.4	3	<0.3	6.54	0.22	2.02	<0.2	0.27	<0.08	0.98	<0.05	<0.01	0.03	0.074	<0.03
14412-0015	CF_HZ01_G	330	604	2886	20263	34	<0.08	69	8	0.19	0.6	<0.2	2.7	1.33	1.6	4.2	<0.3	6.35	0.17	1.83	<0.2	0.18	<0.08	1.13	<0.05	<0.01	0.02	0.068	<0.03
14412-0016	CF_HZ01_Y	242	639	1696	8211	35	<0.08	72	15	0.44	0.9	<0.2	2.8	1.83	0.7	4.1	<0.3	4.38	0.17	2.3	<0.2	0.23	<0.08	1.44	<0.05	<0.01	0.02	0.129	<0.03

Table 23 Water chemical analysis at Cowfield (CF) site (continued)

Sample LIMS Code	Site ID	La	Ce	Pr	Nd	Sm	Eu	Gd	Tb	Dy	Ho	Er	Tm	Yb	Lu	Hf	Ta	W	Tl	Pb	Th	U
		µg l⁻¹	µg l⁻¹	µg l⁻¹	µg l⁻¹	µg l⁻¹	µg l⁻¹	µg l⁻¹	µg l⁻¹	µg l⁻¹	µg l⁻¹	µg l⁻¹	µg l⁻¹	µg l⁻¹	µg l⁻¹	µg l⁻¹	µg l⁻¹	µg l⁻¹	µg l⁻¹	µg l⁻¹	µg l⁻¹	µg l⁻¹
ICP-MS DL		*0.005*	*0.03*	*0.04*	*0.07*	*0.006*	*0.002*	*0.003*	*0.002*	*0.005*	*0.002*	*0.002*	*0.002*	*0.004*	*0.002*	*0.01*	*0.02*	*0.05*	*0.02*	*0.04*	*0.005*	*0.01*
14231-0046	**CF_SW**	0.011	<0.03	<0.04	<0.07	<0.006	<0.002	0.006	<0.002	<0.005	<0.002	0.003	<0.002	<0.004	<0.002	<0.01	<0.02	<0.05	0.05	0.15	<0.005	2.45
14231-0038	**CF_HZ01_B**	0.008	<0.03	<0.04	<0.07	<0.006	0.004	0.004	<0.002	0.005	<0.002	0.003	<0.002	<0.004	<0.002	<0.01	<0.02	0.07	<0.02	0.13	<0.005	1.84
14231-0039	**CF_HZ01_R**	0.011	<0.03	<0.04	<0.07	<0.006	<0.002	0.005	<0.002	<0.005	<0.002	<0.002	<0.002	0.005	<0.002	<0.01	<0.02	0.08	<0.02	0.20	<0.005	1.24
14231-0040	**CF_HZ01_G**	0.037	0.06	<0.04	0.08	<0.006	<0.002	0.011	<0.002	0.009	<0.002	0.006	<0.002	0.008	<0.002	<0.01	<0.02	0.07	0.02	0.20	<0.005	1.81
14231-0041	**CF_HZ01_Y**	0.012	<0.03	<0.04	<0.07	<0.006	0.002	0.005	<0.002	0.005	<0.002	0.005	<0.002	<0.004	<0.002	<0.01	<0.02	<0.05	<0.02	0.19	<0.005	1.94
14231-0042	**CF_HZ02_B**	0.025	0.05	<0.04	<0.07	0.011	0.006	0.010	0.002	0.008	<0.002	0.009	<0.002	0.009	<0.002	<0.01	<0.02	<0.05	0.04	0.28	<0.005	2.59
14231-0043	**CF_HZ02_R**	0.028	0.06	<0.04	<0.07	<0.006	<0.002	0.012	0.002	0.011	0.002	0.010	<0.002	0.008	0.002	<0.01	<0.02	0.07	<0.02	0.25	<0.005	2.43
14231-0044	**CF_HZ02_G**	0.007	<0.03	<0.04	<0.07	<0.006	<0.002	0.005	<0.002	<0.005	<0.002	0.002	<0.002	0.008	<0.002	<0.01	<0.02	<0.05	<0.02	0.12	<0.005	0.160
14231-0045	**CF_HZ02_Y**	0.015	<0.03	<0.04	<0.07	<0.006	<0.002	0.005	<0.002	0.007	<0.002	0.007	<0.002	0.010	<0.002	<0.01	<0.02	<0.05	<0.02	0.13	<0.005	0.690
Sample LIMS Code	Site ID	La	Ce	Pr	Nd	Sm	Eu	Gd	Tb	Dy	Ho	Er	Tm	Yb	Lu	Hf	Ta	W	Tl	Pb	Th	U
		µg l⁻¹	µg l⁻¹	µg l⁻¹	µg l⁻¹	µg l⁻¹	µg l⁻¹	µg l⁻¹	µg l⁻¹	µg l⁻¹	µg l⁻¹	µg l⁻¹	µg l⁻¹	µg l⁻¹	µg l⁻¹	µg l⁻¹	µg l⁻¹	µg l⁻¹	µg l⁻¹	µg l⁻¹	µg l⁻¹	µg l⁻¹
ICP-MS DL		*0.03*	*0.04*	*0.05*	*0.2*	*0.03*	*0.008*	*0.007*	*0.007*	*0.007*	*0.007*	*0.008*	*0.007*	*0.008*	*0.007*	*0.01*	*0.02*	*0.05*	*0.01*	*0.02*	*0.009*	*0.009*
14283-0050	**CF_SW**	<0.03	<0.04	<0.05	<0.2	<0.03	<0.008	<0.007	<0.007	<0.007	<0.007	<0.008	<0.007	<0.008	<0.007	<0.01	<0.02	<0.05	0.06	0.07	<0.009	3.63
14283-0009	**CF_HZ01_B**	<0.03	<0.04	<0.05	<0.2	<0.03	0.012	<0.007	<0.007	0.009	<0.007	<0.008	<0.007	<0.008	<0.007	<0.01	<0.02	0.11	<0.01	0.04	<0.009	1.07
14283-0010	**CF_HZ01_R**	<0.03	<0.04	<0.05	<0.2	<0.03	0.008	<0.007	<0.007	<0.007	<0.007	<0.008	<0.007	<0.008	<0.007	<0.01	<0.02	0.10	<0.01	<0.02	<0.009	0.575
14283-0011	**CF_HZ01_G**	<0.03	<0.04	<0.05	<0.2	<0.03	<0.008	<0.007	<0.007	<0.007	<0.007	<0.008	<0.007	0.010	<0.007	<0.01	<0.02	0.09	<0.01	0.03	<0.009	0.674
14283-0012	**CF_HZ01_Y**	<0.03	<0.04	<0.05	<0.2	<0.03	0.008	<0.007	<0.007	<0.007	<0.007	<0.008	<0.007	<0.008	<0.007	<0.01	<0.02	0.08	<0.01	<0.02	<0.009	1.17
14283-0013	**CF_HZ02_B**	<0.03	<0.04	<0.05	<0.2	<0.03	<0.008	<0.007	<0.007	0.008	<0.007	<0.008	<0.007	<0.008	<0.007	<0.01	<0.02	0.11	<0.01	0.08	<0.009	2.22
14283-0014	**CF_HZ02_R**	<0.03	<0.04	<0.05	<0.2	<0.03	<0.008	<0.007	<0.007	<0.007	<0.007	<0.008	<0.007	0.012	<0.007	<0.01	<0.02	0.11	<0.01	<0.02	<0.009	1.61
14283-0015	**CF_HZ02_G**	0.08	0.21	<0.05	<0.2	<0.03	0.011	0.025	<0.007	0.021	<0.007	0.010	<0.007	0.013	<0.007	<0.01	<0.02	0.06	<0.01	1.19	0.034	0.054
14283-0016	**CF_HZ02_Y**	0.03	0.05	<0.05	<0.2	<0.03	<0.008	<0.007	<0.007	<0.007	<0.007	<0.008	<0.007	<0.008	<0.007	<0.01	<0.02	0.06	<0.01	0.16	<0.009	0.371
Sample LIMS Code	Site ID	La	Ce	Pr	Nd	Sm	Eu	Gd	Tb	Dy	Ho	Er	Tm	Yb	Lu	Hf	Ta	W	Tl	Pb	Th	U
		µg l-1	µg l-1	µg l-1	µg l-1	µg l-1	µg l-1	µg l-1	µg l-1	µg l-1	µg l-1	µg l-1	µg l-1	µg l-1	µg l-1	µg l-1	µg l-1	µg l-1	µg l-1	µg l-1	µg l-1	µg l-1
ICP-MS DL		*0.005*	*0.004*	*0.003*	*0.005*	*0.003*	*0.003*	*0.004*	*0.003*	*0.006*	*0.006*	*0.06*	*0.02*	*0.02*	*0.08*	*0.03*	*0.009*	*0.03*	*0.009*	*0.04*	*0.009*	*0.009*
14412-0013	**CF_SW**	0.022	0.05	0.007	0.022	<0.003	<0.003	0.008	<0.003	0.009	<0.006	<0.06	<0.02	<0.02	<0.08	<0.03	<0.009	<0.03	0.063	0.26	<0.009	3.053
14412-0012	**CF_HZ01_B**	0.006	0.019	<0.003	0.022	0.008	<0.003	0.004	<0.003	<0.006	<0.006	<0.06	<0.02	<0.02	<0.08	<0.03	<0.009	0.09	<0.009	0.04	<0.009	0.517
14412-0014	**CF_HZ01_R**	<0.005	0.02	<0.003	0.007	0.004	<0.003	0.004	<0.003	<0.006	<0.006	<0.06	<0.02	<0.02	<0.08	<0.03	<0.009	0.09	<0.009	<0.04	<0.009	0.414
14412-0015	**CF_HZ01_G**	0.005	0.019	<0.003	0.011	0.006	<0.003	0.004	<0.003	<0.006	<0.006	<0.06	<0.02	<0.02	<0.08	<0.03	<0.009	0.07	<0.009	0.07	<0.009	0.356
14412-0016	**CF_HZ01_Y**	0.025	0.057	0.005	0.029	0.023	<0.003	0.006	<0.003	<0.006	<0.006	<0.06	<0.02	<0.02	<0.08	<0.03	<0.009	0.07	<0.009	0.21	<0.009	1.308

Table 24 Water chemical analysis at Concrete Slab (CS) site

Sample LIMS Code	Site ID	Sampling Date	T	Eh	pH	SEC	DO	TDS	Ca	Mg	Na	K	HCO_3^-	Cl^-	SO_4^{2-}	NO_3^-	Br^-	NO_2^-	HPO_4^{2-}	F^-	NPOC	Total P	Si
			°C	mV		µS cm^{-1}	mg l^{-1}	mg l^{-1}	mg l^{-1}	mg l^{-1}	mg l^{-1}	mg l^{-1}	mg l^{-1}	mg l^{-1}	mg l^{-1}	mg l^{-1}	mg l^{-1}	mg l^{-1}	mg l^{-1}	mg l^{-1}	mg l^{-1}	mg l^{-1}	mg l^{-1}
ICP-MS DL									*0.7*	*0.01*	*0.3*	*0.03*										*0.04*	*0.05*
14231-0051	**CS_SW**	26/04/2018	10.6	372	7.03	1529	10.4	1208	143	77.2	64.9	7.27	463	79.8	367	7.12	<0.1	<0.05	<0.1	0.446	3.16	0.05	3.86
14231-0047	**CS_HZ01_B**	26/04/2018	10.3		7.01	1151	2.5	889	114	53.2	29.0	3.15	581	35.7	71.5	0.488	0.149	<0.05	<0.1	0.265	7.32	<0.04	12.9
14231-0048	**CS_HZ01_R**	26/04/2018	10.4		7.23	1152	1.9	917	108	50.6	29.3	3.17	604	38.9	83.8	0.2	0.169	<0.05	<0.1	0.298	10.3	<0.04	10.5
14231-0049	**CS_HZ01_G**	26/04/2018	10.4	387	7.35	1149	2.3	916	115	52.6	27.5	3.07	622	34.5	61.4	0.2	0.160	<0.05	<0.1	0.486	9.82	<0.04	12.6
14231-0050	**CS_HZ01_Y**	26/04/2018	10.1	350	7.58	953	3.3	766	96.8	49.0	29.4	4.03	455	32.2	100	0.2	<0.1	<0.05	<0.1	0.242	6.80	<0.04	10.5
14231-0052	**CS_HZ02_B**	26/04/2018	10.4	368	7.47	1269	3.8	869	113	51.2	63.7	8.08	507	99.4	26.3	0.2	0.157	<0.05	<0.1	0.211	8.62	<0.04	8.43
14231-0053	**CS_HZ02_R**	26/04/2018	10.4	116	6.96	1372	2.0	1163	116	53.2	70.5	8.87	680	89.7	144	0.2	0.116	<0.05	<0.1	0.223	11.2	<0.04	12.4
14231-0054	**CS_HZ02_G**	26/04/2018	9.8	367	7.13	1352	1.5	1061	128	60.2	27.9	5.70	782	33.6	25.1	0.2	0.225	<0.05	<0.1	0.241	9.74	<0.04	12.4
14231-0055	**CS_HZ02_Y**	26/04/2018	9.7	300	6.98	1192	2.4	920	107	51.3	26.0	3.43	663	30.6	38.6	0.2	0.178	<0.05	<0.1	0.304	9.45	<0.04	11.3
Sample LIMS Code	**Site ID**	**Sampling Date**	**T**	**Eh**	**pH**	**SEC**	**DO**	**TDS**	**Ca**	**Mg**	**Na**	**K**	**HCO_3^-**	**Cl^-**	**SO_4^{2-}**	**NO_3^-**	**Br^-**	**NO_2^-**	**HPO_4^{2-}**	**F^-**	**NPOC**	**Total P**	**Si**
			°C	mV		µS cm^{-1}	mg l^{-1}	mg l^{-1}	mg l^{-1}	mg l^{-1}	mg l^{-1}	mg l^{-1}	mg l^{-1}	mg l^{-1}	mg l^{-1}	mg l^{-1}	mg l^{-1}	mg l^{-1}	mg l^{-1}	mg l^{-1}	mg l^{-1}	mg l^{-1}	mg l^{-1}
									0.6	*0.07*	*0.5*	*0.03*										*0.04*	*0.05*
14283-0001	**CS_SW**	01/08/2018	13.3	376	7.03	1814	8.26	1208	205	116	74.0	9.01	590	55.6	585	2.83	<0.2	<0.1	<0.2	0.328	2.22	0.06	5.00
14283-0049	**CS_HZ01_B**	01/08/2018			8.12			889	159	70.7	35.3	4.96	860	36.4	28	0.3	0.264	<0.1	<0.2	0.249	15.9	<0.04	14.9
14283-0002	**CS_HZ01_R**	01/08/2018			7.99			917	160	69.3	34.8	4.82	927	37.2	21	0.3	0.288	<0.1	<0.2	0.257	16.7	<0.04	15.54
14283-0003	**CS_HZ01_G**	01/08/2018			8.09			916	138	59.9	26.4	3.51	815	29.3	1.3	0.2	0.247	<0.05	<0.1	0.400	10.0	<0.04	17.13
14283-0004	**CS_HZ01_Y**	01/08/2018	20.4	288	7.45	715	3.75	766	86.4	42.2	16.2	1.70	501	18.1	10	0.153	0.111	<0.025	<0.05	0.630	6.34	<0.04	14.79
14283-0005	**CS_HZ02_B**	01/08/2018	18.1	75	7.14	1755	2.7	869	205	98.4	74.1	10.5	848	62.7	337	0.3	<0.2	<0.1	<0.2	0.334	7.21	0.49	10.17
14283-0006	**CS_HZ02_R**	01/08/2018	19.4	44	7.14	1702	0.65	1163	190	78.8	71.1	10.9	1125	75.0	22	0.3	0.281	<0.1	<0.2	0.346	14.9	1.00	17.91
14283-0007	**CS_HZ02_G**	01/08/2018	18	16	7.07	1240	0.19	1061	142	61.8	25.8	5.33	841	29.9	0.25	0.2	0.276	<0.05	<0.1	0.368	8.23	<0.04	16.65
14283-0008	**CS_HZ02_Y**	01/08/2018	18.8	90	7.08	1070	0.6	920	131	58.9	22.0	3.30	747	25.3	1.2	0.2	0.237	<0.05	<0.1	0.474	9.21	<0.04	16.01
Sample LIMS Code	**Site ID**	**Sampling Date**	**T**	**Eh**	**pH**	**SEC**	**DO**	**TDS**	**Ca**	**Mg**	**Na**	**K**	**HCO_3^-**	**Cl^-**	**SO_4^{2-}**	**NO_3^-**	**Br^-**	**NO_2^-**	**HPO_4^{2-}**	**F^-**	**NPOC**	**Total P**	**Si**
			°C	mV		µS cm^{-1}	mg l^{-1}	mg l-1	mg l-1	mg l-1	mg l-1	mg l-1	mg l-1	mg l-1	mg l-1	mg l-1	mg l-1	mg l-1	mg l-1	mg l-1	mg l-1	mg l-1	mg l-1
									0.04	*0.004*	*0.4*	*0.03*	*5.0*									*0.02*	*0.042*
14412-0001-10 aver	**CS_SW**	05/02/2019	5.15	398.85	7.18	1888	10.08	1208	189	97	85	9	537	85	509	5	<0.2	<0.1	<0.2	0.226	1.81	0.025	4.20
14412-0002-3-9 aver	**CS_HZ02_B**	05/02/2019	4.6	87.4	7.4	2036	1.8	869	214	89	75	10	1111	78	175	<0.6	<0.2	<0.1	<0.2	0.209	7.18	0.237	11.31
14412-0004	**CS_HZ02_R**	05/02/2019	4.7	90	7.29	2032	3.8	1163	220	86	65	10	1382	63	1	<0.6	0.235	<0.1	<0.2	0.222	10.9	0.350	16.69
14412-0005	**CS_HZ02_G**	05/02/2019	3.9	84	7.25	1294	2.7	1061	131	54	22	4	808	26	0	<0.3	0.206	<0.05	<0.1	0.212	5.77	<0.02	15.08
14412-0006-7-11	**CS_HZ02_Y**	05/02/2019	4.3	87.4	7.31	1225	3.02	920	131	55	22	3	791	25	1	<0.3	0.195	<0.05	<0.1	0.247	5.70	0.100	14.63

Table 24 Water chemical analysis at Concrete Slab (CS) site (continued)

Sample LIMS Code	Site ID	Ba	Sr	Mn	Fe	Li	Be	B	Al	Ti	V	Cr	Co	Ni	Cu	Zn	Ga	As	Se	Rb	Y	Zr	Nb	Mo	Ag	Cd	Sn	Sb	Cs
		µg l⁻¹	µg l⁻¹	µg l⁻¹	µg l⁻¹	µg l⁻¹	µg l⁻¹	µg l⁻¹	µg l⁻¹	µg l⁻¹	µg l⁻¹	µg l⁻¹	µg l⁻¹	µg l⁻¹	µg l⁻¹	µg l⁻¹	µg l⁻¹	µg l⁻¹	µg l⁻¹	µg l⁻¹	µg l⁻¹	µg l⁻¹	µg l⁻¹	µg l⁻¹	µg l⁻¹	µg l⁻¹	µg l⁻¹	µg l⁻¹	µg l⁻¹
ICP-MS DL		0.1	0.2	0.3	2	3	0.01	18	2	0.2	0.1	0.2	0.02	0.1	0.6	0.8	0.05	0.06	0.1	0.01	0.01	0.09	0.02	0.08	0.05	0.02	0.03	0.02	0.005
14231-0051	**CS_SW**	57.8	471	36.3	37	63	<0.01	104	5	0.3	0.2	0.5	0.17	2.3	1.3	10.1	<0.05	0.23	0.3	4.15	0.02	<0.09	<0.02	0.63	<0.05	0.02	<0.03	0.14	0.009
14231-0047	**CS_HZ01_B**	300	417	1374	62	21	<0.01	80	2	<0.2	<0.1	<0.2	1.41	1.5	2.9	7.4	0.40	0.79	0.3	2.02	0.02	<0.09	<0.02	0.95	<0.05	<0.02	<0.03	0.20	0.009
14231-0048	**CS_HZ01_R**	241	394	1270	34	19	<0.01	71	8	<0.2	0.7	2.4	1.31	2.6	2.5	5.8	0.41	1.44	0.4	2.22	0.06	0.18	<0.02	1.66	<0.05	<0.02	<0.03	0.52	0.015
14231-0049	**CS_HZ01_G**	303	421	1482	66	18	<0.01	73	2	<0.2	<0.1	0.2	1.79	2.0	3.0	5.6	0.47	1.21	0.3	2.11	0.03	<0.09	<0.02	1.13	<0.05	<0.02	<0.03	0.25	0.015
14231-0050	**CS_HZ01_Y**	153	321	1252	7	30	<0.01	80	3	<0.2	0.6	<0.2	1.70	1.4	1.1	7.0	0.38	1.60	0.1	3.09	0.04	<0.09	<0.02	2.19	<0.05	<0.02	<0.03	0.34	0.009
14231-0052	**CS_HZ02_B**	156	357	3204	24	36	0.01	73	3	<0.2	0.9	0.3	3.73	3.3	1.5	8.2	0.87	2.48	0.3	4.95	0.05	0.15	<0.02	2.06	<0.05	0.02	<0.03	0.22	0.009
14231-0053	**CS_HZ02_R**	139	375	3690	45	37	<0.01	77	4	<0.2	1.0	0.4	3.75	3.0	1.3	7.3	1.06	2.93	0.3	6.12	0.05	0.21	<0.02	1.03	<0.05	<0.02	<0.03	0.19	0.012
14231-0054	**CS_HZ02_G**	230	523	3228	56	25	<0.01	91	<2	<0.2	0.4	<0.2	3.24	2.6	5.4	6.7	0.97	1.42	0.2	3.99	0.06	0.16	<0.02	1.07	<0.05	<0.02	0.28	0.22	0.024
14231-0055	**CS_HZ02_Y**	252	483	1514	55	20	<0.01	82	6	<0.2	0.3	2.4	1.53	2.0	2.1	3.4	0.51	1.36	0.1	2.19	0.04	0.14	<0.02	0.97	<0.05	<0.02	0.17	0.17	0.037

Sample LIMS Code	Site ID	Ba	Sr	Mn	Fe	Li	Be	B	Al	Ti	V	Cr	Co	Ni	Cu	Zn	Ga	As	Se	Rb	Y	Zr	Nb	Mo	Ag	Cd	Sn	Sb	Cs
		µg l⁻¹	µg l⁻¹	µg l⁻¹	µg l⁻¹	µg l⁻¹	µg l⁻¹	µg l⁻¹	µg l⁻¹	µg l⁻¹	µg l⁻¹	µg l⁻¹	µg l⁻¹	µg l⁻¹	µg l⁻¹	µg l⁻¹	µg l⁻¹	µg l⁻¹	µg l⁻¹	µg l⁻¹	µg l⁻¹	µg l⁻¹	µg l⁻¹	µg l⁻¹	µg l⁻¹	µg l⁻¹	µg l⁻¹	µg l⁻¹	µg l⁻¹
		0.9	2	2	7	3	0.5	11	2	0.2	0.1	0.3	0.05	0.1	1	2	0.08	0.07	0.1	0.05	0.02	0.05	0.02	0.3	0.05	0.04	0.04	0.05	0.02
14283-0001	**CS_SW**	73.7	750	75.0	19	119	<0.5	140	<2	<0.2	0.2	<0.3	0.21	1.4	18	16	<0.08	0.21	0.3	5.18	0.04	<0.05	<0.02	0.7	<0.05	<0.04	<0.04	0.11	<0.02
14283-0049	**CS_HZ01_B**	261	590	2135	319	23	<0.5	66	10	0.5	0.7	<0.3	1.65	1.7	<1	9	0.95	1.24	0.5	2.31	0.06	0.22	<0.02	0.4	<0.05	<0.04	0.12	0.21	<0.02
14283-0002	**CS_HZ01_R**	288	599	2388	4387	24	<0.5	73	11	0.7	0.4	0.3	1.79	1.6	2	12	0.98	1.19	0.6	2.20	0.06	0.23	<0.02	0.7	<0.05	<0.04	0.05	0.21	<0.02
14283-0003	**CS_HZ01_G**	311	533	2053	11898	19	<0.5	79	11	0.3	0.7	<0.3	1.53	0.9	<1	<2	0.85	1.67	0.3	2.04	0.05	0.11	<0.02	0.4	<0.05	<0.04	<0.04	0.11	<0.02
14283-0004	**CS_HZ01_Y**	138	382	1339	190	18	<0.5	70	17	0.6	0.5	<0.3	1.16	0.7	<1	3	0.60	2.02	0.2	2.08	0.03	0.07	<0.02	0.8	<0.05	<0.04	<0.04	0.13	<0.02
14283-0005	**CS_HZ02_B**	238	722	5459	19589	81	<0.5	93	3	0.3	1.0	<0.3	4.25	1.5	3	9	2.08	5.43	0.3	4.94	0.04	0.23	<0.02	1.2	<0.05	<0.04	0.05	0.17	<0.02
14283-0006	**CS_HZ02_R**	314	667	7893	31463	47	<0.5	73	5	0.7	1.6	0.6	3.72	1.3	2	13	2.96	7.50	0.5	4.30	0.05	0.47	0.02	0.6	<0.05	<0.04	0.08	0.14	<0.02
14283-0007	**CS_HZ02_G**	378	643	3874	46469	26	<0.5	83	5	<0.2	0.7	<0.3	1.95	0.6	<1	9	1.50	9.04	0.3	3.23	0.04	0.22	<0.02	0.4	<0.05	<0.04	0.05	0.09	0.02
14283-0008	**CS_HZ02_Y**	501	638	1370	14249	24	<0.5	83	6	0.4	0.5	<0.3	1.10	0.7	2	14	0.51	5.31	0.2	3.01	0.04	0.15	<0.02	0.4	<0.05	<0.04	<0.04	0.08	0.02

Sample LIMS Code	Site ID	Ba	Sr	Mn	Fe	Li	Be	B	Al	Ti	V	Cr	Co	Ni	Cu	Zn	Ga	As	Se	Rb	Y	Zr	Nb	Mo	Ag	Cd	Sn	Sb	Cs
		µg l-1	µg l-1	µg l-1	µg l-1	µg l-1	µg l-1	µg l-1	µg l-1	µg l-1	µg l-1	µg l-1	µg l-1	µg l-1	µg l-1	µg l-1	µg l-1	µg l-1	µg l-1	µg l-1	µg l-1	µg l-1	µg l-1	µg l-1	µg l-1	µg l-1	µg l-1	µg l-1	µg l-1
		0.05	0.06	0.2	0.4	7	0.08	53	2	0.02	0.4	0.2	0.2	0.05	0.2	0.3	0.3	0.03	0.05	0.05	0.2	0.04	0.08	0.04	0.05	0.01	0.01	0.008	0.03
14412-0001-10 aver	**CS_SW**	65	714	67	45	105	<0.08	122	34	0.26	<0.4	<0.2	0.2	0.93	2.3	11.35	<0.3	0.17	0.265	4.95	<0.2	<0.04	<0.08	0.2	<0.05	0.03	0.025	0.108	<0.03
14412-0002-3-9 aver	**CS_HZ02_B**	248	758	6870	31677	65	<0.08	69	12.7	0.43	0.77	0.3	2.07	0.99	3.57	10.3	<0.3	5.93	0.33	4.26	<0.2	0.37	<0.08	0.48	<0.05	<0.01	0.077	0.133	<0.03
14412-0004	**CS_HZ02_R**	305	762	9580	43399	42	<0.08	57	11	0.38	1.10	0.4	2.00	0.79	1.2	6.2	<0.3	5.89	0.41	3.47	<0.2	0.52	<0.08	0.2	<0.05	<0.01	0.080	0.139	<0.03
14412-0005	**CS_HZ02_G**	343	602	3842	50223	24	<0.08	60	10	0.26	0.40	<0.2	1.10	0.4	0.6	4.2	<0.3	6.80	0.22	2.35	<0.2	0.19	<0.08	0.17	<0.05	<0.01	0.040	0.047	<0.03
14412-0006-7-11	**CS_HZ02_Y**	570	644	2078	29702	21	<0.08	66	12	0.37	0.47	0.2	1.03	0.42	0.2	4	<0.3	6.12	0.18	3.34	<0.2	0.18	<0.08	0.18	<0.05	0.01	0.027	0.063	<0.03

Table 24 Water chemical analysis at Concrete Slab (CS) site (continued)

Sample LIMS Code	Site ID	La	Ce	Pr	Nd	Sm	Eu	Gd	Tb	Dy	Ho	Er	Tm	Yb	Lu	Hf	Ta	W	Tl	Pb	Th	U
		µg l⁻¹	µg l⁻¹	µg l⁻¹	µg l⁻¹	µg l⁻¹	µg l⁻¹	µg l⁻¹	µg l⁻¹	µg l⁻¹	µg l⁻¹	µg l⁻¹	µg l⁻¹	µg l⁻¹	µg l⁻¹	µg l⁻¹	µg l⁻¹	µg l⁻¹	µg l⁻¹	µg l⁻¹	µg l⁻¹	µg l⁻¹
ICP-MS DL		0.005	0.03	0.04	0.07	0.006	0.002	0.003	0.002	0.005	0.002	0.002	0.002	0.004	0.002	0.01	0.02	0.05	0.02	0.04	0.005	0.01
14231-0051	CS_SW	0.006	<0.03	<0.04	<0.07	<0.006	<0.002	0.004	<0.002	<0.005	<0.002	0.004	<0.002	<0.004	<0.002	<0.01	<0.02	<0.05	0.04	0.12	<0.005	2.45
14231-0047	CS_HZ01_B	0.006	<0.03	<0.04	<0.07	<0.006	<0.002	<0.003	<0.002	<0.005	<0.002	0.003	<0.002	0.004	<0.002	<0.01	<0.02	<0.05	<0.02	0.12	<0.005	0.590
14231-0048	CS_HZ01_R	0.013	<0.03	<0.04	<0.07	<0.006	0.004	0.006	<0.002	0.006	<0.002	0.004	<0.002	0.009	<0.002	<0.01	<0.02	0.10	<0.02	0.24	<0.005	0.780
14231-0049	CS_HZ01_G	0.007	<0.03	<0.04	<0.07	0.007	0.002	<0.003	<0.002	0.006	<0.002	0.002	<0.002	<0.004	<0.002	<0.01	<0.02	<0.05	<0.02	0.07	<0.005	0.500
14231-0050	CS_HZ01_Y	0.007	<0.03	<0.04	<0.07	<0.006	0.003	0.004	<0.002	<0.005	<0.002	0.002	<0.002	<0.004	<0.002	<0.01	<0.02	<0.05	<0.02	0.13	<0.005	1.55
14231-0052	CS_HZ02_B	0.008	<0.03	<0.04	<0.07	<0.006	<0.002	0.005	<0.002	0.008	<0.002	0.004	<0.002	0.008	<0.002	<0.01	<0.02	0.07	<0.02	0.12	<0.005	1.48
14231-0053	CS_HZ02_R	0.009	<0.03	<0.04	<0.07	0.006	<0.002	0.006	<0.002	<0.005	<0.002	0.005	<0.002	0.005	<0.002	<0.01	<0.02	0.09	<0.02	0.10	<0.005	0.780
14231-0054	CS_HZ02_G	0.011	<0.03	<0.04	<0.07	<0.006	0.003	0.004	<0.002	<0.005	<0.002	0.002	<0.002	0.009	0.002	<0.01	<0.02	<0.05	<0.02	0.12	<0.005	0.340
14231-0055	CS_HZ02_Y	0.013	<0.03	<0.04	<0.07	0.007	<0.002	<0.003	<0.002	0.007	<0.002	0.002	<0.002	0.005	<0.002	<0.01	<0.02	<0.05	<0.02	0.11	<0.005	0.170

Sample LIMS Code	Site ID	La	Ce	Pr	Nd	Sm	Eu	Gd	Tb	Dy	Ho	Er	Tm	Yb	Lu	Hf	Ta	W	Tl	Pb	Th	U
		µg l⁻¹	µg l⁻¹	µg l⁻¹	µg l⁻¹	µg l⁻¹	µg l⁻¹	µg l⁻¹	µg l⁻¹	µg l⁻¹	µg l⁻¹	µg l⁻¹	µg l⁻¹	µg l⁻¹	µg l⁻¹	µg l⁻¹	µg l⁻¹	µg l⁻¹	µg l⁻¹	µg l⁻¹	µg l⁻¹	µg l⁻¹
		0.03	0.04	0.05	0.2	0.03	0.008	0.007	0.007	0.007	0.007	0.008	0.007	0.008	0.007	0.01	0.02	0.05	0.01	0.02	0.009	0.009
14283-0001	CS_SW	<0.03	<0.04	<0.05	<0.2	<0.03	<0.008	<0.007	<0.007	<0.007	<0.007	<0.008	<0.007	<0.008	<0.007	<0.01	<0.02	<0.05	0.06	0.12	<0.009	3.71
14283-0049	CS_HZ01_B	<0.03	<0.04	<0.05	<0.2	0.07	<0.008	<0.007	<0.007	<0.007	<0.007	<0.008	<0.007	<0.008	<0.007	<0.01	<0.02	0.09	<0.01	0.15	<0.009	0.293
14283-0002	CS_HZ01_R	<0.03	0.05	<0.05	<0.2	<0.03	<0.008	0.008	0.008	0.018	0.008	0.012	0.009	0.011	0.010	0.02	<0.02	0.09	0.01	0.21	0.014	0.165
14283-0003	CS_HZ01_G	<0.03	<0.04	<0.05	<0.2	<0.03	<0.008	0.009	<0.007	0.015	<0.007	<0.008	<0.007	0.008	<0.007	<0.01	<0.02	0.07	<0.01	0.23	0.011	0.116
14283-0004	CS_HZ01_Y	<0.03	0.05	<0.05	<0.2	<0.03	0.011	0.008	<0.007	0.013	<0.007	<0.008	<0.007	0.009	<0.007	<0.01	<0.02	0.10	<0.01	0.29	<0.009	0.224
14283-0005	CS_HZ02_B	<0.03	<0.04	<0.05	<0.2	<0.03	0.009	<0.007	<0.007	0.008	<0.007	<0.008	<0.007	<0.008	<0.007	<0.01	<0.02	0.12	<0.01	0.03	<0.009	2.01
14283-0006	CS_HZ02_R	<0.03	<0.04	<0.05	<0.2	<0.03	0.009	0.009	<0.007	0.008	<0.007	<0.008	<0.007	0.008	<0.007	<0.01	<0.02	0.12	<0.01	0.02	<0.009	0.097
14283-0007	CS_HZ02_G	<0.03	<0.04	<0.05	<0.2	<0.03	<0.008	<0.007	<0.007	<0.007	<0.007	0.011	<0.007	0.012	<0.007	<0.01	<0.02	0.08	<0.01	0.07	0.010	0.031
14283-0008	CS_HZ02_Y	<0.03	0.04	<0.05	<0.2	<0.03	0.012	<0.007	<0.007	<0.007	<0.007	<0.008	<0.007	<0.008	<0.007	<0.01	<0.02	0.08	<0.01	0.12	<0.009	0.028

Sample LIMS Code	Site ID	La	Ce	Pr	Nd	Sm	Eu	Gd	Tb	Dy	Ho	Er	Tm	Yb	Lu	Hf	Ta	W	Tl	Pb	Th	U
		µg l-1	µg l-1	µg l-1	µg l-1	µg l-1	µg l-1	µg l-1	µg l-1	µg l-1	µg l-1	µg l-1	µg l-1	µg l-1	µg l-1	µg l-1	µg l-1	µg l-1	µg l-1	µg l-1	µg l-1	µg l-1
		0.005	0.004	0.003	0.005	0.003	0.003	0.004	0.003	0.006	0.006	0.06	0.02	0.02	0.08	0.03	0.009	0.03	0.009	0.04	0.009	0.009
14412-0001-10 aver	CS_SW	0.006	0.016	0.005	0.011	<0.003	<0.003	0.005	<0.003	0.009	<0.006	<0.06	<0.02	<0.02	<0.08	<0.03	<0.009	<0.03	0.063	0.145	<0.009	3.134
14412-0002-3-9 aver	CS_HZ02_B	0.015	0.041	0.007	0.035	0.005	0.005	0.008	<0.003	0.013	<0.006	<0.06	<0.02	<0.02	<0.08	<0.03	<0.009	0.097	<0.009	0.23	0.013	0.836
14412-0004	CS_HZ02_R	0.011	0.031	0.009	0.045	0.014	<0.003	0.012	<0.003	0.007	<0.006	<0.06	<0.02	<0.02	<0.08	<0.03	<0.009	0.080	<0.009	0.14	<0.009	0.025
14412-0005	CS_HZ02_G	0.01	0.045	0.004	0.011	0.010	<0.003	0.008	<0.003	<0.006	<0.006	<0.06	<0.02	<0.02	<0.08	<0.03	<0.009	0.050	<0.009	0.15	<0.009	0.009
14412-0006-7-11	CS_HZ02_Y	0.022	0.041	0.010	0.028	0.008	<0.003	0.01	<0.003	0.009	<0.006	<0.06	<0.02	<0.02	<0.08	<0.03	<0.009	0.053	<0.009	0.2	0.016	0.016

Table 25 Water chemical analysis at other sites

LIMS Code	Sample Code	Sampling Date	T	pH	SEC	DO	Ca	Mg	Na	K	HCO_3^-	Cl^-	SO_4^{2-}	NO_3^-	Br^-	NO_2^-	HPO_4^{2-}	F^-	NPOC	Total P	Si
			°C		µS cm^{-1}	mg l^{-1}	mg l^{-1}	mg l^{-1}	mg l^{-1}	mg l^{-1}	mg l^{-1}	mg l^{-1}	mg l^{-1}	mg l^{-1}	mg l^{-1}	mg l^{-1}	mg l^{-1}	mg l^{-1}	mg l^{-1}	mg l^{-1}	mg l^{-1}
14283-0061	Bullrushes water	18/07/2018	nd	7.39	2133	nd	210	138	64.2	11.9	649	68.6	654.5	6.00	<0.2	<0.1	<0.2	0.339	12.7	<0.04	6.64
14231-0056	DRAIN 1	24/04/2018	nd	nd	nd	nd	111	39.0	41.4	8.71	328	97.8	100	52.6	0.106	0.424	1.21	0.152	11.0	0.47	4.57
14231-0057	DRAIN 2	24/04/2018	nd	nd	nd	nd	209	122	69.8	8.60	623	52.4	660	3.11	<0.2	<0.1	<0.2	0.367	1.07	<0.04	5.59
14231-0009	DRAIN 3	24/04/2018	nd	nd	nd	nd	125	67.9	59.2	5.97	419	68.4	265	4.12	<0.1	<0.05	<0.1	0.316	1.25	<0.04	4.30
14061-0026	Foumarts Lane Borehole	29/06/2017	nd	8.02	965	nd	90.2	41.07	29.2	1.5	365	51.4	119	1.23	0.153	<0.05	<0.1	1.411	0.584	<0.01	3.85
14067-0016	Stony Hall C Borehole	12/07/2017	11	7.14	2540	n/a	185	78.57	303.9	12.68	661	78.4	751	2.92	<0.5	<0.25	<0.5	<0.25	n/a	<0.04	5.39
14067-0017	Stony Hall L Borehole	12/07/2017	10.9	7.09	2010	0.019	178	81.02	155.5	4.27	539	77.2	570	4.64	<0.5	<0.25	<0.5	0.330	n/a	<0.04	7.11
14067-0018	Low Copelaw Borehole	12/07/2017	10.9	8.15	822	0.015	55	45.32	36.6	6.25	253	51.0	162	3.54	<0.2	<0.1	<0.2	<0.1	n/a	<0.04	1.49
14067-0019	Stillington OBH4 Borehole	12/07/2017	11.5	7.21	775	0.015	86	38.69	34.1	2.42	380	48.4	46	3.33	<0.2	<0.1	<0.2	0.479	n/a	<0.04	4.16
14067-0020	Stillington OBH2 Borehole	12/07/2017	11.6	8.4	433	0.016	13	33.07	21.1	2.6	197	21.1	27	<0.15	0.059	<0.025	<0.05	0.279	n/a	<0.04	0.99
14067-0021	Ketton Hall Borehole	12/07/2017	11.6	9.04	652	0.013	5	43.34	54.2	2.72	186	76.1	67	<0.15	0.324	<0.025	<0.05	0.198	n/a	<0.04	0.88
14283-0060	Quarry AYQ [NZ29524 22571]	17/07/2018	nd	8.17	835	nd	87.9	48.8	16.0	2.33	415	25.0	68.7	16.3	0.060	<0.025	<0.05	0.527	0.45	<0.04	4.18

Table 25 Water chemical analysis at other sites (continued)

LIMS Code	Sample Code	Ba	Sr	Mn	Fe	Li	Be	B	Al	Ti	V	Cr	Co	Ni	Cu	Zn	Ga	As	Se	Rb	Y	Zr	Nb	Mo	Ag	Cd	Sn	Sb	Cs
		µg l^{-1}	µg l^{-1}	µg l^{-1}	µg l^{-1}	µg l^{-1}	µg l^{-1}	µg l^{-1}	µg l^{-1}	µg l^{-1}	µg l^{-1}	µg l^{-1}	µg l^{-1}	µg l^{-1}	µg l^{-1}	µg l^{-1}	µg l^{-1}	µg l^{-1}	µg l^{-1}	µg l^{-1}	µg l^{-1}	µg l^{-1}	µg l^{-1}	µg l^{-1}	µg l^{-1}	µg l^{-1}	µg l^{-1}	µg l^{-1}	µg l^{-1}
14283-0061	Bullrushes water	162	635	601	79	91	<0.5	47	5	<0.2	0.2	<0.3	0.18	0.7	<1	<2	0.26	1.14	0.1	1.31	0.02	0.18	<0.02	<0.3	<0.05	<0.04	0.49	0.12	<0.02
14231-0056	DRAIN 1	104	204	16.9	134	8	<0.01	45	9	1.0	0.8	0.5	0.49	5.8	2.8	14.5	<0.05	1.33	0.2	2.15	0.09	0.10	<0.02	0.75	<0.05	0.03	0.11	0.28	<0.005
14231-0057	DRAIN 2	27.2	759	29.8	4	107	<0.01	155	2	<0.2	<0.1	<0.2	0.09	0.9	0.9	9.2	<0.05	<0.06	0.1	3.64	0.03	<0.09	<0.02	0.18	<0.05	0.03	0.11	0.05	0.009
14231-0009	DRAIN 3	27.6	334	88.4	<2	56	<0.01	123	<2	<0.2	<0.1	<0.2	0.11	2.0	0.8	15.1	<0.05	0.13	0.1	2.81	<0.01	<0.09	<0.02	0.24	<0.05	<0.02	0.08	0.04	0.008
14061-0026	Foumarts Lane Borehole	67.2	226.8	140.1	282	9	<0.01	62	<2	<0.06	<0.5	<0.07	0.19	0.6	<0.5	8	<0.2	0.16	<0.5	0.77	<0.005	0.09	<0.02	0.6	<0.07	<0.04	<0.04	0.12	<0.007
14067-0016	Stony Hall C Borehole	21	4976.7	319.9	3222	242	0.04	1255	<1	<0.2	<1	<0.05	5.97	6.9	<0.4	9	<0.08	0.45	<0.2	22.9	0.059	<0.05	<0.02	0.33	<0.05	<0.02	<0.02	0.13	0.809
14067-0017	Stony Hall L Borehole	12.2	1331.2	187	5192	118	0.04	224	<1	<0.2	<1	<0.05	0.25	0.6	<0.4	6	<0.08	0.12	<0.2	3.81	0.03	<0.05	<0.02	0.5	<0.05	<0.02	<0.02	0.1	0.076
14067-0018	Low Copelaw Borehole	26.4	219.3	123	3466	34	<0.02	101	<1	<0.2	<1	<0.05	0.07	0.7	<0.4	<2	<0.08	0.08	<0.2	2.84	<0.008	<0.05	<0.02	1.46	<0.05	<0.02	<0.02	0.09	0.008
14067-0019	Stillington OBH4 Borehole	51.2	807.2	101.5	2088	58	<0.02	39	<1	<0.2	<1	0.07	0.07	0.3	<0.4	<2	<0.08	0.1	<0.2	2.22	0.01	<0.05	<0.02	1.49	<0.05	<0.02	<0.02	0.12	0.025
14067-0020	Stillington OBH2 Borehole	4.1	55.5	43.7	485	26	<0.02	42	<1	<0.2	<1	<0.05	<0.01	<0.1	<0.4	21	<0.08	0.03	<0.2	2.07	<0.008	<0.05	<0.02	0.17	<0.05	<0.02	0.6	0.12	0.008
14067-0021	Ketton Hall Borehole	1.5	22.5	63.4	38	63	<0.02	67	<1	<0.2	<1	<0.05	<0.01	<0.1	<0.4	<2	<0.08	0.15	<0.2	0.89	<0.008	<0.05	<0.02	4.47	<0.05	<0.02	<0.02	0.1	<0.005
14283-0060	Quarry AYQ [NZ29524 22571]	197	149	<2	<7	10	<0.5	27	10	<0.2	<0.1	<0.3	<0.05	<0.1	<1	10	<0.08	0.08	1.2	1.43	<0.02	<0.05	<0.02	<0.3	<0.05	<0.04	<0.04	<0.05	<0.02

Table 25 Water chemical analysis at other sites (continued)

LIMS Code	Sample Code	La	Ce	Pr	Nd	Sm	Eu	Gd	Tb	Dy	Ho	Er	Tm	Yb	Lu	Hf	Ta	W	Tl	Pb	Th	U
		µg l⁻¹	µg l⁻¹	µg l⁻¹	µg l⁻¹	µg l⁻¹	µg l⁻¹	µg l⁻¹	µg l⁻¹	µg l⁻¹	µg l⁻¹	µg l⁻¹	µg l⁻¹	µg l⁻¹	µg l⁻¹	µg l⁻¹	µg l⁻¹	µg l⁻¹	µg l⁻¹	µg l⁻¹	µg l⁻¹	µg l⁻¹
14283-0061	Bullrushes water	<0.03	<0.04	<0.05	<0.2	<0.03	<0.008	<0.007	<0.007	<0.007	<0.007	<0.008	<0.007	<0.008	<0.007	<0.01	<0.02	<0.05	<0.01	0.02	<0.009	10.8
14231-0056	DRAIN 1	0.067	0.08	<0.04	0.07	0.011	<0.002	0.018	<0.002	0.014	0.004	0.017	0.003	0.026	0.004	<0.01	<0.02	<0.05	<0.02	0.32	0.01	0.980
14231-0057	DRAIN 2	0.008	<0.03	<0.04	<0.07	<0.006	<0.002	0.005	<0.002	<0.005	<0.002	0.002	<0.002	0.006	<0.002	<0.01	<0.02	<0.05	0.17	0.04	<0.005	3.57
14231-0009	DRAIN 3	<0.005	<0.03	<0.04	<0.07	<0.006	<0.002	0.003	<0.002	<0.005	<0.002	0.003	<0.002	<0.004	<0.002	<0.01	<0.02	<0.05	0.36	0.05	<0.005	2.27
14061-0026	Foumarts Lane Borehole	<0.002	<0.002	<0.002	<0.03	<0.005	<0.004	<0.003	<0.002	<0.002	<0.002	<0.002	<0.002	<0.002	<0.002	<0.01	<0.02	<0.07	0.14	<0.1	<0.005	1.11
14067-0016	Stony Hall C Borehole	<0.009	<0.009	<0.008	<0.04	<0.009	<0.007	<0.009	<0.009	<0.009	<0.008	<0.008	<0.01	<0.002	<0.009	<0.01	<0.02	<0.07	<0.01	0.02	<0.02	0.15
14067-0017	Stony Hall L Borehole	<0.009	<0.009	<0.008	<0.04	<0.009	<0.007	<0.009	<0.009	<0.009	<0.008	<0.008	<0.01	0.005	<0.009	<0.01	<0.02	<0.07	0.01	0.03	<0.02	0.65
14067-0018	Low Copelaw Borehole	<0.009	<0.009	<0.008	<0.04	<0.009	<0.007	<0.009	<0.009	<0.009	<0.008	<0.008	<0.01	<0.002	<0.009	<0.01	<0.02	<0.07	<0.01	<0.02	<0.02	0.24
14067-0019	Stillington OBH4 Borehole	<0.009	<0.009	<0.008	<0.04	<0.009	<0.007	<0.009	<0.009	<0.009	<0.008	<0.008	<0.01	<0.002	<0.009	<0.01	<0.02	<0.07	<0.01	<0.02	<0.02	0.54
14067-0020	Stillington OBH2 Borehole	<0.009	<0.009	<0.008	<0.04	<0.009	<0.007	<0.009	<0.009	<0.009	<0.008	<0.008	<0.01	<0.002	<0.009	<0.01	<0.02	<0.07	<0.01	<0.02	<0.02	<0.02
14067-0021	Ketton Hall Borehole	<0.009	<0.009	<0.008	<0.04	<0.009	<0.007	<0.009	<0.009	<0.009	<0.008	<0.008	<0.01	<0.002	<0.009	<0.01	<0.02	<0.07	<0.01	<0.02	<0.02	<0.02
14283-0060	Quarry AYQ [NZ29524 22571]	<0.03	<0.04	<0.05	<0.2	<0.03	<0.008	<0.007	<0.007	<0.007	<0.007	<0.008	<0.007	<0.008	<0.007	<0.01	<0.02	<0.05	<0.01	<0.02	<0.009	1.58

Appendix 4 Clustering

Table 26 Cluster centroids

Variable	Cluster1	Cluster2	Cluster3	Cluster4	Grand centroid
Ca	1.40	-0.75	-0.55	0.10	0.00
Mg	1.55	-0.87	-0.30	-0.06	0.00
Na	1.09	-0.93	0.47	-0.11	-0.00
K	1.30	-1.07	0.32	-0.02	-0.00
HCO3	0.62	-0.90	-0.53	0.93	-0.00
Cl	0.02	-0.58	1.423	-0.27	0.00
SO4	1.59	-0.58	-0.19	-0.51	-0.00
F	0.11	-0.09	-0.23	0.17	0.00
Si	-0.87	0.23	-0.84	1.02	0.00
Ba	-1.05	0.67	-0.35	0.32	-0.00
Sr	1.07	-0.62	-0.28	0.03	0.00
Mn	-0.83	-0.02	-0.32	0.94	-0.00
Fe	-0.60	0.25	-0.57	0.59	-0.00
Li	1.61	-0.80	-0.13	-0.31	-0.00
Rb	1.15	-0.82	0.23	-0.13	-0.00
U	1.45	-0.76	0.22	-0.46	-0.00
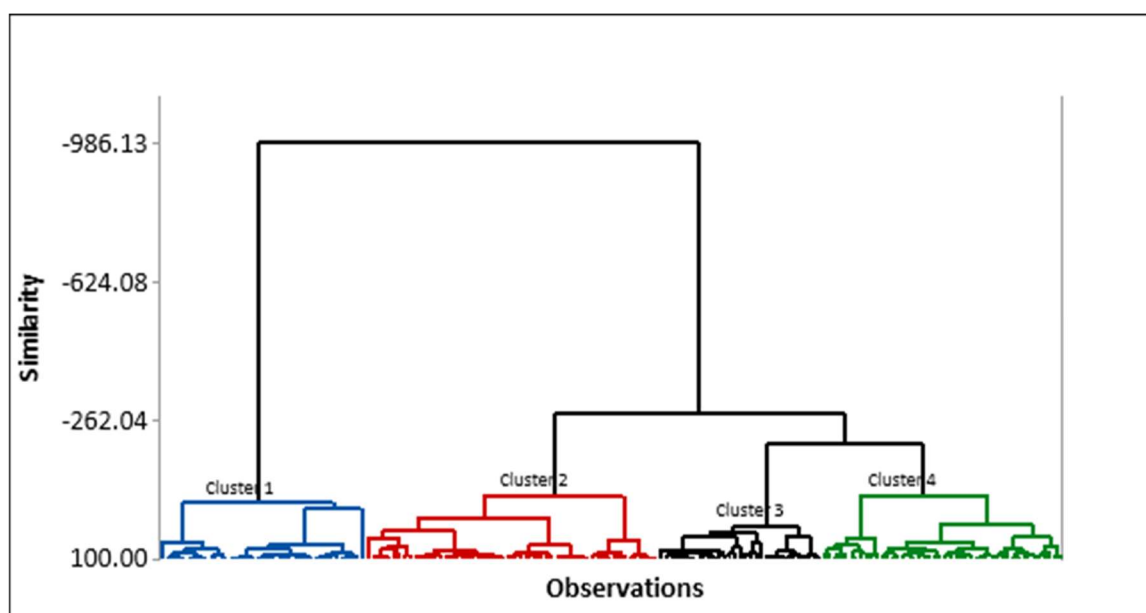
LIMS Code	Sample Code	Type	4 clusters
14283-0061	BULLRUSHES WATER	SPRING	1
14231-010	BP_SEEPAGE_5.1	SPRING	1
14283-0062	BP_SEEPAGE_5.2	SPRING	1
14412-0030	BP_SEEPAGE_5.3	SPRING	1
14067-0016	STONY HALL C BOREHOLE	GW	1
14231-001	BP_HZ01_B_5.1	HZ	1
14283-0041	BP_HZ01_B_5.2	HZ	1
14412-0021	BP_HZ01_B_5.3	HZ	1
14231-004	BP_HZ01_G_5.1	HZ	1
14283-0043	BP_HZ01_G_5.2	HZ	1
14231-003	BP_HZ01_R_5.1	HZ	1

14283-0042	BP_HZ01_R_5.2	HZ	1
14412-0023	BP_HZ01_R_5.3	HZ	1
14231-005	BP_HZ01_Y_5.1	HZ	1
14283-0044	BP_HZ01_Y_5.2	HZ	1
14412-0025	BP_HZ01_Y_5.3	HZ	1
14231-006	BP_HZ02_B_5.1	HZ	1
14283-0045	BP_HZ02_B_5.2	HZ	1
14412-0024	BP_HZ02_G_5.3	HZ	1
14231-007	BP_HZ02_GG_5.1	HZ	1
14283-0047	BP_HZ02_GG_5.2	HZ	1
14231-002	BP_HZ02_R_5.1	HZ	1
14283-0046	BP_HZ02_R_5.2	HZ	1
14231-008	BP_HZ02_Y_5.1	HZ	1
14077-0018	WB/2 ML2 Black	HZ	1
14231-057	DRAIN 2_5.1	SEEPAGE	1
14231-011	BP_SW_5.1	SW	1
14283-0053	BP_SW_5.2	SW	1
14412-0022	BP_SW_5.3	SW	1
14283-0052	Be_SW_5.2	SW	1
14283-0051	LH_SW_5.2	SW	1
14283-0050	CF_SW_5.2	SW	1
14412-0013	CF_SW_5.3	SW	1
14283-0001	CS_SW_5.2	SW	1
14412-0001-10 aver	CS_SW_5.3	SW	1
14077-0006	WB/1 SW	SW	1
14077-0007	WB/2 SW	SW	1
14077-0023	WB/2 SW dupl	SW	1
14283-0059	WOODHAM BURN at BE SITE	SW	1

LIMS Code	Sample Code	Type	4 clusters
14061-0026	FOUMARTS LANE BOREHOLE	GW	2
14283-0060	QUARRY AYQ	GW	2
14067-0019	STILLINGTON OBH4 BOREHOLE	GW	2
14231-013	Be_HZ01_B_5.1	HZ	2
14412-0027	Be_HZ01_B_5.3	HZ	2
14231-015	Be_HZ01_G_5.1	HZ	2
14283-0031	Be_HZ01_G_5.2	HZ	2
14412-0031	Be_HZ01_G_5.3	HZ	2
14231-014	Be_HZ01_R_5.1	HZ	2
14283-0030	Be_HZ01_R_5.2	HZ	2
14412-0029	Be_HZ01_R_5.3	HZ	2
14231-016	Be_HZ01_Y_5.1	HZ	2
14283-0032	Be_HZ01_Y_5.2	HZ	2
14412-0032	Be_HZ01_Y_5.3	HZ	2
14231-017	Be_HZ02_B_5.1	HZ	2
14283-0036	Be_HZ02_B_5.2	HZ	2
14231-019	Be_HZ02_G_5.1	HZ	2
14283-0034	Be_HZ02_G_5.2	HZ	2
14231-018	Be_HZ02_R_5.1	HZ	2

LIMS Code	Sample Code	Type	2
14231-020	Be_HZ02_Y_5.1	HZ	2
14283-0033	Be_HZ02_Y_5.2	HZ	2
14283-0037	Be_HZ03_B_5.2	HZ	2
14231-023	Be_HZ03_G_5.1	HZ	2
14283-0039	Be_HZ03_G_5.2	HZ	2
14283-0038	Be_HZ03_R_5.2	HZ	2
14231-024	Be_HZ03_Y_5.1	HZ	2
14283-0040	Be_HZ03_Y_5.2	HZ	2
14231-025	LH_HZ01_B_5.1	HZ	2
14283-0017	LH_HZ01_B_5.2	HZ	2
14412-0018	LH_HZ01_B_5.3	HZ	2
14231-027	LH_HZ01_G_5.1	HZ	2
14283-0019	LH_HZ01_G_5.2	HZ	2
14412-0026	LH_HZ01_G_5.3	HZ	2
14231-026	LH_HZ01_R_5.1	HZ	2
14283-0018	LH_HZ01_R_5.2	HZ	2
14412-0020	LH_HZ01_R_5.3	HZ	2
14231-028	LH_HZ01_Y_5.1	HZ	2
14283-0020	LH_HZ01_Y_5.2	HZ	2
14412-0019	LH_HZ01_Y_5.3	HZ	2
14231-029	LH_HZ02_B_5.1	HZ	2
14231-031	LH_HZ02_G_5.1	HZ	2
14283-0023	LH_HZ02_G_5.2	HZ	2
14231-030	LH_HZ02_R_5.1	HZ	2
14283-0022	LH_HZ02_R_5.2	HZ	2
14231-032	LH_HZ02_Y_5.1	HZ	2
14283-0024	LH_HZ02_Y_5.2	HZ	2

LIMS Code	Sample Code	Type	4 clusters
14231-033	LH_HZ03_B_5.1	HZ	2
14283-0025	LH_HZ03_B_5.2	HZ	2
14231-035	LH_HZ03_G_5.1	HZ	2
14283-0027	LH_HZ03_G_5.2	HZ	2
14231-034	LH_HZ03_R_5.1	HZ	2
14283-0026	LH_HZ03_R_5.2	HZ	2
14231-036	LH_HZ03_Y_5.1	HZ	2
14283-0028	LH_HZ03_Y_5.2	HZ	2
14283-0004	CS_HZ01_Y_5.2	HZ	2
14077-0022	WB/2 MP1	HZ	2

LIMS Code	Sample Code	Type	4 clusters
14067-0021	KETTON HALL BOREHOLE	GW	3
14067-0018	LOW COPELAW BOREHOLE	GW	3
14067-0020	STILLINGTON OBH2 BOREHOLE	GW	3
14067-0017	STONY HALL L BOREHOLE	GW	3
14231-021	Be_HZ03_B_5.1	HZ	3
14231-022	Be_HZ03_R_5.1	HZ	3
14231-038	CF_HZ01_B_5.1	HZ	3
14231-040	CF_HZ01_G_5.1	HZ	3

LIMS Code	Sample Code	Type	3
14231-039	CF_HZ01_R_5.1	HZ	3
14231-041	CF_HZ01_Y_5.1	HZ	3
14231-042	CF_HZ02_B_5.1	HZ	3
14231-043	CF_HZ02_R_5.1	HZ	3
14231-052	CS_HZ02_B_5.1	HZ	3
14231-053	CS_HZ02_R_5.1	HZ	3
14077-0009	WB/3 ML B	HZ	3
14077-0011	WB/3 ML G	HZ	3
14077-0010	WB/3 ML R	HZ	3
14077-0012	WB/3 ML Y	HZ	3
14077-0024	WB/3 MP1	HZ	3
14077-0025	WB/3 MP2	HZ	3
14231-056	DRAIN 1_5.1	SEEPAGE	3
14231-009	DRAIN 3_5.1	SEEPAGE	3
14231-012	Be_SW_5.1	SW	3
14412-0028	Be_SW_5.3	SW	3
14231-037	LH_SW_5.1	SW	3
14412-0017	LH_SW_5.3	SW	3
14231-046	CF_SW_5.1	SW	3
14231-051	CS_SW_5.1	SW	3
14077-0005	RB/SW	SW	3
14077-0008	WB/3 SW	SW	3
14077-0013	WB/3 SW dupl	SW	3

LIMS Code	Sample Code	Type	4 clusters
14283-0048	BP_HZ02_Y_5.2	HZ	4
14283-0009	CF_HZ01_B_5.2	HZ	4
14412-0012	CF_HZ01_B_5.3	HZ	4
14283-0010	CF_HZ01_R_5.2	HZ	4
14412-0014	CF_HZ01_R_5.3	HZ	4
14283-0013	CF_HZ02_B_5.2	HZ	4
14283-0014	CF_HZ02_R_5.2	HZ	4
14283-0005	CS_HZ02_B_5.2	HZ	4
14412-0002-3-9 aver	CS_HZ02_B_5.3	HZ	4
14283-0006	CS_HZ02_R_5.2	HZ	4
14412-0004	CS_HZ02_R_5.3	HZ	4
14283-0029	Be_HZ01_B_5.2	HZ	4
14283-0035	Be_HZ02_R_5.2	HZ	4
14283-0021	LH_HZ02_B_5.2	HZ	4
14283-0011	CF_HZ01_G_5.2	HZ	4
14412-0015	CF_HZ01_G_5.3	HZ	4
14283-0012	CF_HZ01_Y_5.2	HZ	4
14412-0016	CF_HZ01_Y_5.3	HZ	4
14231-044	CF_HZ02_G_5.1	HZ	4
14283-0015	CF_HZ02_G_5.2	HZ	4
14231-045	CF_HZ02_Y_5.1	HZ	4
14283-0016	CF_HZ02_Y_5.2	HZ	4
14231-047	CS_HZ01_B_5.1	HZ	4
14283-0049	CS_HZ01_B_5.2	HZ	4

14231-049	CS_HZ01_G_5.1	HZ	4
14283-0003	CS_HZ01_G_5.2	HZ	4
14231-048	CS_HZ01_R_5.1	HZ	4
14283-0002	CS_HZ01_R_5.2	HZ	4
14231-050	CS_HZ01_Y_5.1	HZ	4
14231-054	CS_HZ02_G_5.1	HZ	4
14283-0007	CS_HZ02_G_5.2	HZ	4
14412-0005	CS_HZ02_G_5.3	HZ	4
14231-055	CS_HZ02_Y_5.1	HZ	4
14283-0008	CS_HZ02_Y_5.2	HZ	4
14412-0006-7-11	CS_HZ02_Y_5.3	HZ	4
14077-0001	RB/ML Black	HZ	4
14077-0003	RB/ML Green	HZ	4
14077-0002	RB/ML Red	HZ	4
14077-0004	RB/ML Yellow	HZ	4
14077-0014	WB/2 ML1 B	HZ	4
14077-0016	WB/2 ML1 G	HZ	4
14077-0015	WB/2 ML1 R	HZ	4
14077-0017	WB/2 ML1 Y	HZ	4
14077-0020	WB/2 ML2 G	HZ	4
14077-0019	WB/2 ML2 R	HZ	4
14077-0021	WB/2 ML2 Y	HZ	4

References

British Geological Survey holds most of the references listed below, and copies may be obtained via the library service subject to copyright legislation (contact libuser@bgs.ac.uk for details). The library catalogue is available at: https://envirolib.apps.nerc.ac.uk/olibcgi.

BOTTRELL, S H, WEST, L J AND YOSHIDA, K. 2006. Combined isotopic and modelling approach to determining the source of saline groundwaters in the Selby Triassic sandstone aquifer, UK. Geological Society, London, *Special Publications*, 263(1), 325-338.

BRITISH GEOLOGICAL SURVEY. 1969. Geological Sheet, 32. Barnard Castle. 1: 63360. Scale Solid Edition (Keyworth, Nottingham: British Geological Survey).

BRITISH GEOLOGICAL SURVEY. 1989. Geological Sheet, 33. Stockton. Solid and Drift (Keyworth, Nottingham: British Geological Survey).

BRODIE, R, SUNDARAM, B, TOTTENHAM, R, HOSTETLER, S AND RANSLEY, T. 2007. An overview of tools for assessing groundwater–surface water connectivity. *Bureau of Rural Sciences, Canberra, Australia*.

BUSS, S R , CAI, Z, CARDENAS, B, FLECKENSTEIN, J, HANNAH, D M, HEPPELL, K, HULME, P J, IBRAHIM, T G, KAESER, D H, KRAUSE, S, LAWLER, D M, LERNER, D N, MANT, J, MALCOLM, I A, OLD, G, PARKIN, G, PICKUP, R., PINAY, G, PORTER, J, RHODES, G, RITCHIE, A, RILEY, J, ROBERTSON, A I, SEAR, D, SHIELDS, B, SMITH, J W N, TELLAM, J H AND WOOD, P. 2009. The Hyporheic Handbook: A Handbook on the groundwater-surface water interface and hyporheic zone for environmental managers. *Environment Agency Science Report SC050070. EA*, Bristol, UK, 280pp.

CAIRNEY T. 1972. Hydrological investigation of the Magnesian Limestone of south-east Durham, England. *Journal of Hydrology*, 16(4), 323-40.

CAIRNEY T AND HAMILL L. 1977. Interconnection of surface and underground water resources in southeast Durham. *Journal of Hydrology*, 33(1-2), 73-86.

COAL AUTHORITY. 2018. Mining and groundwater constraints for sustainable development and drainage systems (North East England only). *The Coal Authority and Environment Agency Report*, 38 pp.

COOK, P G. 2013. Estimating groundwater discharge to rivers from river chemistry surveys. *Hydrological Processes*, 27(25), 3694-3707.

DAVIES, B J, LIVINGSTONE, S J, ROBERTS, D H, EVANS, D J A, GHEORGHIU D M AND O COFAIGH, C. 2019. Dynamic ice stream retreat in the central sector of the last British-Irish Ice Sheet. *Quaternary Science Reviews* 225.

EDMUNDS, W M. 1975. Geochemistry of brines in the coal measures of northeast England. *Transactions of the Institute of Mining and Metallurgy*. 84, B39-B52.

ENVIRONMENT AGENCY, 2012. Hydrology Flow Investigation Stage 2. Northumbria River Basin District Investigation: NE2010-10005.

FINKELMAN, R.B., DAI, S. AND FRENCH, D. 2019. The importance of minerals in coal as a the hosts of chemical elements: A review. International Journal of Coal Geology, 212, 17pp.

GAMMONS, C H, BROWN, A, POULSON, S R AND HENDERSON, T H. 2013. Using stable isotopes (S, O) of sulfate to track local contamination of the Madison karst aquifer, Montana, from abandoned coal mine drainage. *Applied geochemistry*, 31, 228-238.

HOUSE, A R, SORENSEN, J P R, GOODDY, D C, NEWELL, A J, MARCHANT, B, MOUNTFORD, J O, SCARLETT, P, WILLIAMS, P J AND OLD, G H. 2015. Discrete wetland groundwater discharges revealed with a three-dimensional temperature model and botanical indicators (Boxford, UK). *Hydrogeology Journal,* 23**,** 775-787.

HUGHES D B, CLARKE B G, AND MONEY M S. 1998. The glacial succession in lowland Northern England. *Quarterly Journal of Engineering Geology and Hydrogeology*, 31(3), 211-34.

IBRAHIM, T, THORNTON, S AND WAINWRIGHT, J. 2010. Interplay of Geomorphic and Hydrogeologic Features at Reach- and Channel Unit-Scales on Riverbed Hydrology and Hydrochemistry: A Conceptual Model in the Lower Coal Measures, South Yorkshire, UK. *Hydrogeology Journal*. 18. 1391-1411. 10.1007/s10040-010-0623-z.

KURTAS L AND YOUNGER, P L. 2013. Fracture patterns in the Permian Magnesian Limestone Aquifer, Co. Durham, UK. *Proceedings of the Yorkshire Geological Society*, 59, 3, 161-171.

LANSDOWN, K, HEPPELL, C M, TRIMMER, M, BINLEY, A, HEATHWAITE, A L, BYRNE, P, AND ZHANG, H. 2015. The interplay between transport and reaction rates as controls on nitrate attenuation in permeable, streambed sediments. *Journal of Geophysical Research: Biogeosciences*, 120(6), 1093-1109.

MURTON, D K AND MURTON, J B. 2012. Middle and Late Pleistocene glacial lakes of lowland Britain and the southern North Sea Basin. *Quaternary International*, 260,115-42.

Nuttall, C A and Younger, P L. 2004. Hydrochemical stratification in flooded underground mines: an overlooked pitfall. Journal of Contaminant Hydrology, 69, 101-114.

Ogilvie, A G. 1930. *Great Britain: essays in regional geography by twenty-six authors.* [2nd ed.] Cambridge [Eng.]: The University press.

Palumbo-Roe, B, Banks, V J and Brauns, B. 2019. Characterising the hyporheic zones in the Skerne Catchment. British Geological Survey Commissioned Report, CR/19/004, 173pp.

Plummer, L N, Busby, J F, Lee, R W and Hanshaw, B B. 1990. Geochemical modeling of the Madison aquifer in parts of Montana, Wyoming, and South Dakota. *Water Resources Research*, 26(9), 1981-2014.

Rivett, M O, Ellis, P A, Greswell, R B, Ward, R S, Roche, R S, Cleverly, M G, Walker, C, Conran, D, Fitzgerald, P J, Willcox, T and Dowle, J. 2008. Cost-effective mini drive-point piezometers and multilevel samplers for monitoring the hyporheic zone. *Quarterly Journal of Engineering Geology and Hydrogeology*, 41(1), 49-60.

Rose, A W, and Cravotta III, C A. 1998. Geochemistry of coal mine drainage. Coal mine drainage prediction and pollution prevention in Pennsylvania, 1, 1-22.

Sebok, E and Müller, S. 2019. The effect of sediment thermal conductivity on vertical groundwater flux estimates. *Hydrology & Earth System Sciences*, *23*, 3305–3317.

White Young Green. 2006. Report on Mine Water Contamination of the Permian Aquifer South of the Butterknowle Fault for The Coal Authority. 39 pp and appendices.